

**Synthesis, Chemical Stability and Processing
by Reverse Transcriptases of Abasic RNA**

Inauguraldissertation
der Philosophisch-naturwissenschaftlichen Fakultät
der Universität Bern

vorgelegt von
Pascal André Küpfer
von Lauperswil BE

Leiter der Arbeit:
Prof. Dr. Christian J. Leumann
Departement für Chemie und Biochemie der Universität Bern

**Synthesis, Chemical Stability and Processing
by Reverse Transcriptases of Abasic RNA**

Inauguraldissertation
der Philosophisch-naturwissenschaftlichen Fakultät
der Universität Bern

vorgelegt von
Pascal André Küpfer
von Lauperswil BE

Leiter der Arbeit:
Prof. Dr. Christian J. Leumann
Departement für Chemie und Biochemie der Universität Bern

Von der Philosophisch-naturwissenschaftlichen Fakultät angenommen.

Bern, den 21. Dezember 2006

Der Dekan:



Prof. Dr. P. Messerli

*Die Neugier steht immer an erster Stelle
eines Problems, das gelöst werden will.*

Galileo Galilei (1564-1642)

Acknowledgements

First I would like to thank my supervisor Prof. Dr. Christian J. Leumann who gave me the opportunity to complete this challenging work in his group. I'm grateful for his generous support and invaluable advice over the last years that deeply influenced the outcome of this work.

I am also indebted to Prof. Dr. Andreas Marx from the University of Konstanz who accepted to be a co-referee of this work.

I specially thank Prof. Dr. Robert Häner for reading my thesis and leading the exam.

Moreover I would like to thank the former and current members of the Leumann group who all contributed in a way or the other to the success of this work and made the last four years what they finally were (in alphabetical order): Dae-ro Ahn, Jessica Becaud, Reto Bertolini, Tino Boss, Christine Brotschi, Sabrina Buchini, Caroline Crey-Desbiolles, Christoph Eggenschwiler, Daniel Gautschi (where is he?), Michael Gisler, Adrian Häberli, Caroline Hirz, Marcel Hollenstein, Jürg Hunziker, Damian Ittig, Benno Keller, Sam "sauvage" Luisier, Gerald Mathis, Alain Mayer, Markus Mosimann, Dorte Renneberg, Simon Scheidegger, Rolf Schütz, Andrea Stauffiger, Matthias Stoop, Nadia Waser and Alain Zahn.

Very special thanks go to Dr. Caroline Crey-Desbiolles who greatly supported my work with enzyme assays with her knowledge in this field.

The "Ausgabe" team, the "Hausdienst" team, the "Werkstatt" team and the secretaries are greatly acknowledged for their kind and professional support in all ways. I would also like to specially thank PD Dr. Stefan Schürch and his team for the sometimes difficult and time-consuming mass spectrometry measurements and for the patience.

Finally I would like to thank my family for the support throughout the past years and for the encouragement.

Last but not least I would like to thank all the people I forgot so far for the support over the last years.

During the present work the following articles were or will be published:

- Küpfer P. A., Leumann C. J., "RNA Abasic Sites: Preparation and Trans-Lesion Synthesis by HIV-1 Reverse Transcriptase", *ChemBioChem* **2005**, *6*, 1970-1973.
- Mosimann M., Küpfer P. A., Leumann C. J., "Synthesis and Incorporation into DNA of a Chemically Stable, Functional Abasic Site Analogue", *Org. Lett.* **2005**, *7*, 5211-5214.
- Küpfer P. A., Leumann C. J., "The Chemical Stability of Abasic RNA Compared to Abasic DNA", *Nucleic Acids Res.* **2007**, *35*, 58-68.
- Küpfer P. A., Leumann C. J., "Photochemically Induced RNA and DNA Abasic Sites", *Nucleosides, Nucleotides & Nucleic Acids*, **2007**, submitted.
- Küpfer P. A., Crey-Desbiolles C., Leumann C. J., manuscript in preparation.

Table of Contents

ABSTRACT	1
1 INTRODUCTION	3
1.1 HISTORICAL BACKGROUND	3
1.2 NUCLEIC ACID STRUCTURE	4
1.2.1 Primary structure of nucleic acids	4
1.2.2 DNA secondary structure	5
1.2.3 RNA secondary structure.....	6
1.2.4 From genes to proteins.....	8
1.2.5 RNA species	10
1.3 ABASIC SITES	15
1.3.1 Abasic site structure.....	15
1.3.2 Acidic hydrolysis of <i>N</i> -glycosidic bonds in nucleosides	15
1.4 FORMATION OF SITE SPECIFIC DNA ABASIC SITES.....	18
1.4.1 Synthesis of “true” DNA abasic sites	18
1.4.2 Unnatural and minor DNA abasic site analogues	21
1.5 REACTIVITY OF THE NATURAL DNA ABASIC SITE	23
1.5.1 Abasic site cleavage.....	23
1.5.2 Abasic site detection.....	24
1.5.3 DNA polymerases and reverse transcriptases.....	24
1.5.4 Abasic site repair	25
1.6 FORMATION OF SITE SPECIFIC RNA ABASIC SITES.....	27
1.6.1 Chemically induced RNA abasic sites	27
1.6.2 Abasic sites induced by ribosome inactivating proteins	29
1.6.3 Unnatural RNA abasic site analogues	30
1.7 REACTIVITY OF THE NATURAL RNA ABASIC SITE	31
1.8 MAJOR EFFECTS OF UV RADIATION ON NUCLEIC ACIDS.....	32
1.8.1 Cyclobutane pyrimidine dimers.....	32
1.8.2 Pyrimidine (6-4) pyrimidone photoproducts	33
1.8.3 Mutations from pyrimidine dimers	33
1.9 AIM OF THE WORK	35
2 SYNTHESIS	37
2.1 SYNTHESIS OF THE PHOSPHORAMIDITE BUILDING BLOCKS.....	37
2.1.1 Selection and synthesis of a suitable abasic site protecting group.....	37
2.1.2 Synthesis of the RNA abasic site precursor	38
2.1.3 Synthesis of the 2'- <i>O</i> -Me RNA abasic site precursor.....	42
2.2 SYNTHESIS OF THE DNA ABASIC SITE PRECURSOR.....	43

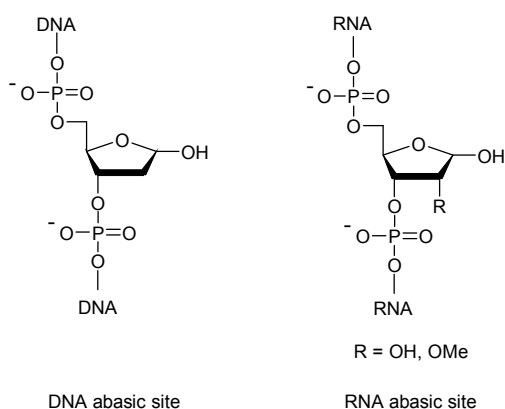
2.3	OLIGONUCLEOTIDE SYNTHESIS	44
3	RESULTS AND DISCUSSION.....	45
3.1	GENERAL REMARKS	45
3.2	DEPROTECTION KINETICS	46
3.2.1	RNA abasic site deprotection kinetics	46
3.2.2	DNA abasic site deprotection kinetics	48
3.2.3	Reaction mechanism of the deprotection reaction	50
3.2.4	Deprotection methods	50
3.3	STRAND CLEAVAGE UNDER BASIC CONDITIONS	52
3.3.1	Cleavage of RNA under basic conditions	52
3.3.2	Kinetics of the β,δ -elimination mechanism of an RNA abasic site.....	53
3.3.3	Cyclophosphate formation mechanism of RNA	56
3.3.4	Strand cleavage mechanism of a natural RNA abasic site	59
3.3.5	Kinetics of the β,δ -elimination mechanism at a natural DNA abasic site.....	62
3.4	STRAND CLEAVAGE UNDER WEAKLY ACIDIC CONDITIONS	64
3.4.1	Kinetics of aniline-induced strand cleavage at an RNA abasic site	64
3.4.2	Kinetics of aniline-induced strand cleavage at a DNA abasic site.....	67
3.5	DISCUSSION OF THE KINETIC RESULTS.....	70
3.6	REVERSE TRANSCRIPTION ASSAYS	74
3.6.1	HIV-1 reverse transcriptase assay.....	75
3.6.2	AMV reverse transcriptase assay.....	79
3.6.3	MMLV RT (H-) reverse transcriptase assay	81
3.6.4	RNase H activity test	83
3.7	INCORPORATION KINETICS OF DNTPS AT ABASIC SITES	87
3.7.1	Michaelis-Menten enzyme kinetics	87
3.7.2	Incorporation kinetics	89
3.8	DISCUSSION OF THE INCORPORATION KINETICS.....	94
4	CONCLUSIONS AND OUTLOOK	95
5	EXPERIMENTAL PART	99
5.1	GENERAL.....	99
5.1.1	Chromatography	99
5.2	INSTRUMENTATION.....	99
5.2.1	NMR spectroscopy	99
5.2.2	Mass spectrometry	100
5.2.3	UV-Vis spectroscopy.....	100
5.2.4	Melting point.....	100
5.3	SYNTHESIS OF THE NATURAL RNA ABASIC SITE PRECURSOR.....	101
5.3.1	1-(2-Nitrophenyl)ethanol (4)	101
5.3.2	1-(2-Nitrophenyl)ethyl-1(<i>S</i>)-camphanate (17).....	103
5.3.3	(<i>R</i>)-, (<i>S</i>)-1-(2-Nitrophenyl)ethanol (4a/b)	106

5.3.4	1'-[(<i>R</i>)-1-(2-Nitrophenyl)ethyl]-2',3',5'-tri- <i>O</i> -acetyl-ribofuranose (5).....	107
5.3.5	1'-[(<i>R</i>)-1-(2-Nitrophenyl)ethyl]-ribofuranose (6).....	109
5.3.6	1'-[(<i>R</i>)-1-(2-Nitrophenyl)ethyl]-5'-[(4,4'-dimethoxy)triphenyl]-ribofuranose (7a)....	111
5.3.7	Triisopropylsilyl(ethylthio)methyl ether (8a).....	115
5.3.8	[(Triisopropylsilyloxy)methyl chloride (8).....	117
5.3.9	1'-[(<i>R</i>)-1-(2-Nitrophenyl)ethyl]-5'-[(4,4'-dimethoxy)triphenyl]-2'- [[[(triisopropyl)silyloxy] methyl]-ribofuranose (9a).....	119
5.3.10	1'-[(<i>R</i>)-1-(2-Nitrophenyl)ethyl]-5'-[(4,4'-dimethoxy)triphenyl]-2'-[[[(triiso- propyl)silyloxy] methyl]-ribofuranose 3'-(2-cyanoethyl diisopropylphosphor- amidite) (1).....	124
5.4	SYNTHESIS OF THE 2'-<i>O</i>-METHYLATED RNA ABASIC SITE PRECURSOR.....	127
5.4.1	1'-[(<i>R</i>)-1-(2-Nitrophenyl)ethyl]-3'-5'- <i>O</i> -(1,1,3,3-tetraisopropylidisiloxane- 1,3-diyl)-ribofuranose (10a).....	127
5.4.2	1'-[(<i>R</i>)-1-(2-Nitrophenyl)ethyl]-2'- <i>O</i> -methyl-3'-5'- <i>O</i> -(1,1,3,3-tetraisopro- pyldisiloxane-1,3-diyl)-ribofuranose (11).....	131
5.4.3	1'-[(<i>R</i>)-1-(2-Nitrophenyl)ethyl]-2'- <i>O</i> -methyl-ribofuranose (12).....	133
5.4.4	1'-[(<i>R</i>)-1-(2-Nitrophenyl)ethyl]-5'-[(4,4'-dimethoxy)triphenyl]-2' <i>O</i> -methyl- ribofuranose (13).....	135
5.4.5	1'-[(<i>R</i>)-1-(2-Nitrophenyl)ethyl]-5'-[(4,4'-dimethoxy)triphenyl]-2'- <i>O</i> -methyl- ribofuranose-3'-cyanoethylphosphoramidite (2).....	137
5.5	SYNTHESIS OF THE DNA ABASIC SITE PRECURSOR.....	140
5.5.1	1', 3', 5'-Tri- <i>O</i> -acetyl-2'-deoxy-D-ribofuranose (16).....	140
5.5.2	1'-[1(<i>S</i>)-(2-Nitrophenyl)-ethyl]-3', 5'-di- <i>O</i> -acetyl-2'-deoxy-ribofuranose (14).....	142
5.5.3	1'-[1(<i>S</i>)-(2-Nitrophenyl)-ethyl]-2'-deoxy-ribofuranose (15).....	144
5.5.4	1'-[1(<i>S</i>)-(2-Nitrophenyl)-ethyl]-5'-[(4,4'-dimethoxy)triphenyl]-2'-deoxy- ribofuranose (16).....	146
5.5.5	1'-[1(<i>S</i>)-(2-Nitrophenyl)-ethyl]-5'-[(4,4'-dimethoxy)triphenyl]-2'-deoxy- ribofuranose-3'-(2-cyanoethyl diisopropylphosphoramidite) (3).....	148
5.6	SYNTHESIS AND PURIFICATION OF OLIGONUCLEOTIDES.....	151
5.6.1	Ribonuclease-free laboratory environment.....	151
5.6.2	Synthesis of oligonucleotides.....	151
5.6.3	Deprotection of oligonucleotides.....	152
5.6.4	Purification of oligonucleotides by RP-HPLC.....	153
5.6.5	Desalting the oligonucleotides.....	154
5.6.6	Purification of oligonucleotides by gel electrophoreses.....	154
5.7	KINETIC STUDIES.....	156
5.7.1	Kinetic studies of abasic site deprotection.....	156
5.7.2	Strand cleavage in the presence of hydroxide at pH 13.....	156
5.7.3	Strand cleavage in the presence of aniline at pH 4.6.....	157
5.7.4	Evaluation of the kinetic parameters.....	157
5.8	ENZYME ASSAYS.....	159
5.8.1	Labeling of the primer.....	159
5.8.2	Preparation of the reaction mix.....	159

5.8.3	Enzyme reaction	160
5.8.4	Enzyme storage buffers.....	160
5.8.5	Kinetic assays	161
6	REFERENCES.....	163
	APPENDIX	173

Abstract

Abasic sites are well known DNA lesions that occur spontaneously under acidic or oxidative stress or as intermediates after enzymatic excision of damaged bases. Due to the missing genetic information such sites are highly mutagenic. Therefore, nature has developed a ubiquitous cellular DNA repair system for genome housekeeping. Spontaneous or induced abasic lesions are *a priori* not restricted to DNA but can also occur in RNA. Given the fact that not only short lived mRNA but long lived tRNAs and ribosomal RNAs are present at all times in a cell in much higher concentrations than DNA, and given also the fact that RNA viruses as well as retroviruses store their genetic information in form of RNA it is not excluded that abasic RNA plays a significant biological role. Literature about the chemistry and chemical biology of RNA abasic sites is, however, scarce and their biological impact is largely unexplored.



This work reports on the synthesis of a natural and a modified RNA abasic site precursor and a natural DNA abasic precursor. After the incorporation in oligonucleotides the synthesized building blocks are shown to transform easily to abasic sites upon irradiation with long-wave UV light. The chemical stabilities of the synthesized abasic sites in alkaline and slightly acidic aqueous solutions were compared. In both cases the abasic RNA was found to be more stable than its DNA analogue.

To evaluate a possible biological role of RNA abasic sites the translesion-synthesis activity of different reverse transcriptases on a RNA template–DNA primer system with an abasic site in the template was studied. HIV-1 reverse transcriptase, an error prone enzyme, and AMV RT to a minor extent showed translesion synthesis in standing and running start experiments with abasic RNA templates. Kinetic studies for HIV-1 RT showed that the incorporation of dATP opposite the abasic lesion is favored over dGTP and the pyrimidine triphosphates. The so called “A-rule” for DNA is also shown to be true for abasic RNA.

1 Introduction

1.1 Historical Background^[1,2]

The discovery of the nucleic acids dates back more than one century and is mainly due to the Swiss physiologist *Friedrich Miescher*,^[3] who isolated in 1869 a phosphorous containing compound from pus cells which he obtained from surgical bandages discarded from the local hospital.^[4] What he called “nuclein” was in reality a nucleoprotein. *Richard Altman* in 1889 then obtained the first protein-free material and coined the name nucleic acid. After the identification of the four nucleobases it was *Phoebus Levene* in 1930 who identified the sugar component of DNA to be 2'-deoxyribose.^[5,6] He also showed that the components were linked in the order phosphate-sugar-base. He called each of these units a nucleotide, and stated that the DNA molecule consisted of a string of nucleotide units linked together through the phosphate groups, which are the 'backbone' of the molecule.^[7] After *George Beadle* and *Edward Tatum* showed that enzyme synthesis was controlled by genes and that there is one gene for each enzyme,^[8] it was *Oswald Avery* in 1944 who published first results demonstrating that DNA was the genetic material.^[9] *Edwin Chargaff* proposed in 1951 the rule that in natural DNA the number of guanine units equals the number of cytosine units and the number of adenine units equals the number of thymine units (Chargaff's rule).^[10] *Maurice Wilkins* and *Rosalind Franklin* in 1950 showed by X-ray that the long, thin DNA molecule in the sample from the Swiss scientist *Rudolf Signer* had a regular, crystal-like structure. These pictures sparked the interest of *Francis Crick* and *James Watson* in DNA. Putting all the pieces of the puzzle together, they published their model in 1953 describing the double-helical structure of DNA.^[11] Articles by Maurice Wilkins^[12] and Rosalind Franklin^[13] illuminating their X-ray diffraction data published in the same time supported the Crick and Watson model for the B-form of DNA. The 1962 Nobel Prize for Physiology or Medicine was subsequently jointly awarded to Francis Crick, James Watson, and Maurice Wilkins.

[1] Macgregor, R. B., Poon, G. M. K., *Comput. Biol. Chem.* **2003**, 27, 461-467.

[2] Klug, A., *J. Mol. Biol.* **2003**, 335, 3-26.

[3] Dahm, R., *Dev. Biol.* **2005**, 278, 274-288.

[4] Miescher, F., *Hoppe-Seyler's Med. Chem. Unters.* **1871**, 4, 441-460.

[5] Levene, P. A., Jacobs, W. A., *Ber.* **1909**, 42, 2102-2106.

[6] Levene, P. A., Jacobs, W. A., *Ber.* **1909**, 42, 3247-3251.

[7] Levene, P. A., Mikeska, L. A., Mori, T., *J. Biol. Chem.* **1930**, 85, 785-787.

[8] Beadle, G. W., Tatum, E. L., *Proc. Natl. Acad. Sci. U. S. A.* **1941**, 27, 499-506.

[9] Avery, O. T., MacLeod, C. M., McCarty, M., *J. Exp. Med.* **1944**, 79, 137-158.

[10] Chargaff, E., *Fed. Proc.* **1951**, 10, 654-659.

[11] Watson, J. D., Crick, F. H., *Nature* **1953**, 171, 737-738.

[12] Wilkins, M. H. F., Stokes, A. R., Wilson, H. R., *Nature* **1953**, 171, 738-740.

[13] Franklin, S. E., Gosling, R. G., *Nature* **1953**, 171, 740-741.

1.2 Nucleic Acid Structure

1.2.1 Primary structure of nucleic acids

Deoxyribonucleic acid (DNA) as well as ribonucleic acid (RNA) is each built from four different nucleobases: the purines adenine and guanine, and the pyrimidines cytosine and thymine (uracil for RNA). The backbone consists of (deoxy)ribose units that are linked with 3'-5' phosphodiester bonds.

These bases pair according to *Watson and Crick* as depicted in Figure 1.1. An A-T(U) base pair is stabilized by two hydrogen bonds. The purine base as well as the pyrimidine base acts as donor and acceptor of the hydrogen bonds. The more stable base pair G-C is stabilized by three hydrogen bonds, where G is a donor of two and acceptor of one hydrogen bond.

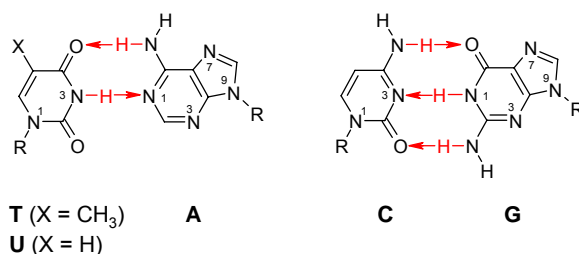


Figure 1.1 Watson-Crick base-pairs of DNA and RNA. R = ribose

The sugar moiety in the backbone can in principle have two different “puckering” modes: C^{2'}-endo and C^{3'}-endo. This puckering describes the major displacement of the 2' or the 3' carbon with respect to the C^{4'}-O^{4'}-C^{1'} plane: if the C^{2'}-endo displacement is bigger than the C^{3'}-exo displacement the conformation is named C^{2'}-endo.

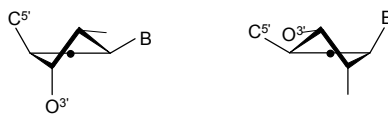


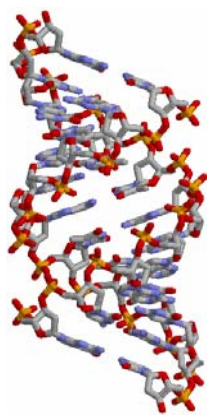
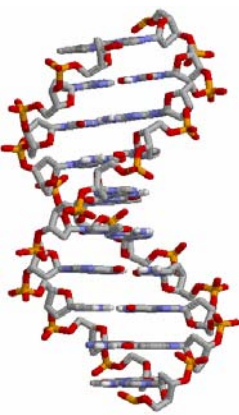
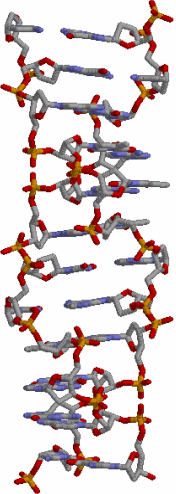
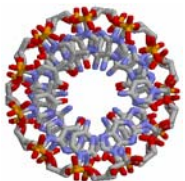
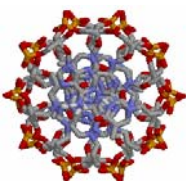
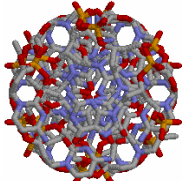
Figure 1.2 Sugar puckering modes of DNA

The base linkage occurs also in two conformations. The plane of the base is virtually perpendicular to the plane of O^{4'}-C^{1'}-C^{2'} of the sugar. This gives rise to two different conformations: *anti* and *syn*. The *anti* conformer has the smaller H-6 (pyrimidines) or H-8 (purines) atom above the sugar ring. The *syn* conformers have the large O-2 (pyrimidines) or N-3 (purines) in that position. In general pyrimidines and purines are found to occupy a narrow or wider range of *anti* conformations.

1.2.2 DNA secondary structure

Double stranded DNA exists in a wide variety of conformations, although these can be classified in two different families: A and B. The difference between these families are the sugar pucker C^3' -*endo* for A-DNA and C^2' -*endo* for B-DNA.

Table 1.1 Structural properties of different types of DNA double helices

	A-DNA	B-DNA	Z-DNA
Double helical structure			
End-on view			
Handedness	Right	Right	Left
Average base pairs per turn	11	10	12
Rise per base pair [Å]	2.9	3.3-3.4	3.7
Base tilt	20 °	-6 °	-7 °
Diameter of the helix [Å]	25.5	23.7	18.4
Sugar pucker	C^3' - <i>endo</i>	C^2' - <i>endo</i>	C^2' - <i>endo</i> (C) C^3' - <i>endo</i> (G)
Major groove: width/depth [Å]	2.7/13.5	11.7/8.8	8.8/3.7
Minor groove: width/depth [Å]	11.0/2.8	5.7/7.5	2.0/13.8

Color scheme for the graphics: grey (C), red (O), blue (N), orange (P); non-hydrogen bonding hydrogen atoms are not shown

A-DNA consists of antiparallel, right-handed double helices, where the sugar rings are parallel to the helix axis and the phosphate backbone is on the outside of the cylinder. The bases are tilted sideways by 20° relative to the helix axis. The double helix moreover forms a hollow core. Glycosidic bonds are in the *anti* conformation. The major groove is very deep and the minor groove extremely shallow.

In **B-DNA** the base-pairs sit directly on the helix axis. This results in similar depths of the minor and the major groove. The bases are perpendicular to the helix axis and predominantly intrastrand stacked. All glycosidic bonds are in the *anti* conformation.

In GC-rich double strand regions another conformation, the **Z-DNA** can be observed. This conformation is also an antiparallel duplex but with the two backbone strands running downward at the left of the major groove and upward at the right. This is the opposite of A- and B-DNA. Cytosines take the *anti* conformation and the guanines the *syn* conformation (zig-zag). The switch from B to Z-DNA appears to be driven by the energetics of base stacking. This Z-conformation is stabilized by high salt concentrations.

1.2.3 RNA secondary structure

In 1953 *Watson* and *Crick* suggested that it was unlikely that RNA could form a double helical structure because the added O2' of the ribose would produce prohibitive van der Waals crowding.^[14] It was in 1956 when *Rich* and *Davies* found that mixing polyuridylic acid (poly(U)) and polyadenylic acid (poly (A)) would form a double helix.^[15] Moreover it was discovered that the sugar puckering mode was exclusively C^{3'}-*endo*, similar to A-DNA.

RNA double helices display two major, structurally similar conformations: **A-RNA** and **A'-RNA**. The conformation depends on the salt concentration of the environment. At low ionic strength the A-RNA double helix predominates which at high salt concentration (> 20 %) is transformed to A'-RNA double helix. Both conformations form a right-handed helix from two antiparallel strands. The most striking difference between the A- and the A'-form is the big difference in the width of the major groove. The major groove of nucleic acids has the potential to interact with proteins. As well as many transcriptional regulatory proteins, several proteins or peptides bind to the major groove of the double helical regions of their target RNAs.^[16,17] The major groove of the A-RNA conformation is too narrow to accommodate a protein. It was in fact observed that binding proteins increased the major groove widths of target RNAs upon binding.^[18] The conclusion is that the A'-RNA conformation, which has a wide major groove, must be taken into consideration for RNA-protein interactions.

[14] Watson, J. D., Crick, F. H. C., *Nature* **1953**, *171*, 737-738.

[15] Rich, A., Davies, D. R., *J. Am. Chem. Soc.* **1956**, *78*, 3548-3549.

[16] Puglisi, J. D., Chen, L., Blanchard, S., Frankel, A. D., *Science* **1995**, *270*, 1200-1203.

[17] Battiste, J. L., Mao, H., Rao, N. S., Tan, R., Muhandiram, D. R., Kay, L. E., Frankel, A. D., Williamson, J. R., *Science* **1996**, *273*, 1547-1551.

[18] Correll, C. C., Freeborn, B., Moore, P. B., Steitz, T. A., *Cell* **1997**, *91*, 705-712.

Table 1.2 Structural properties of the RNA double helices

	A-RNA	A'-RNA
Double helical structure		
End-on view		
Handedness	Right	Right
Average base pairs per turn ^[19]	11	12
Rise per base pair [Å]	2.8	3.0
Base tilt	16-19 °	10 °
Sugar pucker	C ^{3'} -endo	C ^{2'} -endo
Major groove: width/depth [Å]	3.8/very deep	8.0/very deep
Minor groove: width/depth [Å]	10.9/rather shallow	10.8/rather shallow

Color scheme for the graphics: red (bases), black (sugar phosphate backbone), grey (hydrogen bonds); Parts closer to the viewer are indicated in heavier lines^[20]

After the discovery of the left-handed Z-DNA, poly(CG) was reported to form a **Z-RNA** structure in 1984.^[21,22]

[20] Saenger, W., *Principles of Nucleic Acid Structure*, Springer-Verlag, New York, **1984**.

[21] Hall, K., Cruz, P., Tinoco, I., Jr., Jovin, T. M., Van de Sande, J. H., *Nature* **1984**, *311*, 584-586.

[22] Adamiak, R. W., Galat, A., Skalski, B., *Biochim. Biophys. Acta* **1985**, *825*, 345-352.

Just recently the detailed structure could be disclosed.^[23] The left-handed RNA prevails at much higher salt concentration than that noted for $d(CG)_n$ Z-form duplexes.^[24] Today it is a common opinion that B-form RNA does not exist.

1.2.4 From genes to proteins^[25]

Despite the similar structure, DNA and RNA are involved in different tasks in a cell. DNA stores the genetic information of the organism whereas RNA is involved in the synthesis of proteins.

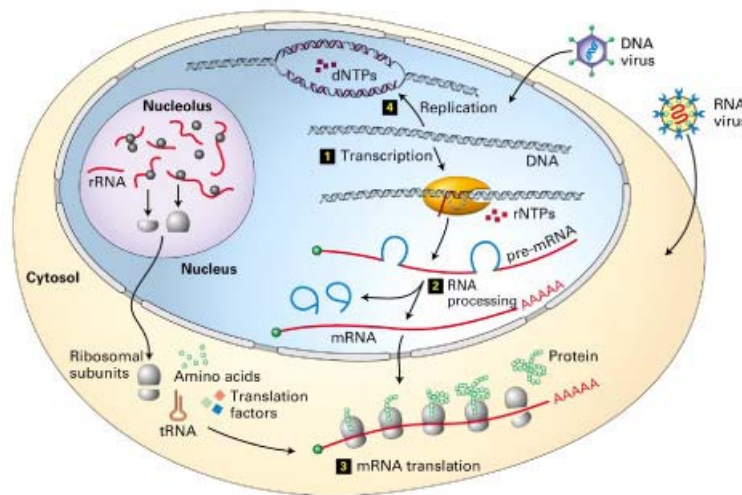


Figure 1.3 Major nucleic acid processes in a cell: transcription (1), RNA processing (2), translation (3) and DNA replication (4)^[26]

Transcription. In the nucleus, the nucleotide sequence of the archival copy of DNA is transcribed to RNA. In the first step in expression of a gene as a polynucleotide chain, an mRNA working copy of the gene is made by RNA polymerase. The polymerase binds to DNA and processes along it, transcribing the gene in a continuous process to produce mRNA, and finally dissociates from the DNA. Every RNA molecule in a cell is synthesized according to the same mechanism. The synthesized nascent mRNA is called pre-mRNA since it contains not only protein coding information (exons) but also non-coding information (introns) which have to be removed prior to protein synthesis.

RNA processing. Eukaryotic mRNA transcripts are extensively modified before transport to the cytosol. At the 5'-end, a structure called cap is introduced: the 5'-triphosphate is hydrolysed to a diphosphate and guanosine 5'-phosphate is transferred from GTP to the 5'-end to give a 5'-5' triphosphosphate linkage. At the 3'-end of the mRNA, a poly A tail of up to 200 residues is added by poly A polymerase. Both the cap

[23] Popenda, M., Milecki, J., Adamiak, R. W., *Nucleic Acids Res.* **2004**, 32, 4044-4054.

[24] Pohl, F. M., Jovin, T. M., *J. Mol. Biol.* **1972**, 67, 375-396.

[25] Knippers, R., *Molekulare Genetik*, 7th ed., Georg Thieme Verlag, Stuttgart, **1997**.

[26] <http://newark.rutgers.edu/~babis/research/cell.jpg>.

and the poly A appear to be important for the stability of the mRNA and for following translation. It may also be necessary for the transport.

Introns, which all begin with the sequence GU and end with AG, are removed by a process called splicing. This can be regarded as a double transesterification reaction. In a first step, the 2'-hydroxyl group of an A-residue within a PyPyPuAPy motive in the intron attacks the phosphodiester bond located at the 5'-exon-intron junction. In a second step the now free 3'-hydroxyl group of the 5'-exon attacks the phosphodiester bond located at the 3'-exon-intron junction. The mature mRNA is then transported to the cytosol.

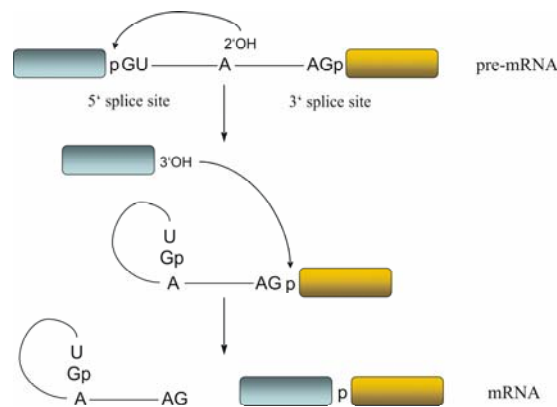


Figure 1.4 The two transesterification reactions of pre-mRNA splicing. In a first step, the 2'-hydroxyl group of an A-residue attacks the phosphodiester bond located at the 5'-exon-intron junction. In a second step the now free 3'-hydroxyl group of the 5'-exon (blue) attacks the phosphodiester bond located at the 3'-exon-intron junction

Translation. The synthesis of proteins takes place in the cytosol. The elongation starts with the formation of the initiation complex. This complex consists of the ribosome, the mRNA and fMet-tRNA. After initiation of the elongation at the AUG start codon, the elongation complex moves in the direction from the 5'-end to the 3'-end along the mRNA. In the A-site of the ribosome the respective tRNA loaded with an amino acid that fits the codon on the mRNA is recognized. In the P-side the amino acid is added to the peptide chain and the unloaded tRNA is liberated.

DNA replication. For cell division a second copy of the DNA molecule is synthesized to pass on the genetic information. To do this, the parental double-strand is unwound by the means of helicases and the single strands are both completed by DNA polymerases. This process is semi-conservative since both resulting double stranded DNA molecules have one parental strand each.

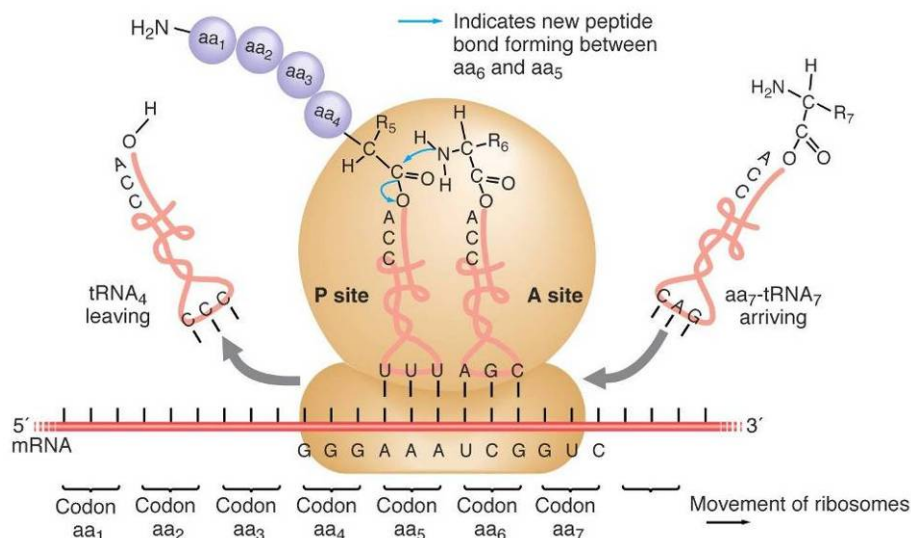


Figure 1.5 Schematic view of the elongation complex [27]

1.2.5 RNA species

In contrast to DNA, RNA occurs mostly as a single polynucleotide chain. By the virtue of the inherent ability of RNA to make up different conformations, many RNAs exist in elaborate, defined structures possibly as distinct as those of proteins. RNA molecules usually contain different structural elements such as short double-helical regions, internal loops, hairpin loops and bulges. RNA structure is much more diverse than DNA structure. In cells three major classes of RNAs have so far been identified: messenger RNA (mRNA), transfer RNA (tRNA) and ribosomal RNA (rRNA). Approximately, 80-85 % of the total RNA is present as rRNA, 10-15 percent is tRNA and only up to 5 % is mRNA. Moreover there is the non-coding RNA that reveals some important properties with regard to regulation processes and furthermore RNA can act as the genome in retroviruses.

1.2.5.1 Transfer RNA

Most cells contain 60-70 different tRNAs which range from 74-95 nucleotides in length. All tRNAs have a characteristic cloverleaf secondary structure. A comparison of the different structures shows some similarities:

- The 5'- and the 3'-end form a seven base-pair stem. The 3'-end forms a four base overhang that ends with the characteristic CCA structure. This overhang is called the acceptor arm.
- The anticodon for which the tRNA is carrying the according amino acid lies in the center of a 7 nucleotide loop.

[27] http://www.mun.ca/biology/scarr/4241F2_ribosome.jpg.

- The left arm, the D-arm, contains dihydrouridine and consists of a stem of variable length.
- The right arm, the T-arm, has a five base-pair stem and a seven nucleotide loop. The arm always contains the characteristic thymidine, pseudouridine, cytosine (TΨC) sequence.
- In-between the anticodon arm and the T-arm lays a variable V-loop.

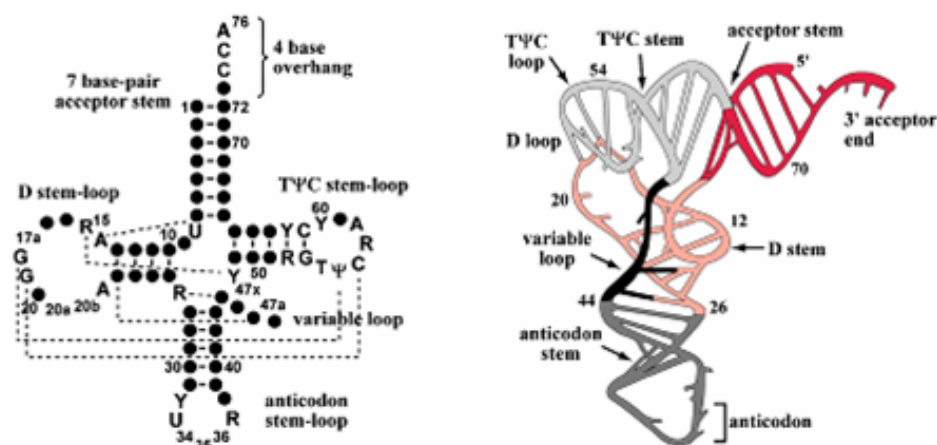


Figure 1.6 Cloverleaf structure of tRNA (left) and the three-dimensional structure^[28]

Around 10 % of the nucleosides in tRNAs are modified. Around one half of the over 95 natural occurring modified RNA nucleosides show up in the different tRNAs.^[29,30] Most of the modified bases occur around the anticodon. The function of transfer RNAs is essentially the delivery of a specific amino acid to the transcribing ribosome.

1.2.5.2 Ribosomal RNA

Ribosomes from bacteria consist of a large and a small subunit that sediment with 50S and 30S, respectively, whereas the complete ribosome sediments with 70S. The large subunit consists of rRNA and proteins. The large subunit is built from a 23S rRNA (2904 nucleotides), a 5S rRNA(120 nucleotides) and the ribosomal proteins L1 to L36. The small subunit consists of a 16S rRNA (1542 nucleotides) and the ribosomal proteins S1 to S21.

Eukaryotic ribosomes are built very similarly. The 80S ribosome divides in a 60S (20S, 5.85S, 5S rRNA and 49 proteins) and a 40S (18S rRNA and 33 proteins) subunit.

Ribosomal RNA is synthesized in the nucleolus and the subunits of the ribosomes are then transported to the cytosol where translation takes place. rRNA molecules are

-
- [28] Blackburn, G. M., Gait, M. J., *Nucleic Acids in Chemistry and Biology*, 2nd ed., Oxford University Press Inc., New York, **1996**.
 [29] Limbach, P. A., Crain, P. F., McCloskey, J. A., *Nucleic Acids Res.* **1994**, 22, 2183-2196.
 [30] Rozenski, J., Crain, P. F., McCloskey, J. A., *Nucleic Acids Res.* **1999**, 27, 196-197.

extremely abundant: they make up at least 80% of the RNA molecules found in a typical eukaryotic cell.

1.2.5.3 Messenger RNA

Compared to tRNA and rRNA messenger RNA makes up the smallest part of RNA in a cell. Typical mRNA has a length from 100 to over 10'000 nucleotides. Messenger RNA is continuously synthesized, utilized and degraded which makes it subject to continual turnover. The half-life time of typical bacterial mRNA is about 2 minutes whereas the other RNA species have a much longer lifetime. Being the transcript of DNA, mRNA contains all the information for the synthesis of proteins. While still in the nucleus mRNA is considered to be immature because it includes not only coding exons but also non-coding introns. The splicing process removes noncoding regions and prepares mRNA for translation.

1.2.5.4 Noncoding RNA

Noncoding RNA (ncRNA) is not directly involved in protein synthesis. Instead it is involved in many other cell processes including the regulation of transcription, DNA replication and RNA processing and modification.

Although only 1.2 % of the human genome encodes protein, a large fraction of it is transcribed. Indeed, ~ 98 % of the transcriptional output in humans and other mammals consists of non-protein-coding RNAs from the introns of protein-coding genes and the exons and introns of non-protein-coding genes, including many that are antisense to or overlapping protein-coding genes.^[31] The size of noncoding RNAs can be anywhere from 21 ribonucleotides to as much as 10'000 or more ribonucleotides in length. In bacteria ncRNA is sometimes referred to as small RNA (sRNA). Some examples of ncRNA are:

- *Xist RNA* inactivates one of the two X chromosomes in females.^[32]
- *snRNA* (small nuclear RNA) is involved with the processing of larger precursor RNA molecules. They are always associated with specific proteins, and the complexes are referred to as small nuclear ribonucleoproteins (snRNP) or sometimes as snurps.^[33]
- *snoRNA* (small nucleolar RNA) is involved in making ribosomes and telomeres. They guide the chemical modification of rRNA.^[34]
- *miRNA* (micro RNA, single stranded), 21-23 nucleotides in length, is involved in the regulation of the expression of mRNA.

[31] Mattick, J. S., Makunin, I. V., *Hum. Mol. Genet.* **2005**, *14*, R121-R132.

[32] Plath, K., Mlynarczyk-Evans, S., Nusinow, D. A., Panning, B., *Annu. Rev. Genet.* **2002**, *36*, 233-278.

[33] Valadkhan, S., *Curr. Opin. Chem. Biol.* **2005**, *9*, 603-608.

[34] Bachellerie Jean, P., Cavaille, J., Huttenhofer, A., *Biochimie* **2002**, *84*, 775-790.

- *siRNA* (small interfering RNA, double stranded) is usually 21 nucleotides in length with 2-nucleotides 3'-overhangs on either end, binds to complementary RNA sequences targeting them for destruction via the RNA interference (RNAi) pathway^[35]

Unlike siRNAs, miRNAs are single stranded and pair with target mRNAs that contain sequences only partially complementary to the miRNA and repress mRNA translation without degrading the mRNA.^[36]

Another class of RNA known in cells is the ribonucleic acid enzymes. Ribozymes are RNA molecules with catalytic activity that were discovered in the early 1980s.^[37] In the recent years a number of ribozymes and their functions were disclosed, the hammerhead ribozyme and the hairpin ribozyme being the most widely known.^[38]

1.2.5.5 Genomic RNA

RNA is not only involved in protein synthesis and regulation of cell processes but in the case of retroviruses it can also contain the genomic information.

The retroviral particle infects cells by binding to a cell surface receptor. The specificity of the virus-cell interaction is determined largely by the envelope proteins of the retrovirus. Infection leads to injection of the virus nucleoprotein core, consisting of proteins, full-length genomic RNA, and the reverse transcriptase protein. Once inside the cell the reverse transcriptase initiates creation of a double-stranded DNA copy of the genome of the virus for integration into the host cell chromosome. Upon completion of reverse transcription, the double-strand viral DNA is moved into the nucleus and integrated into the host DNA. Integration is specific with respect to the viral sequences involved and non-specific to the host sequences. The site of integration in the host genome influences the expression of the integrated provirus. The viral DNA of some complex retroviruses, such as HIV-1, can transit the nuclear membrane. The viral DNA of some simple retroviruses, including MLV, does not transit the nuclear membrane and these viruses cannot infect non-dividing cells. The virus is now prepared to initiate a new round of replication. Once embedded in the host genome, the provirus behaves like a cellular gene. The provirus is transcribed by the host's DNA-dependent RNA polymerase. Translation of the viral mRNA in the cytosol leads to viral enzymes and structural proteins. After the final assembly of the virus budding takes place and a new generation of viruses can infect other cells.

[35] Elbashir, S. M., Lendeckel, W., Tuschl, T., *Genes Dev.* **2001**, *15*, 188-200.

[36] Ambros, V., Bartel, B., Bartel, D. P., Burge, C. B., Carrington, J. C., Chen, X., Dreyfuss, G., Eddy, S. R., Griffiths-Jones, S., Marshall, M., Matzke, M., Ruvkun, G., Tuschl, T., *RNA* **2003**, *9*, 277-279.

[37] Kruger, K., Grabowski, P. J., Zaug, A. J., Sands, J., Gottschling, D. E., Cech, T. R., *Cell* **1982**, *31*, 147-157.

[38] Carola, C., Eckstein, F., *Curr. Opin. Chem. Biol.* **1999**, *3*, 274-283.

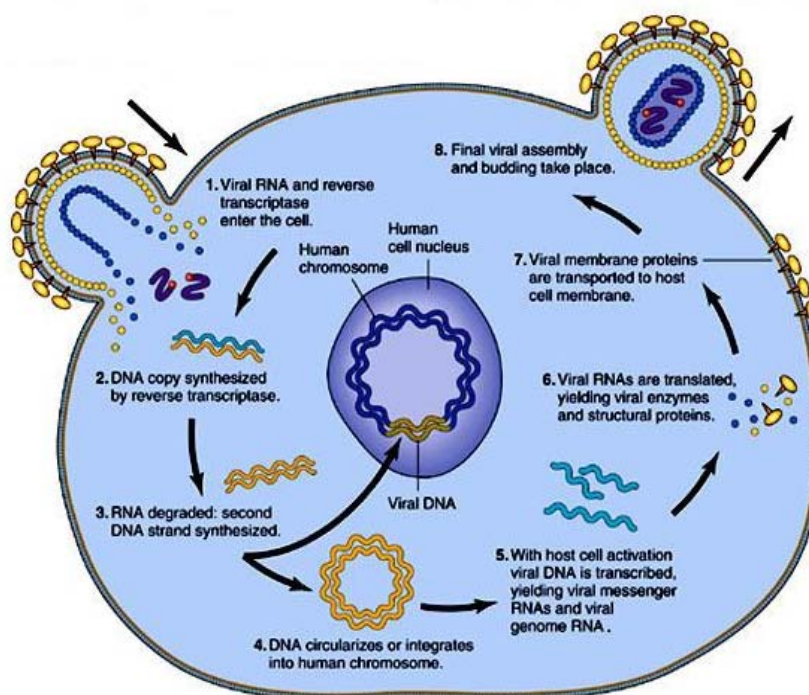


Figure 1.7 Life cycle of the HIV-1 retrovirus^[39]

[39] Byer, C. O., Shainberg, L. W., Galliano, G., Shriver, S. P., Shriver, P., *Dimensions In Human Sexuality*, 5 ed., The McGraw-Hill Companies, 1999.

1.3 Abasic Sites

In general an abasic site is a sugar moiety in a nucleic acid strand where the base was removed by hydrolysis. Abasic sites can be produced by chemical and biological impact but are also natural lesions that occur spontaneously via depurination at a frequency of ca. 10^7 per genome per day in mammalian cells.^[40] Abasic sites are the most common DNA lesions. An important feature is that the depurination rate in DNA single strands is four-fold greater than in double-stranded DNA.^[41]

1.3.1 Abasic site structure

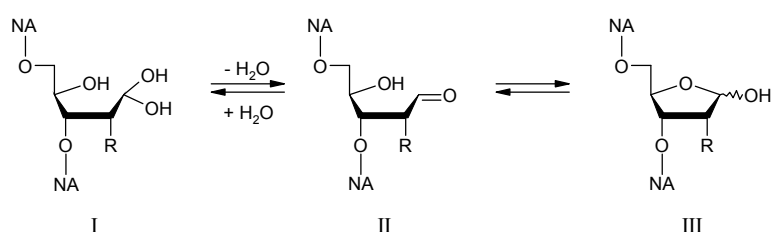


Figure 1.8 Isomers of abasic sites: hydrate form (I), aldehydic form (II) and the hemiacetal form (III); R = H (DNA) or OH (RNA)

The structure of DNA abasic sites has been characterized by ^{13}C -NMR spectroscopy.^[42] From this study it follows that an abasic site occurs in principal in three different forms: the hydrate form (I), the aldehydic form (II) and the hemiacetal form (III). Further investigation by ^{17}O -NMR studies show that not all three forms are present in equal amounts.^[43] It follows that the aldehydic form of the abasic site only represents 1% of the total amount. Furthermore the two anomers of the predominant hemiacetal form are present in a 1:1 ratio. Proof of the occurrence of the hydrate form could not be given from the NMR data. Although up to now no structural studies on RNA abasic sites have been performed it is assumed that the hemiacetal form is also the predominant form in abasic site containing oligoribonucleotides.

1.3.2 Acidic hydrolysis of *N*-glycosidic bonds in nucleosides^[44,45]

In general, abasic sites result from hydrolytic cleavage of the *N*-glycosidic bond. This process is increased by any factor or chemical modification that develops a positive

[40] Lindahl, T., Nyberg, B., *Biochemistry* **1972**, *11*, 3610-3618.

[41] Lindahl, T., Andersson, A., *Biochemistry* **1972**, *11*, 3618-3623.

[42] Manoharan, M., Ransom, S. C., Mazumder, A., Gerlt, J. A., Wilde, J. A., Withka, J. A., Bolton, P. H., *J. Am. Chem. Soc.* **1988**, *110*, 1620-1622.

[43] Wilde, J. A., Bolton, P. H., Mazumder, A., Manoharan, M., Gerlt, J. A., *J. Am. Chem. Soc.* **1989**, *111*, 1894-1896.

[44] Kochetkov, N. K., Budovskii, E. I., in *Organic Chemistry of Nucleic Acids* (Eds.: N. K. Kochetkov, E. I. Budovskii), Plenum, New York, **1972**, pp. 425-448.

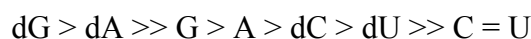
[45] Zielonacka-Lis, E., *Nucleosides Nucleotides* **1989**, *8*, 383-405.

charge on the nucleic base and thus destabilizes the glycosidic bond. Therefore glycoside bond cleavage is highly pH dependent. Aqueous solutions of a variety of strong inorganic acids (HCl, HBr, H₂SO₄ and HClO₄) and organic acids (trichloroacetic acid, acetic acid and formic acid) have been used for hydrolysis reactions. In 1964 Venner reported the first study on the stability of nucleosides at low pH (Table 1.3).^[46]

Table 1.3 Kinetic parameters of acid hydrolysis of nucleosides at pH 1, 37 °C

Nucleoside	k ₁ [sec ⁻¹]
2'-Deoxyadenosine	4.3 · 10 ⁻⁴
2'-Deoxyguanosine	8.3 · 10 ⁻⁴
2'-Deoxycytidine	1.1 · 10 ⁻⁷
2'-Deoxyuridine	< 10 ⁻⁷
Adenosine	3.6 · 10 ⁻⁷
Guanosine	9.36 · 10 ⁻⁷
Cytidine	< 10 ⁻⁹
Uridine	< 10 ⁻⁹

From this work it results that 2'-deoxyribosyl derivatives are hydrolysed 100-1000 times faster than the corresponding ribosyl derivatives. Furthermore, within the two groups the purine nucleosides hydrolyse faster than pyrimidine derivatives:



The mechanism of the hydrolysis reaction introduced by Zoltewicz and Shapiro is shown in Figure 1.9 for purine nucleosides and in Figure 1.10 for pyrimidine nucleosides.^[47,48]

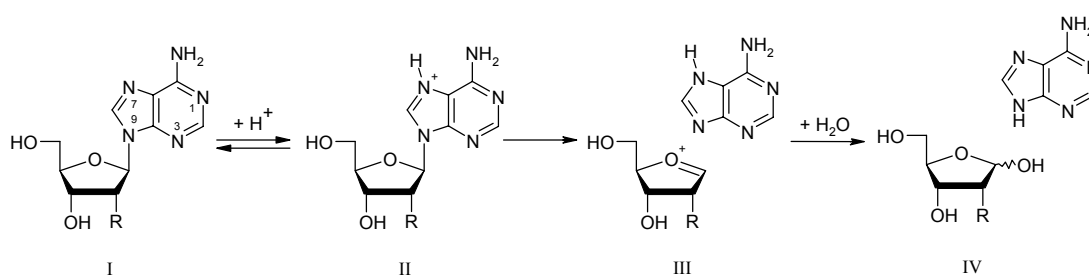


Figure 1.9 Mechanism of the hydrolysis of the N-glycosidic bond of purine nucleosides R = H or OH, respectively

[46] Venner, H., *H.-S. Z. Physiol. Chem.* **1964**, 339, 14-27.

[47] Zoltewicz, J. A., Clark, D. F., Sharpless, T. W., Grahe, G., *J. Am. Chem. Soc.* **1970**, 92, 1741-1750.

[48] Shapiro, R., Danzig, M., *Biochemistry* **1972**, 11, 23-29.

The first stage of the mechanisms now generally accepted, is a protonation of the base of the nucleoside, followed by the formation of a (deoxy)-ribofuranosyl oxocarbenium ion and the free base. *Shapiro* found that the four common naturally occurring deoxyribonucleosides require mono- or diprotonation of the base prior to hydrolysis, whereas the neutral form of deoxyuridine can cleave. The differences of the rate of hydrolysis of deoxynucleosides and ribonucleosides are due to the negative inductive effect of the C2' hydroxyl group in the ribonucleoside derivatives. This hypothesis is underlined by the findings that more electronegative ribose substituents such as tosyl^[49] and 2,4-dinitrobenzoyl groups^[50] lower the rate of hydrolysis of the *N*-glycosidic bond, whereas 2',3'-dideoxynucleosides show even faster rates of hydrolysis than the corresponding 2'-deoxynucleosides. The negative inductive effect of the 2'-hydroxy group therefore hinders the formation of the cyclic ribofuranosyl oxocarbenium ion by its destabilization.

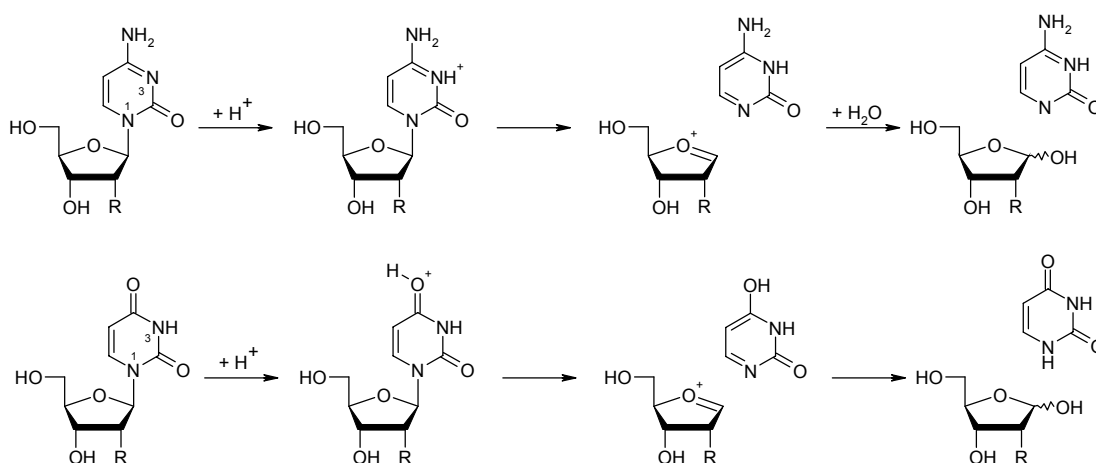


Figure 1.10 Proposed mechanism for the hydrolysis of cytidine and thymine nucleosides

The fact that purine nucleosides are easier hydrolysed than the pyrimidine nucleosides is usually explained by the fact, that purines have a greater ability to stabilize the positive charge induced by protonation.

Other mechanisms, where the oxygen of the furanose moiety is protonated and a quaternary Schiff's base type intermediate is formed, are abandoned nowadays. It has been shown in a wide variety of studies that in general any substitution of the ring of the natural nucleobases leads to a labilization of the *N*-glycosidic bond.^[44] Stabilization on the other side is enhanced when phosphate groups are present at the 5'-hydroxy group and the ribose is substituted with electronegative substituents.

[49] Brown, D. M., Fasman, G. D., Magrath, D. I., Todd, A. R., *J. Chem. Soc., Chem. Commun.* **1954**, 46-52, 1448-1455.

[50] Wempen, I., Doerr, I. L., Kaplan, L., Fox, J. J., *J. Am. Chem. Soc.* **1960**, 82, 1624-1629.

1.4 Formation of Site Specific DNA Abasic Sites

1.4.1 Synthesis of “true” DNA abasic sites^[51]

The known lability of substituted purine nucleosides under acidic conditions was first used by *Vasseur* to generate site specific abasic sites in oligodeoxypyrimidines. The abasic site was introduced by mild acidic treatment of a trimer of the structure TpA^{Bz}pT containing a *N*-benzoyladenine residue (Figure 1.11).^[52]

Another chemical method involves the carefully-controlled acidic hydrolysis of a deoxyadenosine residue that removes only an adenine base followed by stabilization of the resulting abasic site as the methoxyamine derivative.^[52-54] After purification, the abasic site can be generated by an exchange process using acetaldehyde. This method is limited to DNA oligomers having no dG residues and only a single dA group. There is also the risk of forming acetaldehyde adducts with amino groups in other DNA bases.

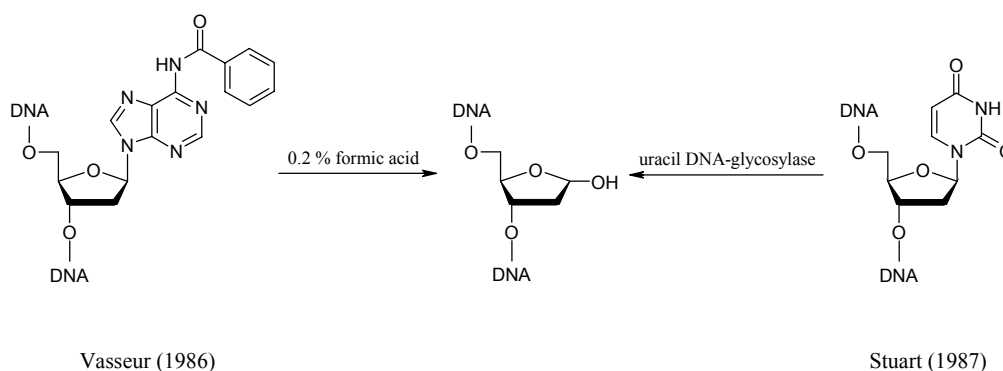


Figure 1.11 Abasic sites generated by acidic treatment (*Vasseur*) and enzymatically (*Stuart*)

Stuart used uracil-DNA glycosylase to efficiently prepare oligonucleotides containing a true abasic site at a predefined position.^[55] Uracil-DNA glycosylase removes uracil residues that are formed in DNA by deamination of cytosines. The use of this enzymatic method may though be compromised by certain elements of DNA structure such as the proximity of the strand termini, noncanonical structures (hairpins, Holliday junctions, etc.), and the presence of noncanonical moieties among bases, sugar or phosphate groups, or proteins bound to DNA.^[56]

[51] Lhomme, J., Constant, J.-F., Demeunynck, M., *Biopolymers* **2000**, *52*, 65-83.

[52] Vasseur, J. J., Rayner, B., Imbach, J. L., *Biochem. Biophys. Res. Commun.* **1986**, *134*, 1204-1208.

[53] Bertrand, J. R., Vasseur, J. J., Rayner, B., Imbach, J. L., Paoletti, J., Paoletti, C., Malvy, C., *Nucleic Acids Res.* **1989**, *17*, 10307-10319.

[54] Bailly, V., Verly, W. G., *Biochem. J.* **1987**, *242*, 565-572.

[55] Stuart, G. R., Chambers, R. W., *Nucleic Acids Res.* **1987**, *15*, 7451-7462.

[56] Kumar, N. V., Varshney, U., *Nucleic Acids Res.* **1994**, *22*, 3737-3741.

Natural abasic sites can also be generated by modified nucleotides that are in a first step incorporated into DNA oligomers via the standard phosphoramidite chemistry and subsequently deprotected in a second step. The α -1'-*O*-TBDMS-protected phosphoramidite from Groebke is deprotected in phosphate buffer pH 2 for 2 hours at room temperature after oligonucleotide synthesis.^[57] The 1'-*O*-nitrobenzyl-protected monomer of Péc'h is deprotected by long wave UV irradiation.^[58]

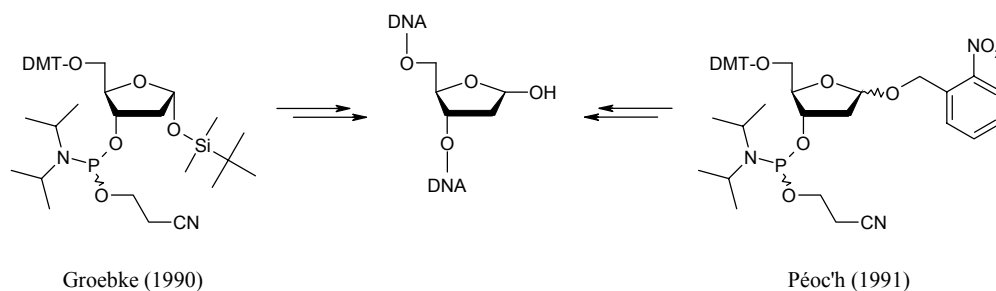


Figure 1.12 Phosphoramidites that can be incorporated into oligomers and converted to natural abasic sites

In 1990 Iocono reported on 2-pyrimidone-2'-deoxynucleosides that release an abasic site upon mild acidic treatment.^[59] In 1994 Laayoun presented a new route to prepare abasic oligonucleotides by hydrolysis of 8-propylthio substituted adenosine.^[60] The substituted adenine was oxidized with aqueous "oxone" for 1 hour and subsequent hydrolysis at 65 °C, pH 3 for 30 min gave the abasic oligonucleotide.

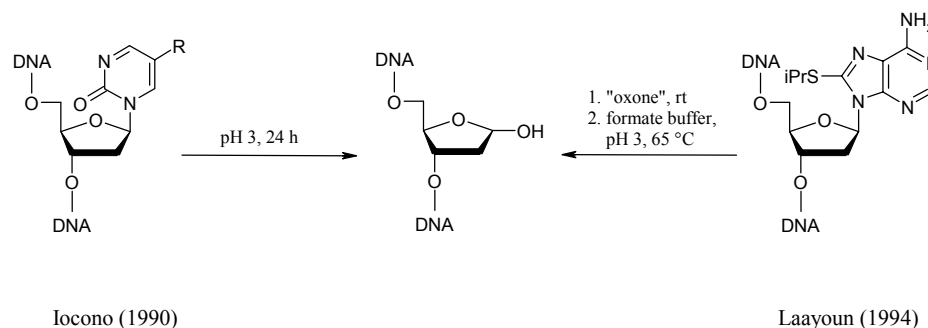


Figure 1.13 Abasic sites generated by Iocono ($R = H, Me$) and Laayoun

In 2000 Shishkina published another phosphoramidite building block that allows the postsynthetic generation of abasic sites in single-or double-stranded DNA oligomers.^[61] An appropriately protected 3-deoxyhexitol was synthesized and incorporated into DNA oligomers. The resulting stable diol-containing oligonucleotides were purified by HPLC

[57] Groebke, K., Leumann, C., *Helv. Chim. Acta* **1990**, *73*, 608-617.

[58] Péc'h, D., Meyer, A., Imbach, J. L., Rayner, B., *Tetrahedron Lett.* **1991**, *32*, 207-210.

[59] Iocono, J. A., Gildea, B., McLaughlin, L. W., *Tetrahedron Lett.* **1990**, *31*, 175-178.

[60] Laayoun, A., Decout, J.-L., Defrancq, E., Lhomme, J., *Tetrahedron Lett.* **1994**, *35*, 4991-4994.

[61] Shishkina, I. G., Johnson, F., *Chem. Res. Toxicol.* **2000**, *13*, 907-912.

and converted quantitatively into the corresponding abasic DNA sequences by mild periodate oxidation. This building block is commercially available since 2001.^[62]

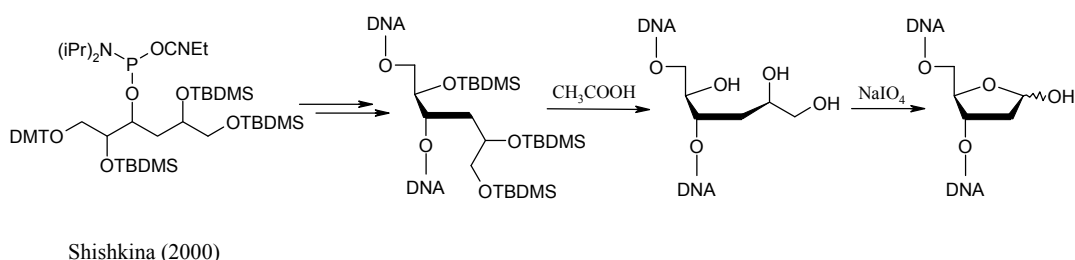


Figure 1.14 Commercially available phosphoramidite building block from Shishkina et al. and its transformation to a natural abasic site

In 2004 Kojima reported on a facile method to generate abasic sites at the 3'-end of oligonucleotides by acidic hydrolysis of a 1-deaza-2'-deoxyguanosine moiety.^[63]

In 1999 Coleman showed another concept of site-specific formation of abasic lesions in DNA.^[64] The approach is based on the formation of a covalent interstrand crosslink between an electrophilic antisense oligonucleotide probe and a deoxyguanosine residue in a native sequence of DNA. This affords a unique dG glycosidic bond with enhanced hydrolytic lability that can be cleaved by neutral and mild thermal hydrolysis to afford an oligonucleotide with a site-specifically incorporated abasic lesion.

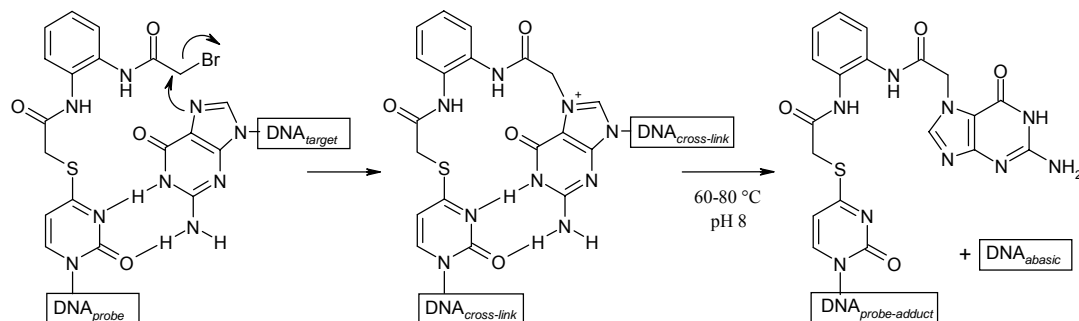


Figure 1.15 Side-specific abasic site formation by a covalent cross-link between an antisense oligonucleotide probe and a target DNA sequence followed by thermal depurination of the target

[62] in *Technical Bulletin Abasic Site*, Glen Research, Sterling, USA, **2001**.

[63] Kojima, N., Sugino, M., Mikami, A., Ohtsuka, E., Komatsu, Y., *Org. Lett.* **2005**, 7, 709-712.

[64] Coleman, R. S., Pires, R. M., *Nucleosides Nucleotides* **1999**, 18, 2141-2146.

1.4.2 Unnatural and minor DNA abasic site analogues

Up to now several chemically stable DNA abasic site analogues have been synthesized, mimicking both, the cyclic and the open chain forms of the deoxyribose unit. *Millican* described the synthesis of the tetrahydrofuran analogous 1,2-dideoxy-D-ribofuranose and its incorporation in oligonucleotides.^[65]

Pochet and coworkers introduced the cyano-1-deoxy-2-D-ribose unit and *Raap* presented the methyl-2'-deoxy- α -D-ribofuranoside shortly after.^[66,67] *Kotera* generated a 2'-deoxyribonolactone unit in oligonucleotides.^[68] This lesion is of major interest since it has been reported to be mutagenic,^[69,70] to be resistant to repair nucleases,^[71] to inhibit transcription^[72] and to lead to DNA strand scission by β - and δ -elimination.^[73] Furthermore it was reported just recently that it disobeys the "A-rule".^[74,75] *Thomas* synthesized in 1999 a carbocyclic abasic site analogue.^[76] *Takeshita* synthesized three open chain abasic site analogues: propandiol, ethylene glycol and the deoxyribitol.^[77] In 2004 *Kim* applied a synthetic route very similar to that published by *Shishkina*, where cleavage with periodate reveals the abasic site, to introduce the 2'-oxidized abasic site.^[61,78] In the same year *Chen* reported on a 1'-oxidized abasic site analogue.^[79]

Very recently *Mosimann* disclosed a stable DNA abasic site analogue.^[80] Due to the replacement of the 3'-oxygen by a methylene group the abasic site can not undergo β - and δ -elimination under basic conditions.

-
- [65] Millican, T. A., Mock, G. A., Chauncey, M. A., Patel, T. P., Eaton, M. A. W., Gunning, J., Cutbush, S. D., Neidle, S., Mann, J., *Nucleic Acids Res.* **1984**, *12*, 7435-7453.
- [66] Pochet, S., Huynh-Dinh, T., Neumann, J. M., Tran-Dinh, S., Taboury, J. A., Taillandier, E., Igolen, J., *Tetrahedron Lett.* **1985**, *26*, 2085-2088.
- [67] Raap, J., Dreef, C. E., Van der Marel, G. A., Van Boom, J. H., Hilbers, C. W., *J. Biomol. Struct. Dyn.* **1987**, *5*, 219-247.
- [68] Kotera, M., Bourdat, A.-G., Defrancq, E., Lhomme, J., *J. Am. Chem. Soc.* **1998**, *120*, 11810-11811.
- [69] Povirk, L. F., Houlgrave, C. W., Han, Y. H., *J. Biol. Chem.* **1988**, *263*, 19263-19266.
- [70] Faure, V., Constant, J.-F., Dumy, P., Sapparbaev, M., *Nucleic Acids Res.* **2004**, *32*, 2937-2946.
- [71] Povirk, L. F., Goldberg, I. H., *Proc. Natl. Acad. Sci. U. S. A.* **1985**, *82*, 3182-3186.
- [72] Wang, Y., Sheppard, T. L., Tornaletti, S., Maeda, L. S., Hanawalt, P. C., *Chem. Res. Toxicol.* **2006**, *19*, 234-241.
- [73] Meijler, M. M., Zelenko, O., Sigman, D. S., *J. Am. Chem. Soc.* **1997**, *119*, 1135-1136.
- [74] Berthet, N., Roupioz, Y., Constant, J.-F., Kotera, M., Lhomme, J., *Nucleic Acids Res.* **2001**, *29*, 2725-2732.
- [75] Kroeger, K. M., Jiang, Y. L., Kow, Y. W., Goodman, M. F., Greenberg, M. M., *Biochemistry* **2004**, *43*, 6723-6733.
- [76] Thomas, M., Castaing, B., Fourrey, J.-L., Zelwer, C., *Nucleosides Nucleotides* **1999**, *18*, 239-243.
- [77] Takeshita, M., Chang, C. N., Johnson, F., Will, S., Grollman, A. P., *J. Biol. Chem.* **1987**, *262*, 10171-10179.
- [78] Kim, J., Weledji, Y. N., Greenberg, M. M., *J. Org. Chem.* **2004**, *69*, 6100-6104.
- [79] Chen, J., Stubbe, J., *Biochemistry* **2004**, *43*, 5278-5286.
- [80] Mosimann, M., Kuepfer, P. A., Leumann, C. J., *Org. Lett.* **2005**, *7*, 5211-5214.

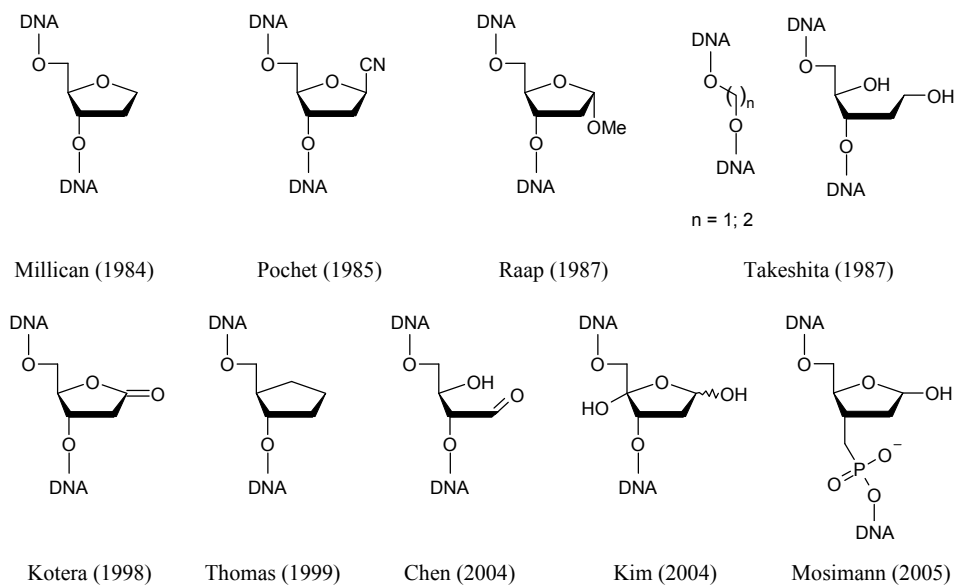


Figure 1.16 Abasic site analogues that were incorporated into oligomers via the phosphoramidite method

1.5 Reactivity of the Natural DNA Abasic Site

1.5.1 Abasic site cleavage

Abasic site strand cleavage has been extensively studied under different conditions. *Bailly* showed that abasic sites undergo fast β -elimination followed by slow δ -elimination under alkaline treatment.^[81,82]

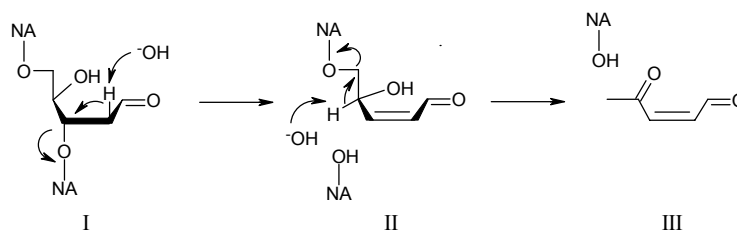


Figure 1.17 Mechanism of β -elimination and following slow δ -elimination

Vodička studied the phosphodiester cleavage in apurinic dinucleotides.^[83] *Suzuki* in 1994 extended the study to the cleavage of apurinic sites at different sites in tetramers when treated with heat.^[84]

The aldehydic form of DNA apurinic sites is known to react with amines to give a Schiff base that leads to β -elimination.^[85]

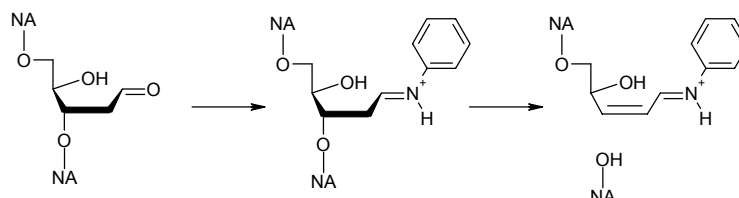


Figure 1.18 Mechanism of the Schiff base formation of the aldehydic abasic site and an amine

Up to now, a wide variety of chemical agents have been reported to undergo this process. Polyamines like *N,N*-dimethylethylenediamine, spermine, spermidine and putrescine are found to be the simplest ones.^[86-88]

[81] Bailly, V., Verly, W. G., *Biochem. J.* **1988**, 253, 553-559.

[82] Bailly, V., Derydt, M., Verly, W. G., *Biochem. J.* **1989**, 261, 707-713.

[83] Vodička, P., Hemminki, K., *Chem.-Biol. Interact.* **1988**, 68, 153-164.

[84] Suzuki, T., Ohsumi, S., Makino, K., *Nucleic Acids Res.* **1994**, 22, 4997-5003.

[85] Livingston, D. C., *Biochim. Biophys. Acta* **1964**, 87, 538-540.

[86] McHugh, P. J., Knowland, J., *Nucleic Acids Res.* **1995**, 23, 1664-1670.

[87] Male, R., Fosse, V. M., Kleppe, K., *Nucleic Acids Res.* **1982**, 10, 6305-6318.

[88] Georgakilas Alexandros, G., Bennett Paula, V., Sutherland Betsy, M., *Nucleic Acids Res.* **2002**, 30, 2800-2808.

Intercalating agents such as 9-aminoellipticine^[53] and 3-aminocarbazole^[89] and the tripeptide Lys-Trp-Lys^[90,91] have been shown to act as artificial AP lyases. Fkyerat, Belmont and Alarcon reported on molecules that incorporate in their structure 2,6-diaminopurine as a nucleic base analogue linked to 9-aminoaciridine as an intercalator.^[92-94] These compounds also recognize and cleave abasic sites.

1.5.2 Abasic site detection

Most reported methods to detect abasic sites are based on the condensation between the aldehydic function of the deoxyribose and amino reporter groups. More sensitive assays are the ARP (for Aldehyde Reactive Probe) and the Lissamine Probe that allow the detection of one AP-site per 10⁴ and 10⁵ nucleotides of DNA, respectively.^[95-97]

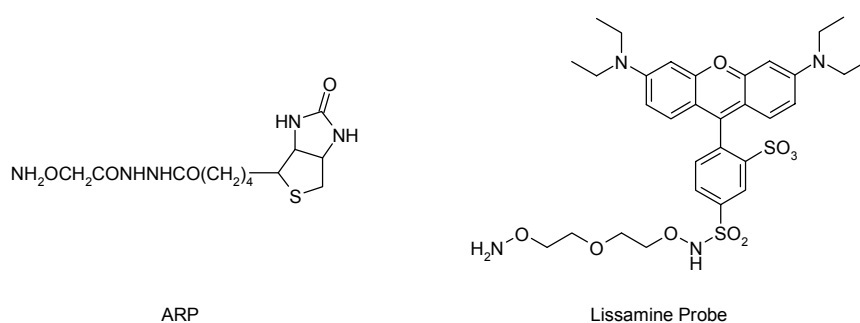


Figure 1.19 Biotin derivative ARP and Lissamine-Rhodamine B used to detect abasic sites

1.5.3 DNA polymerases and reverse transcriptases^[98,99]

DNA abasic sites are reported to have mutagenic effects when they are bypassed by polymerases. In *Escherichia coli*, synthesis past abasic sites *in vitro* shows preferential incorporation of adenine opposite the abasic lesion.^[77,100,101] The same phenomenon has

- [89] Vasseur, J. J., Rayner, B., Imbach, J. L., Verma, S., McCloskey, J. A., Lee, M., Chang, D. K., Lown, J. W., *J. Org. Chem.* **1987**, *52*, 4994-4998.
- [90] Behmoaras, T., Toulme, J. J., Helene, C., *Nature* **1981**, *292*, 858-859.
- [91] Pierre, J., Laval, J., *J. Biol. Chem.* **1981**, *256*, 10217-10220.
- [92] Fkyerat, A., Demeunynck, M., Constant, J. F., Michon, P., Lhomme, J., *J. Am. Chem. Soc.* **1993**, *115*, 9952-9959.
- [93] Belmont, P., Boudali, A., Constant, J.-F., Demeunynck, M., Fkyerat, A., Michon, P., Serratrice, G., Lhomme, J., *New J. Chem.* **1997**, *21*, 47-54.
- [94] Alarcon, K., Demeunynck, M., Lhomme, J., Carrez, D., Croisy, A., *Bioorg. Med. Chem. Lett.* **2001**, *11*, 1855-1858.
- [95] Nakamura, J., Swenberg, J. A., *Cancer Res.* **1999**, *59*, 2522-2526.
- [96] Atamna, H., Cheung, I., Ames, B. N., *Proc. Natl. Acad. Sci. U. S. A.* **2000**, *97*, 686-691.
- [97] Boturnyn, D., Constant, J.-F., Defrancq, E., Lhomme, J., Barbin, A., Wild, C. P., *Chem. Res. Toxicol.* **1999**, *12*, 476-482.
- [98] Loeb, L. A., Preston, B. D., *Annu. Rev. Genet.* **1986**, *20*, 201-230.
- [99] Pages, V., Fuchs, R. P. P., *Oncogene* **2002**, *21*, 8957-8966.
- [100] Sagher, D., Strauss, B., *Biochemistry* **1983**, *22*, 4518-4526.
- [101] Randall, S. K., Eritja, R., Kaplan, B. E., Petruska, J., Goodman, M. F., *J. Biol. Chem.* **1987**, *262*, 6864-6870.

been shown for *in vivo* transcription. The selectivity of the incorporation of purines over pyrimidines and the preference of adenine- over guanine-incorporation is known as the “A-rule”.^[102] In the lab of *Arthur Grollman*, *Takeshita* showed that the tetrahydrofuran abasic site analogue is read over by calf thymus DNA polymerase- α as well as by avian myeloblastosis virus reverse transcriptase (AMV-RT), following the A-rule.^[77] Furthermore significant read-through could only be observed in the case of a cyclic abasic site analogue whereas the acyclic deoxyribitol and other acyclic abasic site mimics blocked the polymerases. At about the same time *Randall* from the lab of *Myron Goodman* reported the translesion synthesis of *Drosophila* DNA polymerase α obeying the A-rule.^[101] In 1993 *Cai* from the same lab presented a study on the deoxyribonucleotide insertion efficiencies opposite abasic template lesions in DNA for HIV-1 reverse transcriptase.^[103,104] In 1997 *Shibutani*, again from the *Grollman* lab, confirmed the A-rule for the Klenow fragment of *Escherichia coli* DNA polymerase I and for calf thymus DNA polymerase- α .^[105] *Shibutani* furthermore showed that the frequency of translesion synthesis past abasic sites follows the order tetrahydrofuran > deoxyribose > deoxyribitol.

1.5.4 Abasic site repair^[106-108]

The maintenance of the integrity of the genome is crucial for all organisms. DNA abasic sites can occur spontaneously as described above but they are also intermediates of the base-excision repair pathway (BER, Figure 1.20).^[109,110] Damage to DNA bases resulting from deamination, oxidation and alkylation is mainly repaired by BER.^[111] The repair pathway is initiated by DNA glycosylases, which recognize damaged bases, excise them by hydrolysis of the *N*-glycosidic bond and generate an abasic site. It follows a strand cleavage 5' to the abasic site by AP endonuclease APE1 to generate a nick. Polymerase β (Pol β) then incorporates a single nucleotide and removes the abasic moiety by its AP lyase activity. In the final step the nick is ligated by DNA ligase III.

[102] Strauss, B. S., *BioEssays* **1991**, *13*, 79-84.

[103] Cai, H., Bloom, L. B., Eritja, R., Goodman, M. F., *J. Biol. Chem.* **1993**, *268*, 23567-23572.

[104] Cancio, R., Spadari, S., Maga, G., *Biochem. J.* **2004**, *383*, 475-482.

[105] Shibutani, S., Takeshita, M., Grollman, A. P., *J. Biol. Chem.* **1997**, *272*, 13916-13922.

[106] Dianov, G. L., Sleeth, K. M., Dianova, I. I., Allinson, S. L., *Mutat. Res.* **2003**, *531*, 157-163.

[107] Friedberg Errol, C., *Nature* **2003**, *421*, 436-440.

[108] Fleck, O., Nielsen, O., *J. Cell Sci.* **2004**, *117*, 515-517.

[109] Schaerer, O. D., *Angew. Chem., Int. Ed. Engl.* **2003**, *42*, 2946-2974.

[110] Hoeijmakers, J. H., *Nature* **2001**, *411*, 366-374.

[111] Cappelli, E., Hazra, T., Hill, J. W., Slupphaug, G., Bogliolo, M., Frosina, G., *Carcinogenesis* **2001**, *22*, 387-393.

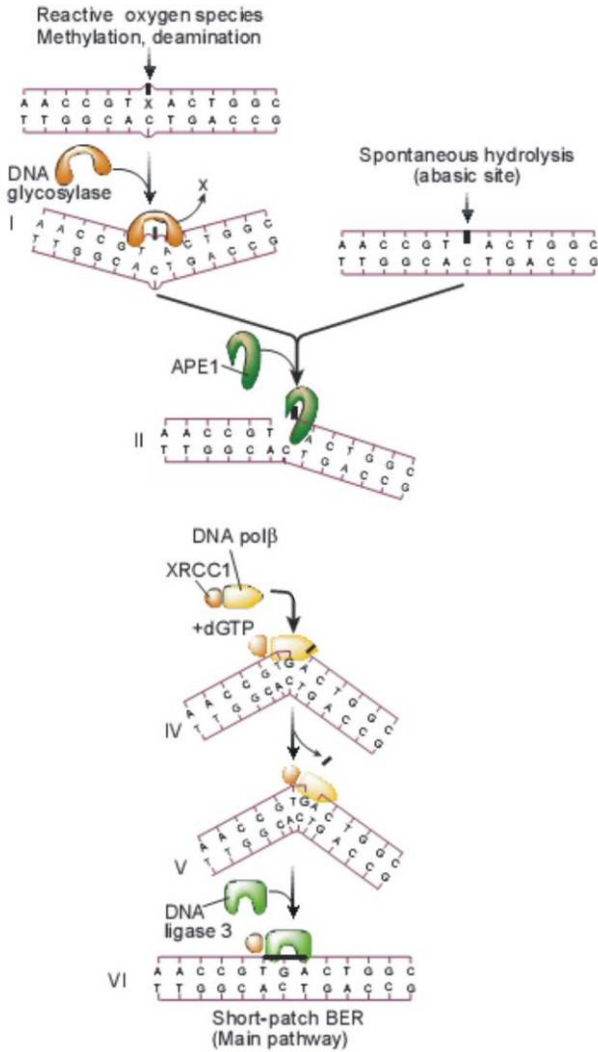


Figure 1.20 Main pathway of the base-excision repair mechanism (Figure adapted from [110])

1.6 Formation of Site Specific RNA Abasic Sites

1.6.1 Chemically induced RNA abasic sites

Besides the published methods for chemical RNA sequencing where chemical steps for removal of specific bases are proposed, literature on formation of site specific RNA abasic sites is still scarce.^[112,113]

Up to now just a few examples have been published where RNA abasic sites are formed on specific sites in oligoribonucleotides. These examples are based on natural occurring modified nucleobases, preliminary from tRNAs where modifications are omnipresent. Two of these modified RNA nucleosides in tRNA^{Phe} have shown to be easily hydrolysed under mild conditions to give abasic sites: wybutosine (37) and 7-methylguanosine (46). The generation of abasic sites was just an intermediate step on the way to explore the structure of tRNA^{Phe}. The abasic sites were therefore never thoroughly characterized.

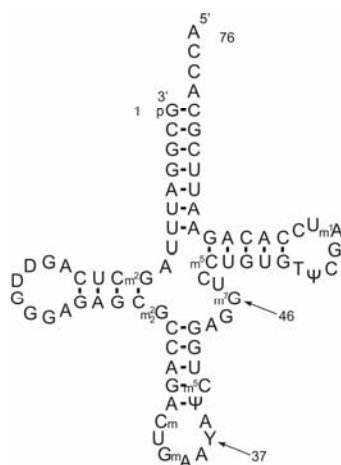


Figure 1.21 Cloverleaf structure of tRNA^{Phe} with wybutosine (37) and 7-methylguanosine (46), two nucleobases that are easily hydrolysed under mild acidic conditions

In 1968 Zachau generated an abasic site by removal of the base of the wybutosine nucleoside in tRNA^{Phe} under mild conditions (pH 2.9, 37 °C, 3-4 hours).^[114] Two years later it was found that 7-methylguanosine can be transformed to a 4-ribosylamino pyrimidine by alkaline treatment (pH 9.5, 37 °C, 4 hours).^[115] This conversion product can then be further transformed to an abasic site by acidic treatment (pH 3.0, 37 °C, 4 hours or 22 °C, 15 hours). Another way to transform 7-methylguanosine into an abasic

[112] Peattie, D. A., *Proc. Natl. Acad. Sci. U. S. A.* **1979**, 76, 1760-1764.

[113] Waldmann, R., Gross, H. J., Krupp, G., *Nucleic Acids Res.* **1987**, 15, 7209.

[114] Thiebe, R., Zachau, H. G., *Eur. J. Biochem.* **1968**, 5, 546-555.

[115] Wintermeyer, W., Zachau, H. G., *FEBS Lett.* **1970**, 11, 160-164.

site is the treatment with NaBH_4 , which leads to several reaction products that can be cleaved by treatment with aniline.^[116]

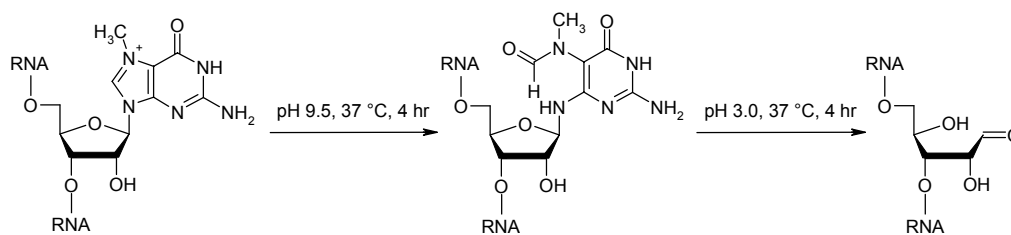


Figure 1.22 Transformation of 7-methylguanosine into an abasic site

Nishikawa used the known lability of wybutosine to generate an abasic site in tRNA^{Phe} in order to perform an enzymatic excision of the apurinic site.^[117] In a first step an abasic site is induced at position 37 of eukaryotic tRNA^{Phe} . Wybutosine, which can be regarded as a highly substituted guanine derivative, has a high capability to stabilize a positive charge and can therefore be easily hydrolysed under slightly acidic conditions. *Nishikawa* in a first step generated the abasic site by treatment of the tRNA^{Phe} according to *Zachau*. In a second step the tRNA molecule is cleaved at the apurinic site by treatment with aniline/2-aminopyridine (pH 5.5, 0.25 M each, 45 °C, up to 72 hrs). With bacterial alkaline phosphatase the phosphate groups of the remaining 3'-end of the RNA is removed and the 5' phosphate groups are replaced by incubation with polynucleotide kinase and ATP. The anticodon loop could then be resealed quantitatively by incubation of the reannealed RNA molecules in the presence of RNA ligase and ATP.

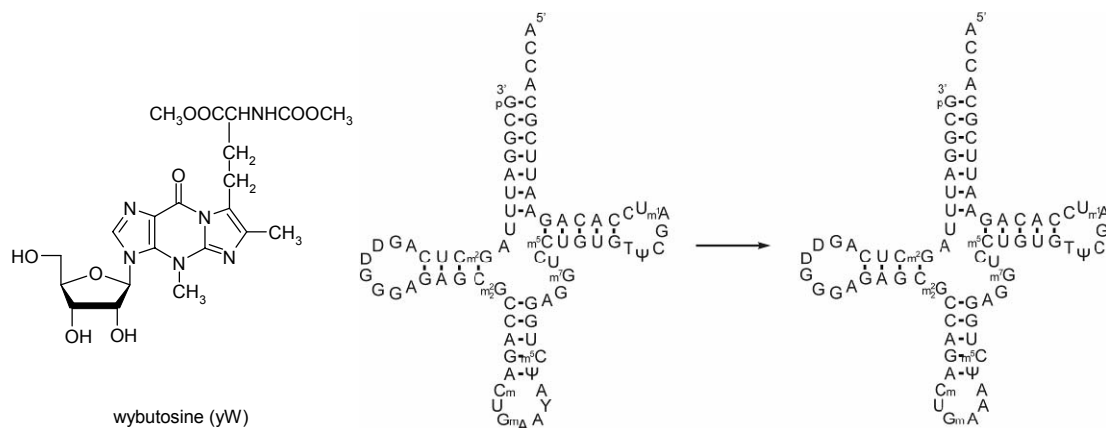


Figure 1.23 Structure of wybutosine (left). Apurinic site excision experiment: Y is removed by acidic hydrolysis, the molecule is cleaved and resealed by RNA ligase

[116] Wintermeyer, W., Zachau, H. G., *FEBS Lett.* **1975**, 58, 306-309.

[117] Nishikawa, K., Adams, B. L., Hecht, S. M., *J. Am. Chem. Soc.* **1982**, 104, 326-328.

In parallel to the research presented in this work a similar approach to generate abasic sites in oligoribonucleotides by photochemical treatment was disclosed by Trzupek in early 2005.^[118]

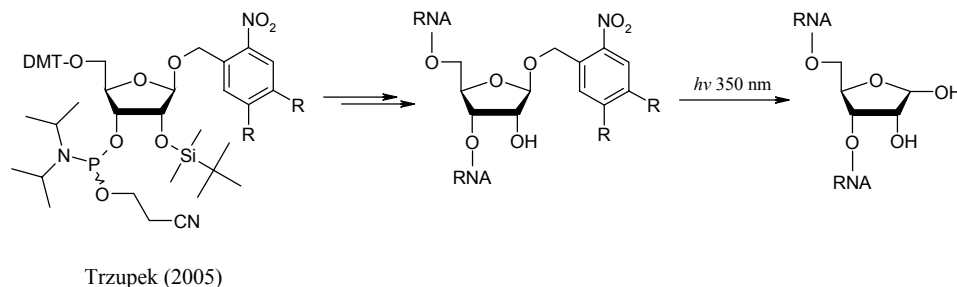


Figure 1.24 Incorporation of a phosphoramidite building block that can be deprotected by long-wave UV light ($R = H$ or OCH_3)

1.6.2 Abasic sites induced by ribosome inactivating proteins^[119,120]

Ribosome inactivating proteins (RIP) are a group of proteins that damage ribosomes in an irreversible manner, acting catalytically.^[121] Ricin is a widely and long known protein of this class.^[122] Ricin is a highly toxic RNA *N*-ribohydrolase that has a k_{cat} for mammalian ribosomes of 1800 min^{-1} .^[123] Thus a single molecule is capable of killing a mammalian cell. The mechanism of the ribosomal damage was discovered by Endo et al., who found that ricin cleaved the glycosidic bond of a single adenine residue (A_{4324} in rat liver rRNA).^[124] This residue is adjacent to the site of cleavage of rRNA by α -sarcin (which cleaves the phosphodiester bond between G_{4325} and A_{4326} in rat 28S rRNA), in a tetranucleotide $GA_{4324}GA$ in a highly conserved loop at the top of a stem, for this called α -sarcin/ricin loop (Figure 1.25). This loop is involved in the binding of elongation factors and the modified ribosomes are, therefore, unable to support protein synthesis.^[125] This observation was extended to other RIPs, which were officially classified as rRNA *N*-glycosidases.^[126] RIPs depurinate also non-mammalian ribosomes, from insects, plants, yeast and bacteria. Subsequently, it was found that some RIPs remove more than one adenine residue per ribosome and that RIPs also remove adenine residues from DNA.^[119,127]

[118] Trzupek, J. D., Sheppard, T. L., *Org. Lett.* **2005**, *7*, 1493-1496.

[119] Stirpe, F., *Toxicon* **2004**, *44*, 371-383.

[120] Stirpe, F., Battelli, M. G., *Cell. Mol. Life Sci.* **2006**, *63*, 1850-1866.

[121] Peumans, W. J., Hao, Q., Van Damme, E. J. M., *FASEB J.* **2001**, *15*, 1493-1506.

[122] Olsnes, S., *Toxicon* **2004**, *44*, 361-370.

[123] Schramm, V. L., *Curr. Opin. Chem. Biol.* **1997**, *1*, 323-331.

[124] Endo, Y., Mitsui, K., Motizuki, M., Tsurugi, K., *J. Biol. Chem.* **1987**, *262*, 5908-5912.

[125] Endo, Y., Gluck, A., Wool, I. G., *J. Mol. Biol.* **1991**, *221*, 193-207.

[126] Stirpe, F., Bailey, S., Miller, S. P., Bodley, J. W., *Nucleic Acids Res.* **1988**, *16*, 1349-1357.

[127] Barbieri, L., Ferreras, J. M., Barraco, A., Ricci, P., Stirpe, F., *Biochem. J.* **1992**, *286*, 1-4.

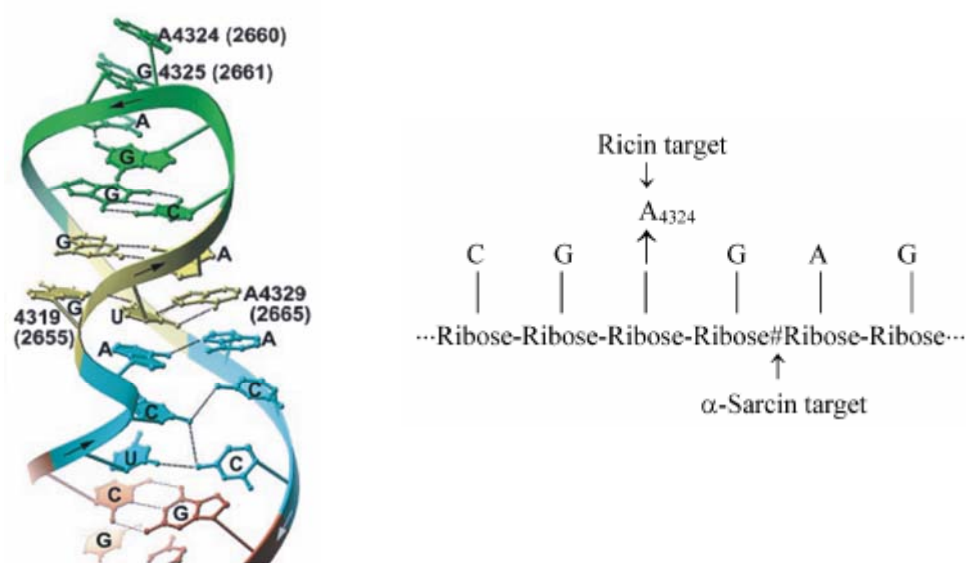


Figure 1.25 Crystal structure of the sarcin-ricin loop (left).^[128] Numbering for the rat 28S rRNA, with corresponding number for *E. coli* 23S rRNA in parentheses. Schematic representation of the enzymatic reaction of ribosome-inactivating proteins on rRNA (right).^[119]

1.6.3 Unnatural RNA abasic site analogues

Just one chemically stable RNA abasic site analogue has been synthesized, mimicking the tetrahydrofuranose ring.^[129] A slightly modified building block is now commercially available.^[130]



Figure 1.26 RNA abasic site analogues that were incorporated into oligomers via the phosphoramidite method

- [128] Correll, C. C., Munishkin, A., Chan, Y.-L., Ren, Z., Wool, I. G., Steitz, T. A., *Proc. Natl. Acad. Sci. U. S. A.* **1998**, *95*, 13436-13441.
 [129] Beigelman, L., Karpeisky, A., Usman, N., *Bioorg. Med. Chem. Lett.* **1994**, *4*, 1715-1720.
 [130] *Glen Report* **2003**, *16*.

1.7 Reactivity of the Natural RNA Abasic Site

From literature there is not much information available on the reactivity of RNA abasic sites. As described above, *Nishikawa* showed that abasic lesion in RNA can be cleaved by treatment with aniline.^[117] It will be shown later in this work that RNA abasic sites show a similar behavior with regard to strand cleavage as DNA abasic sites.

In 1999 *Ogasawara* and co-workers reported on a novel enzyme that specifically cleaves RNA abasic sites.^[131,132] The protein, ribosomal RNA apurinic site specific lyase (RALyase), was found in wheat germ embryos and has a molecular weight of 50625 Da. The enzyme cleaves the phosphodiester bond at the 3' side of the apurinic site introduced by ribosome-inactivating proteins into the sarcin-ricin domain of 28S rRNA. The substrate specificity of the enzyme was found to be extremely high: it acts only at the apurinic site in the sarcin/ricin domain of intact ribosomes, not on deproteinized rRNA or DNA containing apurinic sites. A survey focused on RIP containing plants suggested that there is a wide distribution of RALyase among RIP-producing plants. In a later study it was found that phosphodiester bond cleavage of depurinated ribosomes by RALyase leads to a complete inactivation of the depurinated ribosomes.^[133] The authors think that it is possible that plants acquired this system of completely inactivating their depurinated ribosomes in order to stop protein synthesis reliably, since it is conceivable that viral proteins, for example, have found ways of exploiting the residual ribosome function. RALyase might also be involved in inactivating mutated ribosomes and restoring accurate translation depending on the undamaged ribosomes.

[131] Ogasawara, T., Sawasaki, T., Morishita, R., Ozawa, A., Madin, K., Endo, Y., *EMBO J.* **1999**, *18*, 6522-6531.

[132] Sawasaki, T., Morishita, R., Ozawa, A., Ogasawara, T., Madin, K., Endo, Y., *Nucleic Acids Symp. Ser.* **1999**, *42*, 257-258.

[133] Ozawa, A., Sawasaki, T., Takai, K., Uchiumi, T., Hori, H., Endo, Y., *FEBS Lett.* **2003**, *555*, 455-458.

1.8 Major Effects of UV Radiation on Nucleic Acids

The generation of abasic sites by UV irradiation has besides its easiness and elegance the one major drawback that the UV radiation can in principle damage nucleic acids. Two major products are formed in DNA upon irradiation with UV-light: cyclobutane pyrimidine dimers (CPD) and pyrimidine (6-4) pyrimidones ((6-4)PP).^[134-136] These two major products are formed at a ratio of 3:1. The induction of the various lesions is wavelength dependent. Most photoproducts are induced efficiently at the absorption maximum of DNA, i.e. 260 nm, but the UVB wavelength range (290–320nm) is still very effective in this respect.

1.8.1 Cyclobutane pyrimidine dimers^[137-139]

Cyclobutane pyrimidine dimers (CPD) constitute the major DNA photoproducts upon exposure to UVB light (280-320 nm). They arise from a [2+2] cycloaddition of the C5-C6 double bonds of two adjacent pyrimidine bases. Due to steric constraints in DNA only *cis* isomers can be generated. The relative orientation of the C5-C6 double bonds gives rise to *syn* and *anti* regioisomers.^[140] The *cis-syn* form is produced in large excess with respect to the *trans-syn* form which is only present in single-stranded and denaturated DNA.

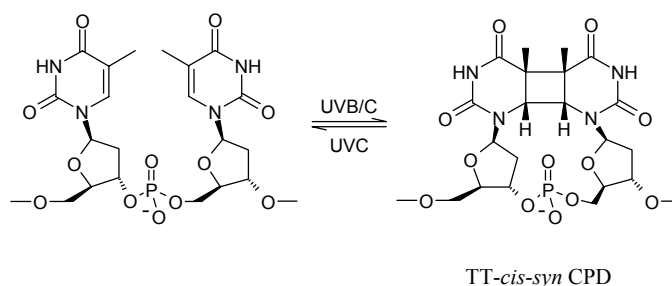


Figure 1.27 The most prominent DNA lesion induced by UVB/C light are *cis-syn* cyclobutane pyrimidine dimers (CPD) from a [2+2] cycloaddition of two adjacent pyrimidine bases

The cyclobutane pyrimidine dimer formation can be reversed upon UVC irradiation through the photo-induced splitting of the cyclobutane ring. It is known, that *E. coli* DNA photolyase specifically reverses cyclobutane CPDs, but not (6-4) photoproducts.

-
- [134] Yoon, J.-H., Lee, C.-S., O'Connor, T. R., Yasui, A., Pfeifer, G. P., *J. Mol. Biol.* **2000**, *299*, 681-693.
 [135] Ravanat, J.-L., Douki, T., Cadet, J., *J. Photochem. Photobiol., B* **2001**, *63*, 88-102.
 [136] Sinha, R. P., Hader, D.-P., *Photochem. Photobiol. Sci.* **2002**, *1*, 225-236.
 [137] Liu, F.-T., Yang, N. C., *Biochemistry* **1978**, *17*, 4865-4876.
 [138] Vink, A. A., Roza, L., *J. Photochem. Photobiol., B* **2001**, *65*, 101-104.
 [139] Durbeej, B., Eriksson, L. A., *J. Photochem. Photobiol., A* **2002**, *152*, 95-101.
 [140] Koning, T. M. G., Van Soest, J. J. G., Kaptein, R., *Eur. J. Biochem.* **1991**, *195*, 29-40.

1.8.2 Pyrimidine (6-4) pyrimidone photoproducts

Pyrimidine (6-4) pyrimidine adducts are the second class of relevant photoproducts. They arise from a [2+2] cycloaddition of the C5-C6 double bond of the 5'-end pyrimidine with the C4 carbonyl bond of the 3'-end pyrimidine. The resulting oxetane (an azetidine is formed when the 3'-end pyrimidine is a cytosine) rearranges spontaneously to give rise to the pyrimidine (6-4) pyrimidone adducts. Further exposure of the (6-4) photoproduct to UVB light leads to the Dewar valence isomer.

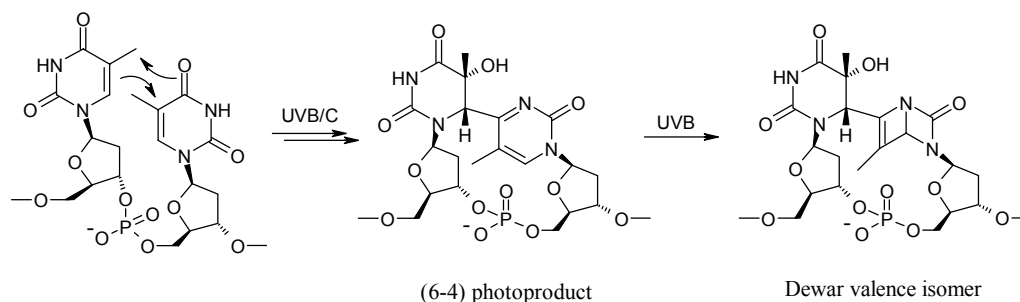


Figure 1.28 Formation of the pyrimidine (6-4) pyrimidone photoadducts

1.8.3 Mutations from pyrimidine dimers^[141,142]

CPD is the most likely product to be encountered by a polymerase during repair or replication.^[143] Saturation of the 5,6 double bond like in a CPD is known to facilitate tautomerization and deamination of cytidine. It has been shown that two adenosine residues are incorporated opposite the *cis-syn* dimer of TU. Deamination of the TC dimer then explains the origin of UV-induced CT, TC, CC→TT mutations.

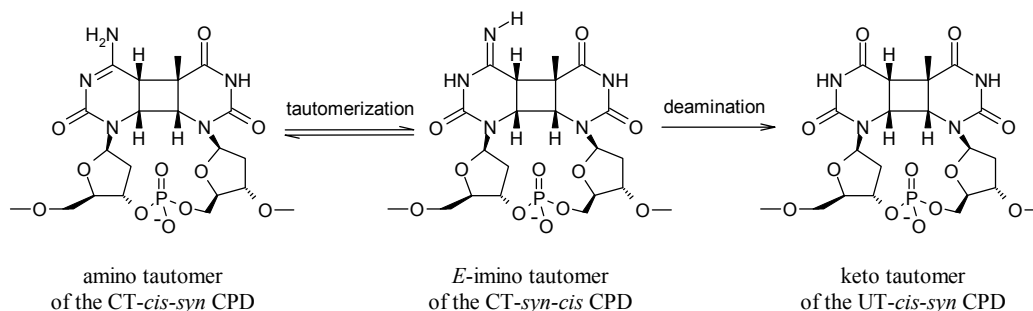


Figure 1.29 Tautomerization and deamination of a CT-*syn-cis* CPD to a UT-*syn-cis* CPD result a CT→TT mutation

[141] Gibbs, P. E. M., Lawrence, C. W., *Nucleic Acids Res.* **1993**, *21*, 4059-4065.

[142] Taylor, J.-S., *Mutat. Res.* **2002**, *510*, 55-70.

[143] Glickman, B. W., Schaaper, R. M., Haseltine, W. A., Dunn, R. L., Brash, D. E., *Proc. Natl. Acad. Sci. U. S. A.* **1986**, *83*, 6945-6949.

A recent study comes to the conclusion that in general the formation of UV-induced DNA lesions is strongly sequence and conformation dependent.^[144] Moreover the authors conclude that RNA is more UV resistant than DNA.

[144] Kundu, L. M., Linne, U., Marahiel, M., Carell, T., *Chem. Eur. J.* **2004**, *10*, 5697-5705.

1.9 Aim of the Work

In the recent years, the DNA abasic site and its stable analogues were extensively studied with regard to their stability and their mutagenic effects on different polymerases. Compared to that, little attention was given to the RNA abasic site up to now. The recent discovery of the mechanism by which *E. coli* repairs RNA alkylation damage points into the direction that cells also care about the integrity of RNA and that there might exist more unknown RNA repair mechanisms.^[145-147]

Two facts underline that RNA abasic sites might not form in nature or won't have an impact when formed:

- hydrolysis of the *N*-glycosidic bond in ribonucleotides is slower by a factor of 1000 compared to the deoxyribonucleotides
- the life-time of an RNA molecule is much shorter compared to DNA

On the other side there are arguments that underline that RNA abasic sites might occur and have a biological impact:

- RNA concentration is much higher than DNA concentration
- Over 95 % of the cellular RNA is long living rRNA and tRNA
- The life-time of an abasic RNA moiety is expected to be higher than for the DNA analogue
- Ribosome inactivating proteins are known to depurinate polynucleotide chains
- RALyase specifically cleaves RNA abasic sites
- RNA viruses and retroviruses rely on RNA as their genetic material. Any damage to it may be live-threatening

These arguments lead to the conclusion that the high concentration of relatively stable RNA enhances the chance that abasic sites are formed. Moreover the expected higher stability of a formed RNA abasic site might lead to a higher influence in the cell. Adding to this the discovery of RALyase, an enzyme with no other known function than to cut abasic rRNA, indicates that such lesions are so important to nature that a special enzyme was created.

The aim of this study is set to explore natural RNA abasic sites more closely.

In a first part the phosphoramidites **1-3** are synthesized that can be incorporated into oligonucleotides by standard phosphoramidite chemistry. The incorporated building

-
- [145] Aas, P. A., Otterlei, M., Falnes, P. O., Vagbo, C. B., Skorpen, F., Akbari, M., Sundheim, O., Bjoras, M., Slupphaug, G., Seeberg, E., Krokan, H. E., *Nature* **2003**, *421*, 859-863.
 - [146] Bellacosa, A., Moss, E. G., *Curr. Biol.* **2003**, *13*, R482-R484.
 - [147] Bregeon, D., Sarasin, A., *Mutat. Res.* **2005**, *577*, 293-302.

blocks will then be tested with regard to their deprotection kinetics to reveal a natural abasic site.

In a second step the stability of the abasic RNA is compared to that of the abasic DNA under basic (pH 13) and slightly acidic (pH 4.6) conditions. Furthermore the different strand cleavage mechanisms that can occur at an RNA abasic site in a basic medium (β -elimination and cyclophosphate formation) are measured independently and the arithmetic product of the two mechanisms is then correlated to the overlay of the measured cleavage at a natural abasic site.

In a third part the processing of abasic RNA by different reverse transcriptases is investigated. The question is whether an RNA abasic site will lead to translesion synthesis of the tested enzymes or to abortion of the reverse transcription process. This would give a theoretical answer to the question whether RNA abasic sites are a possible source of retroviral mutation. Furthermore the incorporation kinetics will be measured for successful enzymes and the kinetic data will show whether the A-rule for DNA abasic sites can be expanded to RNA. The influence of an abasic site on the RNase H mechanism will also be determined.

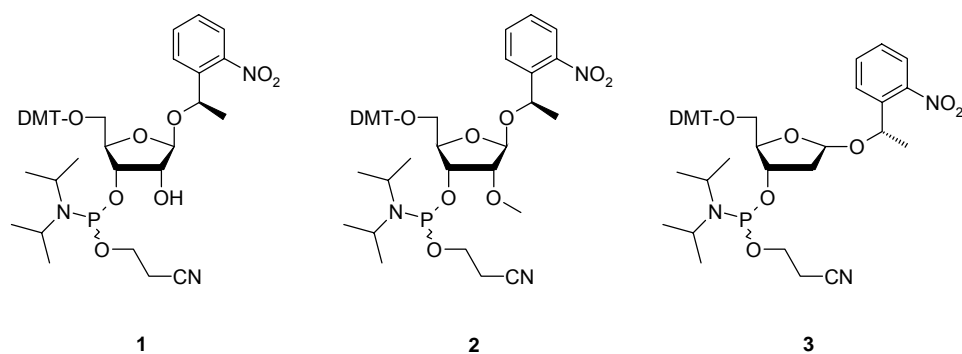


Figure 1.30 Synthesized phosphoramidite building blocks: mimicking a natural RNA (1), a 2'-O-methylated RNA (2) and a natural DNA abasic site (3)

2 Synthesis

2.1 Synthesis of the Phosphoramidite Building Blocks

2.1.1 Selection and synthesis of a suitable abasic site protecting group

The design of potential assays using true abasic site containing oligonucleotides demands the final deprotection step to occur fast, under mild conditions and merely quantitative in order not to interfere unnecessarily with the assay conditions. Moreover the deprotection conditions of a chosen protecting moiety have to be orthogonal to standard oligonucleotide chemistry to ensure a wide usability of the designed phosphoramidite building block. Photocleavable protecting groups fulfill these conditions to a satisfying extent.^[148] The usage of the simple 2-nitrobenzyl moiety (NB) was first adopted for ribonucleoside protection in 1974 and has since then been widely described in literature.^[149-151] Therefore it was chosen as the starting point. Nevertheless, this protecting unit usually used to cage the 2'-hydroxy position of the furanose ring had shown not to be fully stable under treatment with fluoride ions used in standard RNA of 2'-*O*-TBDMS deprotection chemistry.^[152,153] Because changing the 2'-hydroxy protecting groups would interfere with the desired wide usability of the synthesized building block, a 2-nitrobenzyl derivative with higher stability against fluoride treatment was looked for. Moreover the use of the 2-nitrobenzyl unit needs the work to be performed under attenuated light.^[154] Although there is no data available that shows that the used 1NPE group is more stable under normal lab conditions, no noticeable decomposition of 1NPE containing intermediates was identified when work was performed under normal lab conditions.

The 1-(2-nitrophenyl)ethyl (1NPE) unit was shown to be fully stable under the deprotection conditions mentioned above. Besides this, deprotection of the 1NPE unit gives rise to the less reactive 2-nitrosoacetophenone compared to the biologically toxic 2-nitrosobenzaldehyde that arises from 2-nitrobenzyl deprotection. 1NPE adducts are additionally known to photolyse 20 times more rapidly than the NB adducts.^[155] The

[148] Bochet, C. G., *J. Chem. Soc., Perkin Trans. 1* **2002**, 125-142.

[149] Ohtsuka, E., Tanaka, S., Ikehara, M., *Nucleic Acids Res.* **1974**, *1*, 1351-1357.

[150] Bartholomew, D. G., Broom, A. D., *J. Chem. Soc., Chem. Commun.* **1975**, 38.

[151] Hayes, J. A., Brunden, M. J., Gilham, P. T., Gough, G. R., *Tetrahedron Lett.* **1985**, *26*, 2407-2410.

[152] Walker, J. W., Reid, G. P., McCray, J. A., Trentham, D. R., *J. Am. Chem. Soc.* **1988**, *110*, 7170-7177.

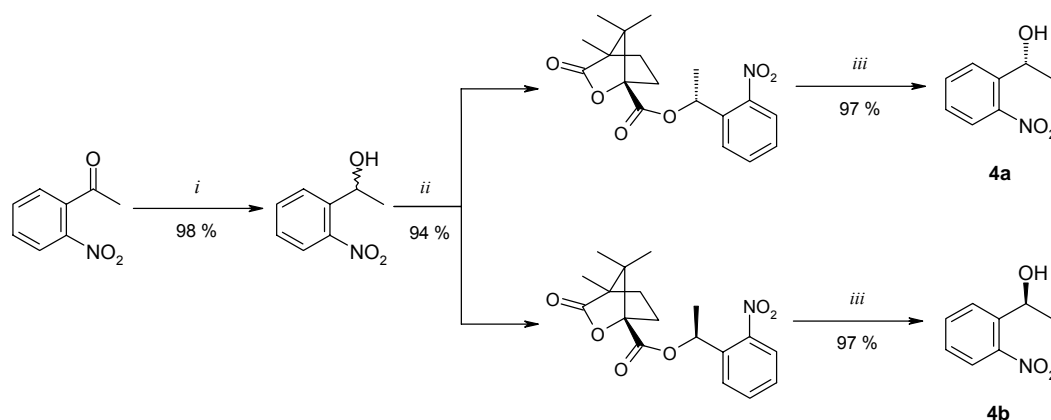
[153] Chaulk, S. G., MacMillan, A. M., *Nucleic Acids Res.* **1998**, *26*, 3173-3178.

[154] Schwartz, M. E., Breaker, R. R., Asteriadis, G. T., deBear, J. S., Gough, G. R., *Bioorg. Med. Chem. Lett.* **1992**, *2*, 1019-1024.

[155] Walker, J. W., McCray, J. A., Hess, G. P., *Biochemistry* **1986**, *25*, 1799-1805.

only drawback is the newly introduced chiral centre. Nevertheless it was shown in the synthesis for the RNA building block that a diastereomeric mixture is separable during the synthesis.

The desired (*R*)- and (*S*)-1-(2-nitrophenyl)ethanol were synthesized after the method of Corrie et al.^[156] Commercially available 2-nitroacetophenone was reduced in a first step in almost quantitative yield using NaBH₄. Subsequent esterification of the secondary alcohol with camphanic acid chloride gave the diastereomeric mixture of the esters in high yield.^[157] Fractional crystallization from hot methanol and repeated recrystallization of the two fractions from hot methanol for the (*R,S*)-isomer or from hot isopropyl alcohol for the (*S,S*)-isomer lead to the two pure diastereomeric esters. Separate saponification of the two esters gave the enantiopure alcohols in high yield, ready to couple to the sugar moiety.



Scheme 2.1 i) NaBH₄, MeOH, 0° → 20 °C; ii) (-)-(1*S*,4*R*)-camphanic acid chloride, pyridine; iii) KOH, MeOH/H₂O, reflux

2.1.2 Synthesis of the RNA abasic site precursor

The first step was the formation of the acetal under *Vorbrüggen* conditions of enantiopure 1-(*R*)-(2-nitrophenyl)ethanol **4a** with commercially available (1,2,3,5)-tetra-*O*-acetyl-ribofuranose.^[158,159] Because of the participation of the 2'-*O*Ac group after the 1'-*O*Ac group leaves, pure beta anomer of nucleoside **5** was obtained. Deacetylation of **5** gave triol **6** in good yield. Protection of the primary alcohol lead to the DMT-protected nucleoside **7a**. For the protection of the 2'-hydroxyl group [(triisopropylsilyl)oxy]methyl chloride **8** was used. This group is sterically less demanding than the TBDMS group and shows high deprotection yields using methylamine in ethanol/water. Moreover the TOM group does not undergo 2' to 3'

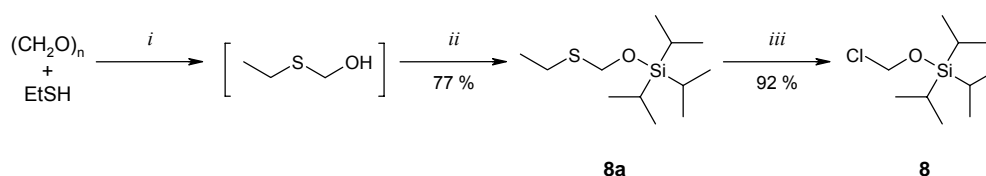
[156] Corrie, J. E. T., Reid, G. P., Trentham, D. R., Hursthouse, M. B., Mazid, M. A., *J. Chem. Soc., Perkin Trans. 1* **1992**, 1015-1019.

[157] Gerlach, H., Kappes, D., Boeckman, R. K., Jr., Maw, G. N., *Org. Synth.* **1993**, *71*, 48-55.

[158] Vorbrueggen, H., Krolikiewicz, K., Bennua, B., *Chem. Ber.* **1981**, *114*, 1234-1255.

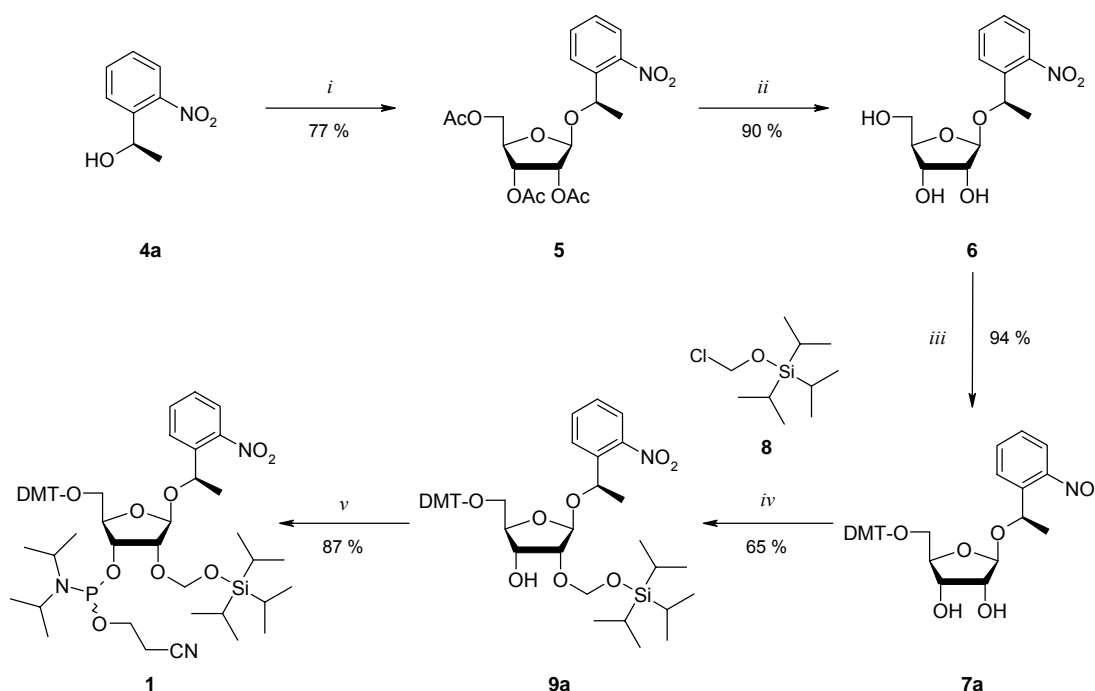
[159] Vorbrueggen, H., Hoefle, G., *Chem. Ber.* **1981**, *114*, 1256-1268.

migration under basic conditions.^[160] The reagent [(triisopropylsilyloxy)methyl chloride (**8**, TOM-Cl) was synthesized by modifying the general procedure for the synthesis of [(trialkylsilyloxy)methyl chlorides by *Benneche* and co-workers: silylation of (ethylthio)methanol^[161] with triisopropylsilylchloride/*1H*-imidazole in dichloromethane gave, after extraction and distillation, the silylated derivative **8a** in good yield.



Scheme 2.2 i) NaOH (cat), 40 °C; ii) $i\text{Pr}_3\text{SiCl}$, *1H*-imidazole, CH_2Cl_2 , r.t.; iii) SO_2Cl_2 , CH_2Cl_2 , r.t.

This intermediate was transformed with SO_2Cl_2 in CH_2Cl_2 into TOM-Cl **8** according to a known procedure.^[162] Distillation below 70 °C gave **8** in an excellent yield.



Scheme 2.3 i) Tetra-*O*-acetyl-ribofuranose, TMSOTf, CH_3CN , -20 °C; ii) Na_2CO_3 , MeOH; iii) DMT-Cl, pyridine; iv) a) Bu_2SnCl_2 , $i\text{Pr}_2\text{NEt}$, (CH_2Cl_2); b) TOM-Cl, 80 °C; v) CEP, $i\text{Pr}_2\text{NEt}$, THF

Attachment of the TOM-group in 94 % yield was achieved after the method developed by *Pitsch*.^[163] The ratio of the 2'- and 3'- regioisomers was determined to be

[161] Benneche, T., Gundersen, L. L., Undheim, K., *Acta Chem. Scand.* **1988**, B42, 384-389.

[162] Benneche, T., Strande, P., Undheim, K., *Synthesis* **1983**, 762-763.

[163] Pitsch, S., Weiss, P. A., Jenny, L., Stutz, A., Wu, X., *Helv. Chim. Acta* **2001**, 84, 3773-3795.

65 % in favor of the 2'-*O*-TOM protected nucleoside **9a**, according to ¹H-NMR analysis (Figure 2.1). Comparison of the achieved selectivity of 1-NPE to the natural nucleobases in the 1' position is shown in Table 2.1. According to *Pitsch*, the selectivity of the alkylation reaction is decreasing with longer reaction times. In this synthesis however, a high yield conversion was desired since the 3'-*O*-alkylated product could easily be treated with tetrabutylammonium fluoride to recover the educt **7a**. The structure of nucleoside **9a** was proven by ¹H-NOE measurements (Figure 2.2). Repeated column chromatography yielded 37% of the pure 2'-*O*-TOM nucleoside and 57% of an inseparable 2'-, 3'-*O*-TOM mixture. Reaction of **9a** with 2-cyanoethyl diisopropylchlorophosphoramidite gave compound **1**.

Table 2.1 Comparison of base induced 2'/3'-regioselectivity of TOM coupling

Base	Alkylation product		Overall yield [%]	Ratio 2'/3'
	2'-O [%]	3'-O [%]		
AAc	40	25	65	1.6
GAc	60	5	65	12
U	40	25	65	1.6
CAC	40	25	65	1.6
1NPE	61	33	94	1.85

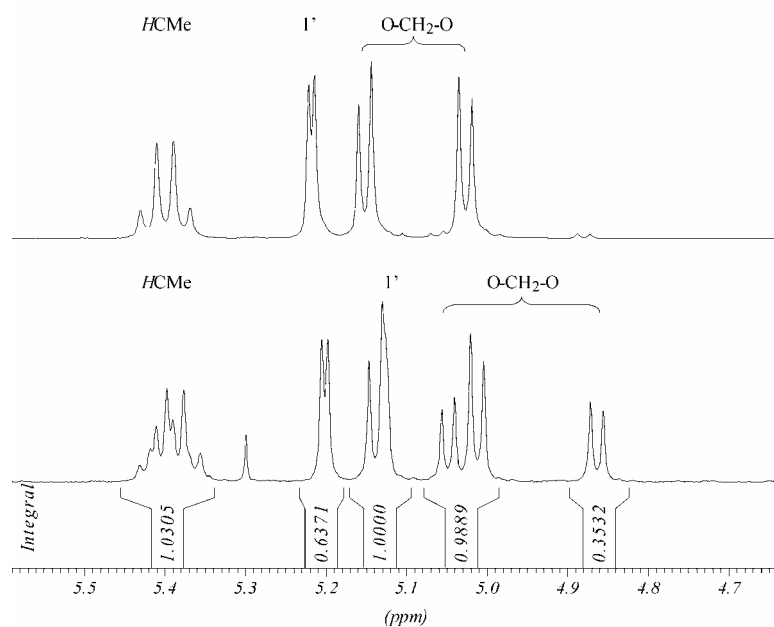


Figure 2.1 ¹H-NMR spectra of pure 2'-*O*-TOM nucleoside **9a** (upper) and the purified mixture of the 2',3'-*O*-TOM regioisomers **9a** and **9b** after synthesis (lower). Comparison of the spectra shows a ratio of almost 2 to 1 in favor of the desired 2'-*O*-TOM nucleoside **9a**

If racemic 1-(2-nitrophenyl)ethanol was used for the synthesis, the two diastereomeric nucleosides could be separated by column chromatography at the stage of intermediate

7. The further synthesis was performed using **7a**. For both diastereomers **7a** and **7b** spectroscopic data were collected.

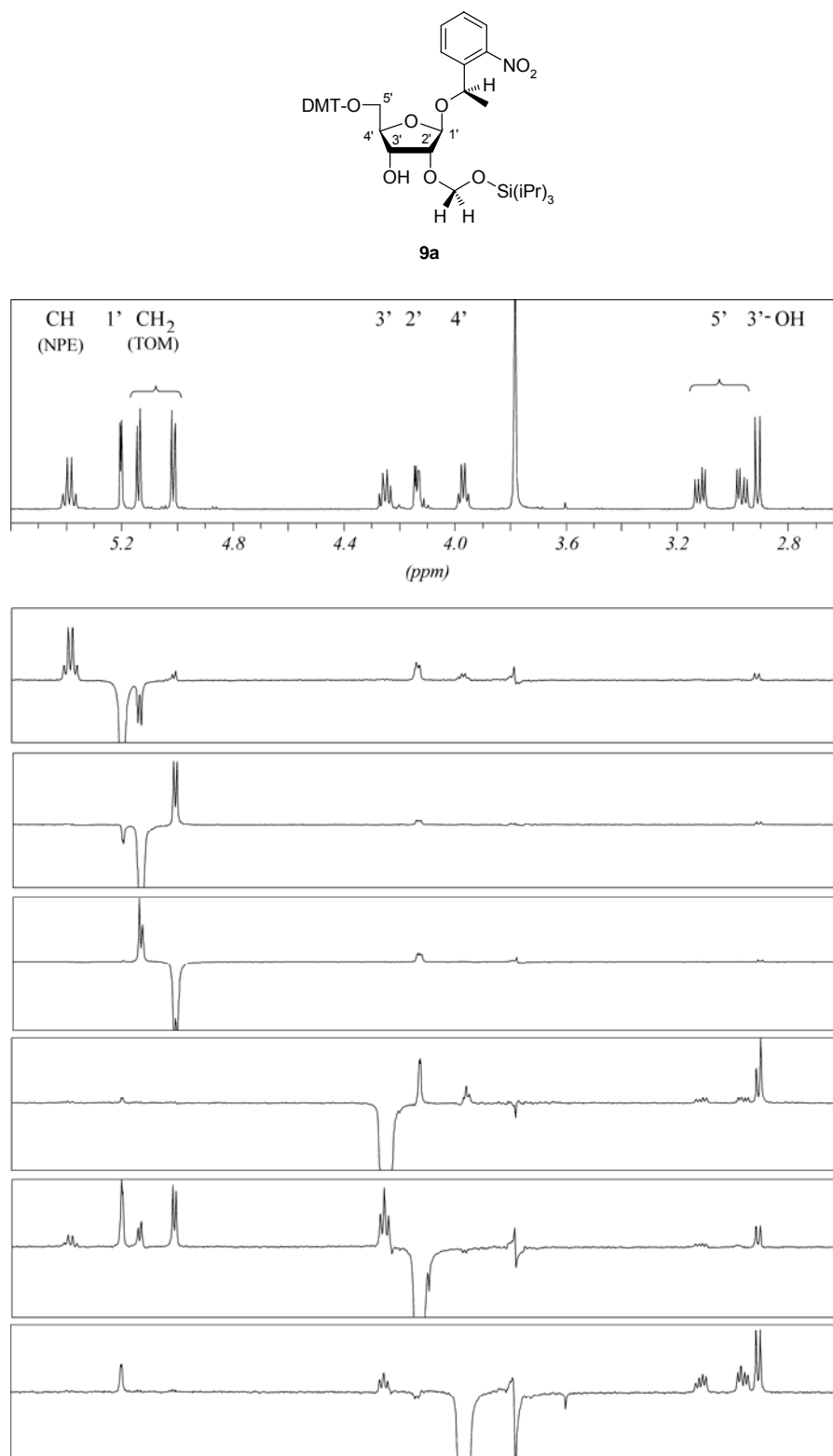
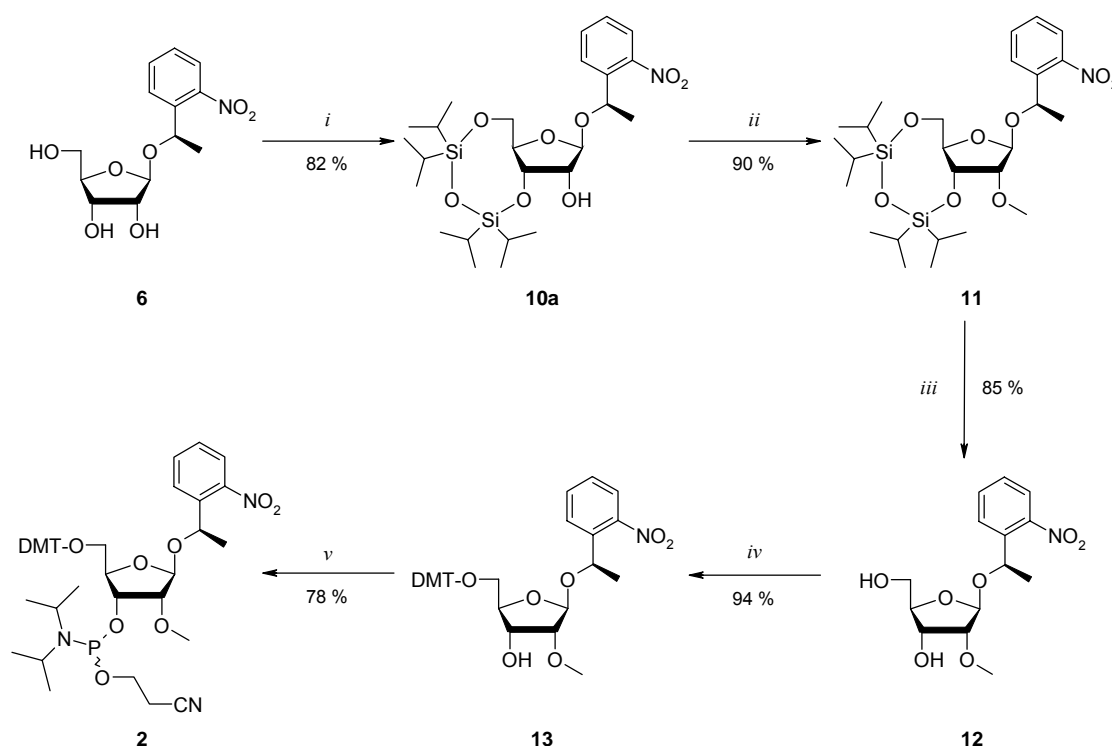


Figure 2.2 NOE spectra of 2'-O-TOM nucleoside **9a**

2.1.3 Synthesis of the 2'-O-Me RNA abasic site precursor

Intermediate **6** was TIPDS protected to give **10**.^[164] The 2'-hydroxyl group was then methylated using methyl iodide and silver(I)oxide to give **11**.^[165] Deprotection with TBAF yielded diol **12**. Protection with DMT-chloride and the formation of the phosphoramidite **2** was performed as already described.

If a mixture of diastereomers of **6** was used for synthesis, the two isomers could be separated by column chromatography at the stage of intermediate **10**. Spectroscopic data were collected for both diastereomers **10a** and **10b**. Stereoisomer **10a** was used for further synthesis.



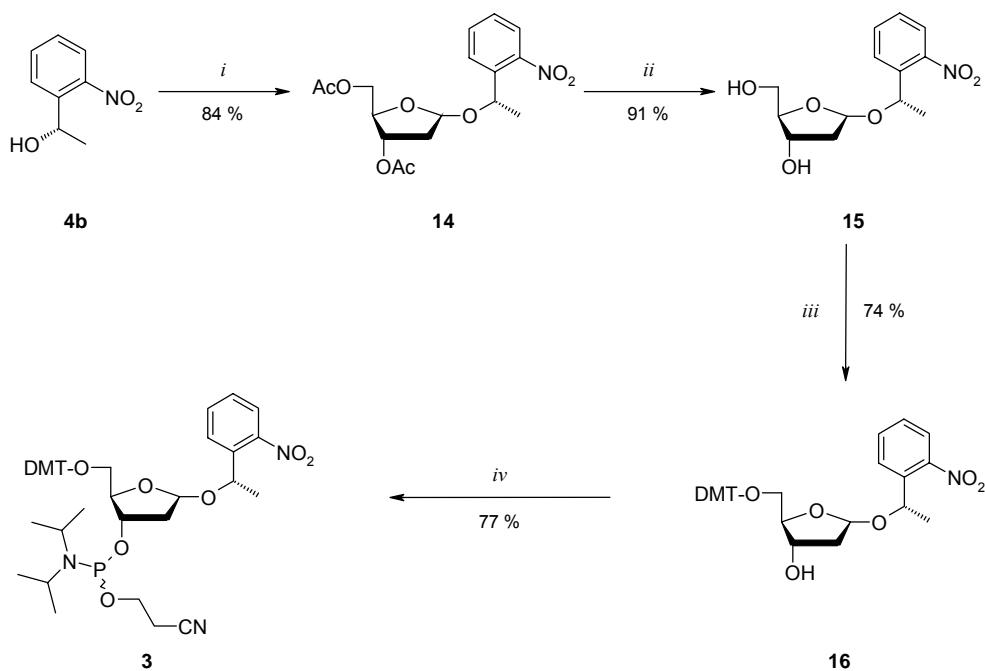
Scheme 2.4 i) TIPDS-Cl, pyridine; ii) MeI, AgO, 50 °C; iii) TBAF, THF; iv) DMT-Cl, pyridine; v) CEP, *i*Pr₂NEt, THF

[164] Markiewicz, W. T., *J. Chem. Res., Synop.* **1979**, 24-25.

[165] Zhang, N., Chen, H.-M., Koch, V., Schmitz, H., Liao, C.-L., Bretner, M., Bhaddi, V. S., Fattom, A. I., Naso, R. B., Hosmane, R. S., Borowski, P., *J. Med. Chem.* **2003**, *46*, 4149-4164.

2.2 Synthesis of the DNA Abasic Site Precursor

(1',3',5')-Tri-*O*-acetyl-2'-deoxy-D-ribofuranose was synthesized according to the method of *Robins* et al.: 2-deoxyadenosine was acetylated and the product was subsequently acetolysed to give the desired starting material.^[166] The synthesis was performed with 1-(*S*)-(2-nitrophenyl)ethanol **4b** as described for the RNA abasic site precursor with comparable yields.



Scheme 2.5 *i*) *Tri-O*-acetyl-2'-deoxyribofuranose, *TMSOTf*, CH_3CN , $-20\text{ }^\circ\text{C}$; *ii*) Na_2CO_3 , *MeOH*; *iii*) *DMT-Cl*, *pyridine*; *iv*) *CEP*, iPr_2Net , *THF*

The synthesis was performed with the mixture of the anomers although at the stages of the intermediates **14** and **16** the anomers would be separable, according to TLC.

2.3 Oligonucleotide Synthesis

All oligonucleotides were prepared by automated oligonucleotide synthesis by using the cyanoethyl-phosphoramidite approach.^[167,168] For RNA synthesis, 2'-*O*-TBDMS protected PAC-phosphoramidites were used. For DNA synthesis benzoyl (dA, dC) and isobutyryl (dG) protected phosphoramidites and controlled pore-glass solid supports (*Glen Research*) were used. The synthesis was performed by using the same standard coupling protocol for DNA and RNA with 5-(ethylthio)-1*H*-tetrazole as activator and a coupling time of 90 seconds for DNA and 6 minutes for RNA. The modified phosphoramidites were allowed to couple for 6 min and 12 min for DNA and RNA, respectively. Solid supports were treated with EtOH/NH₄OH (1:4) at 55 °C, overnight.

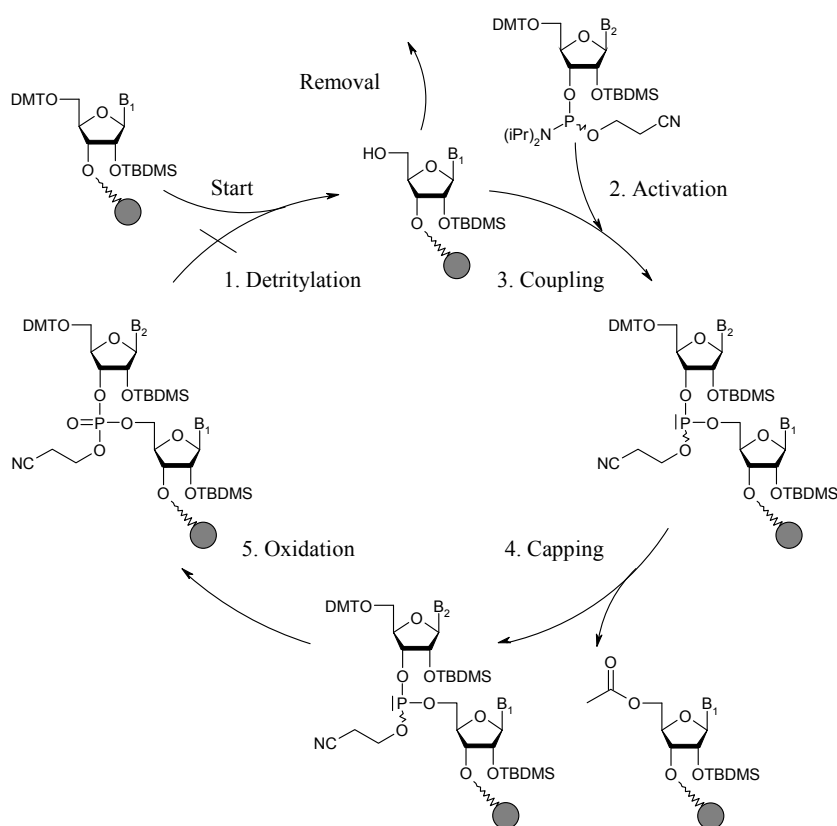


Figure 2.3 Automated RNA synthesis cycle (DMT: 4,4'-dimethoxy-triphenyl; TBDMS: *tert.*-butyldimethylsiloxy; B₁, B₂: protected nucleobases or INPE)

[167] Beaucage, S. L., *Methods Mol. Biol.* **1993**, 20, 33-61.

[168] Mueller, S., Wolf, J., Ivanov, S. A., *Curr. Org. Synth.* **2004**, 1, 293-307.

3 Results and Discussion

3.1 General Remarks

The synthesized abasic site precursors are incorporated via automated oligonucleotide chemistry into heptamers of the general form $5' \text{AGG-}AS_p\text{-UUC}3'$, where AS_p is the protected abasic site. This sequence is chosen for several reasons:

- Oligonucleotides are of a length that they can be easily purified by RP-HPLC
- The sequence is not self-complementary: no stable secondary structure is possible and could disturb kinetic measurements. The shortness of the oligonucleotide furthermore prevents double stranded structures
- Fragments arising from the cleavage at the abasic site have distinguishable masses: a heavier 5' fragment consisting of three purine bases and a lighter 3' fragment consisting of three pyrimidine bases
- The resulting fragments allow that the reactions can be followed by RP-HPLC since the fragments will have different UV-absorption properties and they will most likely have different retention times
- Kinetic results of the different reactions are directly comparable if the very same oligonucleotide sequence is used for all experiments and possible differences in kinetic parameters are not due to structural influence

It was found that the chosen heptamer structure gives HPLC spectra with reasonable resolution. Moreover the deprotection step of the embedded abasic site precursor can be followed easily since the change in retention time is around 4 minutes.

The abbreviations used for the different natural and modified nucleotides are shown in Table 3.1.

Table 3.1 *Used abbreviations of the different nucleotides*

Abbreviation	Structure
A, G, C, T, U	unmodified nucleotides
a, g, u	2'-O-methylated nucleotides
X_p/X	protected/unprotected RNA abasic site
x_p/x	protected/unprotected 2'-O-methylated RNA abasic site
Y_p/Y	protected/unprotected DNA abasic site

3.2 Deprotection Kinetics

3.2.1 RNA abasic site deprotection kinetics

To verify the clean deprotection of the natural abasic site precursor, ribonucleotide heptamers of the structure $r(\text{AGGX}_p\text{UUC})$, containing a protected abasic site X_p (= 1'-1NPE-protected ribose) at position four, were irradiated for different time intervals with a UV lamp. The concentration of the oligonucleotides for the deprotection step was chosen to be $1 \text{ OD}_{260}\text{mL}^{-1}$.

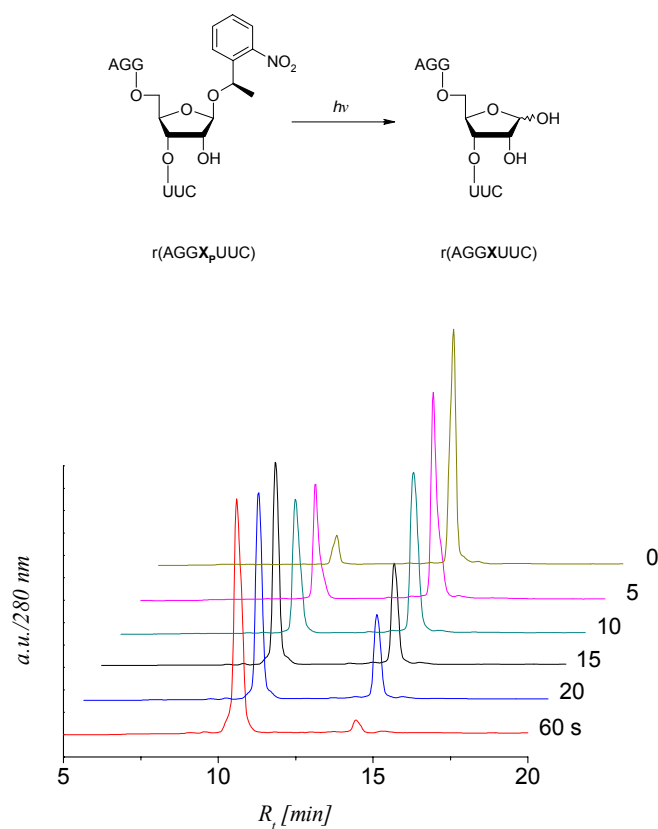


Figure 3.1 280 nm RP-HPLC traces for different UV-irradiation intervals: the integral of the protected heptamer $r(\text{AGGX}_p\text{UUC})$ ($R_t = 14.5$ min) decreases to give the abasic heptamer $r(\text{AGGXUUC})$ ($R_t = 10.8$ min). HPLC gradient: 0-50 % B in 30 min

The HPLC traces in Figure 3.1 show that the deprotection step is clean and that the oligonucleotide is not digested under the applied conditions. The integrals of the protected and the deprotected oligonucleotide were calculated and the time dependent change of the substrate integral was plotted (Figure 3.2), assuming the combined integrals of one run to be constantly 100%. Since the loss of the aromatic abasic site protecting group decreases the overall UV absorption with increasing time intervals, this assumption produces a mistake with longer irradiation intervals. Nevertheless, this minor influence was neglected here.

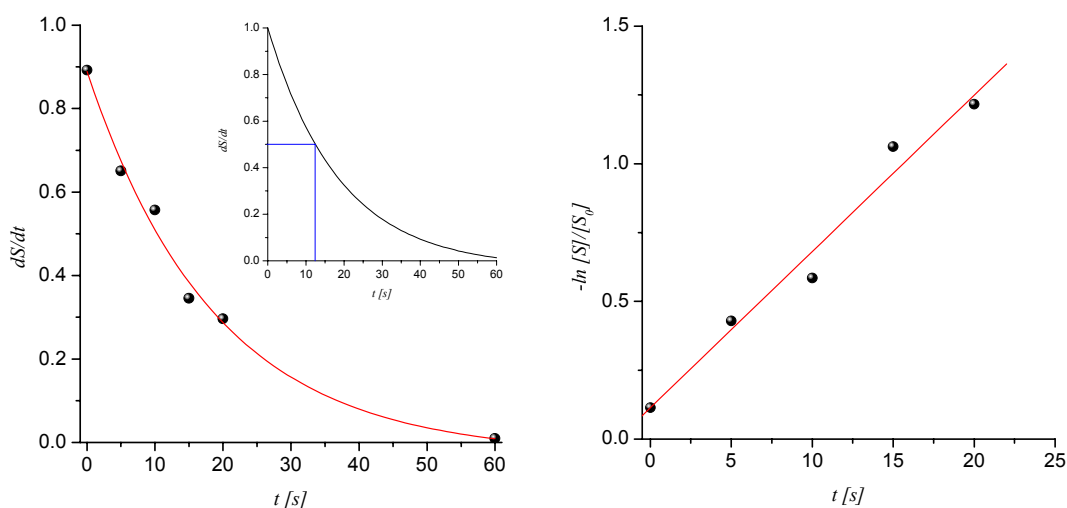


Figure 3.2 First order exponential fit of $d[S]/dt$ after different deprotection intervals of $r(\text{AGGX}_p\text{UUC})$ calculated from the HPLC traces (left). Linear fit of the five first data points to prove first order character of the reaction (right)

The calculation of the first order exponential fit gave a half-life time of $T_{1/2} = 12.5$ seconds and the linear fit of $-\ln[S]/[S_0]$ gave the velocity constant $k = 5.68 \cdot 10^{-2} \text{ s}^{-1}$.

Since the synthesis demonstrated that the 1NPE group is chemically stable against a variety of chemical conditions, this loss can therefore be explained by the action of residual light at low oligonucleotide concentration. For further deprotection reactions an irradiation time of 2 minutes was found to be sufficient to achieve almost quantitative deprotection. It was found later that high yield deprotection can be obtained by irradiation with a slide projector for 6 up to 10 minutes. Moreover it was shown that the tungsten halogen projector does not emit UV light below 320 nm due to its lens system. This is a very elegant and soft deprotection method that was preferably applied.

Table 3.2 Fragment masses of the educt and the product of the photochemical deprotection

Nr	R_t [min]	Structure	Formula	m/z calc	m/z found
1	10.8	$r(\text{AGGXUUC})$	$\text{C}_{62}\text{H}_{79}\text{N}_{22}\text{O}_{48}\text{P}_6$	2086.28	2086.32
2	14.5	$r(\text{AGGX}_p\text{UUC})$	$\text{C}_{70}\text{H}_{86}\text{N}_{23}\text{O}_{50}\text{P}_6$	2235.42	2236.44

3.2.2 DNA abasic site deprotection kinetics

To be able to compare RNA abasic sites to DNA abasic sites in further experiments, the same deprotection kinetics were also performed for a natural DNA abasic site precursor. Deoxyribonucleotide heptamers of the same sequence $d(\text{AGGY}_p\text{TTC})$ (Y_p being the 1'-(1-(2-nitrophenyl)ethyl)-protected deoxyribose unit) were irradiated at the same concentration of $1 \text{ OD}_{260}\text{mL}^{-1}$ for different time intervals.

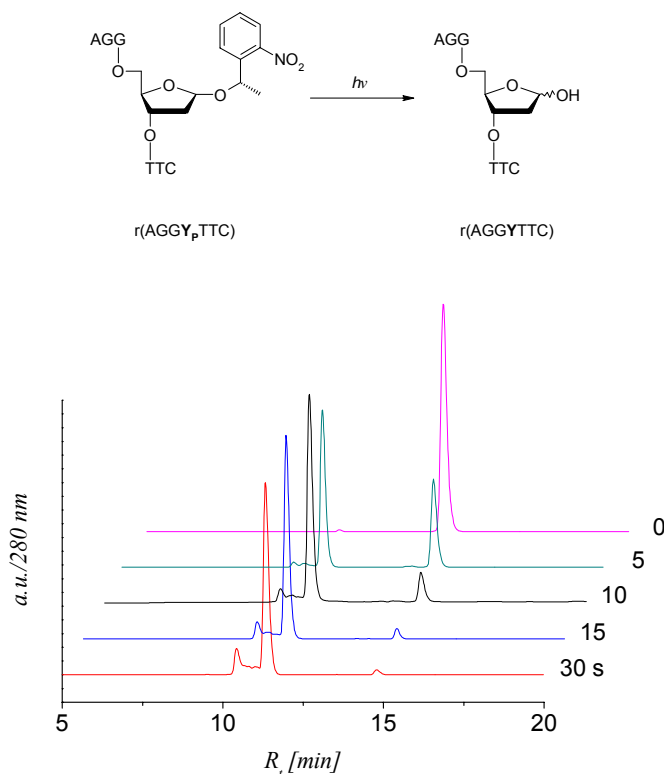


Figure 3.3 280 nm RP-HPLC traces for different UV-irradiation intervals: the integral of the protected heptamer $d(\text{AGGY}_p\text{TTC})$ ($R_t = 14.7 \text{ min}$) decreases to give the abasic heptamer $d(\text{AGGYTTC})$ ($R_t = 11.3 \text{ min}$). HPLC gradient: 0-50 % B in 30 min

The experiments were performed in a similar way described in the section above. Remarkable is that the deprotection reaction is even faster compared to the RNA analogue. The calculation of the first order exponential fit gave a half-life time of $T_{1/2} = 3.4 \text{ seconds}$ and the linear fit of $-\ln[S]/[S_0]$ gave the velocity constant $k = 2.11 \cdot 10^{-1} \text{ s}^{-1}$.

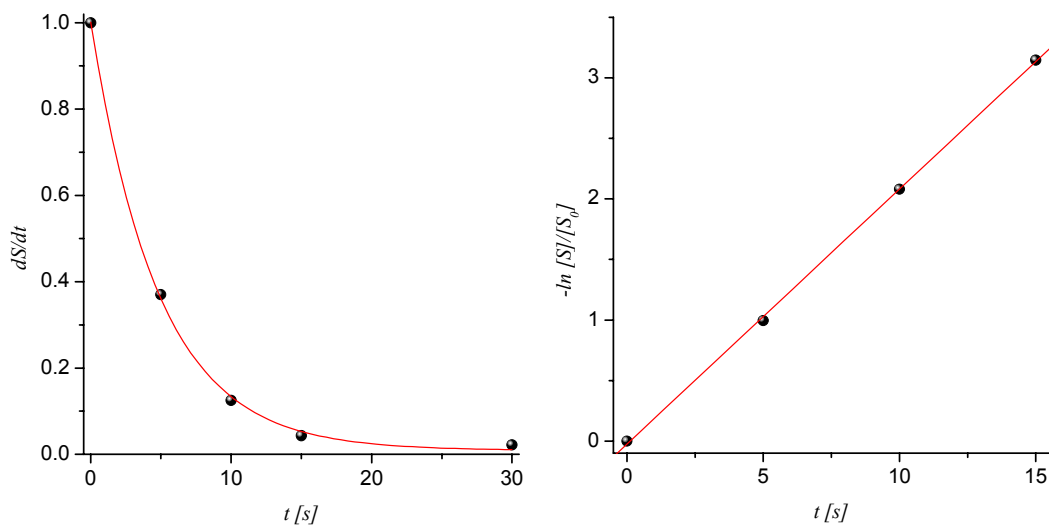


Figure 3.4 First order exponential fit of $d[S]/dt$ after different deprotection intervals of $r(\text{AGGY}_p\text{TTC})$ calculated from the HPLC traces. Linear fit of the four first data points to prove first order character of the reaction (right)

UV deprotection with longer irradiation time gave rise to a side product with $R_t = 10.4$ minutes, as can be seen in Figure 3.3. This side product has not been identified so far. From experiments that will be discussed later in this section it followed that this side product is not due to strand cleavage. It has also been observed, that using a slide projector as light source for 5 minutes did not give rise to this side product. We thus conclude that this side product most likely results from UV-induced base damage.

Table 3.3 Fragment masses of the educt and the product of the photochemical deprotection

Nr	R_t [min]	Structure	Formula	m/z calc	m/z found
1	11.3	$r(\text{AGGYTTC})$	$\text{C}_{64}\text{H}_{83}\text{N}_{22}\text{O}_{41}\text{P}_6$	2002.33	2002.88
2	14.7	$r(\text{AGGY}_p\text{TTC})$	$\text{C}_{72}\text{H}_{90}\text{N}_{23}\text{O}_{43}\text{P}_6$	2151.47	2151.88

3.2.3 Reaction mechanism of the deprotection reaction

The mechanism of the deprotection of nitrobenzyl units has been widely described.^[169-171] For photoreactions in neutral aqueous media the following reaction mechanism is proposed. The reaction is initiated by a very fast intramolecular 1,5-*H* shift yielding an *aci*-nitro protomer as a primary photoproduct. The next step is a cyclization to form a short-living benzisoxazolidine. The nitrophenyl unit is then released as a carbonyl hydrate which then further dehydrates to give nitrosoacetophenone. In a closer view the initial step is the result of the activation of the nitro group by UV light. The formed unstable biradical then very fast abstracts a benzylic hydrogen and forms a more stable benzylic radical. The benzylic radical is in equilibrium with the *aci*-nitro isomer. The latter then cyclizes to give the short living benzisoxazolidine.

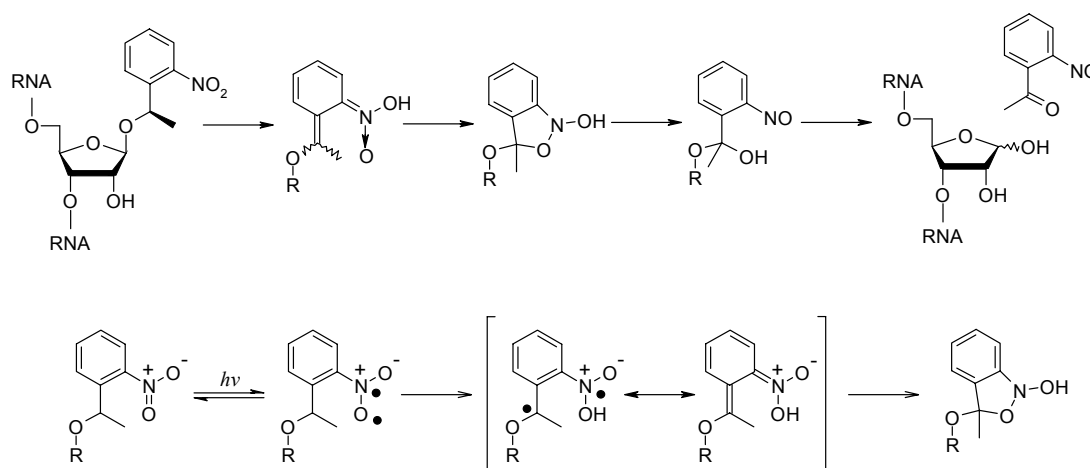


Figure 3.5 Reaction mechanism of the deprotection of a 1-(2-nitrophenyl)ethyl-protected sugar moiety

3.2.4 Deprotection methods

For the kinetic studies of the deprotection reaction a medium pressure UV immersion lamp (150W) was used. The spectrum of the relative spectral radiant flux shows that there is considerable emission at wavelengths below 315 nm (Figure 3.6). The deprotection reactions were carried out in quartz cuvettes. Because quartz glass does not absorb wavelengths above ~180 nm the UV-C and UV-B light could eventually damage the nucleic acids. Therefore a smother deprotection method was looked for. For the deprotection of oligoribonucleotides carrying a [(2-nitrobenzyl)oxy]methyl (= nbm) moiety as a 2'-hydroxy protecting group, Pitsch used a slide projector.^[172]

[169] Blanc, A., Bochet, C. G., *J. Am. Chem. Soc.* **2004**, *126*, 7174-7175.

[170] Il'ichev, Y. V., Schwoerer, M. A., Wirz, J., *J. Am. Chem. Soc.* **2004**, *126*, 4581-4595.

[171] Gaplovsky, M., Il'ichev, Y. V., Kamdzhilov, Y., Kombarova, S. V., Mac, M., Schwoerer, M. A., Wirz, J., *Photochem. Photobiol. Sci.* **2005**, *4*, 33-42.

[172] Pitsch, S., *Helv. Chim. Acta* **1997**, *80*, 2286-2314.

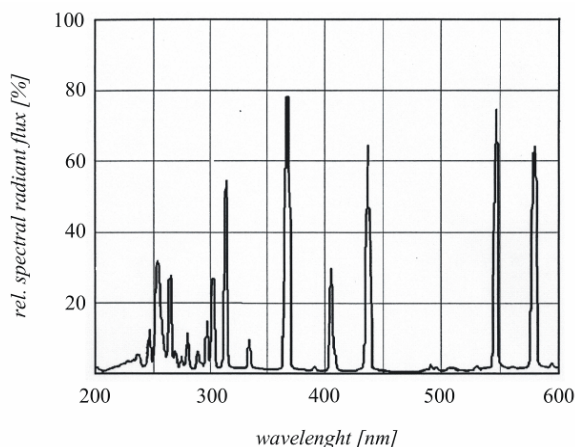


Figure 3.6 Relative spectral radiant flux of the medium pressure UV immersion lamp from Heraeus

In contrary to the experiment of *Pitsch* where he used the nbm-group on every sugar moiety, in the here used heptamers just one photocleavable group is present. No quenching effect of the 2-nitrosoacetophenone should therefore be observed in this case.

The slide projector was used with its two beam focusing lenses in place but with the final zooming lens removed. Additionally a slide-frame with a thin glass plate was placed in the beam. The distance between the lamp and the irradiated sample was approximately 20 cm. The relative emission spectrum of the unshielded 250 W tungsten lamp is shown in Figure 3.7. The relative intensity of the wavelengths below 350 nm is very small and with the focusing lens system and the additional glass plate placed in the beam it can be assumed that wavelengths below 320 nm are almost completely cut out.

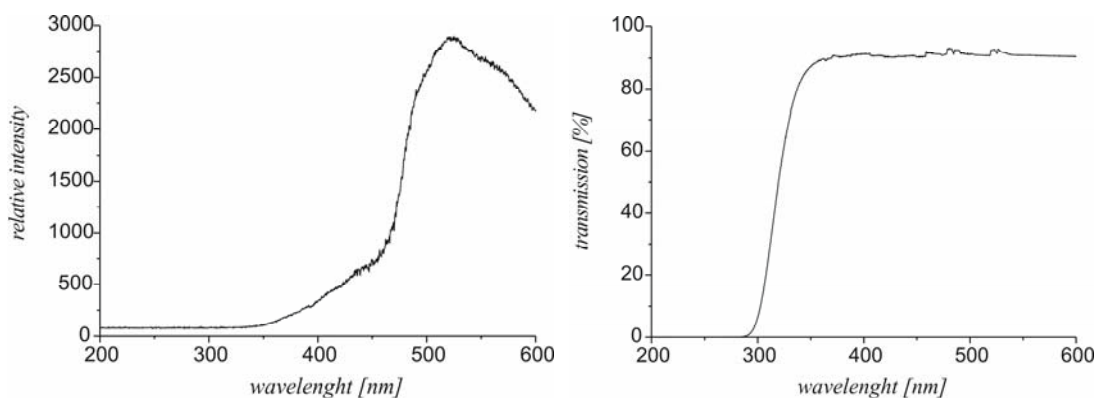


Figure 3.7 Relative emission spectrum of the used slide projector and the absorption spectrum of the used glass filter

For heptamers containing protected RNA or DNA abasic sites a deprotection time of 6 minutes showed to be sufficient for high yield deprotection. This method was further applied in this study.

3.3 Strand Cleavage under Basic Conditions

3.3.1 Cleavage of RNA under basic conditions

In order to study the stability of a natural RNA abasic site, a heptamer of the sequence $r(\text{AGGX}_p\text{UUC})$ was deprotected and $1 \text{ OD}_{260}\text{ml}^{-1}$ of the resulting abasic heptamer $r(\text{AGGXUUC})$ is incubated with a NaOH of a final concentration of 0.1 M for 30 minutes. *Bailly* reported that incubation at 37°C for 15 minutes with 0.2 M NaOH is sufficient to cleave all present abasic sites.^[81]

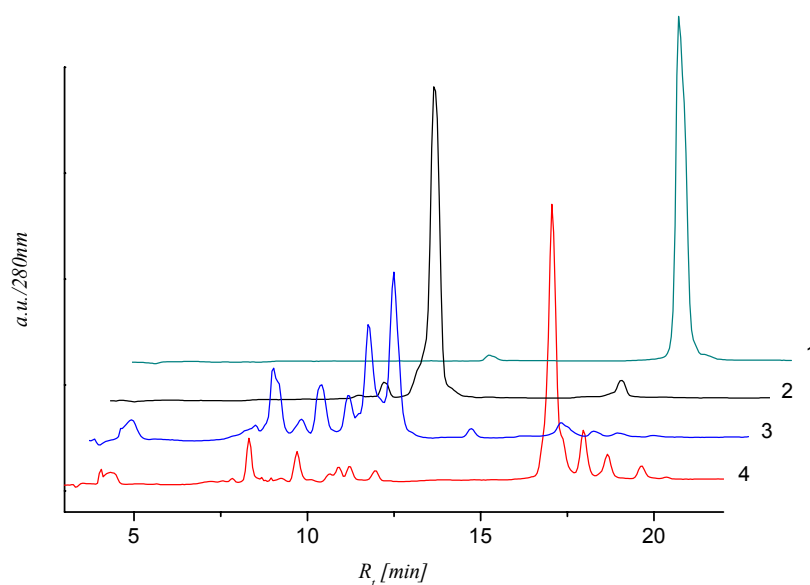


Figure 3.8 280 nm HPLC traces of decay of RNA heptamer $r(\text{AGGX}_p\text{UUC})$. Lane 1: protected heptamer $r(\text{AGGX}_p\text{UUC})$; lane 2: deprotected heptamer $r(\text{AGGXUUC})$ (60 s deprotection time with UV lamp); lane 3: deprotected heptamer $r(\text{AGGXUUC})$ (60 s deprotection time), 0.1 M NaOH, 30 min, 37°C ; lane 4: protected heptamer $r(\text{AGGX}_p\text{UUC})$, 0.1 M NaOH, 30 min, 37°C . HPLC gradient: 0-40 % B in 30 min

The HPLC chromatograms show that the abasic oligoribonucleotide is cleaved quantitatively. The control shows that even the protected heptamer is cleaved to a non negligible amount. Both oligomers give rise to a similar fragment pattern. The protected heptamer is cleaved via cyclophosphate formation.^[173-175] For the abasic heptamer we have an overlay of the cyclophosphate formation and the β,δ -elimination reaction mechanisms. In the following experiments heptamers with protected 2'-hydroxyl groups were used in order to be able to investigate both mechanisms combined and separately. Already from this preliminary result it is obvious that the abasic site strongly enhances the digestion of the heptamer under basic conditions.

[173] Anslyn, E., Breslow, R., *J. Am. Chem. Soc.* **1989**, *111*, 4473-4482.

[174] Breslow, R., *Acc. Chem. Res.* **1991**, *24*, 317-324.

[175] Breslow, R., *Proc. Natl. Acad. Sci. U. S. A.* **1993**, *90*, 1208-1211.

3.3.2 Kinetics of the β,δ -elimination mechanism of an RNA abasic site

To study the two strand cleavage mechanisms β,δ -elimination and cyclophosphate formation independently, a fully 2'-*O*-methylated RNA heptamer containing an abasic site precursor x_p is chosen: $r(\text{agg}x_p\text{uuC})$. By the 2'-*OMe* modification any cyclophosphate formation and thus undesired strand cleavage can be excluded. The oligomer ($c = 1 \text{ OD}_{260}\text{mL}^{-1}$) was deprotected by UV light with a slide projector for 6

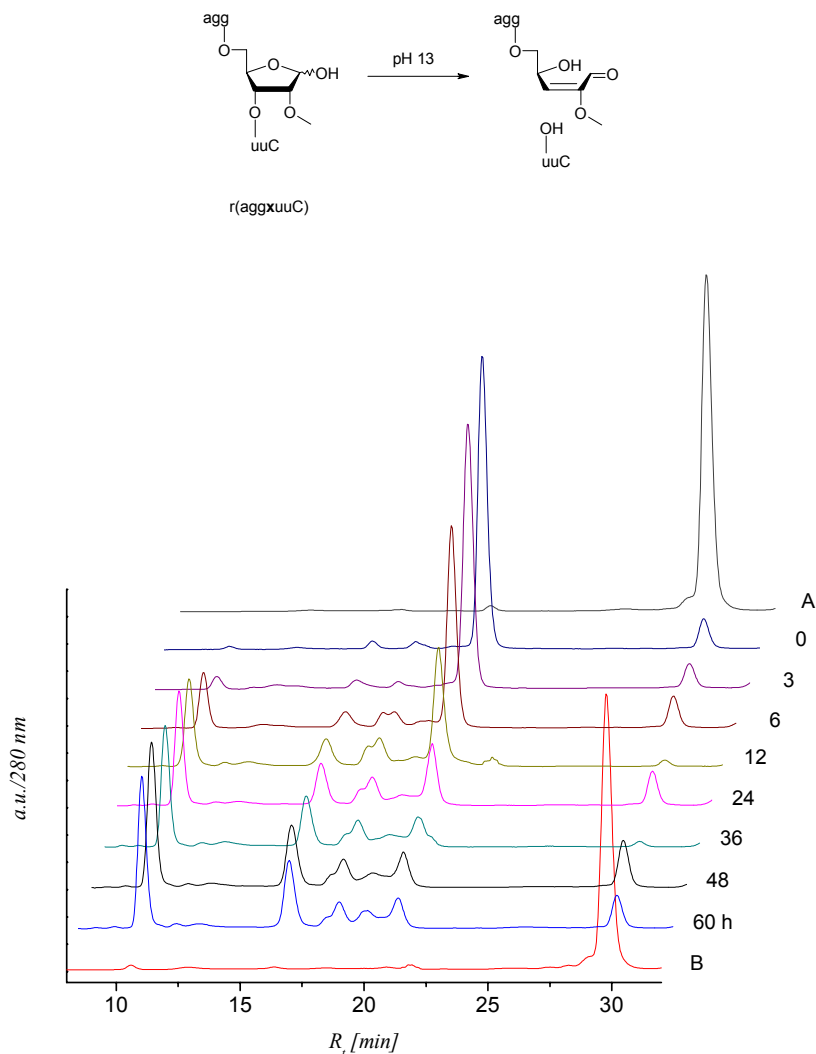


Figure 3.9 280 nm HPLC traces of β -elimination reaction of a fully 2'-*O*-methylated heptamer $r(\text{agg}x\text{uuC})$. Lane A: protected heptamer $r(\text{agg}x_p\text{uuC})$; lane B: protected heptamer $r(\text{agg}x_p\text{uuC})$, 0.1 M NaOH, 48 h, 37 °C. HPLC gradient: 0-30 % B in 40 min

minutes and the resulting abasic oligonucleotide was then submitted to basic conditions (0.1 M NaOH) at 37 °C. Strand cleavage was followed by RP-HPLC. From the HPLC traces in Figure 3.9 it is observed that the integral of the abasic heptamer $r(\text{agg}x\text{uuC})$ ($R_t = 20.6$ min) decreases while at the same time the integrals of three fragments with lower retention times are increasing ($R_t = 10.5, 16.1, 18.2$ min).

Furthermore lane B in Figure 3.9 proves that no cyclophosphate formation occurred: the protected heptamer r(aggx_puuC) ($R_t = 29.2$ min) is completely stable against the basic treatment.

To calculate the half-life time of the β -elimination strand cleavage reaction, the integrals for the peaks 1 to 4 (Figure 3.11) for the different reaction times were calculated and the percentage of integral 4 from the total integral was plotted and fitted with a first order exponential decay (Figure 3.10).

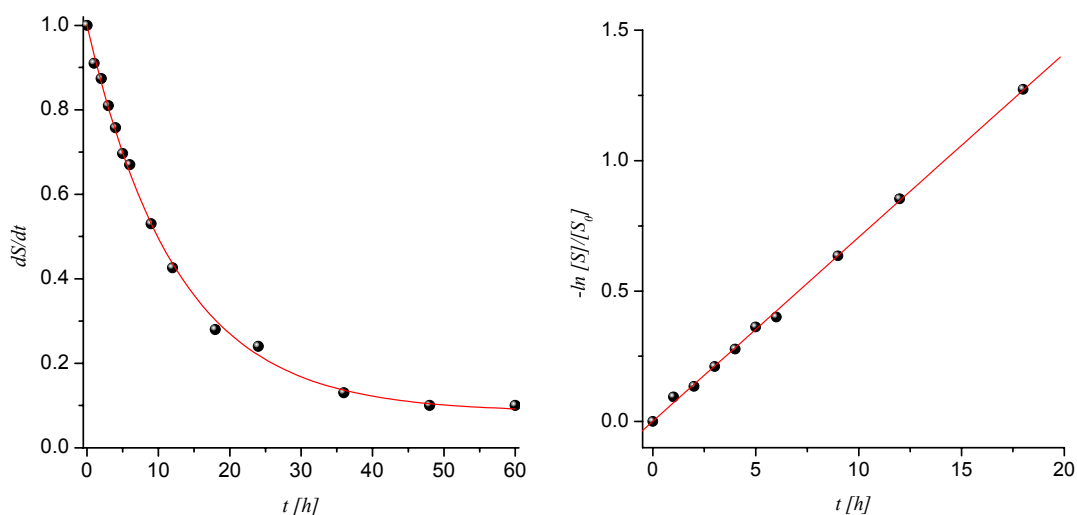


Figure 3.10 First order exponential fit of $d[S]/dt$ after different incubation intervals of r(aggxuuc) calculated from the HPLC traces. Linear fit without the last data points to prove first order character of the reaction (right)

The calculation of the first order exponential fit gave a half-life time of $T_{1/2} = 9 \text{ h } 54 \text{ min}$ and the linear fit of $-\ln[S]/[S_0]$ gave the velocity constant $k = 1.96 \cdot 10^{-5} \text{ s}^{-1}$.

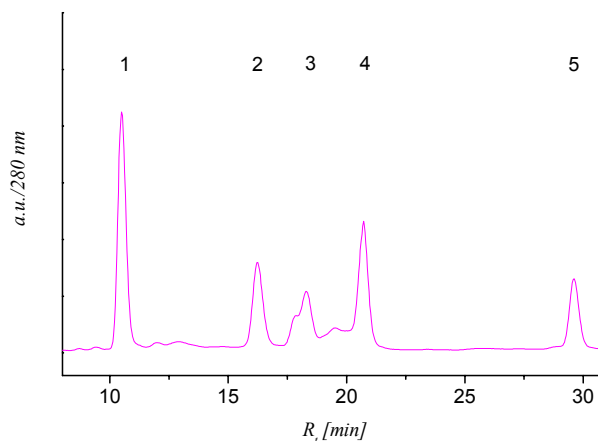


Figure 3.11 Fragment analysis of the β,δ -elimination mechanism. Heptamer $r(\text{aggxuuc})$ is treated with 0.1 M NaOH for 24 h at 37 °C and analyzed by RP-HPLC (gradient: 0-30 % in 40 min)

To prove the expected β,δ -elimination, heptamer $r(\text{aggxuuc})$ was incubated at 0.1 M NaOH at 37 °C for 24 hours. The different fragments **1** to **3** were then separated by RP-HPLC (Figure 3.11) and analyzed by ESI⁺ mass spectrometry. The fragment masses found corresponded to the expected fragments calculated for the β,δ -elimination as shown in Table 3.4. Fragments **1** and **3** correspond to the expected fragments after a β -elimination, whereas fragment **2** corresponds to fragment **3** after the subsequent δ -elimination reaction.

Table 3.4 Identified fragments of heptamer $r(\text{aggxuuc})$ cleavage

Nr	R_t [min]	Structure	Formula	m/z calc	m/z found
1	10.5	$r(\text{puuC})$	$\text{C}_{29}\text{H}_{40}\text{N}_7\text{O}_{24}\text{P}_3$	963.60	963.64
2	16.1	$r(\text{aggp})$	$\text{C}_{33}\text{H}_{44}\text{N}_{15}\text{O}_{21}\text{P}_3$	1079.73	1079.26
3	18.2	$r(\text{aggp-rb})$	$\text{C}_{39}\text{H}_{52}\text{N}_{15}\text{O}_{24}\text{P}_3$	1207.86	1207.34
4	20.6	$r(\text{aggxuuc})$	$\text{C}_{68}\text{H}_{92}\text{N}_{22}\text{O}_{48}\text{P}_6$	2171.45	2171.00
5	29.2	$r(\text{aggx}_p\text{uuc})$	$\text{C}_{76}\text{H}_{99}\text{N}_{23}\text{O}_{50}\text{P}_6$	2320.60	2320.13

$rb = 4,5$ -dihydroxy-2-methoxy-2-pentenal

3.3.3 Cyclophosphate formation mechanism of RNA

In order to study the cyclophosphate formation independently from the β,δ -elimination an oligonucleotide without a free abasic site was chosen. Furthermore the oligonucleotide should just have one possibility for a cyclophosphate formation to occur in order to avoid the generation of numerous different fragments. The oligonucleotide $r(\text{aggX}_p\text{uuC})$ fulfilled these demands: just one 2'-hydroxy group was not methylated and thus reactive and the abasic site precursor remained protected so that no β -elimination was possible. The oligonucleotide ($c = 1 \text{ OD}_{260}\text{mL}^{-1}$) was submitted to basic conditions (0.1 M NaOH) at 37 °C. Strand cleavage was then again followed by HPLC.

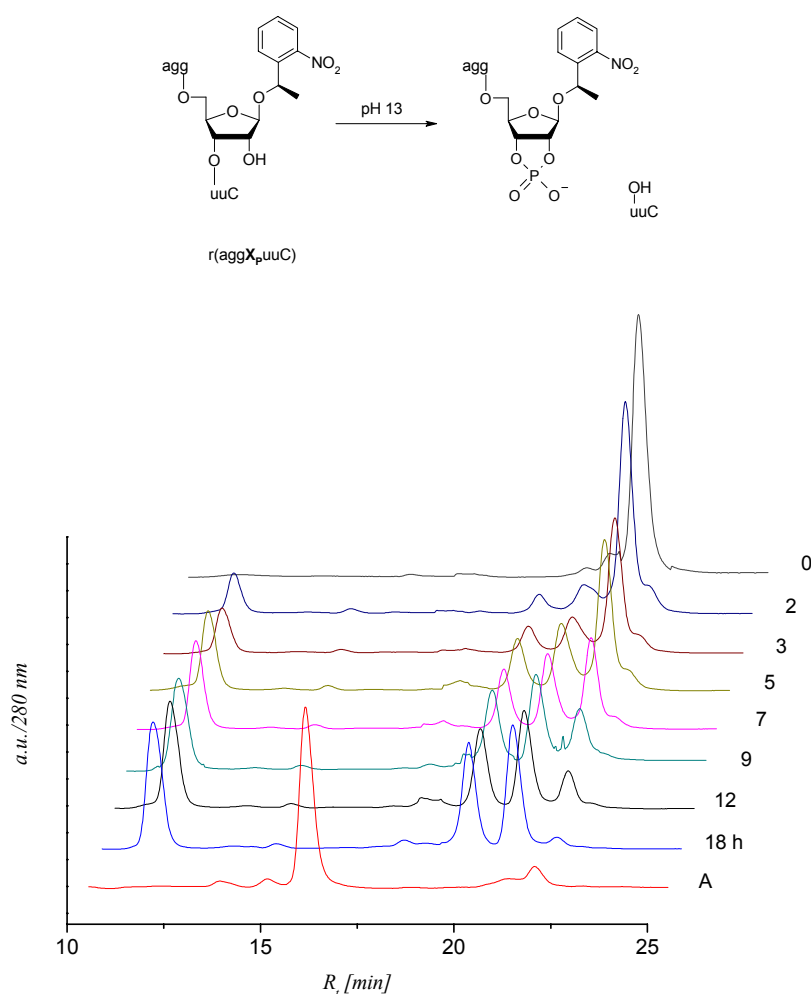


Figure 3.12 280 nm HPLC traces of the cyclophosphate reaction of a partially 2'-O-methylated heptamer $r(\text{aggX}_p\text{uuC})$. Lane A: deprotected heptamer $r(\text{aggXuuC})$. HPLC gradient: 0-30 % B in 30 min

The collected HPLC traces in Figure 3.12 show that the integral of the protected heptamer $r(\text{aggX}_p\text{uuC})$ ($R_t = 21.7 \text{ min}$) is decreasing while the integrals of one fragment with a significantly ($R_t = 11.6 \text{ min}$) and two fragments with slightly lower retention times ($R_t = 19.5, 20.6 \text{ min}$) are increasing. Lane A shows the oligonucleotide

r(aggXuuC) with a free abasic site. Since this peak does not occur in the other lanes it can be followed that the 1NPE group is totally stable under the applied basic conditions and thus no β -elimination is possible.

To calculate the half-life time of the cyclophosphate strand cleavage reaction, the integrals for the peaks **1** to **4** (Figure 3.14) for the different reaction times were calculated and the percentage of integral **4** from the total integral was plotted and fitted with a first order exponential decay (Figure 3.13).

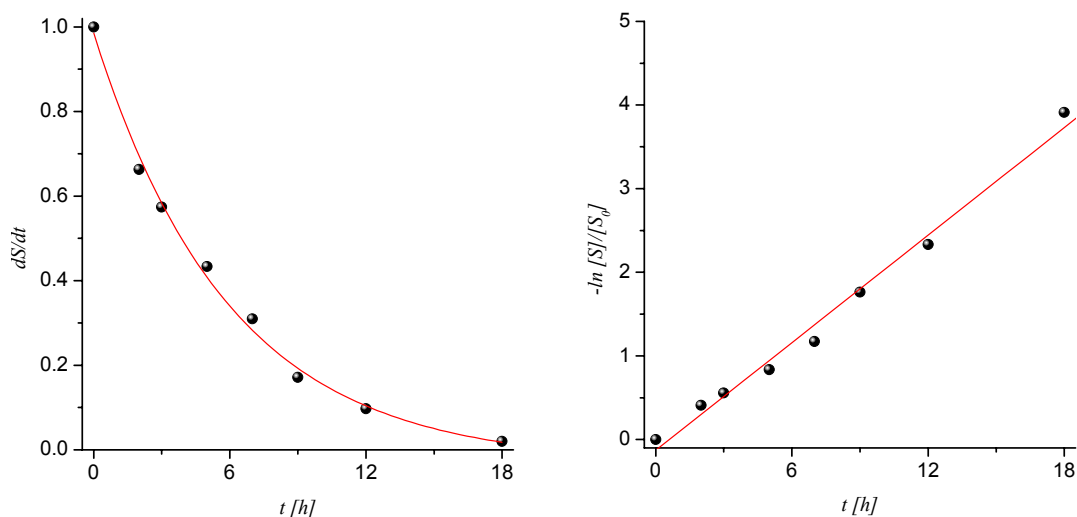


Figure 3.13 First order exponential fit of $d[S]/dt$ after different incubation intervals of r(aggX_puuC) calculated from the HPLC traces. Linear fit using all data points to prove first order character of the reaction (right)

The calculation of the first order exponential fit gave a half-life time of $T_{1/2} = 3 \text{ h } 41 \text{ min}$ and the linear fit of $-\ln[S]/[S_0]$ gave the velocity constant $k = 5.95 \cdot 10^{-5} \text{ s}^{-1}$.

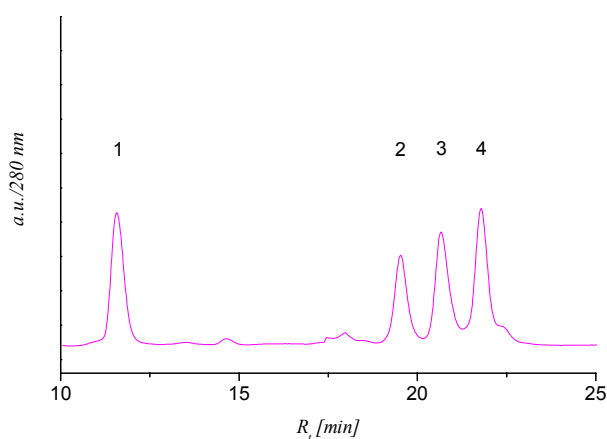


Figure 3.14 Fragment analysis of the cyclophosphate formation mechanism. Heptamer r(aggX_puuC) is treated with 0.1 M NaOH for 7 h at 37 °C and analyzed by RP-HPLC (gradient: 0-30 % in 30 min)

To prove the expected cyclophosphate formation, heptamer $r(\text{aggX}_p\text{uuC})$ was incubated at 0.1 M NaOH at 37 °C for 7 hours. The different fragments **1** to **4** were then separated by RP-HPLC (Figure 3.14) and analyzed by ESI⁻ mass spectroscopy. The neutral fragment masses found corresponded to the expected fragments calculated for the cyclophosphate formation as shown in Table 3.5.

Table 3.5 Identified fragments of heptamer $r(\text{aggX}_p\text{uuC})$ cleavage

Nr	R _t [min]	Structure	Formula	m/z calc	m/z found
1	11.6	$r(\text{uuC})$	$\text{C}_{29}\text{H}_{39}\text{N}_7\text{O}_{21}\text{P}_2$	883.62	883.20
2	19.5	$r(\text{aggX}_p\text{p})$	$\text{C}_{46}\text{H}_{60}\text{N}_{16}\text{O}_{30}\text{P}_4$	1440.98	1440.35
3	20.6	$r(\text{aggX}_p\text{p})$	$\text{C}_{46}\text{H}_{60}\text{N}_{16}\text{O}_{30}\text{P}_4$	1440.98	1440.34
4	21.7	$r(\text{aggX}_p\text{uuC})$	$\text{C}_{75}\text{H}_{97}\text{N}_{23}\text{O}_{50}\text{P}_6$	2306.58	2306.57

Fragments **2** and **3** showed the exact same mass. Whether the fragments correspond to the 2'- or 3'-phosphate or a mixture of both can not be determined from these data. For the question why there are two different peaks ($R_t = 19.5, 20.6$ min) with the same mass, there are two answers:

- one peak corresponds to the 2'-phosphate, whereas the other one corresponds to the 3'-phosphate
- one peak corresponds to the mixture of the 2'/3'- phosphates and the second peak contains the cyclophosphate

We assume that the cyclophosphate does not survive the lyophilisation after HPLC and that it is cleaved ruling out the second line of explanation.

3.3.4 Strand cleavage mechanism of a natural RNA abasic site

Since the two common strand cleavage mechanisms in RNA were studied in detail, it was necessary to study the combination of both.

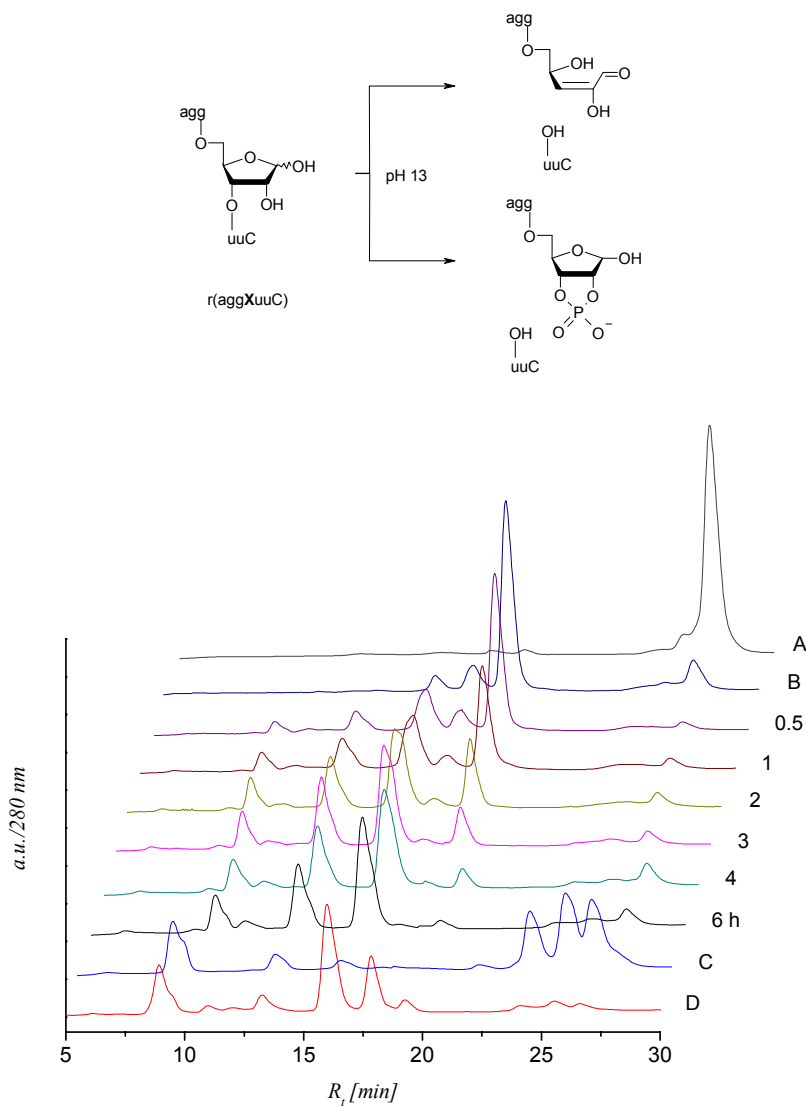


Figure 3.15 280 nm HPLC traces of the cleavage reaction of a true abasic site embedded in a 2'-methylated heptamer $r(\text{aggXuuC})$. Lane A: protected heptamer $r(\text{aggX}_p\text{uuC})$; lane B: deprotected heptamer $r(\text{aggXuuC})$; lane C: protected heptamer $r(\text{aggX}_p\text{uuC})$, 0.1 M NaOH, 6.5 h, 37 °C; lane D: protected heptamer, 0.1 M NaOH, 6.5 h, 37 °C, → deprotected after reaction. HPLC gradient: 0-30% B in 40 min

For this purpose an oligonucleotide of the form $r(\text{aggXuuC})$ was chosen. At position four this oligonucleotide contained a natural abasic site. This position is the only one susceptible to strand cleavage reactions by β,δ -elimination and cyclophosphate formation.

The oligonucleotide ($c = 1 \text{ OD}_{260}\text{mL}^{-1}$) was deprotected as usual with a slide projector for 6 minutes and then submitted to basic conditions (0.1 M NaOH) at 37 °C. Strand cleavage was then again followed by RP-HPLC.

The overlay of different mechanisms gives rise to a higher number of possible fragments. Again just the main fragments are further investigated. Protected heptamer $r(\text{aggX}_p\text{uuC})$ ($R_t = 27.3 \text{ min}$) is deprotected and is transformed to $r(\text{aggXuuC})$ ($R_t = 19.4 \text{ min}$). During the reaction the integral of this heptamer decreases and three main peaks with shorter retention times ($R_t = 10.2, 13.7, 16.4 \text{ min}$) arise. To have a first indication whether cyclophosphate formation would be dominant, protected heptamer $r(\text{aggX}_p\text{uuC})$ was submitted to basic conditions (0.1 M NaOH at 37 °C for 6.5 h) as can be seen in lane C (Figure 3.15) and deprotected afterwards (lane D). Although the fragments and retention times are quite similar to the digested real abasic site heptamer, no clear answer as to the nature of the intermediates could be given prior to fragment analysis.

The integrals of peaks **1** to **4** (Figure 3.17) were calculated and the relative ratio of integral **4** was fitted by a first order exponential fit as depicted in Figure 3.16.

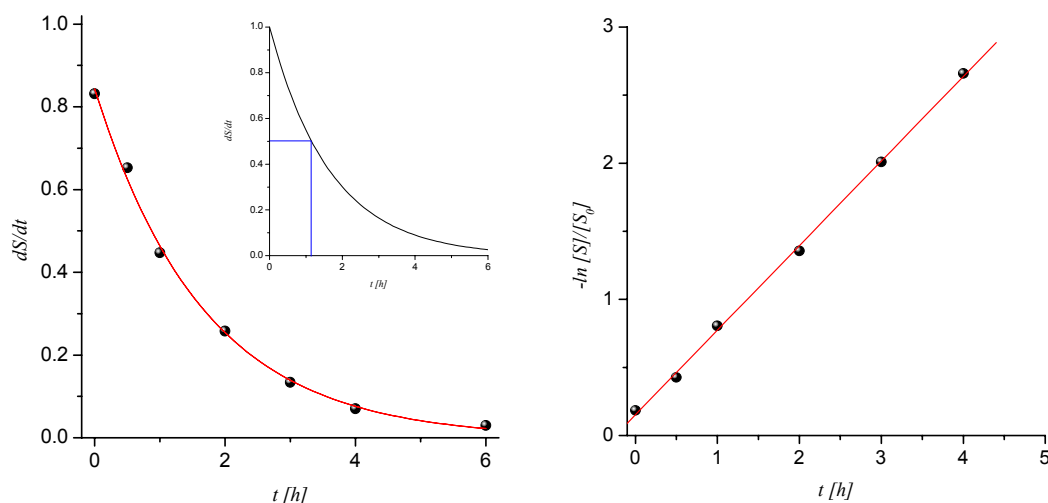


Figure 3.16 First order exponential fit of $d[S]/dt$ of $r(\text{aggXuuC})$ calculated from the HPLC traces. Linear fit using the first six data points to prove first order character of the reaction (right)

The calculation of the first order exponential fit gave a half-life time of $T_{1/2} = 69 \text{ min}$ and the linear fit of $-\ln[S]/[S_0]$ gave the velocity constant $k = 1.73 \cdot 10^{-4} \text{ s}^{-1}$.

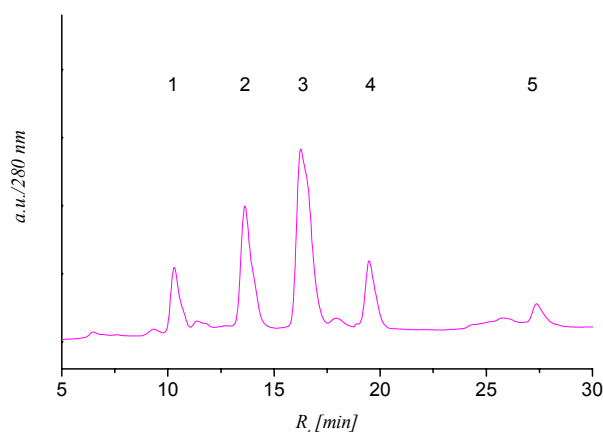


Figure 3.17 Fragment analysis of a true abasic site. Heptamer *r*(aggXuuC) is treated with 0.1 M NaOH for 3 h at 37 °C and analyzed by RP-HPLC (gradient: 0-30 % in 40 min)

To prove the expected β,δ -elimination/cyclophosphate formation overlap, heptamer *r*(aggXuuC) was incubated at 0.1 M NaOH at 37 °C for 3 hours. The different fragments **1** to **4** were then separated by RP-HPLC (Figure 3.17) and analyzed by ESI⁺ mass spectrometry. All expected fragments that theoretically result from the two parallel strand cleavage mechanisms could be detected (Table 3.4).

Table 3.6 Identified fragments of heptamer *r*(aggXuuC) cleavage

Nr	R _t [min]	Structure	Formula	m/z calc	m/z found
1	10.3	<i>r</i> (puuC)	C ₂₉ H ₄₀ N ₇ O ₂₄ P ₃	963.60	963.26
2	13.6	<i>r</i> (uuC)	C ₂₉ H ₃₉ N ₇ O ₂₁ P ₂	883.62	883.22
3a	16.2	<i>r</i> (aggp)	C ₃₃ H ₄₄ N ₁₅ O ₂₁ P ₃	1079.73	1079.34
3b	16.2	<i>r</i> (agg-rb)	C ₃₈ H ₅₂ N ₁₅ O ₂₅ P ₃	1211.85	1211.51
3c	16.2	<i>r</i> (agg-rbcp)	C ₃₈ H ₅₁ N ₁₅ O ₂₇ P ₄	1273.81	1273.36
3d	16.2	<i>r</i> (agg-rbp)	C ₃₈ H ₅₃ N ₁₅ O ₂₈ P ₄	1291.83	1291.34
4	19.5	<i>r</i> (aggXuuC)	C ₆₇ H ₉₀ N ₂₂ O ₄₈ P ₆	2157.43	2157.54
5	27.3	<i>r</i> (aggX _p uuC)	C ₇₅ H ₉₇ N ₂₃ O ₅₀ P ₆	2306.58	2306.57

rb = 4,5-dihydroxy-2-oxo-pentanal, *cp* = 2',3'-cyclophosphate

Surprisingly, in this case it was possible to find the cyclophosphate fragment **3c** compared to the cyclophosphate formation kinetics where it could not be detected.

3.3.5 Kinetics of the β,δ -elimination mechanism at a natural DNA abasic site

To finally compare the natural RNA abasic site with its DNA analogue, a heptamer containing a caged abasic site Y_p was deprotected ($c = 1 \text{ OD}_{260}\text{mL}^{-1}$, UV lamp for 2 minutes) and the resulting abasic DNA heptamer $d(\text{AGGYTTC})$ was treated with sodium hydroxide as in the preceding experiments (0.1 M NaOH , 37°C).

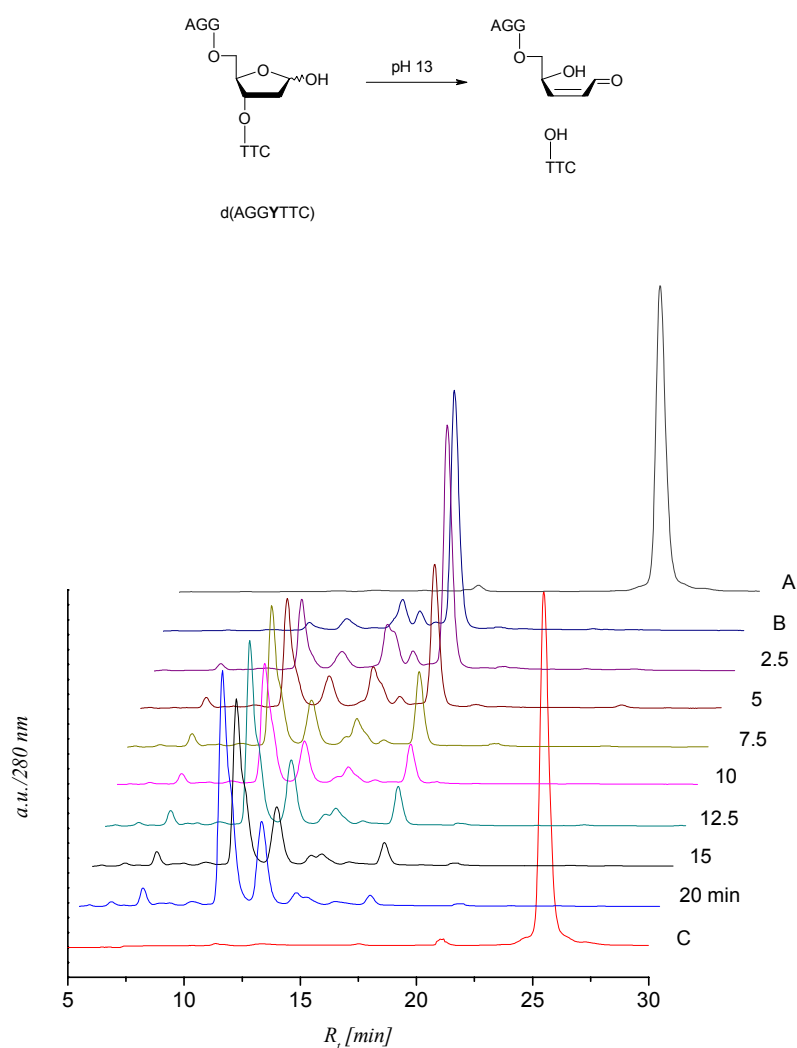


Figure 3.18 280 nm HPLC traces of a true abasic site containing DNA heptamer $d(\text{AGGYTTC})$. Lane A: protected heptamer $d(\text{AGGY}_p\text{TTC})$; lane B: deprotected heptamer $d(\text{AGGYTTC})$; lane C: protected heptamer $d(\text{AGGY}_p\text{TTC})$, 0.1 M NaOH , 37°C , 20 min. HPLC gradient: 0-30 % B in 40 min

The protected heptamer $d(\text{AGGY}_p\text{TTC})$ ($R_t = 25.7 \text{ min}$) was easily deprotected to give abasic heptamer $d(\text{AGGYTTC})$ ($R_t = 17.6 \text{ min}$). The abasic heptamer almost completely disappeared within 20 minutes. Within the first few minutes a fragment with lower retention time ($R_t = 14.9 \text{ min}$) appeared but disappeared again very fast. It seems that this fragment was an unstable intermediate. The two major fragments have significantly lower retention times than $d(\text{AGGYTTC})$: ($R_t = 11.2, 13.0 \text{ min}$).

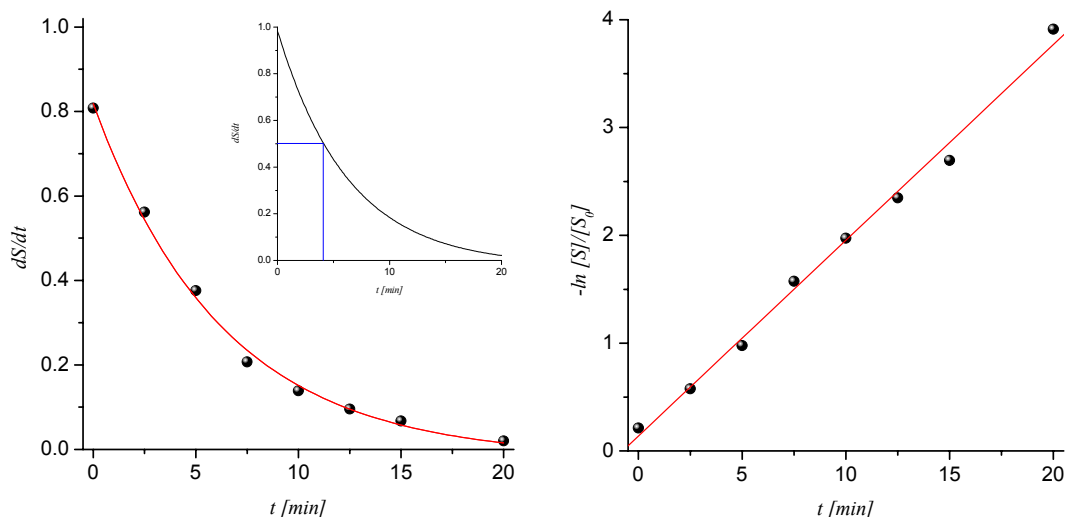


Figure 3.19 First order exponential fit of $d[S]/dt$ of $d(AGGYUUC)$ calculated from the HPLC traces. Linear fit using all data points to prove first order character of the reaction (right)

The calculation of the first order exponential fit gave a half-life time of $T_{1/2} = 4.1$ min and the linear fit of $-\ln[S]/[S_0]$ gave the velocity constant $k = 3.02 \cdot 10^{-3} \text{ s}^{-1}$.

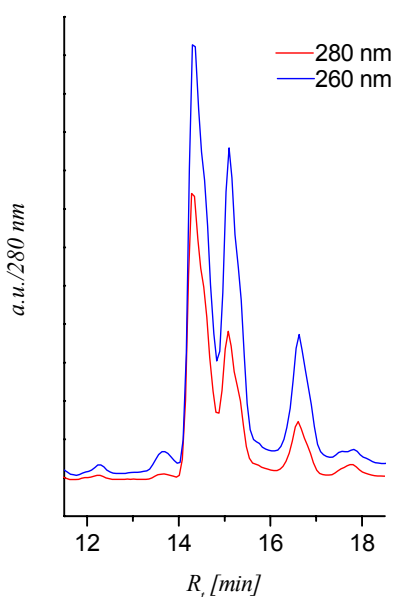


Figure 3.20 The two DNA fragments could not be easily isolated. However it is assumed that the fragment with $R_t = 14.3$ min corresponds to $[P]$ -TTC ($m/z = 915.15$) whereas the fragment with $R_t = 15.1$ min corresponds to AGG - $[P]$ ($m/z = 989.38$). The first fragment is considered to be the pyrimidine fragment due to its absorption properties

3.4 Strand Cleavage under Weakly Acidic Conditions

3.4.1 Kinetics of aniline-induced strand cleavage at an RNA abasic site

To investigate strand cleavage reactions without interfering cyclophosphate formation, strand scission reactions were performed at slightly acidic pH. At pH 4.6 strand cleavage is achieved by Schiff base formation of aniline and the 1'-aldehyde of the abasic ribose residue.

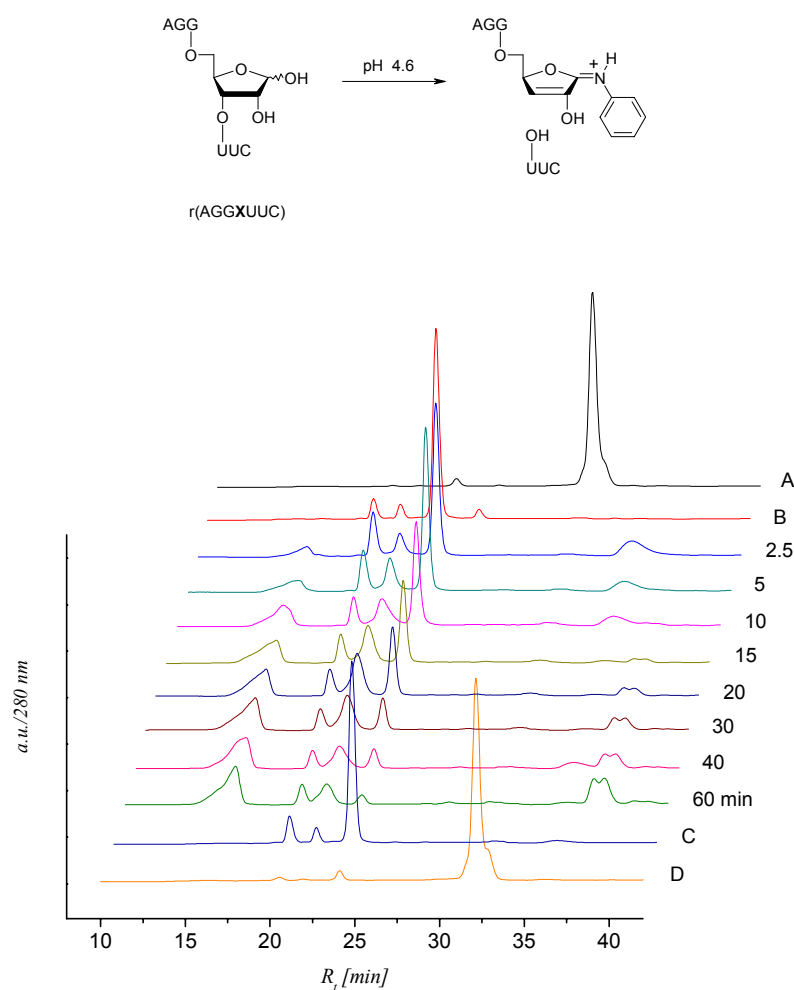


Figure 3.21 260 nm HPLC traces of aniline-induced strand cleavage reaction of $r(\text{AGGXUUC})$. Lane A: protected heptamer $r(\text{AGGX}_p\text{UUC})$; lane B: deprotected heptamer $r(\text{AGGXUUC})$; lane C: deprotected heptamer $r(\text{AGGXUUC})$ after 60 min in 0.3 M TEAA buffer at 37 °C; lane D: protected heptamer $r(\text{AGGX}_p\text{UUC})$ after 60 min aniline. HPLC gradient: 0 % B for 10 min, 0-30 % B in 40 min

The protected heptamer $r(\text{AGGX}_p\text{UUC})$ ($R_t = 32.0$ min) was again completely deprotected within 6 minutes irradiation with a slide projector to give abasic heptamer $r(\text{AGGXUUC})$ ($R_t = 24.0$ min). The deprotected heptamer was then incubated with 0.5 M aniline-HCl at 37 °C for different time intervals. It is clearly visible from Figure 3.21

that the deprotected abasic heptamer disappears with increasing reaction times. For short reaction times a fragment with an absorption ratio 280/260 nm of ~ 2.4 showed up ($R_t = 35.7$ min). It is not fully clear from the collected data whether this fragment was a rather short living intermediate or an aniline impurity that was not removed prior to RP-HPLC. But since the excess aniline was removed by the same procedure throughout all experiments it seems to be an aniline containing intermediate that vanishes with longer reaction times. The double-peak fragment with a slightly higher retention time ($R_t = 37.7$ min) that came up after 15 minutes reaction time has different absorption properties: the absorption ratio 280/260 nm is ~ 0.46 .

The fragment with the shortest retention time was identified by mass and absorption properties to be the pyrimidine trimer. The fragment increased with longer reaction times but was not present after deprotection (lane B). This fact indicates that the little fragments already present after simple deprotection are not due to strand cleavage. The latter would give rise to a pyrimidine fragment with or without a 5'-terminal phosphate group following the β -elimination mechanism. Nevertheless this fragments with lower retention times ($R_t = 20.3, 21.9$ min) present at the beginning of the reaction were growing with increasing reaction times. From mass spectra no evidence could be found that this fragments are the missing purine trimers. These two fragments also occurred in a small amount in an environment where no primary amine is present (lane C). The proof that the cleavage of the heptamer was due to the abasic site is shown in lane D. The protected heptamer was incubated with aniline-HCl (0.5 M) for an hour and no reaction could be monitored.

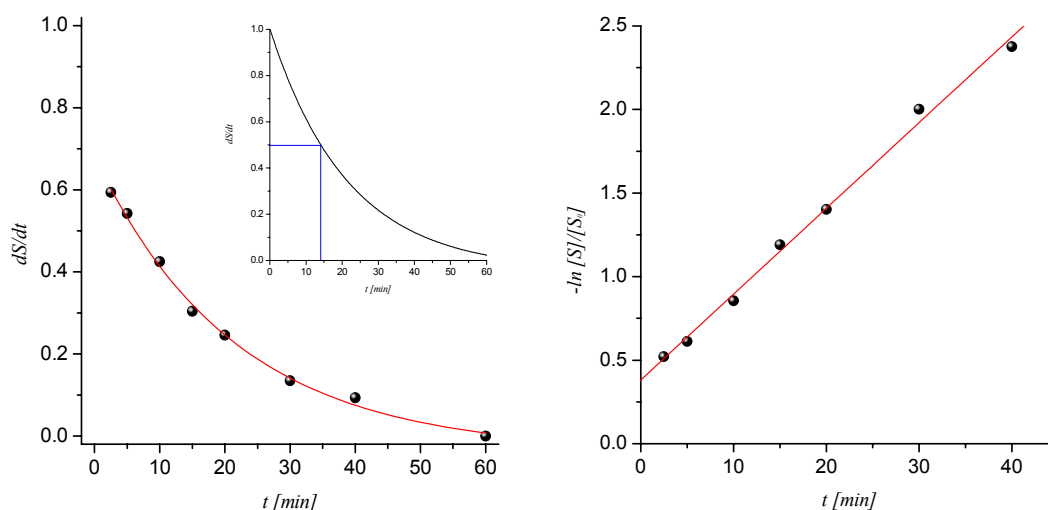


Figure 3.22 First order exponential fit of $d[S]/dt$ of $r(AGGXUUC)$ calculated from the HPLC traces. Linear fit using all data points to prove first order character of the reaction (right)

The integrals of peaks **1-4** and **6** (Figure 3.23) were calculated and the relative ratio of the abasic oligonucleotide was fitted by a first order exponential fit as depicted in Figure 3.22

The calculation of the first order exponential fit gave a half-life time of $T_{1/2} = 14 \text{ min}$ and the linear fit of $-\ln[S]/[S_0]$ gave the velocity constant $k = 8.56 \cdot 10^{-4} \text{ s}^{-1}$.

For fragment analysis the deprotected heptamer r(AGGXUUC) was incubated for 30 minutes. After removal of the excess aniline, the mixture of the fragments was directly measured by mass spectrometry.

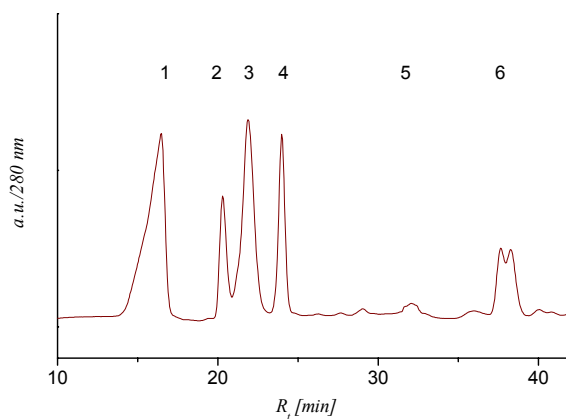


Figure 3.23 Fragment analysis of a true abasic site. Heptamer r(AGGXUUC) is treated with 0.5 M aniline-HCl for 30 min at 37 °C and analyzed by RP-HPLC (gradient: 0 % B for 10 min, 0-30 % in 40 min)

The following fragments could be found. Surprisingly no purine fragment could be identified by mass spectrometry.

Table 3.7 Identified fragments of heptamer r(AGGX_pUUC)

Nr	R _t [min]	Structure	Formula	m/z calc	m/z found
1	16.5	r(pUUC)	C ₂₇ H ₃₆ N ₇ O ₂₄ P ₃	935.54	935.11
2	20.3	r(UUC)	C ₂₇ H ₃₅ N ₇ O ₂₁ P ₂	855.56	855.14
4	24.0	r(AGGXUUC)	C ₆₂ H ₇₉ N ₂₂ O ₄₈ P ₆	2086.28	2086.32
5	32.0	r(AGGX _p UUC)	C ₇₀ H ₈₆ N ₂₃ O ₅₀ P ₆	2235.42	2236.44

3.4.2 Kinetics of aniline-induced strand cleavage at a DNA abasic site

The same experiment was repeated with a heptamer containing a DNA abasic lesion.

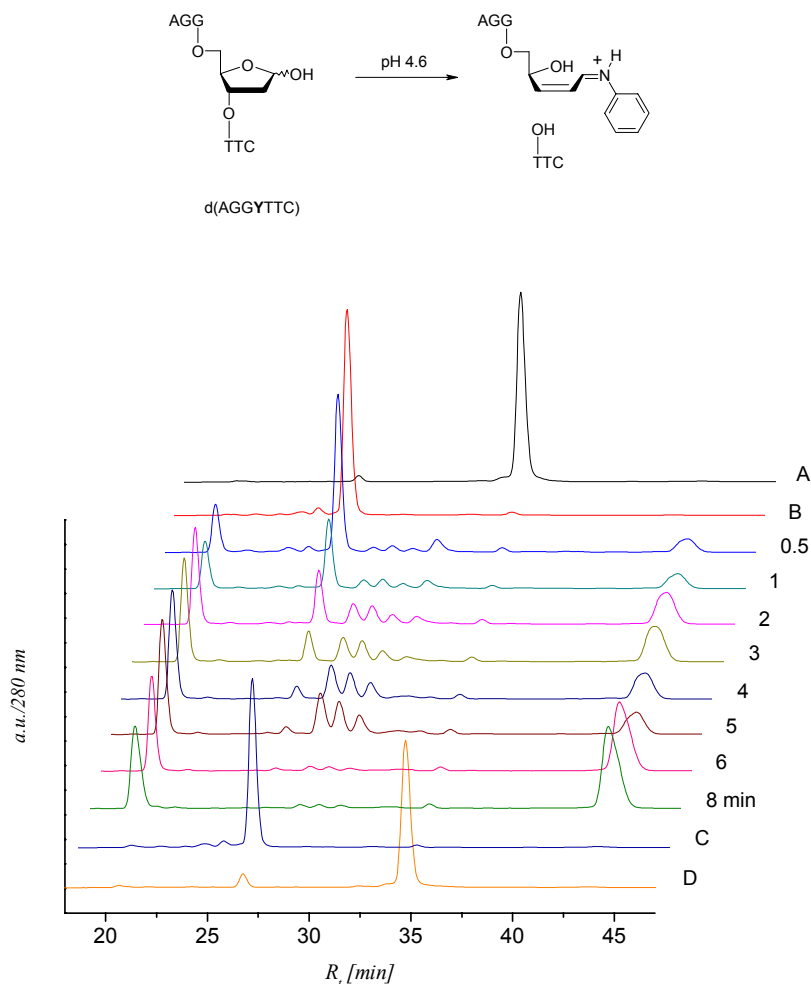


Figure 3.24 260 nm HPLC traces of aniline-induced strand cleavage reaction of $d(\text{AGGY}_p\text{TTC})$. Lane A: protected heptamer $d(\text{AGGY}_p\text{TTC})$; lane B: deprotected heptamer $d(\text{AGGYUUC})$; lane C: deprotected heptamer $d(\text{AGGYUUC})$ after 10 min in 0.3 M TEAA buffer at 37 °C; lane D: protected heptamer $d(\text{AGGY}_p\text{UUC})$ after 10 min aniline. HPLC gradient: 0 % B for 10 min, 0-30 % B in 40 min

The deprotection of $d(\text{AGGY}_p\text{TTC})$ ($R_t = 34.5$ min) was performed with a slide projector for 6 minutes. The abasic heptamer $d(\text{AGGYTTC})$ ($R_t = 26.5$ min) was then diluted to a final concentration of 0.5 M aniline-HCl and incubated for different time intervals at 37 °C. The slowest fragment was identified to be the pyrimidine fragment ($R_t = 20.5$ min). Compared to the digestion of the abasic RNA heptamer with aniline, the slow eluting fragment ($R_t = 43.7$ min) showed also an absorption ratio 280/260 nm of ~ 0.4 . The three fragments ($R_t = 26.6, 28.4, 30.3$ min) occurred at short reaction times and merely disappeared at a reaction time of 6 minutes and longer. The fact that these fragments have a longer retention time than the abasic heptamer indicated that the

fragments might contain an aniline moiety. After completed reaction only two fragment peaks remained. Lane C proves that the abasic heptamer did not show any decay without a primary amine present. Also the heptamer with the protected abasic site did not show any cleavage during incubation in 0.5 M aniline-HCl at 37°C.

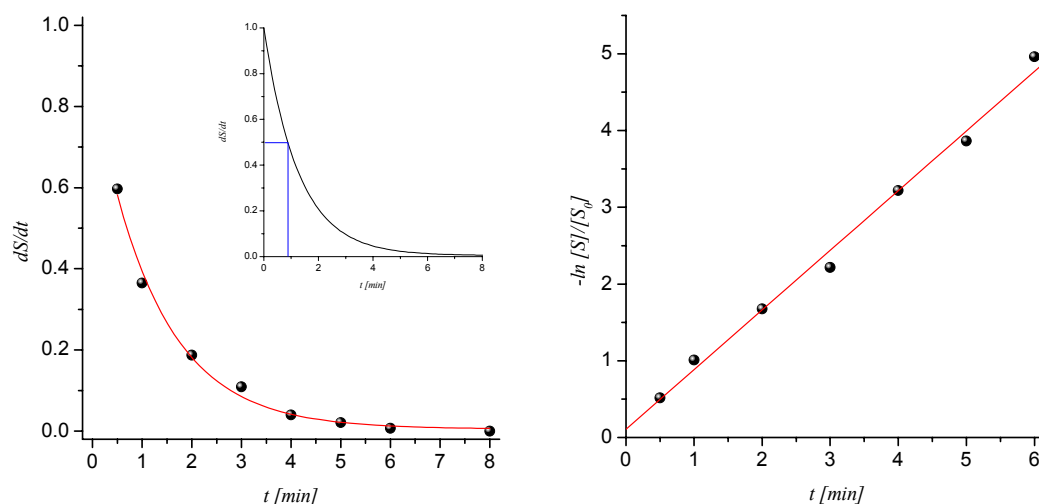


Figure 3.25 First order exponential fit of $d[S]/dt$ of $d(\text{AGGYUUC})$ calculated from the HPLC traces. Linear fit using all data points to prove first order character of the reaction (right)

The usual calculation of the first order exponential fit gave a half-life time of $T_{1/2} = 53$ sec and the linear fit of $-\ln[S]/[S_0]$ gave the velocity constant $k = 1.29 \cdot 10^{-2} \text{ s}^{-1}$.

To prove the expected β -elimination, heptamer $d(\text{AGGYTTC})$ was incubated at 0.5 M aniline-HCl at 37 °C for 4 minutes (Figure 3.26). The fragment mixture was then cleaned from excess aniline and analyzed by ESI mass spectroscopy.

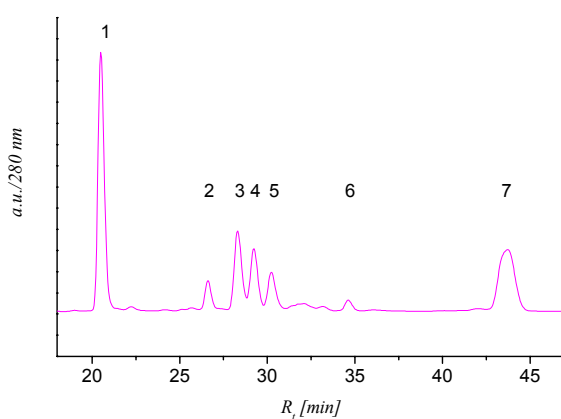


Figure 3.26 Fragment analysis of a true DNA abasic site. Heptamer $d(\text{AGGYTTC})$ is treated with 0.5 M aniline-HCl for 4 min at 37 °C and analyzed by RP-HPLC (gradient: 0 % B for 10 min, 0-30 % B in 40 min)

All detected fragments are shown in Table 3.8. Since the whole mixture was analyzed, not all fragments could be assigned to a specific peak. Compared to the same experiment done with the abasic RNA heptamer, a purine fragment mass could be found. Moreover the abasic site-aniline adduct could also be detected.

Table 3.8 Identified fragments of heptamer *d*(AGGYTTC) cleavage with aniline

Nr	R _t [min]	Structure	Formula	m/z calc	m/z found
1	20.5	d(pTTC)	C ₂₉ H ₄₀ N ₇ O ₂₁ P ₃	915.60	915.15
		d(TTC)	C ₂₉ H ₃₉ N ₇ O ₁₈ P ₂	835.62	835.18
2	26.6	d(AGGYTTC)	C ₆₄ H ₈₃ N ₂₂ O ₄₁ P ₆	2002.33	2002.88
3-5, 7	28.3	d(AGGY-NHC ₆ H ₅)	C ₄₁ H ₄₈ N ₁₆ O ₁₉ P ₃	1161.86	1062.26
		d(AGGY-NHC ₆ H ₅)·H ₂ O	C ₄₁ H ₄₈ N ₁₆ O ₁₉ P ₃ ·H ₂ O	1079.34	1080.27
		d(AGGY-NHC ₆ H ₅ -TTC)	C ₇₀ H ₈₈ N ₂₃ O ₄₀ P ₆	2077.45	2077.38
6	34.6	d(AGGY _p TTC)	C ₇₂ H ₉₀ N ₂₃ O ₄₃ P ₆	2151.47	2151.88

3.5 Discussion of the Kinetic Results

The following tables contain a summary of all determined kinetic parameters.

Table 3.9 Summary of the $T_{1/2}$, k_s and k_{rel} data measured for alkaline induced strand scission of the abasic RNA and DNA heptamers

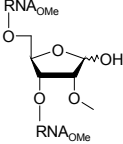
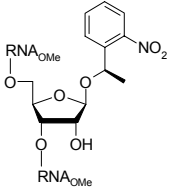
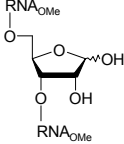
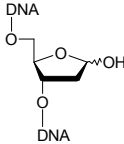
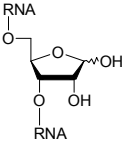
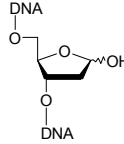
Abasic site				
Mechanism of strand scission	β,δ -elimination	cyclophosphate formation	β,δ -elimination + cyclophosphate formation	β,δ -elimination
$T_{1/2}$ [min]	594	221	69	4.1
k_s [s^{-1}]	$1.96 \cdot 10^{-5}$	$5.95 \cdot 10^{-5}$	$1.73 \cdot 10^{-4}$	$3.02 \cdot 10^{-3}$
k_{rel}	1	3	9	154

Table 3.10 Summary of the $T_{1/2}$, k_s and k_{rel} data measured for aniline-HCl induced strand scission of the abasic RNA and DNA heptamers

Abasic site		
$T_{1/2}$ [min]	14	0.88
k_s [s^{-1}]	$8.56 \cdot 10^{-4}$	$1.29 \cdot 10^{-2}$
k_{rel}	1	15

In a first step the validity of the 2'-*O*-methylated RNA abasic site **x** as an adequate natural RNA abasic analogue **X** is to be discussed. This was *a priori* not clear because reversible, competitive deprotonation at 2'-OH or the shift of the keto function from C1' to C2' via the intermediate C1'-C2' dienolate could interfere with the β -elimination kinetics (Figure 3.27). The half-life times of strand cleavage for **X** are therefore on the one side measured directly and on the other side calculated from the cyclophosphate kinetics of **X_p** and the β -elimination kinetics of **x**. From this calculation it follows that the half-life time for the decay of **X** is expected to be $T_{1/2} = 165$ min (Figure 3.28). Direct measurement of the cleavage of **X** shows a half-life time of 69 minutes. From the calculation we would expect the half-life of **X** to be ~ 2.5 fold higher than actually measured. From this the conclusion is that O2'-methylation slightly but not significantly retards β -elimination in abasic RNA which validates the O2'-methylated ribose unit as

an abasic model. At the same time this comparison also validates the 1-NPE protected abasic RNA unit X_p with a free 2'-OH group as a model to study cyclophosphate formation.

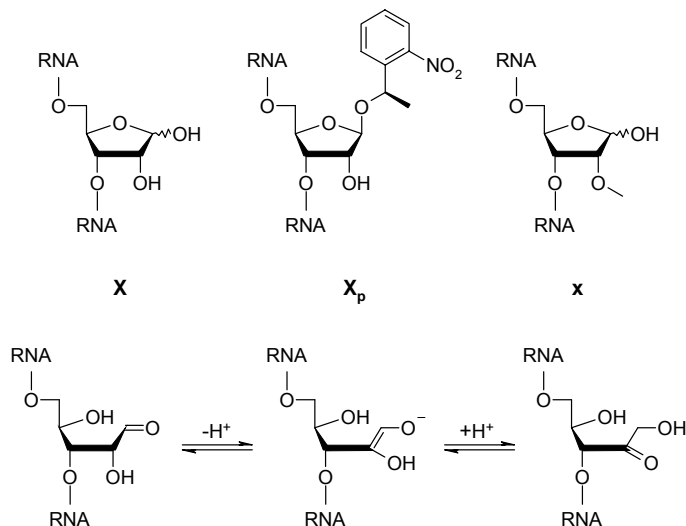


Figure 3.27 RNA abasic site analogues used in the kinetic studies (above) and the 1',2'-shift of the keto function via a dienolate intermediate

In a true abasic site not only the hemiacetal form but also the open chain, the aldehydic form can undergo strand cleavage via cyclophosphate formation. The above described comparison underlines that if this is the case there is either no significant difference in the velocity of cyclophosphate formation between the open chain and the furanose form, or the open chain form is kinetically not relevant.

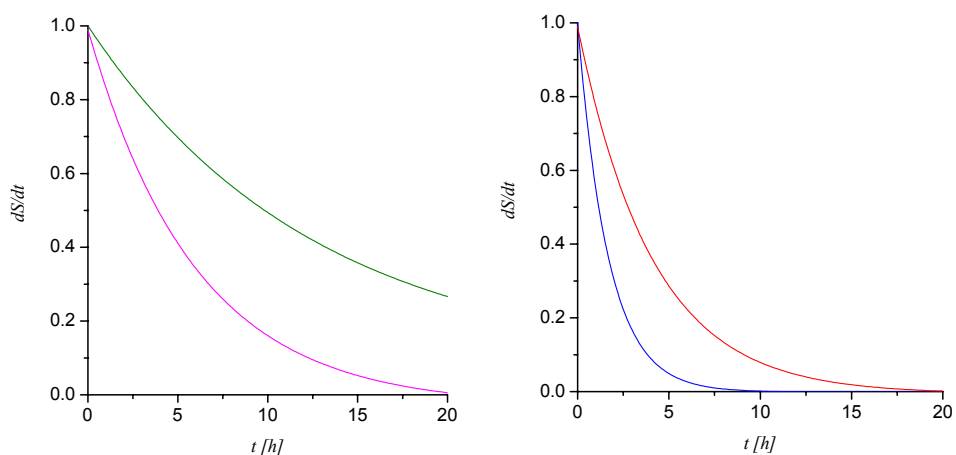


Figure 3.28 Left: comparison of the exponential decay of β -elimination mechanism ($T_{1/2} = 9$ h 54 min; green) and the cyclophosphate formation ($T_{1/2} = 3$ h 41 min; cyan). Right: measured ($T_{1/2} = 69$ min; blue) and calculated ($T_{1/2} = 165$ min; red) exponential decay of the cleavage of a natural RNA abasic site

By comparing the relative rate of strand cleavage we noted that cleavage via cyclophosphate formation is ca 3-fold faster than cleavage by β -elimination.

Extrapolated to longer RNA as e.g. viral RNA this means that under basic conditions strand scission via cyclophosphate formation is clearly the dominant mechanism of decay even in the presence of an abasic site.

Comparison of the kinetic parameters for the β -elimination mechanism shows that the **X** is around 154 times more stable than a DNA abasic site. A thermodynamic argument for this would invoke differences in pK_a of the C2'-H as a function of the presence or absence of a hydroxyl function. Therefore a variety of pK_a values have been calculated using the *SPARC* calculator.^[176] The calculated pK_a values for the C2'-H show just minor differences between RNA and DNA, whether the abasic site is in the cyclic or open chain form (Figure 3.29). In theory, the C2'-H of the RNA abasic site is slightly more basic compared to DNA but the ΔpK_a of only 0.34 can not explain the difference in reactivity.

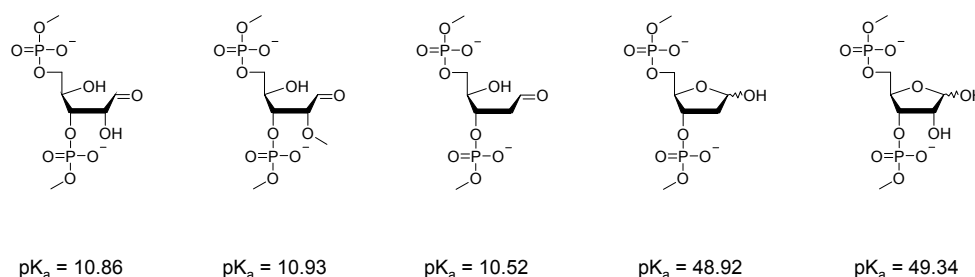


Figure 3.29 2'-H pK_a values calculated with *SPARC* at 25 °C

Also retardation of β -elimination via competitive, reversible deprotonation of the 2'-hydroxyl group can be excluded as the reason due to the fact that the corresponding 2'-O-Me derivative **x** shows slower strand scission compared to the non-methylated abasic residue **X**. It therefore seems likely that C2'-H dissociation is not rate determining and that most likely dissociation of the C3'-O3' bond is the rate limiting step. A working hypothesis which is in agreement with the current experimental observations attributes an important role to the C2'-O2' σ -bond which renders dissociation of the C3'-O3' bond more difficult compared to the analogous C2'-H bond in DNA due to less hyperconjugative stabilization of the transition state upon progressing C3'-O3' bond dissociation (Figure 3.30).

[176] Hilal, S. H., Karickhoff, S. W., Carreira, L. A., *Quant. Struct.-Act. Relat.* **1995**, *14*, 348-355.

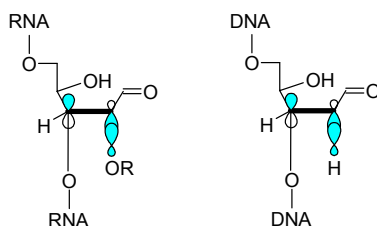


Figure 3.30 Model of the differential hyperconjugative assistance of the C3'-O3' bond dissociation by a C2'-OH or C2'-H σ -bond in a RNA and DNA abasic site

In the *Schiff*-base induced β -elimination at pH 4.6 the relative rates of cleavage between an RNA and a DNA abasic site are less different. Under these conditions abasic RNA is still 15-fold more stable compared to abasic DNA. It may well be that under these conditions the deprotonation of the 2'C-H becomes kinetically more dominant compared to the C3'-O3' bond dissociation in the overall β -elimination mechanism due to the increased difference of the pH of the medium compared to the pK_a of the C2'-H. Thus the differences in kinetics between RNA and DNA decay are expected to correlate with the differences of the pK_a of the respective C2'-H which is at least qualitatively the case. As a bottom line it appears that also under these more biorelevant conditions there is an advantage in stability of abasic RNA over abasic DNA.

3.6 Reverse Transcription Assays

To prove the possibility whether natural RNA abasic sites could have a mutagenic effect, a reverse transcriptase assay was performed. Reverse transcriptases highly vary in fidelity. Therefore three different types of RNA dependent DNA polymerases were chosen: HIV-1 RT, AMV RT and MMLV-(H⁻) RT.^[177]

As a primer-template system, the following RNA and DNA sequences are selected:

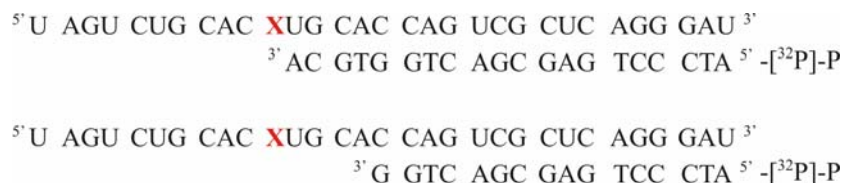


Figure 3.31 Primer-template systems used for standing start (upper) and running start (lower) reverse transcription assays

The sequence of the template is random besides consisting of 60 % G-C base pairs in the primer region to enhance stability of the primer-template duplex. Furthermore, neither the template nor the primer is self-complementary in any way to avoid disturbance of the duplex formation.^[178] For any of the used reverse transcriptases the primer region is long enough to initiate transcription. The template overhang allows the reverse transcriptases to pass the abasic lesion completely. In the template overhang each nucleotide is incorporated at least twice. The DNA primer is labeled at the 5'-end with [γ -³²P]ATP and T4 kinase. This allows the detection of pmol amounts of material.

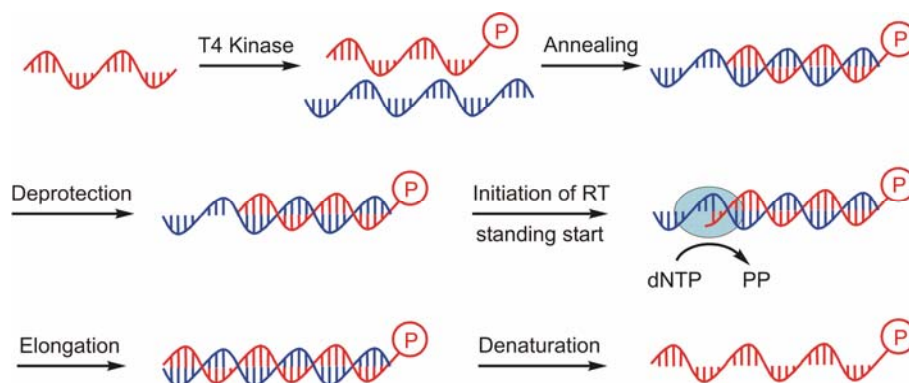


Figure 3.32 Standing start reverse transcription assay. After annealing of the [³²P]-phosphorylated DNA primer (red) to the AS-protected RNA template (blue) the abasic site is deprotected and the reverse transcription is initiated. After elongation and denaturation the radioactively labeled primer is analyzed.

[177] Stahlberg, A., Kubista, M., Pfaffl, M., *Clin. Chem.* **2004**, *50*, 1678-1680.

[178] Zuker, M., *Nucleic Acids Res.* **2003**, *31*, 3406-3415.

In the assay conditions applied, the final concentration of the DNA primer is chosen to be 50 nM, whereas the RNA template concentration is 100 nM and the final dNTP concentration is 20 μ M. The 2-fold concentration of the template ensures that all primer is in its duplex state during the reaction. This allows the quantification of the processed material by autoradiography after gel electrophoresis. The goal of the performed assays is to show whether the different tested enzymes incorporate the different deoxynucleotides opposite the abasic site.

3.6.1 HIV-1 reverse transcriptase assay^[179]

Human Immunodeficiency Virus reverse transcriptase is the most error prone DNA polymerase known and therefore the most promising enzyme to start with.^[180-182] HIV-1 RT has two distinct enzymatic activities, an RNA- or DNA dependent DNA polymerase and a ribonuclease RNase H activity. Functional HIV-1 RT is a heterodimer of two related chains, a 66-kD subunit (p66) and a 51-kD subunit (p51) derived from p66 by proteolytic cleavage. The two chains have in common four domains: “fingers”, “palm” “thumb” and “connection”, and p66 additionally also has an RNase H activity on the carboxy terminus (Figure 3.33). The palm contains residues critical for polymerase catalytic activity, and its folded structure resembles that of a corresponding catalytic domain in other DNA and RNA polymerases.

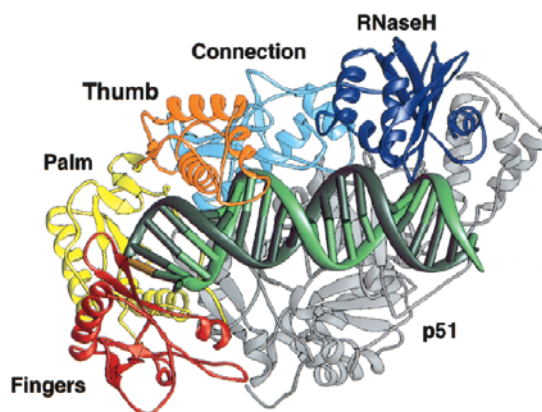


Figure 3.33 Structure of the HIV-1 RT catalytic complex. p51 is shown in gray, whereas p66 domains are colored: “fingers” (red), “palm” (yellow) “thumb” (orange), “connection” (cyan) and RNase H (blue). DNA template is shown in light-green, RNA primer strand in dark-green and the last incorporated deoxynucleotide is shown in gold^[183]

[180] Yu, H., Goodman, M. F., *J. Biol. Chem.* **1992**, 267, 10888-10896.

[179] Castro, H. C., Loureiro, N. I. V., Pujol-Luz, M., Souza, A. M. T., Albuquerque, M. G., Santos, D. O., Cabral, L. M., Frugulhetti, I. C., Rodrigues, C. R., *Curr. Med. Chem.* **2006**, 13, 313-324.

[181] Kati, W. M., Johnson, K. A., Jerva, L. F., Anderson, K. S., *J. Biol. Chem.* **1992**, 267, 25988-25997.

[182] Bebenek, K., Abbotts, J., Wilson, S. H., Kunkel, T. A., *J. Biol. Chem.* **1993**, 268, 10324-10334.

[183] Huang, H., Chopra, R., Verdine, G. L., Harrison, S. C., *Science* **1998**, 282, 1669-1675.

Standing start experiments with two different enzyme concentrations show that HIV-1 reverse transcriptase incorporates all four natural dNTPs opposite an abasic RNA lesion (Figure 3.34). With all four dNTPs available both experiments show full length elongation with the incorporation opposite the abasic site being the slowest step. The qualitative comparison between the four dNTPs shows that the proposed “A-rule” is also expandable to RNA abasic lesions. The “A-rule” states, that opposite a template lesion without information, DNA polymerases incorporate bases preferentially in the following order: $A > G \gg C \sim T$.

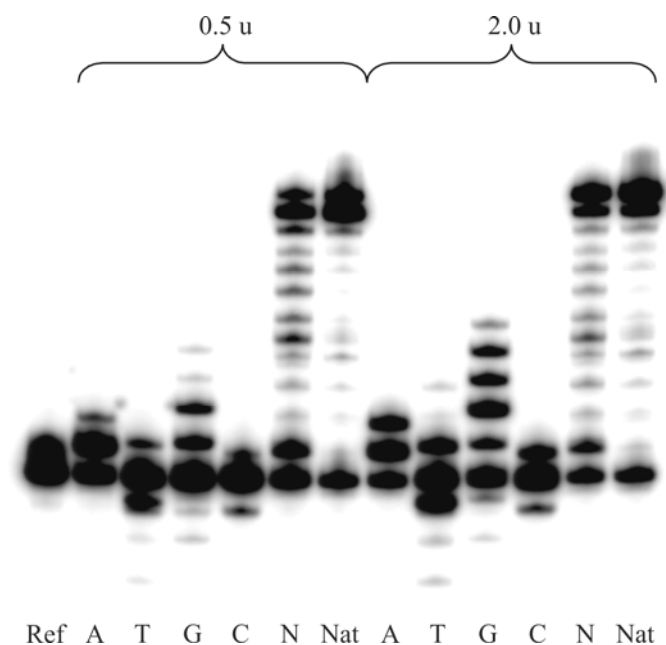


Figure 3.34 Standing start HIV-1 RT assay with abasic template, enzyme concentrations 0.5 and 2.0 units, reaction time 1 hour. Ref: without enzyme and dNTPs. A, T, G, C: reactions in presence of the according dNTPs; N: reactions in presence of all four dNTPs; Nat: unmodified template ($X=U$) and all four dNTPs

Quantitation of the incorporation of the different dNTPs is shown in Table 3.11. Although the used recombinant HIV-1 reverse transcriptase (*Worthington*), lacks its 3'-5' exonuclease activity (according to the manufacturer's manual), shorter primer products are detected for elongation reactions with dTTP, dGTP and dCTP. It follows that the faster the incorporation of the dNTP opposite an abasic site is, the less exonuclease activity is observed.

Table 3.11 Quantitation of the primer elongation with 2 units of HIV-1 reverse transcriptase in %

dNTP	- 3	- 2	- 1	primer	+ 1	+ 2	+ 3	+ 4	+ 5
dATP	-	-	-	30.9	42.4	26.6	-	-	-
dTTP	0.7	1.2	25.5	46.6	26.1	-	-	-	-
dGTP	-	0.6	3.8	29.2	12.6	24.3	14.6	12.2	2.8
dCTP	-	-	10.8	60.4	28.8	-	-	-	-

Whether the shortened primer fragments origin from the original primer 20-mer or from elongated and further processed primer can not be directly determined. In the first case the “A-rule” could be interpreted as follows (percentages in parenthesis display not elongated primer): A (30.9 %) ~ G (33.6 %) >> C (71.2 %) ~ T (74 %). In the case that the fragments result from elongated and processed primer the “A-rule” needs to be interpreted as follows: G (29.2 %) ~ A (30.9 %) > T (46.6 %) > C (60.4 %). In this case elongated primer that is processed back to the original primer size is just treated like not elongated material. Therefore this interpretation is not accurate. In either way purines are incorporated in higher rates than pyrimidines.

To investigate the selectivity of the HIV-1 reverse transcriptase the identical assay is repeated with the protected template, i.e. the masked abasic site (Figure 3.35). This lesion also carries no information for the enzyme.

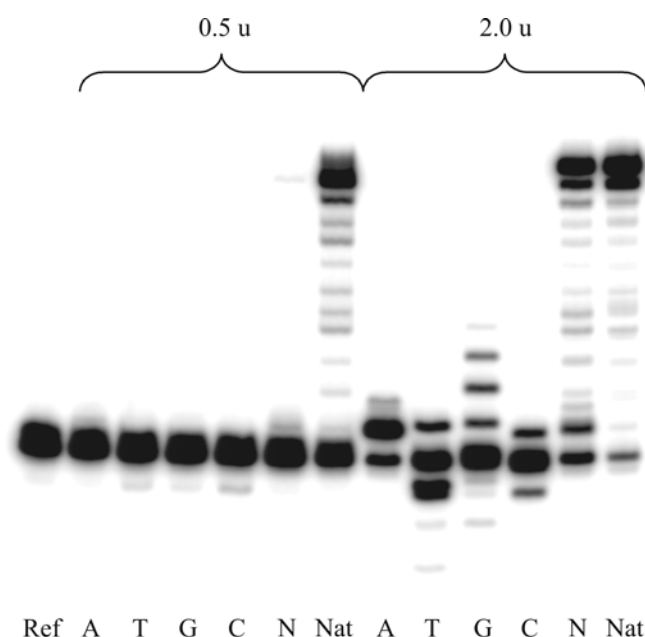


Figure 3.35 Standing start HIV-1 RT assay with protected abasic template, enzyme concentrations 0.5 and 2.0 units, reaction time 1 hour. Ref: without enzyme and dNTPs. A, T, G, C: reactions in presence of the according dNTPs; N: reactions in presence of all four dNTPs; Nat: unmodified template (X=U) and all four dNTPs

At lower enzyme concentration it is found that the enzyme does not elongate the primer, independent on the dNTPs provided (Figure 3.35). At higher enzyme concentration the observed elongation pattern is almost identical to that of the low enzyme concentration assay in Figure 3.34. From these data it follows that the reverse transcriptase prefers an abasic site over a no information carrying hydrophobic group. Nonetheless full-length product is provided at high enzyme concentration. Whether this enzyme could be used to incorporate dNTPs of non-hydrogen bonding base analogues or even abasic site precursor triphosphates was not investigated. This would be of particular interest for the synthesis of kilobase DNA fragments with masked abasic sites at predefined positions.

To investigate the influence of an RNA abasic site on the reverse transcriptase already in action a running start experiment was performed.



Figure 3.36 Comparison of standing start (left) and running start (right) elongation experiments with HIV-1 reverse transcriptase, reaction time 1 hour P_{ss} : primer standing start, P_{rs} : primer running start, T_m : modified template (e.g. abasic template), T_n : natural template

For lower enzyme concentrations neither the standing start nor the running start assays show elongation. This fact is due to the lower activity of the used enzyme batch, in accordance to Figure 3.34, where elongation with 0.5 units of enzyme could be observed. With higher enzyme concentrations the standing start as well as the running start assay showed high read-through. The running start assay confirms that the slowest incorporations occur at the positions of the AP site and AP site - 1. From there on the

rate of the subsequent incorporations is higher, although lower than in the natural primer/template system. From this it follows that an abasic lesion in the template is read over in either way: standing start or running start.

3.6.2 AMV reverse transcriptase assay

Avian Myeloblastosis Virus reverse transcriptase is less error prone than HIV-1 reverse transcriptase: compared to the latter there is a 10 times higher fidelity.^[180,184] The active reverse transcriptase is a heterodimer composed of a 95 kDa and a 63 kDa subunit. AMV RT has two distinct enzymatic activities, an RNA- or DNA dependent DNA polymerase and a ribonuclease (RNase) H.

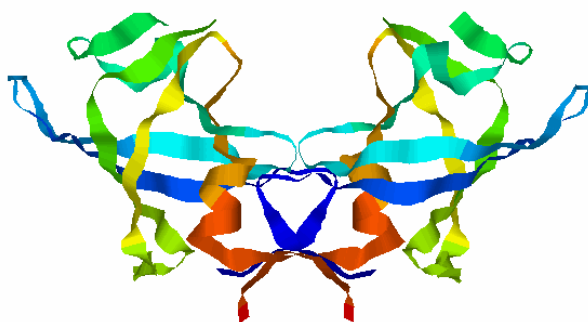


Figure 3.37 Structure of AMV reverse transcriptase

Standing start experiments with two different enzyme concentrations show almost no elongation of the primer with 2.0 units but considerable elongation with 8.0 units (Figure 3.38). For both enzyme concentrations the natural template is fully elongated. For low enzyme concentrations just faint bands are visible for single incorporations of dATP and in the presence of all four dNTPs. For the incorporation of dTTP, dGTP and dCTP some exonuclease activity is present at low enzyme concentration. For higher enzyme concentrations in the presence of all four dNTPs there is a considerable amount of full length elongation. The purine dNTPs are incorporated opposite the abasic site whereas the pyrimidine dNTPs show no incorporation. In the cases of dTTP, dGTP and dCTP enhanced exonuclease activity is observed.

[184] Roberts, J. D., Preston, B. D., Johnston, L. A., Soni, A., Loeb, L. A., Kunkel, T. A., *Mol. Cell. Biol.* **1989**, *9*, 469-476.

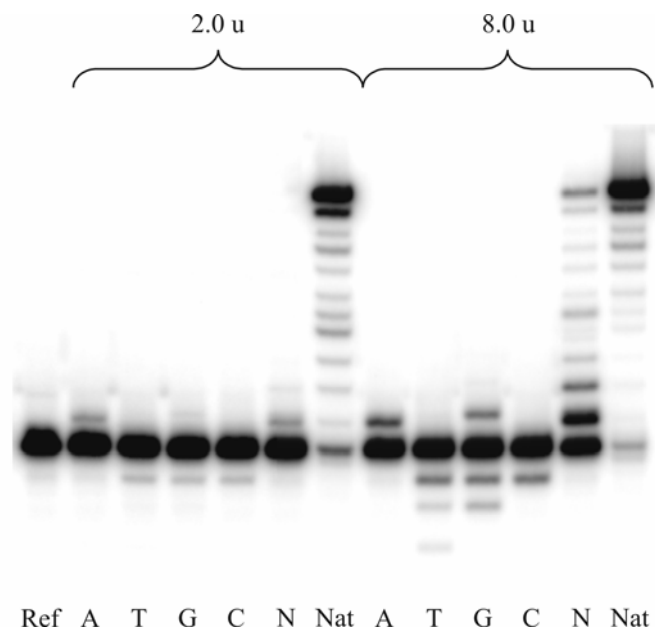


Figure 3.38 Standing start AMV RT assay with abasic template, enzyme concentrations 2.0 and 8.0 units, reaction time 1 hour. Ref: without enzyme and dNTPs. A, T, G, C: reactions in presence of the according dNTPs; N: reactions in presence of all four dNTPs; Nat: unmodified template (X=U) and all four dNTPs

The comparison of standing and running start experiments in the presence of all dNTPs is shown in Figure 3.39. The lacking full elongation for the experiments with 8.0 units can be explained by the fact that a new enzyme batch was used for this series of tests and that the activity of the new batch is lower compared to the first one used. This assumption is supported by the fact that the standing start experiment does not show full elongation either. The running start series shows that the enzyme stops one base before or even two bases before the abasic site. This might be due the fact that the abasic site disturbs the duplex geometry.

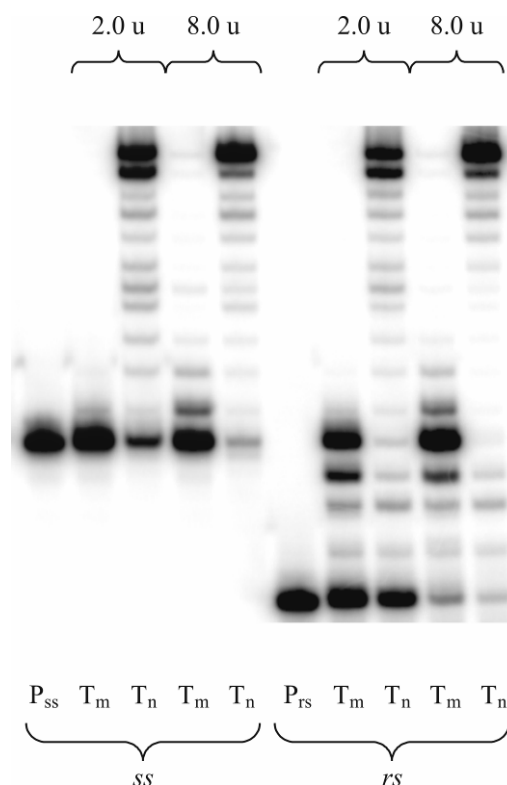


Figure 3.39 Comparison of standing start (left) and running start (right) elongation experiments with AMV reverse transcriptase, reaction time 1 hour. P_{ss} : primer standing start, P_{rs} : primer running start, T_m : modified template (e.g. abasic template), T_n : natural template

3.6.3 MMLV (H-) reverse transcriptase assay

Moloney Murine Leukemia Virus Reverse Transcriptase (MMLV-RT) is an RNA- and DNA-dependent DNA polymerase requiring an oligodeoxyribonucleotide primer for initiation of elongation.^[185] The monomeric enzyme consists of a single polypeptide chain with five domains with a mass of 75 kDa. MMLV-RT lacks a 3'-5' exonucleolytic proofreading function and has a weak RNase H activity.^[186] The here used MMLV-RT(H-) contains a point mutation which results in the lack of the intrinsic RNase H activity. MMLV-RT has the highest fidelity of the reverse transcriptases used in these experiments: MMLV-RT is considered to have an 18 times higher fidelity than HIV-1 RT.^[184]

[185] Roth, M. J., Tanese, N., Goff, S. P., *J. Biol. Chem.* **1985**, 260, 9326-9335.

[186] Das, D., Georgiadis, M. M., *Structure (Cambridge, MA, U. S.)* **2004**, 12, 819-829.

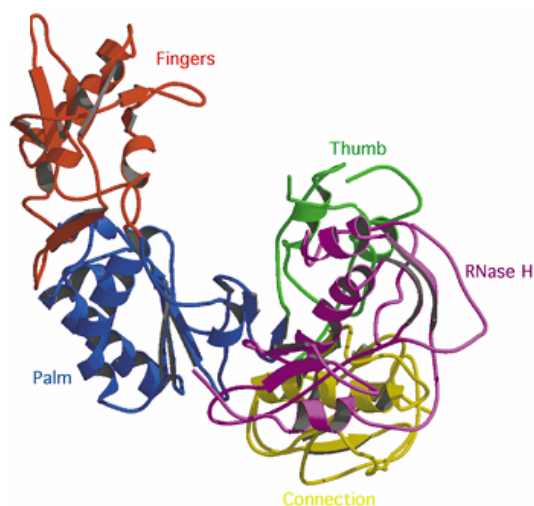


Figure 3.40 X-ray structure of MMLV reverse transcriptase^[186]

It is known that MMLV-RT is not as active as HIV-1 RT and therefore more units of the enzyme are used to get full length products. Standing start experiments with three different enzyme concentrations (4, 16 and 32 units) show high yield elongation for the natural template (Figure 3.41). Nevertheless, no primer elongation could be determined for the abasic template. The very weak bands that can be observed for 16 and 32 units with all dNTPs present seem to be artifacts from the application of the samples to the gel.

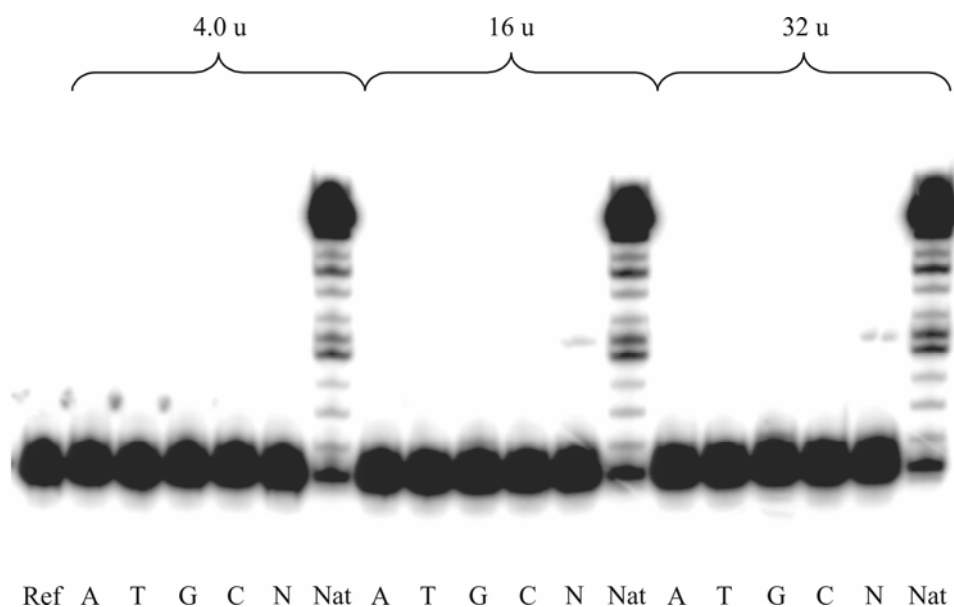


Figure 3.41 Standing start M-MLV RT (H-) assay with abasic template, enzyme concentrations 4.0, 16 and 32 units, reaction time 1 hour. Ref: without enzyme and dNTPs. A, T, G, C: reactions in presence of the according dNTPs; N: reactions in presence of all four dNTPs; Nat: unmodified template (X=U) and all four dNTPs

3.6.4 RNase H activity test

We also checked for the RNase H activity of the used reverse transcriptases (Figure 3.42).^[187] For this, the abasic and unmodified (X = U) template strands were [³²P]- 5'-end labeled and the DNA primer was not labeled. Control standing start experiments performed in the absence of any reverse transcriptase show that the RNA template is partially cleaved at the abasic site, presumably by β -elimination at the 3'-terminus of the RNA.

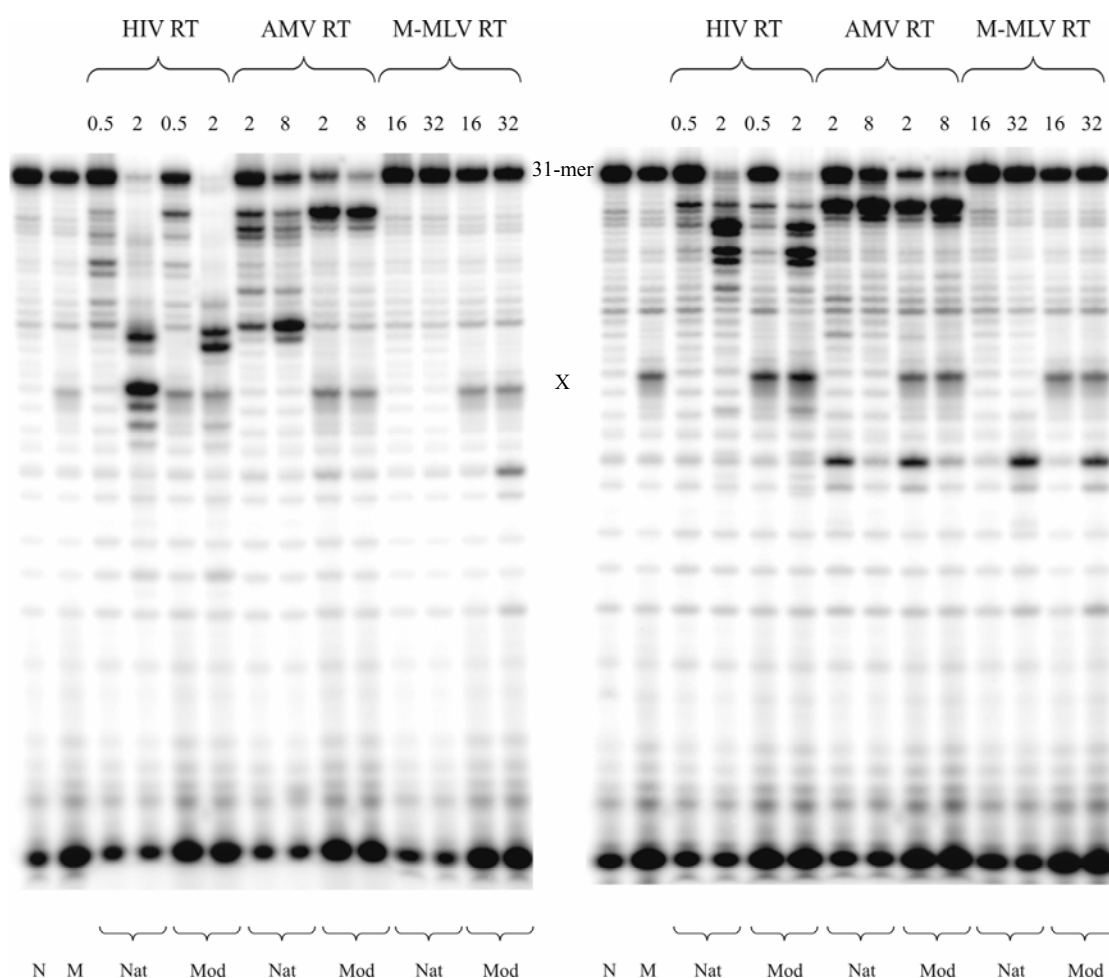


Figure 3.42 RNase H activity test for HIV-1-, AMV- and MMLV-(H-) reverse transcriptases. The assay is performed at 37 °C for one hour in the presence (left) or in the absence of dNTPs (right). The RNA template is ³²P 5'-end labeled, the primer is not labeled. N = natural template, M = abasic template, both without enzyme. Nat = natural template and the according enzyme; Mod = abasic template and the according enzyme. The shortest shown fragment is excess ³²P-ATP

[187] DeStefano, J. J., Mallaber, L. M., Fay, P. J., Bambara, R. A., *Nucleic Acids Res.* **1994**, *22*, 3793-3800.

We assume that most of this cleavage occurs under the conditions of denaturation (5 min, 90 °C) prior to application to the gel and not during incubation. Partial cleavage is not expected to interfere with primer extension as the RNA template is used in a twofold excess. A more detailed analysis of RNase H activity is given in the following sections.

HIV-1 RT: At low enzyme concentration just minor RNase H activity is observed for both templates not depending on the presence of dNTPs (lanes 1, 3, 5 and 7 in Figure 3.43). Increasing the enzyme concentration to 2 units results in complete disappearance of the full length RNA template in all cases (lanes 2, 4, 6 and 8). Interestingly, in the presence of dNTPs there are differences in the RNA degradation pattern as a function of the presence or absence of the RNA abasic site. In the unmodified RNA template, cleavage occurs predominantly at the junction between the doublehelical part and the RNA single strand. However, in the abasic template, cleavage is effected predominantly in the doublehelical primer–template region. This differential cleavage pattern is in accord with the enzyme predominantly cleaving in the unextended primer part, 3 to 4 nucleotides before the abasic site, due to slow elongation in the latter case. The same experiment performed in the absence of dNTPs shows in general the same degradation characteristics for the natural and the abasic template. At high enzyme concentration the double strand is efficiently cleaved in the center of the primer-template duplex region since there is no elongation of the primer.

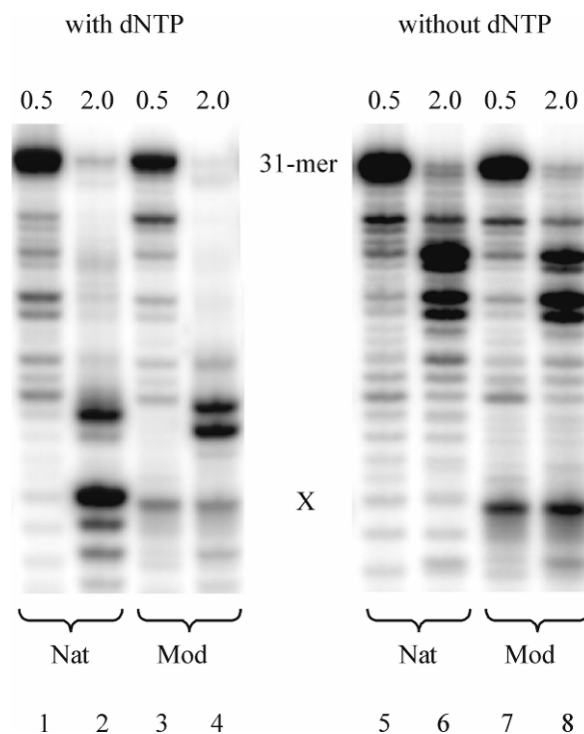


Figure 3.43 Comparison of the RNase H activity of HIV-1 reverse transcriptase with (lanes 1-4) and without (lanes 5-8) dNTPs with different enzyme concentrations: 0.5 units (lanes 1, 3, 5, 7) and 2.0 units (lanes 2, 4, 6, 8). X = U for natural template (lanes 1, 2, 5, 6) or X = AS for modified template (lanes 3, 4, 7, 8)

AMV-RT: At low enzyme concentration the enzyme shows slightly more RNase H activity for the natural primer-template duplex compared to HIV-1 RT (lanes 1, 2, 5, 6 in Figure 3.44). For the modified primer-template duplex results an almost complete disappearance of the full length RNA template in the presence of dNTPs (lanes 3, 4). The most striking fact is that for the modified template the cleavage is almost complete, not depending on the enzyme concentration (lanes 3, 4). For the modified template the cleavage pattern is independent of the presence of dNTPs (lanes 3, 4, 7, 8). This can just be due the fact that elongation is very slow and thus translesion synthesis is blocking the transcription. This is underlined by the comparison of the natural template reactions with or without dNTPs (lanes 1, 2, 5, 6): the cleavage for the presence of dNTPs occurs near to the junction site between the doublehelical part and the RNA single strand for high enzyme concentration (lane 2) and cleavage is deeper in the double helix part when no elongation occurs (lanes 5 and 6). If elongation takes place but slow, then there's cleavage at both sites mentioned above (lane 1).

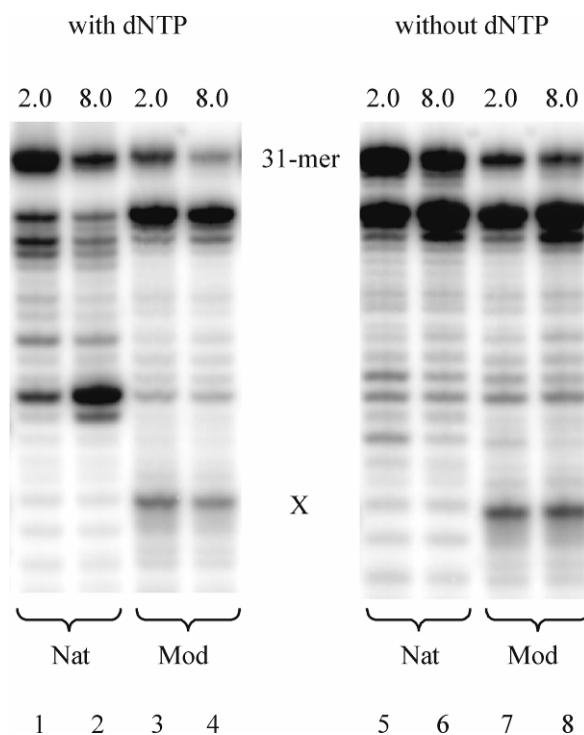


Figure 3.44 Comparison of the RNase H activity of *AMV* reverse transcriptase with (lanes 1-4) and without (lanes 5-8) dNTPs for different enzyme concentrations: 2.0 units (lanes 1, 3, 5, 7) and 8.0 units (lanes 2, 4, 6, 8). $X = U$ for natural template (lanes 1, 2, 5, 6) or $X = AS$ for modified template (lanes 3, 4, 7, 8)

MMLV-(H-) RT: As could be expected, no RNase H activity could be observed with MMLV-(H-) reverse transcriptase. The weak cleavage is similar to the controls where no enzyme was present. The weak bands that occur with the abasic template underline the assumption that they arise from β -elimination at the 3'-end of the abasic site.

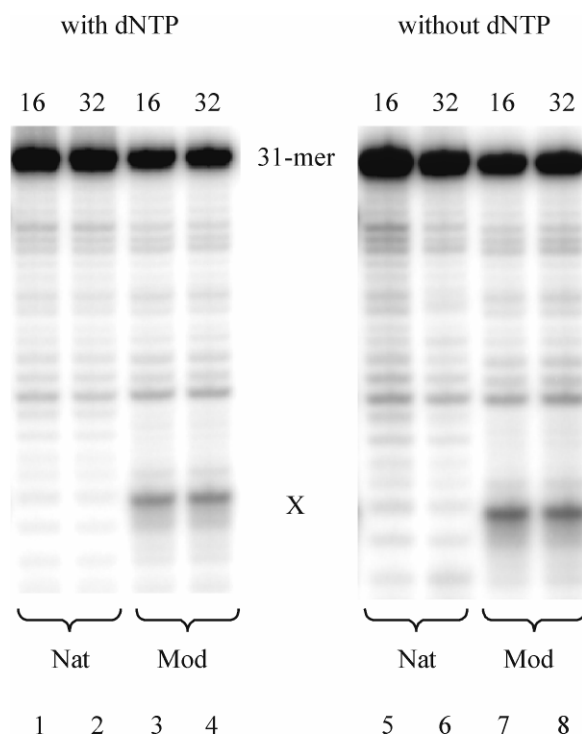


Figure 3.45 Comparison of the RNase H activity of MMLV-(H-) reverse transcriptase with (lanes 1-4) and without (lanes 5-8) dNTPs for different enzyme concentrations: 16 units (lanes 1, 3, 5, 7) and 32 units (lanes 2, 4, 6, 8). X = U for natural template (lanes 1, 2, 5, 6) or X = AS for modified template (lanes 3, 4, 7, 8)

Previous studies showed that the RNase H activity of the polymerases accompanying RNA-directed DNA synthesis is not sufficient to eliminate all of the template RNA.^[181,188-190] While HIV-RT and MMLV-RT generated small products, AMV-RT generated mostly large products. In all cases some of the template RNA remained undigested. In a further study, the amount of degradation that accompanied RNA directed DNA synthesis by AMV- and HIV-RT was measured.^[187] Results showed that with HIV-RT ~20% of the template RNA remained annealed, while with AMV-RT ~80% of the template RNA remained annealed after one round of processive DNA synthesis. In both cases, the template that remained annealed to the newly synthesized DNA was composed of oligoribonucleotides 13–49 nt long.

- [188] DeStefano, J. J., Buiser, R. G., Mallaber, L. M., Myers, T. W., Bambara, R. A., Fay, P. J., *J. Biol. Chem.* **1991**, 266, 7423-7431.
 [189] Dudding, L. R., Nkabinde, N. C., Mizrahi, V., *Biochemistry* **1991**, 30, 10498-10506.
 [190] Fuentes, G. M., Fay, P. J., Bambara, R. A., *Nucleic Acids Res.* **1996**, 24, 1719-1726.

3.7 Incorporation Kinetics of dNTPs at Abasic Sites

3.7.1 Michaelis-Menten enzyme kinetics

In 1913 Michaelis and Menten proposed a model for the kinetics of enzyme reactions. They assumed that the formation of the enzyme-substrate complex ES is reversible, while the release of the product P is irreversible and thus the overall reaction $S \rightarrow P$ is irreversible.



From this assumption the following equation was derived:

$$v = k_2 \cdot [E_T] \frac{[S]}{K_M + [S]} = \frac{V_{\max} \cdot [S]}{K_M + [S]} \quad \text{with } K_M = \frac{k_{-1} + k_2}{k_1}$$

$[E_T]$ is the total concentration of the enzyme, k_2 is k_{cat} . K_M is the dissociation constant of the enzyme-substrate complex. V_{\max} is the maximum rate while v is the reaction rate dP/dt .

In principle, the analysis of the dNTP concentration dependent primer elongation is done after the method of Lineweaver and Burk.

$$\frac{1}{v} = \frac{1}{V_{\max}} + \frac{K_M}{V_{\max} [S]}$$

For the incorporation of dATP vs. U this plot did not give concluding results. Because of the high velocity of the incorporation reaction the data in the linear region of the Michaelis-Menten plot could not be reasonably fitted. Due to this the evaluation of this incorporation is done after the method of Hanes and Woolf. In this linearization the data points are spread over the whole $[S]$ axis.

Compared to the Lineweaver-Burk plot this allows simple outliers to have just a minimal effect on the outcome of the linear regression. To plot the data after Hanes-Woolf the Michaelis-Menten equation is transformed into

$$\frac{[S]}{v} = \frac{1}{V_{\max}} \cdot [S] + \frac{K_M}{V_{\max}}$$

The values for K_M/V_{\max} and $-K_M$ can be easily derived from the linear equation by simply setting $[S]$ and $[S]/v$ to zero.

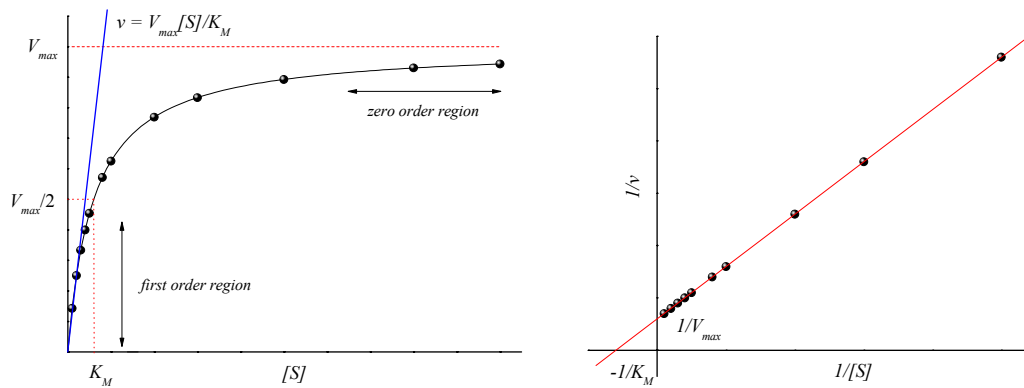


Figure 3.46 Michaelis-Menten enzyme kinetics: the reaction rate shows a hyperbolic behavior (left). By plotting the data after the method of Lineweaver and Burk the according values for K_M and V_{max} can be directly determined (right)

To calculate the velocity of the reactions the concentration of the primer-template complex is assumed to be 50 nM. This assumption is valid since the double-fold concentration of the template (100 nM) ensures that after the annealing all primer (50 nM) is bound in a complex that can be elongated by the enzyme. Excess RNA template will not disturb the elongation reaction since the chosen sequence does not allow the RNA molecules to form double strand structures that could be efficiently elongated at 37 °C. From the gels of the elongation assays the percentage of the elongated material is determined for each dNTP concentration and converted to nM min^{-1} . This allows then to directly determine K_M and V_{max} from the linear regression in the Lineweaver-Burk plot.

To calculate the k_{cat} of the incorporation reaction the concentration of the enzyme is needed:

$$k_{cat} = \frac{V_{max}}{[E_T]} \quad \text{with } [E_T] = \text{total enzyme concentration } [E] + [ES]$$

From the given specific activity of the enzyme (21600 U/mg according to the manufacturer) and the known mass (117 kDa for the heterodimer) the concentration of the enzyme is calculated to be $3.95 \cdot 10^{-13}$ M·unit. Since the volume of the reactions performed is 10 μl the concentration of the enzyme is $3.95 \cdot 10^{-8}$ M·unit or 39.5 nM·unit.

3.7.2 Incorporation kinetics

To determine the initial velocity of an enzymatic reaction with HIV-1 reverse transcriptase it is necessary to follow the incorporation reactions in the first order region. An elongation of less than 20 % is considered to be suitable.^[103] Time course experiments were performed in order to find the appropriate reaction conditions regarding the enzyme concentration and the range of substrate concentrations (Figure 3.47). The following parameters were fixed: reaction temperature (37 °C), reaction time (2 min), concentration of the primer (50 nM) and the concentration of the template (100 nM).

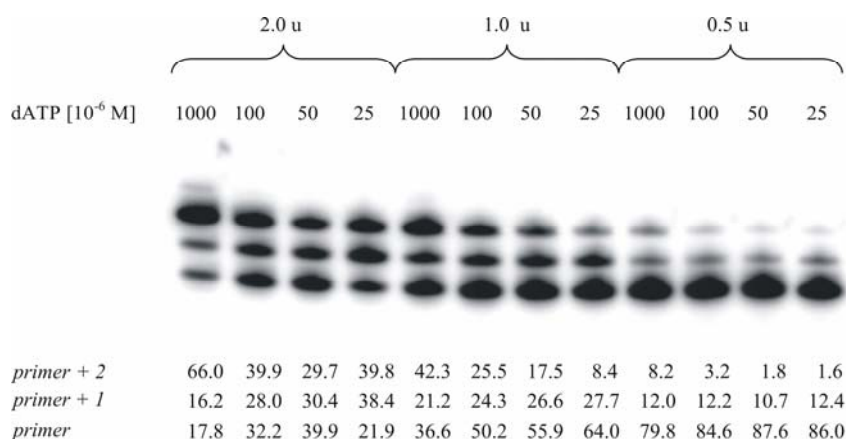


Figure 3.47 Time course experiment of the incorporation of dATP opposite of uracil. The elongation is quantified for different enzyme concentrations. The reactions with 0.5 units show the desired range of elongation

The time course experiments were repeated for all dNTPs and the following enzyme concentrations of HIV-1 RT were found to work best: 0.5 u (dATP vs AS), 1.0 u (dGTP) and 1.5 u (dTTP and dCTP). For all experiments the same range of substrate concentrations was used: 1000, 800, 500, 300, 200, 100, 80, 50, 40, 30, 20 and 10 μ M.

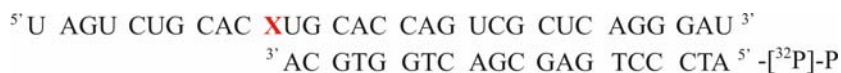


Figure 3.48 Primer-template systems used for standing start reverse transcription assays

3.7.2.1 Incorporation of purine nucleoside triphosphates opposite an abasic site

Analysis of the incorporation kinetics of dATP opposite an abasic site in the template shows an elongation of the primer by one at lower or two bases at higher dATP concentrations, respectively. For the calculation both bands are taken into account (Figure 3.49). For two incorporations A is placed opposite C. The weakness of this

[103] Cai, H., Bloom, L. B., Eritja, R., Goodman, M. F., *J. Biol. Chem.* **1993**, 268, 23567-23572.

basepair seems to inhibit further incorporations. For the elongation reaction of dGTP up to four incorporations are observed with high nucleoside triphosphate concentrations.

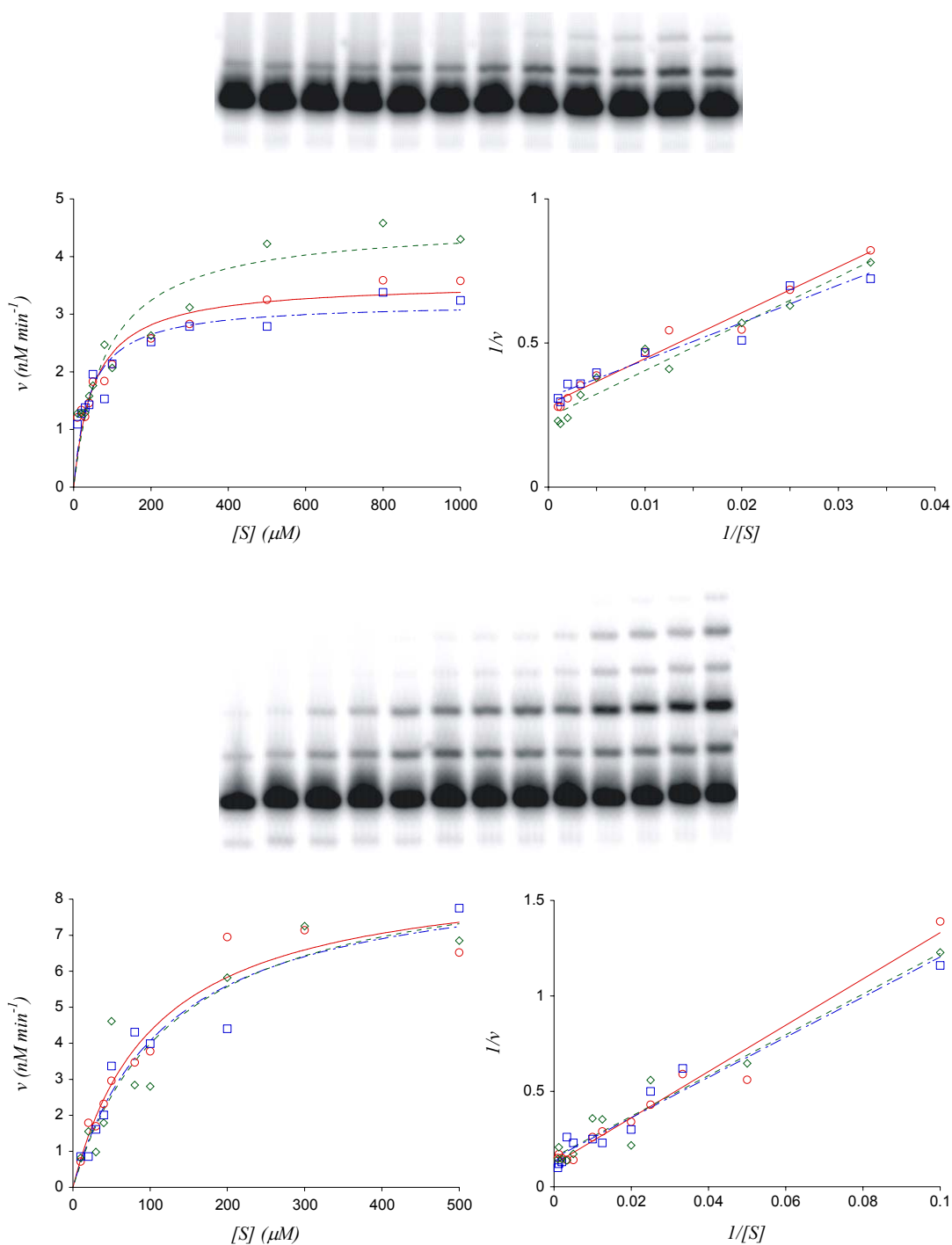


Figure 3.49 Incorporation of dATP (upper) and dGTP (lower) opposite an abasic site: evaluated gel with the dATP concentration rising from left to right (upper), fitted Michaelis-Menten curves (left) and Lineweaver-Burk fits (right)

From the primer and template sequences it follows that G is also incorporated against A. This incorporation seems to be stabilized by the two adjacent G-C basepairs in the

up- and downstream direction. The following G-G basepair is weak and therefore inhibits further elongation of the primer. In both cases no exonuclease activity could be observed. This can be explained by the fact that high exonuclease activity is just present when the RNA dependent DNA polymerase activity is low. Furthermore, shorter primer would again be elongated very fast.

3.7.2.2 Incorporation of pyrimidine nucleoside triphosphates opposite an abasic site

The rates of incorporation of pyrimidine nucleoside triphosphates are lower than for purine nucleoside triphosphates. For both pyrimidines 1.5 units of the enzyme are needed to follow the incorporation kinetics. Since the base following the abasic site in the template is a C, incorporation of a second pyrimidine is highly unfavored. In both cases just incorporation opposite the abasic site is observed. Given the fact that polymerase activity is slow the exonuclease activity gains more influence: in both cases a considerable amount of shortened primer is observed, especially when dNTP concentrations are low. For the lowest dCTP concentration the amount of shortened primer is measured to be over 9 %. In the case of TTP the amount of shortened primer is over 12 %. Since the exonuclease activity is increased at low dNTP concentration and decreased at high dNTP concentrations it is not trivial to include this fact into the calculations.

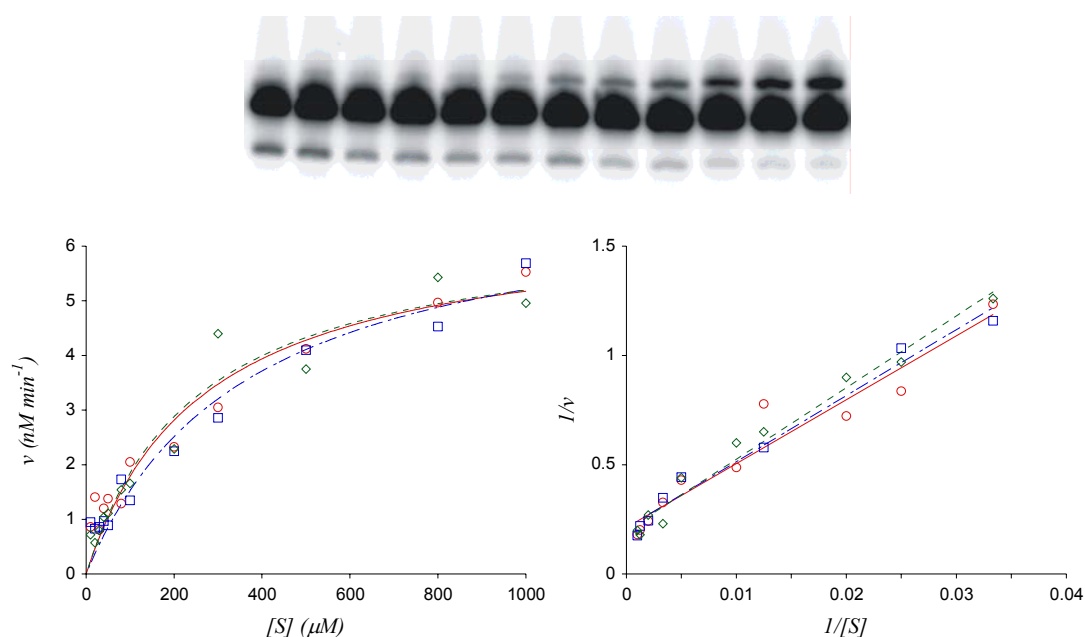


Figure 3.50 Incorporation dCTP opposite an abasic site: evaluated gel with the dATP concentration rising from left to right (upper), fitted Michaelis-Menten curves (left) and Lineweaver-Burk fits

Therefore it was decided not to consider this fact in the calculations and just to focus on primer elongation. This consideration is viable since in the case of the purines exonuclease activity is also not included because not observable (this does not mean that it does not occur).

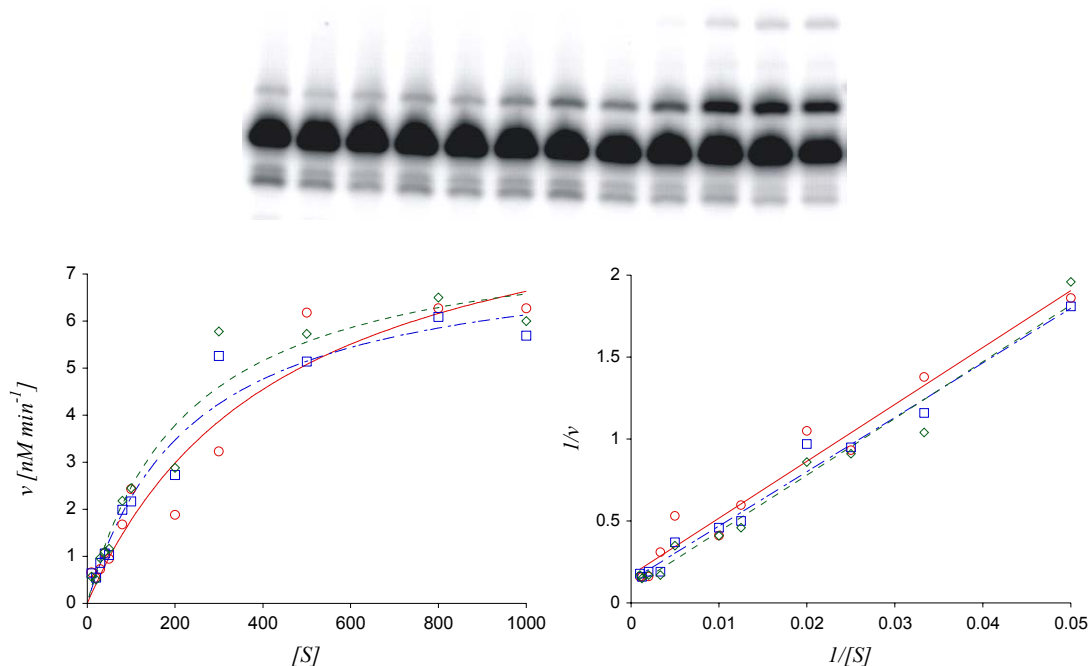


Figure 3.51 Incorporation of dTTP opposite an abasic site: evaluated gel with the dATP concentration rising from left to right (upper), fitted Michaelis-Menten curves (left) and Lineweaver-Burk fits

3.7.2.3 Incorporation of dATP versus U

To be able to compare the incorporation velocities of the four natural dNTPs opposite an abasic template the incorporation kinetics of the incorporation of dATP opposite the natural template containing a uracil residue were also measured.

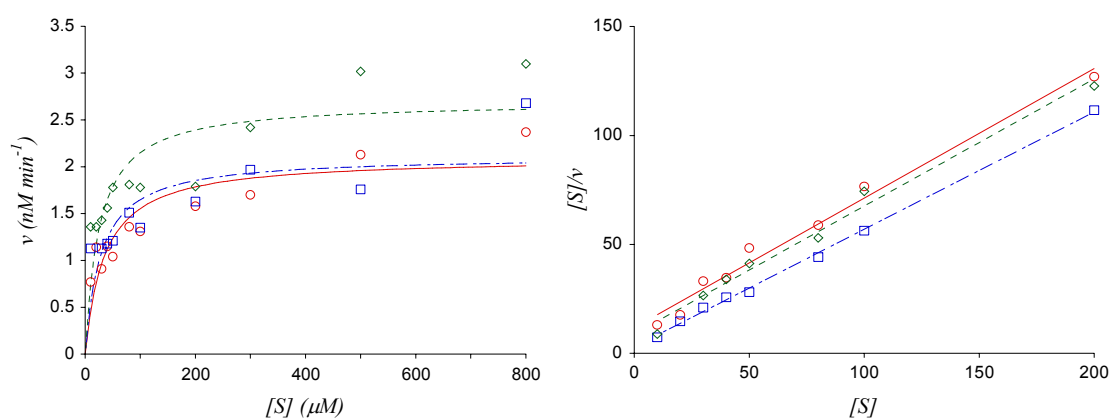


Figure 3.52 Incorporation of dATP opposite U: fitted Michaelis-Menten curves (left) and Hanes-Woolf fits

Unfortunately the Lineweaver-Burk plot did not give a linear result. The second method of choice, the plot after Hanes and Woolf gave a result that could be interpreted via linear regression.

3.7.2.4 Determination and evaluation of the kinetic parameters

The following parameters are determined:

K_M : the *Michaelis-Menten* constant [μM] describes the affinity of an enzyme to the substrate. The constant gives the necessary substrate concentration for the reaction velocity to be $\frac{1}{2} V_{max}$.

V_{max} : maximum velocity [$\text{nM}\cdot\text{min}^{-1}$] of the reaction for a given substrate.

k_{cat} : characteristic constant [min^{-1}] for the velocity of the enzyme.

k_{cat}/K_M : specificity constant for a given substrate.

For each incorporation assay three measurements were evaluated. The data was then taken from the *Lineweaver-Burk* plots (*Hanes-Woolf* plot for the incorporation of dATP vs U) and the standard deviation of the single measurements was determined.

Table 3.12 Measured and calculated kinetic parameters

<i>dNTP</i>	V_{max} [$\text{nM}\cdot\text{min}^{-1}$]	K_M [μM]	k_{cat} [min^{-1}]	k_{cat}/K_M [$\mu\text{M}^{-1}\cdot\text{min}^{-1}$]	k_{rel}
dATP vs U	1.75 ± 0.08	13.47 ± 5.99	0.089 ± 0.004	$6.57 \cdot 10^{-3}$	13.32
dATP vs X	3.61 ± 0.40	54.84 ± 10.64	0.183 ± 0.020	$3.33 \cdot 10^{-3}$	6.76
dGTP vs X	7.19 ± 0.92	80.62 ± 15.87	0.182 ± 0.023	$2.26 \cdot 10^{-3}$	4.58
dCTP vs X	4.83 ± 0.15	148.75 ± 12.05	0.082 ± 0.003	$0.55 \cdot 10^{-3}$	1.11
dTTP vs X	8.05 ± 2.17	275.21 ± 75.95	0.136 ± 0.037	$0.50 \cdot 10^{-3}$	1

k_{rel} is the ratio of k_{cat}/K_M of the measured incorporations over the value of k_{cat}/K_M for the incorporation of dTTP vs. X. This allows a direct comparison of the velocities of the measured incorporations with the slowest incorporation of dTTP vs. X.

3.8 Discussion of the Incorporation Kinetics

From similar experiments done it follows that the accuracy of such measurements is not too high. In 1993 *Cai* and *Goodman* reported on HIV-1 reverse transcriptase incorporating dNTPs opposite a DNA template.^[103,191] The measurements done differed about 20 % between experiments.

From the results presented in Table 3.12, it follows immediately that incorporations opposite abasic sites are slower than the incorporation of dATP opposite a U residue. dATP is built-in opposite U 2, 3 and 13 times faster than dATP, dGTP and dCTP/TTP are incorporated opposite an abasic site. Most striking is the fact, that the incorporation of dATP versus U is only two times faster than the incorporation of dATP vs AS. This absolutely correlates with the findings in Figure 3.34 from the standing start experiments where most of the abasic template is transcribed to full length in the presence of all dNTPs.

Most important it can be proved that the “A-rule” proposed for DNA abasic sites is also valid for RNA abasic sites: $A > G \gg C \sim T$. Incorporation of dATP opposite an abasic site is 1.5 and 6.5 times faster than for dGTP and dCTP/TTP, respectively.

[191] Goodman, M. F., Cai, H., Bloom, L. B., Eritja, R., in *Ann. N. Y. Acad. Sci.*, Vol. 726, **1994**, pp. 132-143.

4 Conclusions and Outlook

This work presents for the first time a comparison of the chemical stabilities of natural RNA and DNA abasic sites. RNA abasic sites are shown to be more stable compared to their DNA analogue. Moreover it could be shown that RNA abasic sites are overread in high yield by HIV-1 reverse transcriptase and that the “A-rule” known for DNA abasic sites can be extended to RNA abasic lesions.

The synthesis of the abasic site building blocks is straight forward and resulted in overall yields of 21 % for the natural RNA abasic precursor **1** and 32 % for the 2'-*O*-methylated RNA abasic precursor **2** starting from tetraacetyl ribose, as well as 44 % for the DNA abasic site precursor **3** starting from 1,3,5-tri-*O*-acetyl-2'-deoxy-D-ribose. These phosphoramidites were completely stable over more than one year when kept in the dark at -20°C. All three building blocks could be incorporated with slightly increased coupling times in comparable yields to natural phosphoramidites by standard oligonucleotide synthesis. Deprotection studies with heptamers containing **1** and **3** showed fast and clean release of the appropriate abasic sites. Kinetic studies under strongly basic conditions (pH 13) showed the RNA abasic site to be more stable than the DNA abasic site by a factor of 150 with regard to the β -elimination mechanism. Moreover natural RNA abasic sites that undergo strand cleavage by β -elimination and cyclophosphate formation are measured to be more stable by a factor of 15 compared to natural DNA abasic sites. If cyclophosphate formation and β -elimination are compared it follows that strand cleavage by cyclophosphate formation is faster by a factor of 3. In slightly acidic media (pH 4.6) where strand cleavage only occurs by β -elimination the RNA abasic site shows to be more stable by a factor of 15 compared to a DNA abasic site.

Reverse transcription assays show that HIV-1 reverse transcriptase as well as AMV-RT perform efficient translesion synthesis. For HIV-1 RT the incorporation kinetics could be measured and the existing “A-rule” could be extended also to RNA. From the measurements it follows that the incorporation of dATP vs. U compared to dATP vs. AS is faster by a factor of only two. This suggests that RNA abasic sites in the HIV-1 genome would be highly mutagenic.

While the influence of DNA abasic sites in DNA duplexes have been explored, due to the unavailability of an RNA building block, data on the effect of an RNA abasic site on a RNA:DNA duplex is unknown.^[192-199] In addition to this, the destabilizing effect of an abasic RNA lesion has not been determined either. With the building blocks at hand these basic experiments might be performed for short duplexes. Whether the abasic lesion would endure the heating and cooling process has to be investigated first. The data would allow a more detailed comparison of DNA and RNA abasic lesions. For example it would provide information on the question which RNA:DNA duplex is more stable: the one with an abasic site in the DNA or the one with the lesion in the RNA strand.

The ability to easily generate site-specific RNA abasic sites makes it possible to study the influence of abasic lesions in more detail and different environments. Here it has been shown that in retroviruses abasic sites in the genomic RNA can lead to mutations in the reverse transcript. If one expands the question to whether abasic lesions in RNA would also lead to mutations in more complex systems it might be interesting to have a closer look on the mRNA level in eukaryotes. According to the central dogma of molecular biology the genomic information is stored in DNA, transcribed to mRNA and translated from there to proteins. So the question is, whether an abasic lesion introduced in a coding mRNA would give rise to a modified protein. The proposed experiment is based on the work of *Moore*, who could efficiently ligate a modified RNA oligomer into an mRNA by the means of the T4 DNA ligase.^[200] The principal idea is to take two parts of a mature coding mRNA without introns and a missing exon part and ligate in-between a synthesized oligoribonucleotide containing the caged abasic site in a predefined position. The synthetic oligoribonucleotides mimics the missing exon part in a way that the double ligated mRNA contains the complete code for the protein. This modified mRNA could then be deprotected and translated by means of an *in vitro* translation assay.

-
- [192] Withka, J. M., Wilde, J. A., Bolton, P. H., Mazumder, A., Gerlt, J. A., *Biochemistry* **1991**, *30*, 9931-9940.
- [193] Goljer, I., Withka, J. M., Kao, J. Y., Bolton, P. H., *Biochemistry* **1992**, *31*, 11614-11619.
- [194] Fouilloux, L., Berthet, N., Coulombeau, C., Coulombeau, C., Dheu-Andries, M. L., Garcia, J., Lhomme, J., Vatton, P., *J. Mol. Struct. (Theochem)* **1995**, *330*, 417-422.
- [195] Coppel, Y., Berthet, N., Coulombeau, C., Coulombeau, C., Garcia, J., Lhomme, J., *Biochemistry* **1997**, *36*, 4817-4830.
- [196] Wang, K. Y., Parker, S. A., Goljer, I., Bolton, P. H., *Biochemistry* **1997**, *36*, 11629-11639.
- [197] Gelfand, C. A., Plum, G. E., Grollman, A. P., Johnson, F., Breslauer, K. J., *Biochemistry* **1998**, *37*, 7321-7327.
- [198] Barsky, D., Foloppe, N., Ahmadi, S., Wilson, D. M., III, MacKerell, A. D., Jr., *Nucleic Acids Res.* **2000**, *28*, 2613-2626.
- [199] Sagi, J., Guliaev, A. B., Singer, B., *Biochemistry* **2001**, *40*, 3859-3868.
- [200] Moore, M. J., Sharp, P. A., *Science* **1992**, *256*, 992-997.

Combined transcription/translation or simple translation assays have been described in literature.^[201-204] In the case of an mRNA of a fluorescent protein where the abasic lesion is placed in the codon of the amino acid that enables the protein to fold correctly, proper protein folding could be monitored by fluorescence. Sequencing of the protein would clarify the effect of the abasic site on the translation process.

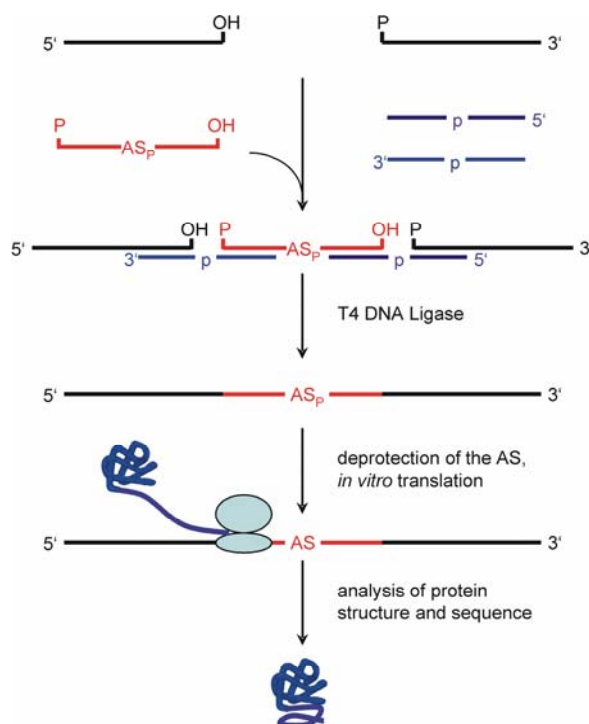


Figure 4.1 In a first step, the two mRNA parts and the modified part are annealed by short complementary DNA strands. Ligation with T4 DNA Ligase and deprotection give the abasic mRNA. *In vitro* transcription gives a protein that can be analyzed by sequencing of by structure properties

This experiment would give a great insight on the fidelity of ribosomes.

-
- [201] Spirin, A. S., Baranov, V. I., Ryabova, L. A., Ovodov, S. Y., Alakhov, Y. B., *Science* **1988**, 242, 1162-1164.
 [202] Nakano, H., Yamane, T., *Biotechnol. Adv.* **1998**, 16, 367-384.
 [203] Shimizu, Y., Inoue, A., Tomari, Y., Suzuki, T., Yokogawa, T., Nishikawa, K., Ueda, T., *Nat. Biotechnol.* **2001**, 19, 751-755.
 [204] Katzen, F., Chang, G., Kudlicki, W., *Trends Biotechnol.* **2005**, 23, 150-156.

5 Experimental Part

5.1 General

All reactions were carried out under argon in distilled, anhydrous solvents. The solvents were either purchased over molsieves or dried by filtration over activated aluminiumoxide (group owned device). All reagents were used as supplied by *Fluka*, *Sigma*, *Acros Chemicals* or *Aldrich* in the highest purity available.

5.1.1 Chromatography

TLC is performed using pre-coated silica gel plates SIL-G-25 UV₂₅₄ (*Macherey-Nagel*). Visualization is performed under UV light (254 nm) and by using following staining reagents:

<i>Cerium reagent:</i>	10.5 g Ce(SO ₄) ₂ , 21 g phosphomolybdic acid, 60 ml conc. H ₂ SO ₄ and 900 ml H ₂ O
<i>Anisaldehyde reagent:</i>	10 ml anisaldehyde, 10 ml conc. H ₂ SO ₄ , 2 ml acetic acid and 180 ml ethanol

Stained TLC plates are heated until stains remained visible. Colum chromatography is performed using *Silica gel 60* (40-63 μm) from *Fluka* or *SDS*. Technical grade solvents were distilled before use.

5.2 Instrumentation

5.2.1 NMR spectroscopy

All NMR spectra were measured at room temperature on *BRUKER AVANCE* (300MHz) or *BRUKER DRX* (400MHz/500MHz) spectrometers. For ¹H-NMR spectra shifts δ are given in ppm relative to residual undeuterated solvents^[205] (CDCl₃ = 7.24, DMSO-*d*₆ = 2.49), coupling constants *J* are given in Hz. Multiplicities are abbreviated as follows: s = singlet, d = doublet, t = triplet, q = quadruplet, m = multiplet, br = broad. For ¹³C-NMR spectra the shifts δ are given in ppm relative to residual solvent peaks (CDCl₃ = 77.00, DMSO-*d*₆ = 39.70). Multiplicities were established by DEPT experiments and are abbreviated as follows: s = singlet, d = doublet, t = triplet, q = quadruplet. ³¹P-NMR spectra were recorded at 162 MHz or 202 MHz. Chemical shifts δ are reported in ppm relative to 85 % H₃PO₄ as an external standard. Difference NOE experiments were recorded at 400 MHz.

[205] Gottlieb, H. E., Kotlyar, V., Nudelman, A., *J. Org. Chem.* **1997**, *62*, 7512-7515.

5.2.2 Mass spectrometry

Electrospray ionization mass spectra (ESI-MS) were recorded on *VG platform Fisons* instruments. Electron impact mass spectra (EI-MS) were recorded on *Micromass Autospec Q* (Manchester, UK), with sector field MS, electron impact 70 eV, solid sample injection, acceleration voltage 8 kV, and external calibration with perfluorokerosen (PFK).

5.2.3 UV-Vis spectroscopy

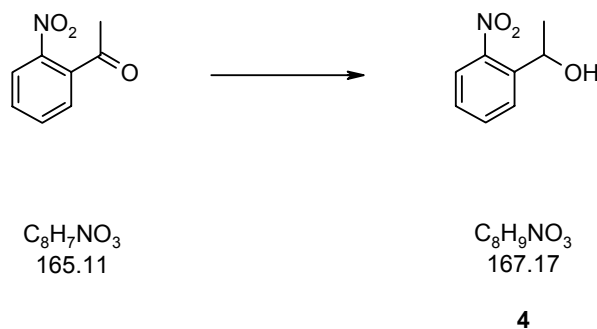
A *Perkin Elmer Lambda 16 UV/Vis* spectrophotometer was used. Samples were measured using a quartz cuvette with a path length of 1 cm. The wavelength (λ_{\max}) is indicated in nm.

5.2.4 Melting point

A *Büchi SMP-510* apparatus was used. The melting points of solids were measured in glass capillaries and indicated without correction in °C.

5.3 Synthesis of the Natural RNA Abasic Site Precursor

5.3.1 1-(2-Nitrophenyl)ethanol (**4**)



A solution of 2-nitroacetophenone (10 g, 60.06 mmol) in methanol (245 ml) is cooled to 0° C. After addition of NaBH₄ (2.29 g, 60.06 mmol, 1 eq.) the solution is stirred for 1 h under argon in the ice-bath and is finally neutralized with glacial acetic acid (ca. 10 ml). The mixture is then concentrated under reduced pressure. The residue is diluted in ethyl acetate (240 ml) and washed with water (120 ml), saturated NaHCO₃ (120 ml) and saturated NaCl (120 ml). The aqueous layers are extracted with ethyl acetate (3 x 120 ml). The organic layers are dried (Na₂SO₄) and evaporated. The oily residue is chromatographed on silica gel (250 g, eluted with ethyl acetate/hexane 1:4) to give racemic alcohol **4** as a yellow oil (9.93 g, 98 %).

TLC (ethyl acetate/hexane 1:2): *R_f* 0.38

¹H-NMR (300 MHz, CDCl₃): δ 7.81-7.90 (*m*, 2 H, H-C(3), H-C(4)); 7.61-7.66 (*m*, 1 H, H-C(5)); 7.37-7.43 (*m*, 1 H, H-C(6)); 5.37-5.44 (*m*, 1 H, H-C(7)); 2.27 (*d*, *J* = 4.1, 1 H, HO-C(7)); 1.56 (*d*, *J* = 6.6, 3 H, H₃C(8)).

¹³C-NMR (75 MHz, CDCl₃): δ 147.7 (*s*, C(2)); 140.9 (*s*, C(1)); 133.6 (*d*, C(5)); 128.1 (*d*, C(6)); 127.5 (*d*, C(4)); 124.2 (*d*, C(3)); 65.5 (*d*, C(7)); 24.2 (*q*, C(8)).

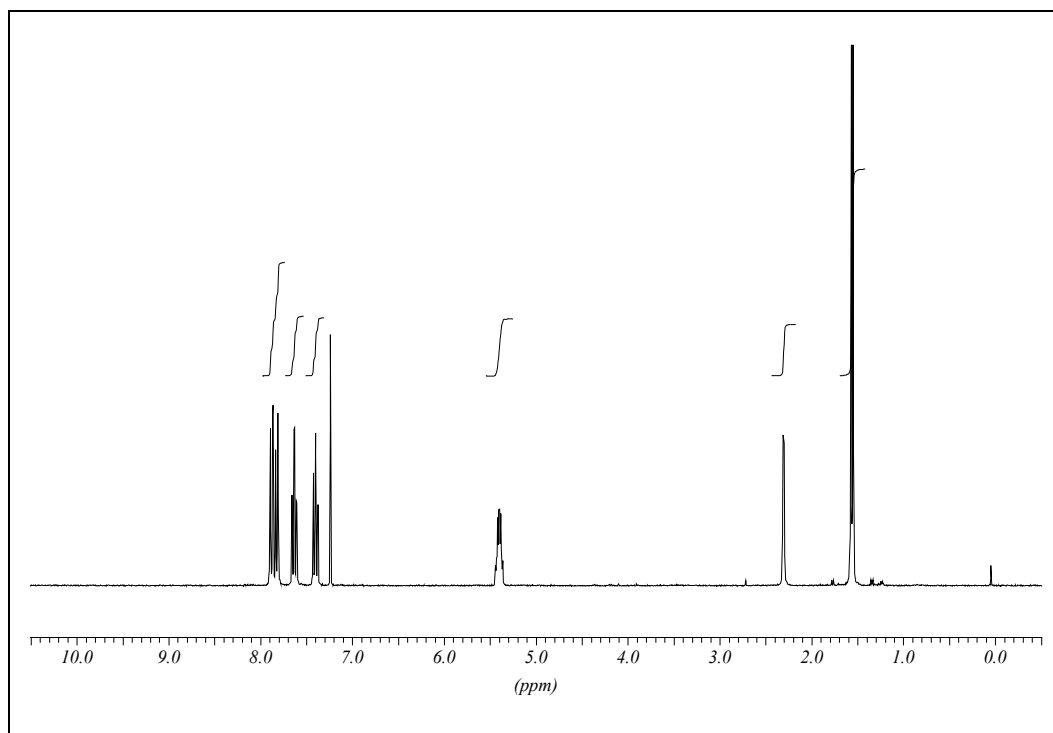


Figure 5.1 $^1\text{H-NMR}$ spectrum of **4**

^{13}C -NMR (75 MHz, CDCl_3): δ 178.16 (*s*, C=O); 166.56 (*s*, C=O); 147.57 (*s*, Ar); 137.04 (*s*, Ar); 133.70, 128.76, 127.39, 124.57 (*4d*, Aryl-C); 90.73 (*s*, C-O); 69.41 (*d*, HCMe); 54.80 (*s*, CMe); 54.40 (*s*, CMe₂); 30.81 (*t*, CH₂); 28.90 (*t*, CH₂); 22.04 (*q*, HCMe); 16.69 (*q*, CH₃); 16.60 (*q*, CH₃); 9.61 (*q*, CH₃).

Spectroscopic data for (*S,S*)-ester **17b**:

^1H -NMR (300 MHz, CDCl_3): δ 7.95-7.98 (*m*, 1 H, Ar); 7.71-7.74 (*m*, 1 H, Ar); 7.61-7.67 (*m*, 1 H, Ar); 7.41-7.47 (*m*, 1 H, Ar); 6.50 (*dd*, 1 H, $J = 6.6, 6.3$, HCMe); 2.30-2.39 (*m*, 1 H, CH₂); 1.84-1.98 (*m*, 2 H, CH₂); 1.60-1.69 (*m*, 1 H, CH₂); 1.68 (*d*, $J = 6.3$, 3 H, HCMe); 1.10, 1.02, 0.97 (*3s*, 9 H, 3 Me).

^{13}C -NMR (75 MHz, CDCl_3): δ 178.33 (*s*, C=O); 166.56 (*s*, C=O); 147.48 (*s*, Ar); 137.04 (*s*, Ar); 133.90, 128.72, 127.39, 124.57 (*4d*, Aryl-C); 90.87 (*s*, C-O); 69.43 (*d*, HCMe); 54.87 (*s*, CMe); 54.35 (*s*, CMe₂); 30.54 (*t*, CH₂); 28.80 (*t*, CH₂); 22.15 (*q*, HCMe); 16.73 (*q*, CH₃); 16.62 (*q*, CH₃); 9.67 (*q*, CH₃).

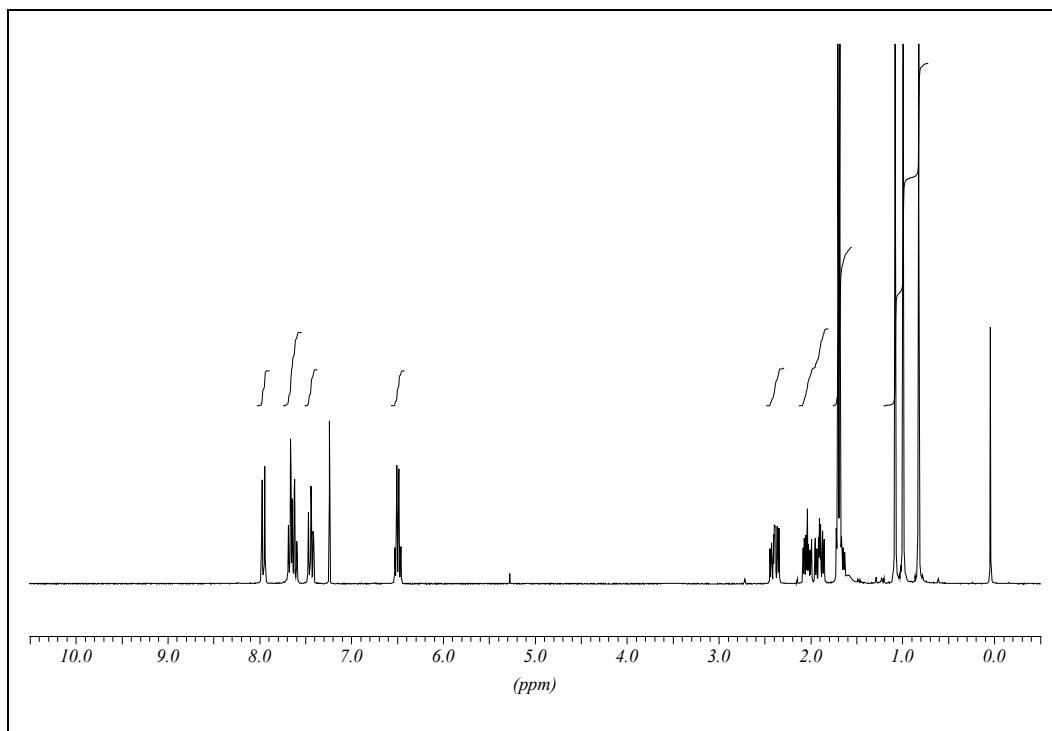


Figure 5.2 $^1\text{H-NMR}$ spectrum of **17a**

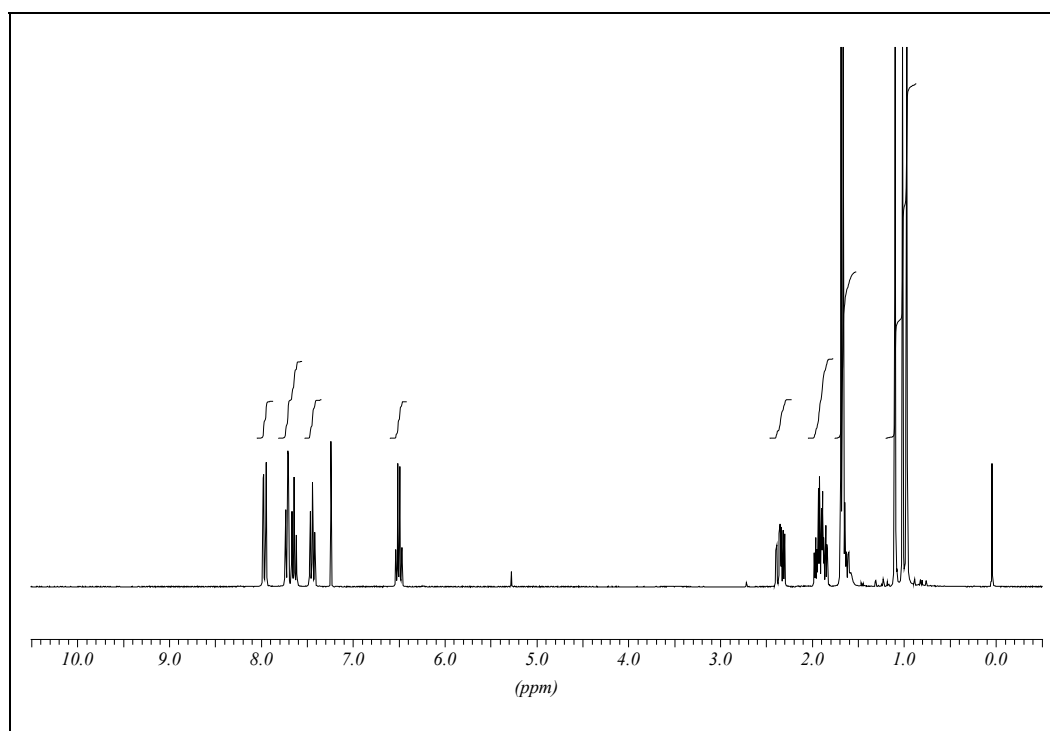
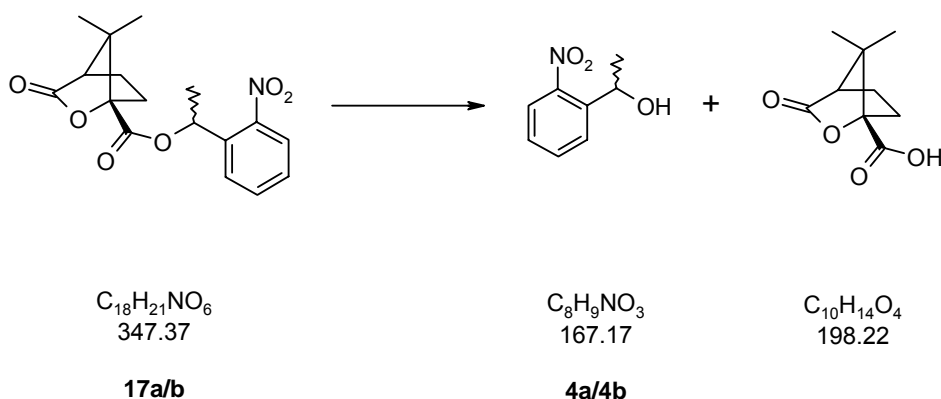


Figure 5.3 $^1\text{H-NMR}$ spectrum of **17b**

5.3.3 (*R*)-, (*S*)-1-(2-Nitrophenyl)ethanol (**4a/b**)



(*R,S*)-ester **17a** (2.78 g) is dissolved in a mixture of methanol (45 ml) and KOH (2 M, 6 ml) and the solution is heated under reflux for 45 min. The mixture is then allowed to cool to room temperature, neutralized with HCl (2 M, 6 ml) and concentrated under reduced pressure. The residue is extracted with ethyl acetate (2 x 50 ml) and the organic extract is washed with sat. NaHCO₃ (2 x 50 ml), dried (Na₂SO₄) and evaporated. Column chromatography of the residue on silica gel (50 g, eluted with ethyl acetate/hexane 1:2) gave 1(*R*)-(2-nitrophenyl)ethanol **4a** (1.34 g, 97 %). The aqueous layers are then acidified to pH = 1 by addition of concentrated HCl and extracted with CH₂Cl₂ (3 x 50 ml). The organic layers are dried (Na₂SO₄) and evaporated to give camphanic acid as a colorless solid.

(*S,S*) ester **17b** is saponificated in an identical manner to give alcohol **4b** and camphanic acid with the same yields.

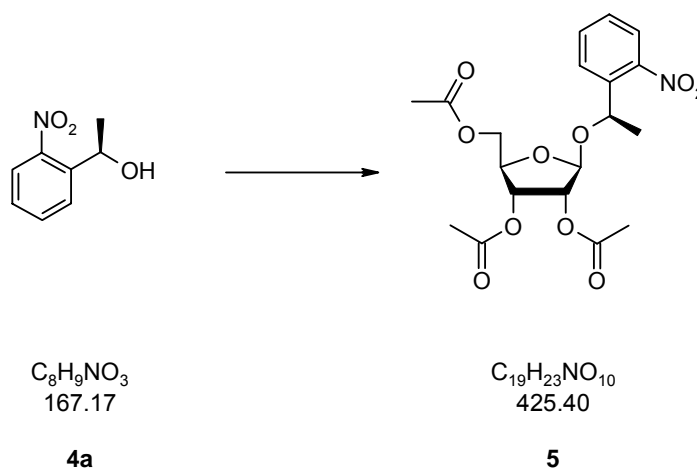
TLC (ethyl acetate/hexane 1:2): *R_f* 0.38

Spectroscopic data for (*R*)-, (*S*)-1-(2-nitrophenyl)ethanol **4a/4b**:

The ¹H-NMR spectra of the enantiomers are identical to the spectrum of the racemic alcohol **4**.

Spectroscopic data for camphanic acid:

¹H-NMR (300 MHz, CDCl₃): δ 8.80 (*s br*, 1 H, OH); 2.48 (*ddd*, *J* = 13.5, 10.6, 4.2, 1 H, CH₂); 2.11 (*ddd*, *J* = 13.5, 9.3, 4.5, 1 H, CH₂); 1.98 (*ddd*, *J* = 13.2, 10.6, 4.5, 1 H, CH₂); 1.74 (*ddd*, *J* = 13.2, 9.3, 4.3, 1 H, CH₂); 1.15 (*s*, 3 H, CH₃); 1.11 (*s*, 3 H, CH₃); 1.03 (*s*, 3 H, CH₃).

5.3.4 1'-[(*R*)-1-(2-Nitrophenyl)ethyl]-2',3',5'-tri-*O*-acetyl-ribofuranose (**5**)

(1,2,3,5)-Tetra-*O*-acetyl-ribofuranose (11.61 g, 36.5 mmol, 1.22 eq.) is added under argon to a solution of (*R*)-1-(2-nitrophenyl)ethanol **4a** (5 g, 29.9 mmol) in absolute acetonitrile (225 ml). The mixture is cooled to -20 °C and trimethylsilyl-trifluoromethanesulfonate (1.9 ml, 10.1 mmol, 0.35 eq.) is added slowly in four equal portions every 30 min. After two hours the reaction mixture is taken up in ethyl acetate (300 ml) and washed with saturated NaHCO₃ (3 x 100 ml). The water layer is extracted with ethyl acetate (3 x 100 ml). The organic layers are dried (Na₂SO₄) and evaporated under reduced pressure. The residue is chromatographed on silica gel (300 g, eluted with ethyl acetate/hexane 1:3) to give nucleoside **5** (9.6 g, 77 %) as a yellow oil.

TLC (ethyl acetate/hexane 1:3): *R_f* 0.29

¹H-NMR (300 MHz, CDCl₃): δ 7.85-7.88 (*m*, 1 H, Ar); 7.71-7.74 (*m*, 1 H, Ar); 7.59-7.64 (*m*, 1 H, Ar); 7.36-7.41 (*m*, 1 H, Ar); 5.34 (*q*, *J* = 6.3, 1 H, H-CMe); 5.27 (*d*, *J* = 4.8, 1 H, H-C(1'))); 5.15-5.20 (*m*, 2 H, H-C(2'), H-C(3')); 4.14-4.20 (*m*, 1 H, H-C(4')); 3.97-4.02, 3.56-3.62 (2*m*, 2 H, H₂-C(5')); 2.08, 2.01, 1.89 (3*s*, 9 H, 3 Ac); 1.50 (*d*, *J* = 6.3, 3 H, H-CMe).

¹³C-NMR (75 MHz, CDCl₃): δ 170.4, 169.7, 169.6 (3*s*, C=O); 147.2, 139.4 (2*s*, Ar); 133.4, 128.4, 128.0, 124.0 (4*d*, Ar); 103.9 (*d*, C(3')); 78.2 (*d*, C(4')); 74.8 (*d*, C(1')); 71.3 (*d*, C(2')); 71.0 (*s*, H-CMe); 64.2 (*t*, C(5')); 22.5 (*q*, H-CMe); 20.6, 20.5 (2*q*, 3 Ac).

ESI-MS: 873.22 (10), 851.20 (5), 648.21 (25), 448.17 (5), 426.46 (2), 259.07 (100).

HR-ESIMS ($M + Na^+$) for $C_{19}H_{23}NO_{10}$. Calculated: 448.1219. Found: 448.1240.

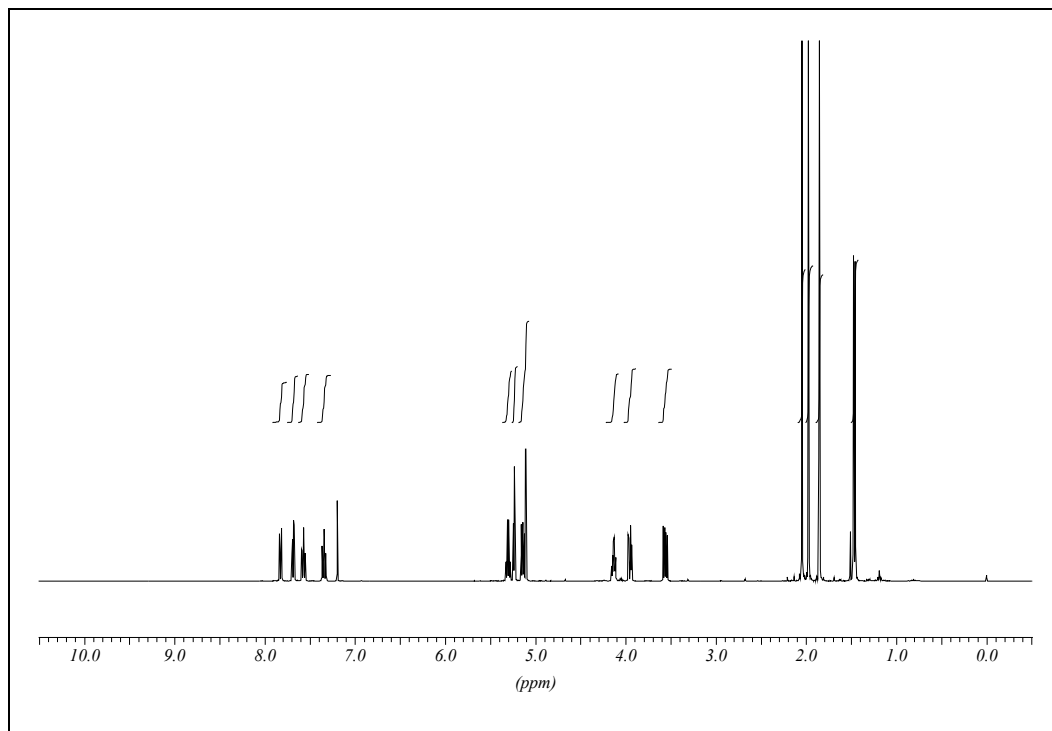
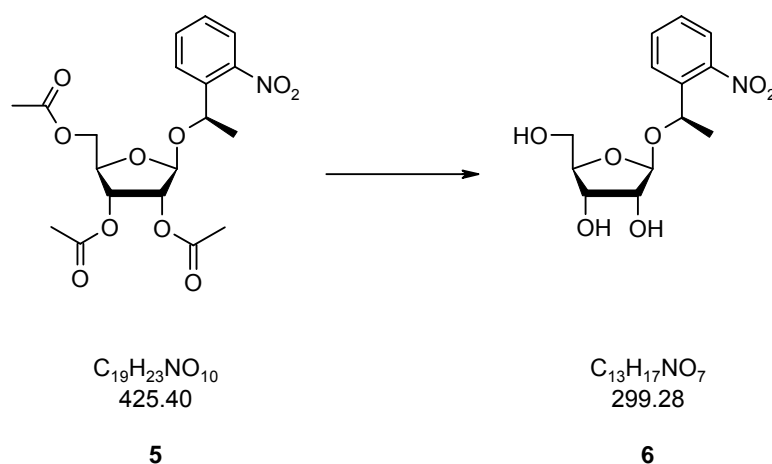


Figure 5.4 1H -NMR spectrum of 5

5.3.5 1'-[(R)-1-(2-Nitrophenyl)ethyl]-ribofuranose (**6**)

Na_2CO_3 (406 mg, 3.83 mmol, 1 eq.) is added to a solution of 1'-(2-nitrophenyl)ethyl-(2',3',5')-tri-*O*-acetyl-ribofuranose **5** (1.63 g, 3.83mmol) in methanol (12 ml) under argon. The mixture is stirred for 22 hours at room temperature. The reaction mixture is diluted with ethyl acetate (150 ml) and washed with saturated NaHCO_3 (2 x 70 ml). The water layer is then extracted with ethyl acetate (3 x 70 ml). The organic layers are dried (Na_2SO_4) and evaporated under reduced pressure. The residue is chromatographed on silica gel (60 g, eluted with ethyl acetate) to give nucleoside **6** (1.03 g, 90 %) as a white solid.

To get compound **6** in a powdered form, it is recrystallized from hot ethyl acetate, washed with hexane and dried.

TLC (ethyl acetate): R_f 0.31

UV (EtOH): $\epsilon_{260} = 6000$

$^1\text{H-NMR}$ (300 MHz, $\text{DMSO-}d_6$): δ 7.88-7.91 (*m*, 1 H, Ar); 7.71-7.72 (*m*, 2 H, Ar); 7.46-7.54 (*m*, 1 H, Ar); 5.14 (*q*, $J = 6.6$, 1 H, *HCM*e); 5.07 (*d*, $J = 4.0$, 1 H, OH); 5.06 (*s*, 1 H, H-C(1')); 4.81 (*d*, $J = 5.9$, 1 H, OH); 4.38 (*t*, $J = 5.5$, 1 H, HO-C(5')); 3.73-3.76 (*m*, 2 H, H-C(2'), H-C(3')); 3.65-3.67 (*m*, 1 H, H-C(4')); 3.21-3.28, 2.94-3.00 (2*m*, 2 H, $\text{H}_2\text{-C}(5')$); 1.40 (*d*, $J = 6.6$, 3 H, *HCM*e).

^{13}C -NMR (75 MHz, $\text{DMSO-}d_6$): δ 147.4, 139.3 (2s, Ar); 133.6, 128.6, 128.5, 124.0 (4d, Ar); 105.8 (d, C(1')); 83.9 (d, C(4')); 74.9, 71.3 (2d, C(3'), C(2')); 69.7 (d, HCMe); 63.0 (t, C(5')); 22.5 (q, HCMe).

ESI-MS: 621.15 (60), 599.27 (25), 432.14 (25), 321.95 (100), 300.01 (80), 132.91 (50).

HR-ESIMS ($\text{M} + \text{Na}^+$) for $\text{C}_{13}\text{H}_{17}\text{NO}_7$. Calculated: 322.0902. Found: 322.0904.

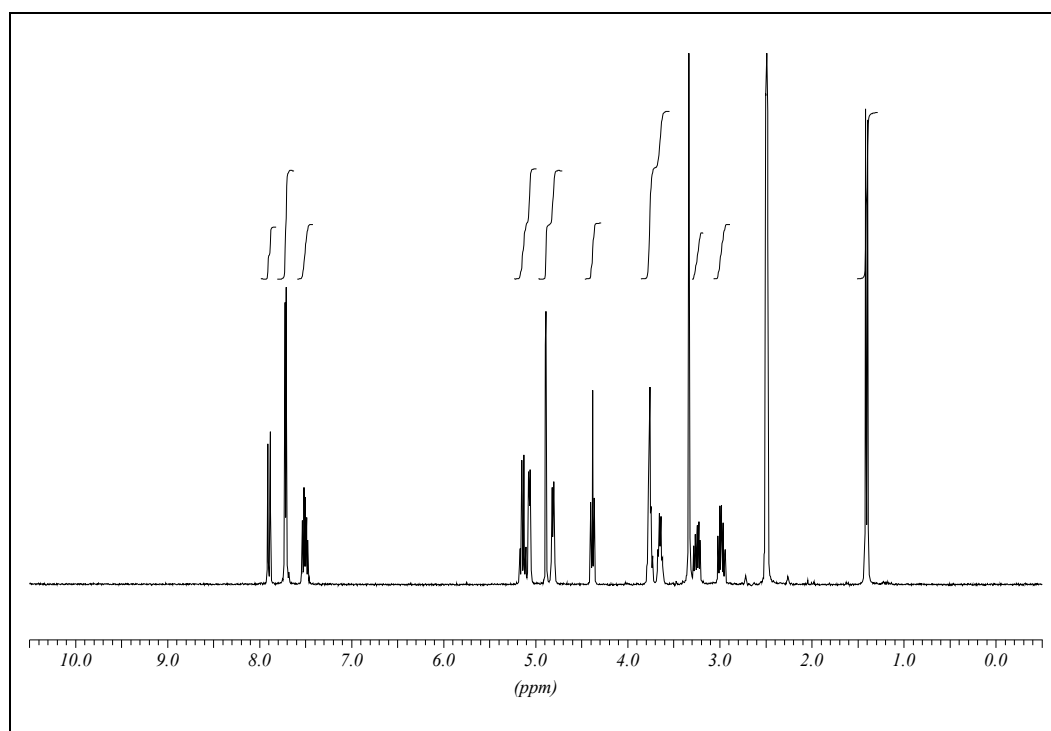
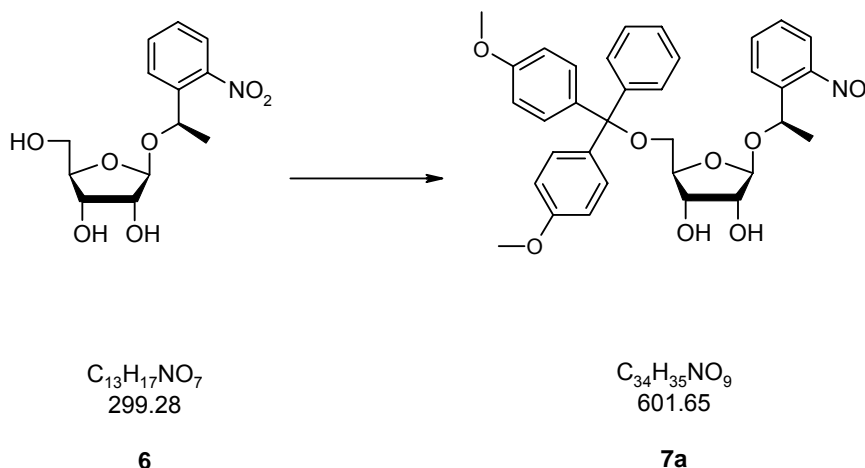


Figure 5.5 ^1H -NMR spectrum of **6**

5.3.6 1'-[(*R*)-1-(2-Nitrophenyl)ethyl]-5'-[(4,4'-dimethoxy)triphenyl]-ribofuranose (**7a**)



Triol **6** (800 mg, 2.7 mmol) is co-evaporated with pyridine (2 x 3 ml) and diluted under argon in 8.5 ml of pyridine. 4,4'-Dimethoxytriphenylmethyl chloride (1.09 g, 3.2 mmol, 1.2 eq.) is added in four equal portions every 15 min. After 90 min. the solution is taken up in ethyl acetate (25 ml) and washed with NaHCO₃ (3 x 15 ml). The aqueous phases are extracted with ethyl acetate (2 x 15 ml) and the organic layers are dried (Na₂SO₄) and evaporated. The residue is chromatographed on silicagel (50 g, eluted with ethyl acetate/hexane + 1 % triethylamine) to give (*R*)-isomer **7a** (1.51 g, 94 %) as a pale yellow foam.

Diastereomers are separable.

TLC (ethyl acetate/hexane 2:1): **7a** *R_f* 0.48; **7b** *R_f* 0.35

Spectroscopic data for **7a**:

¹H-NMR (300 MHz, CDCl₃): δ 7.82-7.85 (*m*, 1 H, Ar); 7.63-7.65 (*m*, 1 H, Ar); 7.20-7.34 (*m*, 12 H, Ar); 6.78 (*m*, 4 H, Ar); 5.31 (*q*, *J* = 6.3, 1 H, HCMe); 5.09 (*s*, 1 H, H-C(1')); 4.21-4.27 (*m*, 1 H, H-C(2')); 4.14-4.17 (*m*, 1 H, H-C(3')); 3.91-3.97 (*m*, 1 H, H-C(4')); 3.80 (*s*, 6 H, OMe); 3.08-3.12 (*m*, 1 H, H-C(5')); 2.89-2.95 (*m*, 1 H, H-C(5')); 2.66 (*s*, 1 H, HO); 2.42 (*s*, 1 H, HO); 1.49 (*d*, *J* = 6.3, 3 H, HCMe).

¹³C-NMR (75 MHz, CDCl₃): δ 158.4 (*s*, Ar); 147.0 (*s*, npe); 144.6 (*s*, Ar); 140.0 (*s*, npe), 135.8, 135.7 (2*s*, Ar); 133.2 (*d*, npe), 130.0, 129.9, 129.1 (3*d*, Ar); 128.3 (*d*, npe),

128.0 (*d*, npe), 127.8, 127.6, 126.8 (3*d*, Ar); 124.0 (*d*, npe), 113.1 (*d*, Ar); 106.0 (*d*, C(1')); 86.2 (*s*, Ar₃-C-O); 81.6 (*d*, C(4')); 75.6 (*d*, C(3')); 73.2 (*d*, C(2')); 71.1 (*d*, HCMe); 64.3 (*t*, C(5')); 55.2 (*q*, OMe); 22.7 (*q*, HCMe).

ESI-MS: 624.27 (35), 448.16 (100), 303.20 (80).

HR-ESIMS (M + Na⁺) for C₃₄H₃₅NO₉. Calculated: 624.2209. Found: 624.2208.

Spectroscopic data for **7b**:

¹H-NMR (300 MHz, CDCl₃): δ 7.88-7.91 (*m*, 1 H, Ar); 7.59-7.68 (*m*, 1 H, Ar); 7.16-7.51 (*m*, 12 H, Ar); 6.85-6.88 (*m*, 4 H, Ar); 5.39 (*q*, *J* = 6.3, 1 H, HCMe); 4.70 (*s*, 1 H, H-C(1')); 4.30-4.35 (*m*, 1 H, H-C(2')); 4.04-4.11 (*m*, 2 H, H-C(3'), H-C(4')); 3.80 (*s*, 6 H, OMe); 3.30 (*dd*, *J* = 3.3, 1.8, 2 H, H-C(5')); 2.51 (*d*, *J* = 3.7, 1 H, HO); 2.28 (*d*, *J* = 5.9, 1 H, HO); 1.37 (*d*, *J* = 6.3, 3 H, HCMe).

¹³C-NMR (75 MHz, CDCl₃): δ 158.5 (*s*, Ar); 148.6 (*s*, npe); 144.8 (*s*, Ar); 138.8 (*s*, npe), 136.0, 135.9 (2*s*, Ar); 133.5 (*d*, npe), 130.1, 130.0 (2*d*, Ar); 128.2 (*d*, npe), 128.1 (*d*, npe), 128.0, 127.9, 126.8 (3*d*, Ar); 124.3 (*d*, npe), 113.2 (*d*, Ar); 104.8 (*d*, C(1')); 86.1 (*s*, Ar₃-C-O); 82.2 (*d*, C(4')); 75.4 (*d*, C(3')); 72.7 (*d*, C(2')); 69.9 (*d*, HCMe); 64.0 (*t*, C(5')); 55.2 (*q*, OMe); 23.7 (*q*, HCMe).

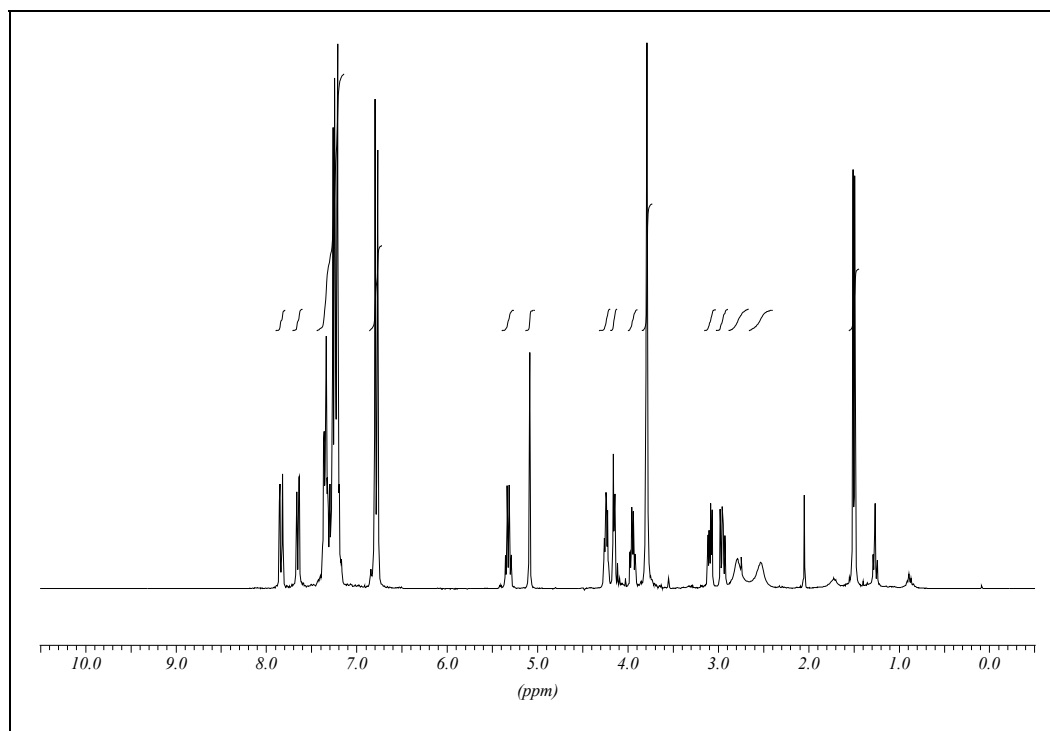


Figure 5.6 $^1\text{H-NMR}$ spectrum of **7a**

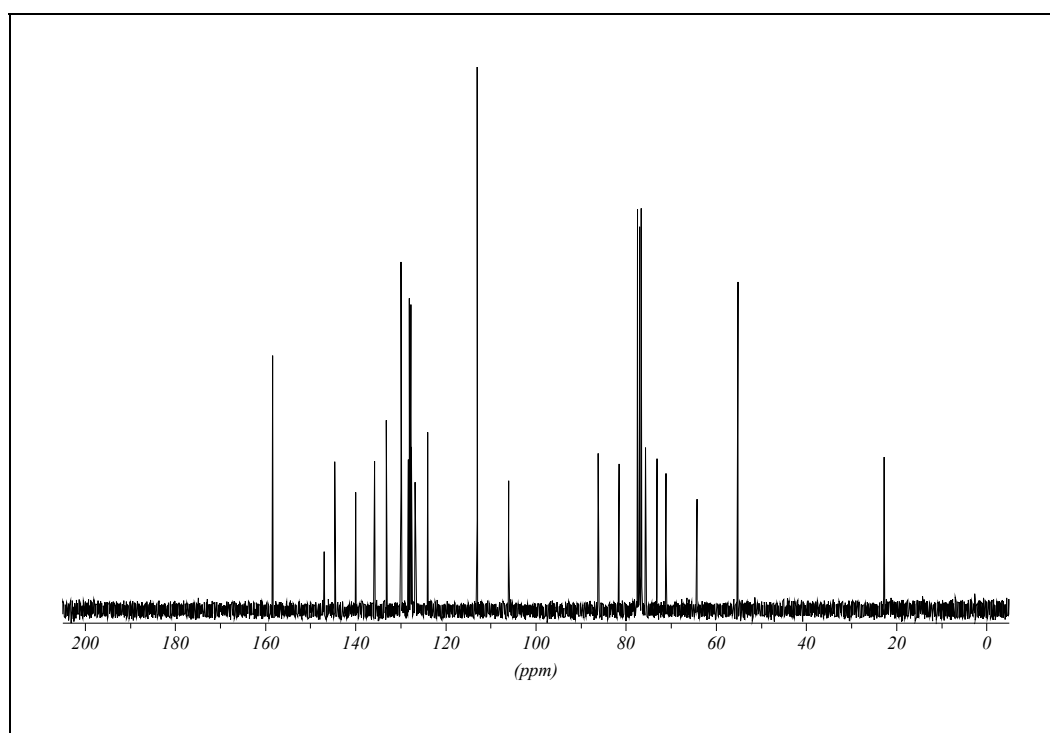


Figure 5.7 $^{13}\text{C-NMR}$ spectrum of **7a**

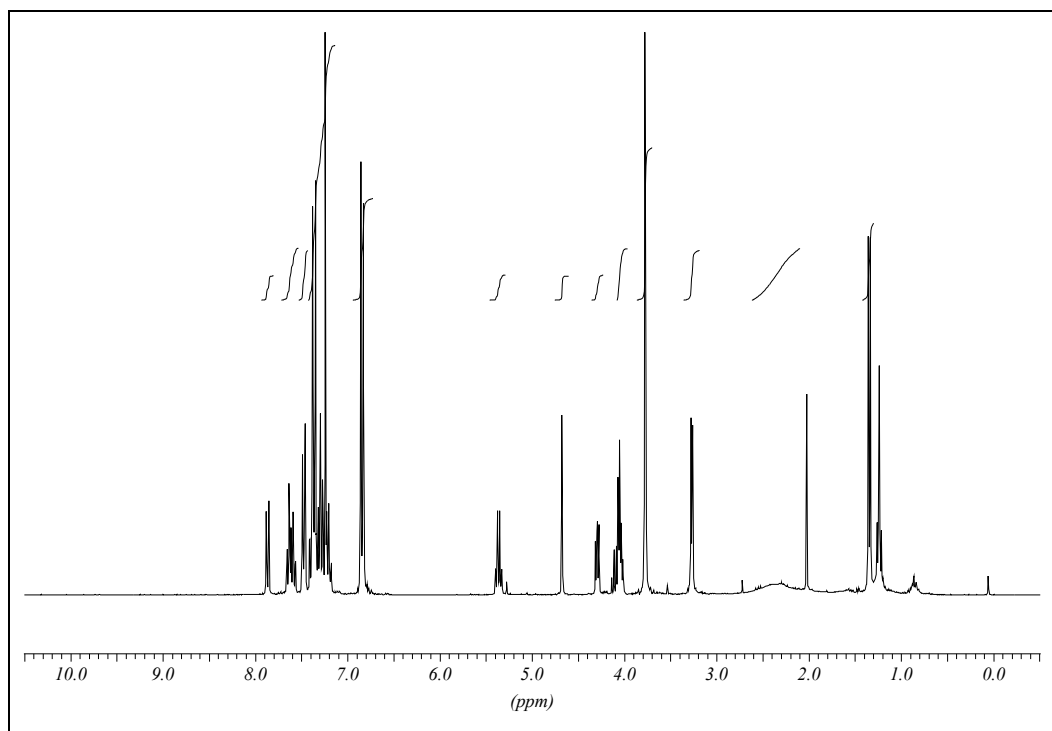


Figure 5.8 $^1\text{H-NMR}$ spectrum of **7b**

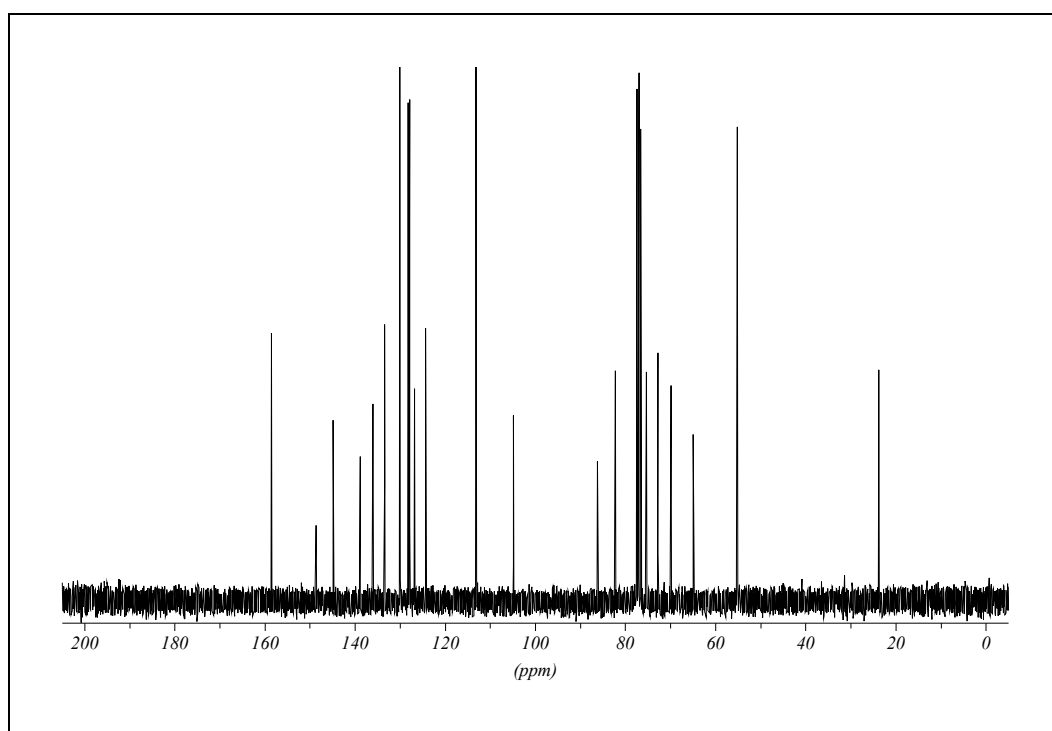
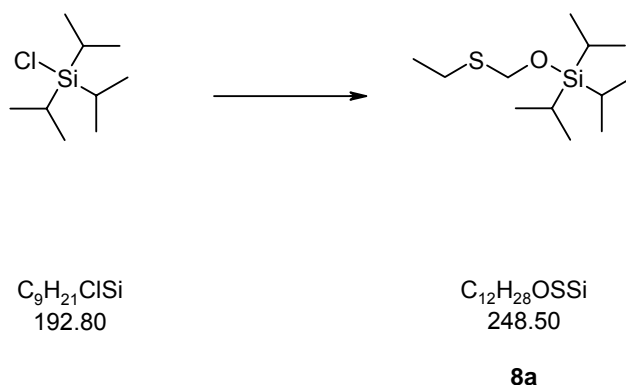


Figure 5.9 $^{13}\text{C-NMR}$ spectrum of **7b**

5.3.7 Triisopropylsilyl(ethylthio)methyl ether (8a)

To a suspension of paraformaldehyde (306 mg, 10.2 mmol) in ethanethiol (750 μ l, 10.2 mmol, 1 eq.) at 0 °C is added one drop of 10 M NaOH aq. The mixture is then slowly allowed to warm up and is stirred at 40 °C for one hour. After addition of CH_2Cl_2 (10 ml) to the solution, 1*H*-imidazole (1.38 g, 20.4 mmol, 2 eq.) and chlorotriisopropylsilane (2.05 ml, 9.7 mmol) are added and the resulting suspension is stirred for 14 hours. The reaction mixture is then taken up in hexane (20 ml) and washed with NaH_2PO_4 (10 %, 2 x 5 ml). The organic phase is then dried, evaporated and distilled in a Kugelrohr oven at 75 °C/0.05 Torr to give thioether **8a** (1.85 g, 77 %) as a colorless liquid.

1H -NMR (300 MHz, $CDCl_3$): δ 4.85 (*s*, 2 H, SCH_2O); 2.69 (*q*, $J = 7.4$, 2 H, $MeCH_2$); 1.29 (*t*, $J = 7.4$, 3 H, $MeCH_2$); 1.03-1.09 (*m*, 21 H, iPr_3Si).

^{13}C -NMR (75 MHz, $CDCl_3$): δ 66.0 (*t*, SCH_2O); 24.7 (*t*, $MeCH_2$); 17.9 (*q*, $MeCH_2$); 15.0 (*q*, Me_2CH); 11.9 (*q*, Me_2CH).

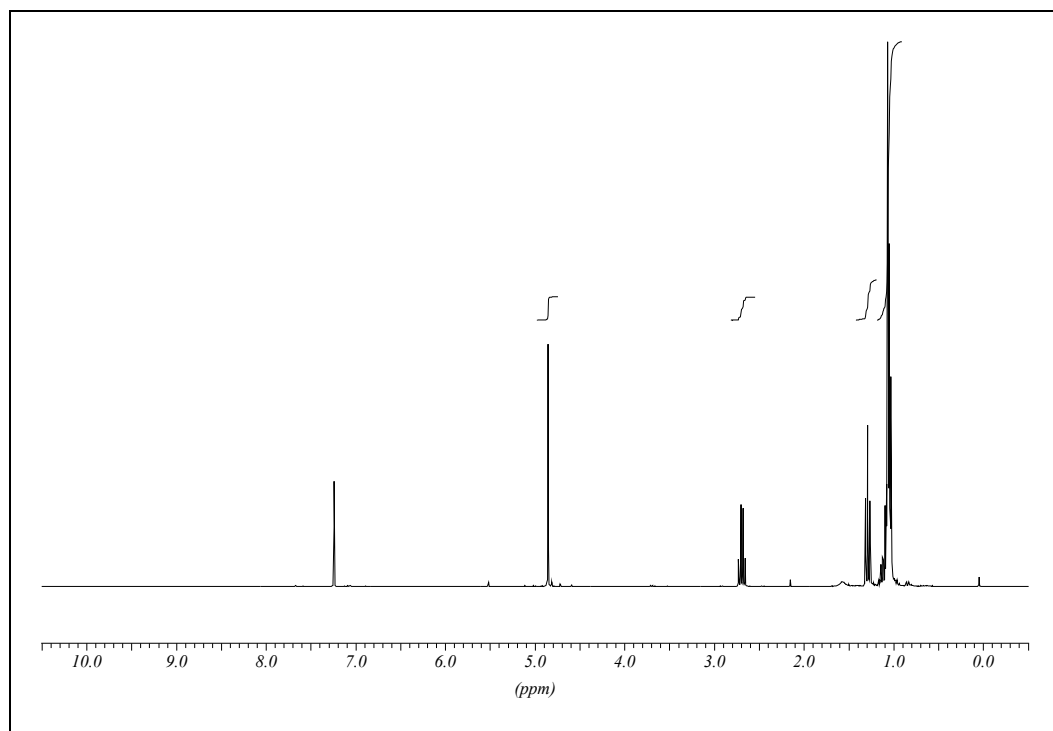
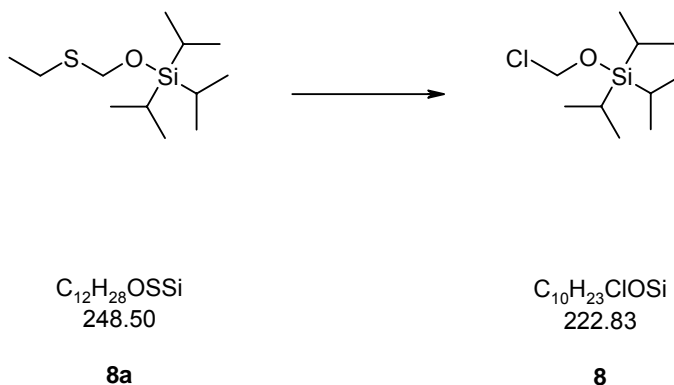


Figure 5.10 $^1\text{H-NMR}$ spectrum of **8a**

5.3.8 [(Triisopropylsilyl)oxy]methyl chloride (8**)**

A solution of **8a** (2.32 g, 9.3 mmol) in CH_2Cl_2 (7 ml) under argon is treated at 0 °C with sulfonyl chloride (9.3 ml, 9.3 mmol, 1 eq., 1 M in CH_2Cl_2). The solution is allowed to stand for one hour at room temperature and is then evaporated under reduced pressure. The residue is distilled in a Kugelrohr apparatus at 50 °C/0.05 Torr to give **8** (1.90 g, 92 %) as a colorless liquid.

$^1\text{H-NMR}$ (300 MHz, CDCl_3): δ 5.64 (*s*, 2 H, ClCH_2O); 1.06-1.08 (*m*, 21 H, $^i\text{Pr}_3\text{Si}$).

$^{13}\text{C-NMR}$ (75 MHz, CDCl_3): δ 76.6 (*t*, ClCH_2O); 17.7 (*q*, Me_2CH); 11.8 (*d*, Me_2CH).

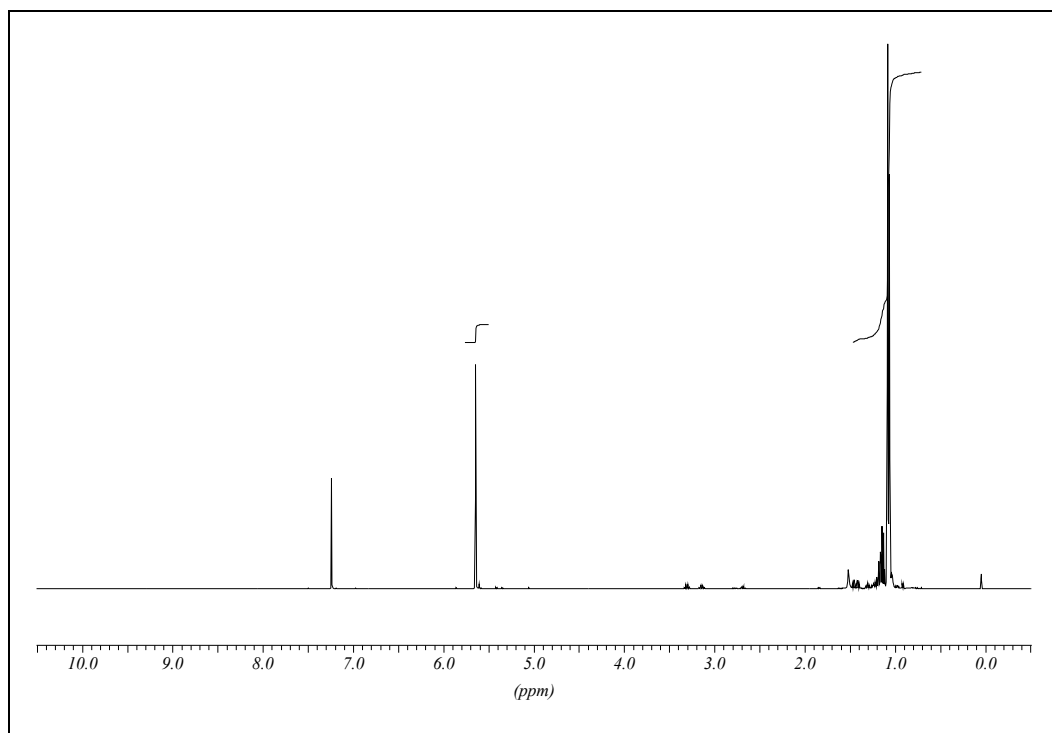
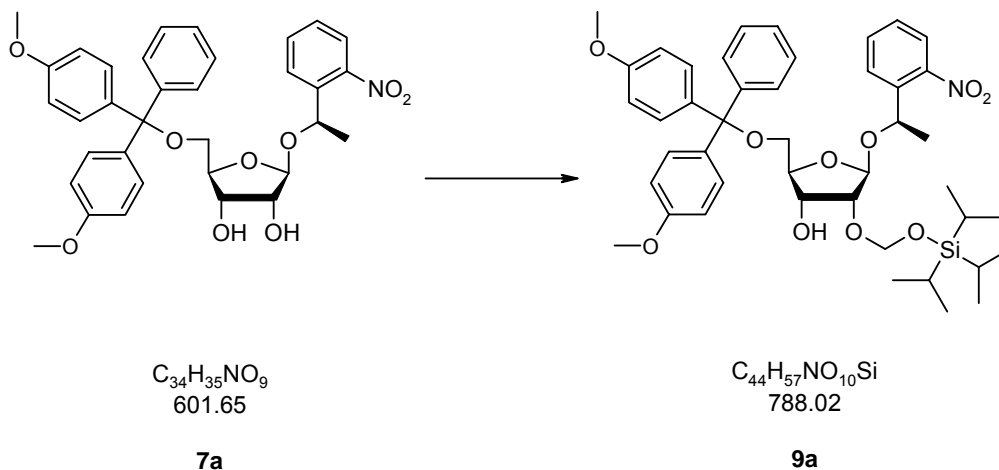


Figure 5.11 $^1\text{H-NMR}$ spectrum of **8**

5.3.9 1'-[(R)-1-(2-Nitrophenyl)ethyl]-5'-[(4,4'-dimethoxy)triphenyl]-2'-[[[(triisopropyl)silyloxy] methyl]-ribofuranose (9a)

A solution of diol **7a** (2.3 g, 3.8 mmol) in 1,2-dichloroethane (25 ml) is treated with iPr_2NEt (2.29 ml, 13.4 mmol, 3.5 eq.), Bu_2SnCl_2 (1.28 g, 4.2 mmol, 1.1 eq.) and stirred for one hour at room temperature. The solution is then heated to 80 °C and treated with chloromethylether **8** (1.11 g, 5 mmol, 1.1 eq.). After 30 minutes, the reaction mixture is allowed to cool to room temperature, is taken up in CH_2Cl_2 (100 ml) and washed with $NaHCO_3$ (3 x 50 ml). The aqueous layer is then extracted with CH_2Cl_2 (2 x 50 ml). The organic layers are dried (Na_2SO_4), filtered over Celite and evaporated under reduced pressure. The residue is chromatographed on silicagel (240 g, eluted with ethyl acetate/hexane 1:2 + 1 % triethylamine) to give **9a** and regioisomer **9b** (2.83 g, 94 %) as a yellow resin.

NMR spectroscopy shows a ratio of 65/35 in favor of 2'-alkylated **9a**. Repeated column chromatography over silicagel (2 x 300 g, 1 x 200 g; eluted with ethyl acetate/hexane 1:4 + 1 % triethylamine) gives pure **9a** (1.12 g, 37%), as a yellow resin.

The remaining mixture of **9a** and **9b** is dissolved in THF, tetrabutylammonium fluoride trihydrate is added (3 eq.) and the reaction mixture was allowed to stand for 30 min. at room temperature. The solution is then evaporated under reduced pressure, the resulting brown oil is chromatographed twice on silicagel (eluted with ethyl acetate/hexane + 1 % triethylamine) to give **8** as a colorless foam.

TLC (ethyl acetate/hexane 1:4): **9a** R_f 0.30; **9b** R_f 0.27

Spectroscopic data of **9a**:

$^1\text{H-NMR}$ (300 MHz, CDCl_3): δ 7.85-7.89 (*m*, 1 H, Ar); 7.73-7.76 (*m*, 1 H, Ar); 7.15-7.41 (*m*, 12 H, Ar); 6.75-6.78 (*m*, 4 H, Ar); 5.40 (*q*, $J = 6.3$, 1 H, *HCMe*); 5.22 (*s*, 1 H, H-C(1')); 5.15, 5.02 (*2d*, $J = 4.8$, 2 H, O-CH₂-O); 4.10-4.16 (*m*, 1 H, H-C(2')); 3.93-4.02 (*m*, 1 H, H-C(4')); 3.79 (*s*, 6 H, OMe); 3.11-3.16 (*m*, 1 H, H-C(5')); 2.93-3.00 (*m*, 1 H, H-C(5')); 2.94 (*d*, $J = 6.3$, 1 H, HO-C(3')); 1.52 (*d*, $J = 6.6$, 1 H, *HCMe*); 0.86-1.29 (*m*, 21 H, $^1\text{Pr}_3\text{Si}$).

$^{13}\text{C-NMR}$ (75 MHz, CDCl_3): δ 158.3 (*s*, Ar); 147.0 (*s*, npe); 144.8 (*s*, Ar); 140.1 (*s*, npe), 136.1, 136.0 (*2s*, Ar); 133.2 (*d*, npe), 130.0, 129.1 (*2d*, Ar); 128.5 (*d*, npe), 128.2 (*d*, npe), 127.8, 127.6, 127.0, 126.6 (*3d*, Ar); 124.0 (*d*, npe), 113.1 (*d*, Ar); 105.1 (*d*, C(1')); 90.7 (*t*, OCH₂O); 85.9 (*s*, Ar₃-C-O); 83.9 (*d*, C(2')); 83.1 (*d*, C(4')); 71.8 (*d*, C(3')); 71.6 (*d*, *HCMe*); 64.0 (*t*, C(5')); 55.2 (*q*, OMe); 23.0 (*q*, *HCMe*); 17.8 (*q*, Me₂CH); 11.8 (*d*, Me₂CH).

ESI-MS: 1598.00 (20), 1201.62 (5), 1090.57 (90), 810.51 (100).

HR-ESIMS ($\text{M} + \text{Na}^+$) for C₄₄H₅₇NO₁₀Si. Calculated: 810.3649. Found: 810.3662.

Spectroscopic data of **9b**:

$^1\text{H-NMR}$ (300 MHz, CDCl_3): δ 7.85-7.88 (*m*, 1 H, Ar); 7.73-7.75 (*m*, 1 H, Ar); 7.17-7.38 (*m*, 12 H, Ar); 6.73-6.78 (*m*, 4 H, Ar); 5.41 (*q*, $J = 6.2$, 1 H, *HCMe*); 5.14 (*s*, 1 H, H-C(1')); 5.06, 4.88 (*2d*, $J = 4.8$, 2 H, O-CH₂-O); 4.22-4.25 (*m*, 2 H, H-C(2'), H-C(3')); 4.10-4.15 (*m*, 1 H, H-C(4')); 3.78 (*s*, 6 H, OMe); 3.11-3.15 (*m*, 1 H, H-C(5')); 2.93-3.00 (*m*, 2 H, H-C(5'), HO-C(3')); 1.52 (*d*, $J = 6.2$, 1 H, *HCMe*); 1.05-1.10 (*m*, 21 H, $^1\text{Pr}_3\text{Si}$).

$^{13}\text{C-NMR}$ (75 MHz, CDCl_3): δ 158.3 (*s*, Ar); 147.0 (*s*, npe); 144.8 (*s*, Ar); 140.1 (*s*, npe), 136.1, 136.0 (*2s*, Ar); 133.2 (*d*, npe), 130.0, 129.1 (*2d*, Ar); 128.4 (*d*, npe), 128.1 (*d*, npe), 127.8, 127.6, 127.0, 126.6 (*3d*, Ar); 124.1 (*d*, npe), 113.0 (*d*, Ar); 105.9 (*d*, C(1')); 90.4 (*t*, OCH₂O); 85.8 (*s*, Ar₃-C-O); 80.9 (*d*, C(2')); 80.1 (*d*, C(4')); 75.3 (*d*, C(3')); 70.7 (*d*, *HCMe*); 63.7 (*t*, C(5')); 55.1 (*q*, OMe); 22.6 (*q*, *HCMe*); 17.8 (*q*, Me₂CH); 11.8 (*d*, Me₂CH).

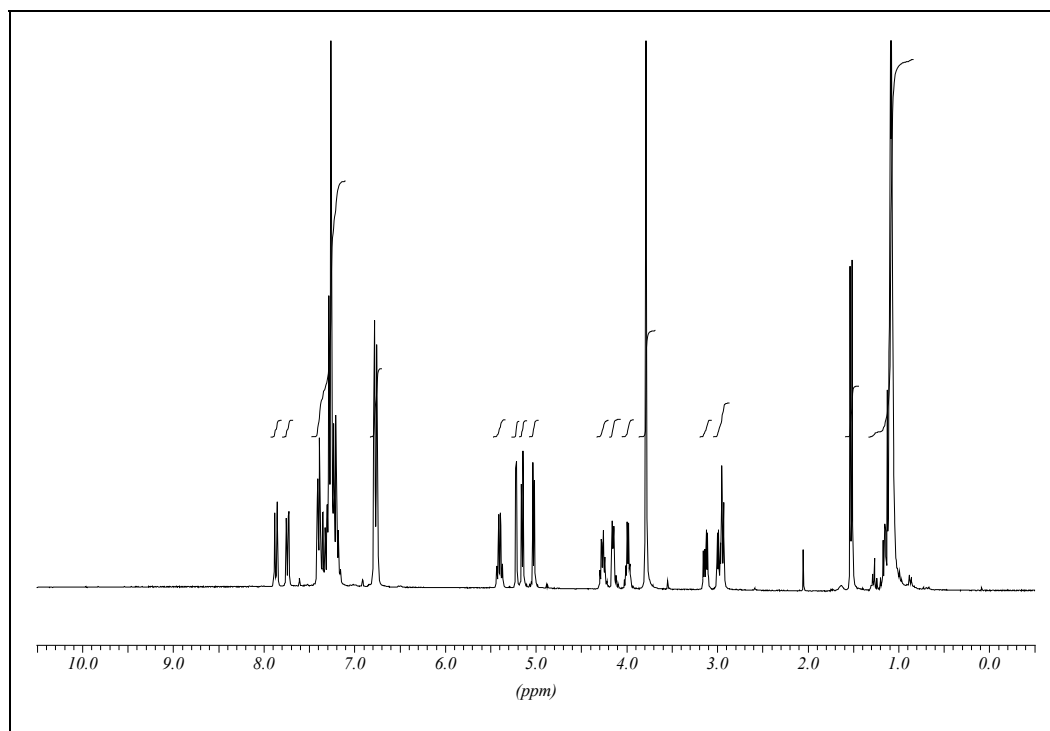


Figure 5.12 $^1\text{H-NMR}$ spectrum of **9a**

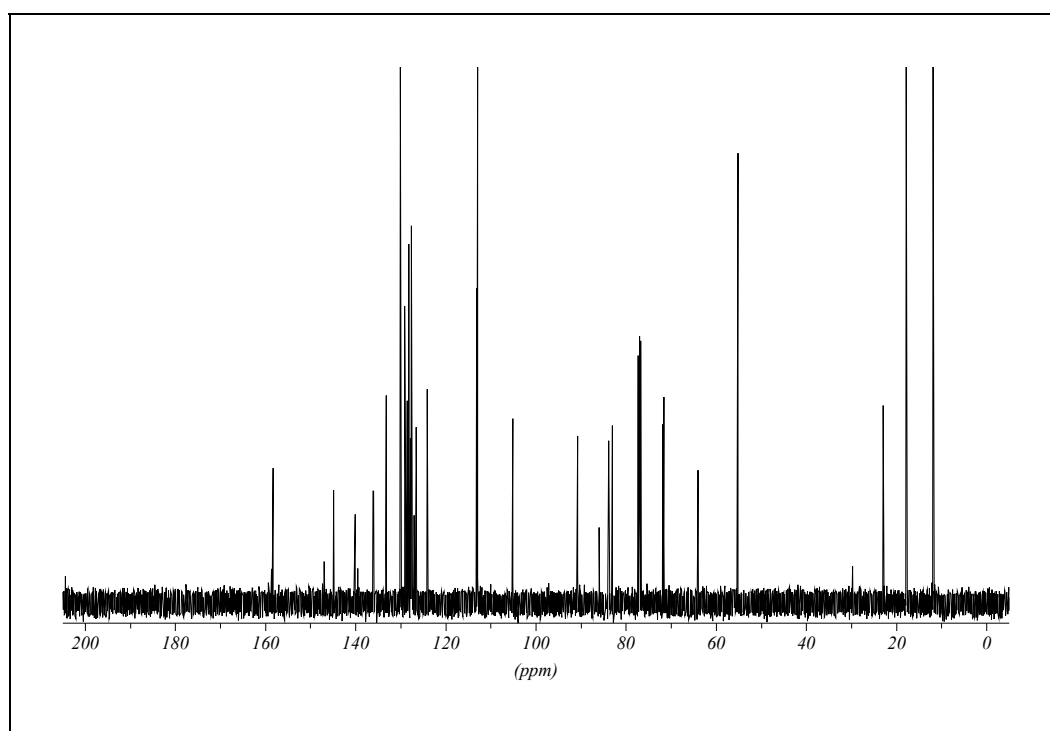


Figure 5.13 $^{13}\text{C-NMR}$ spectrum of **9a**

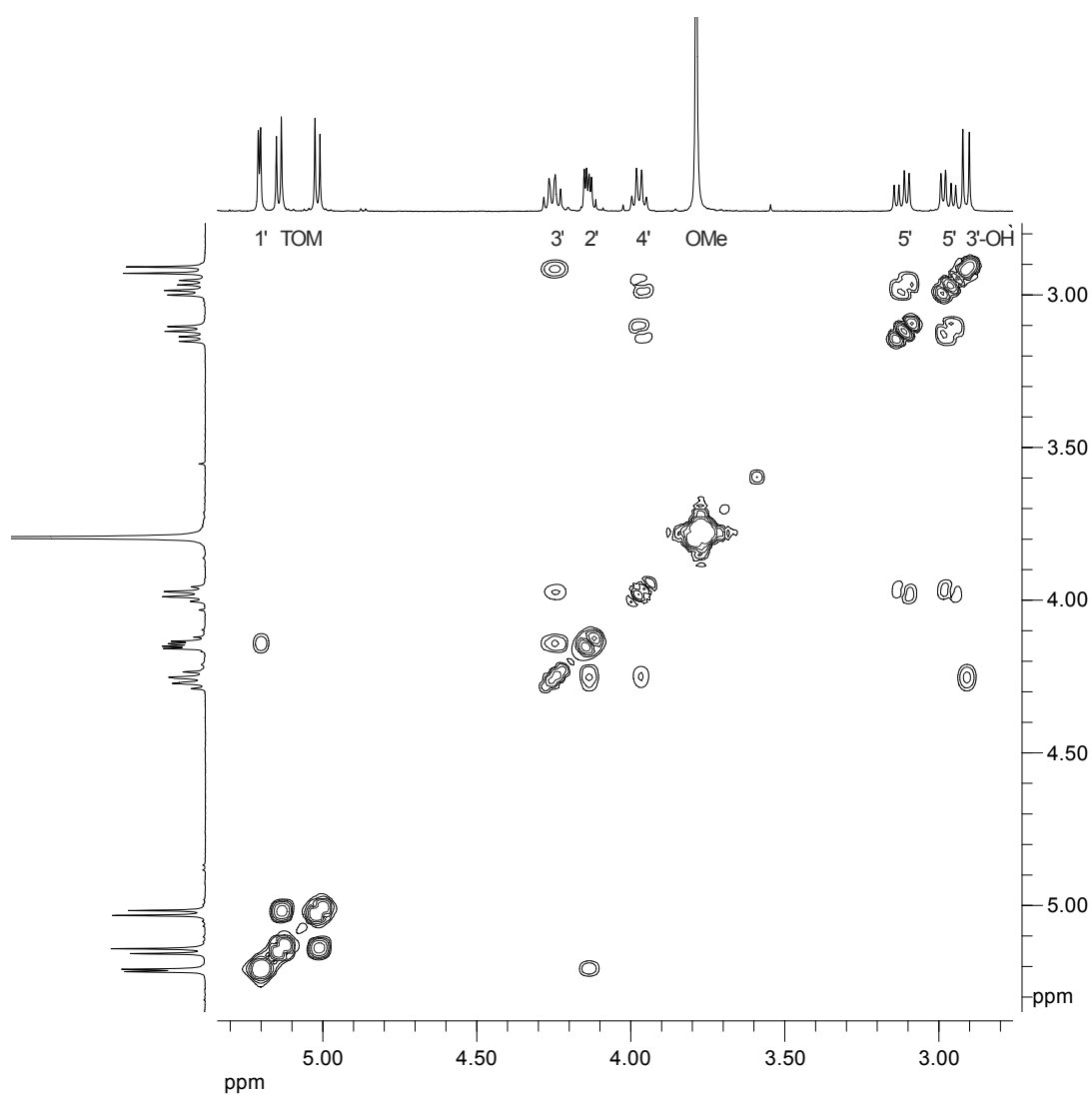


Figure 5.14 $^1\text{H}, ^1\text{H}$ correlation spectrum of **9a**.

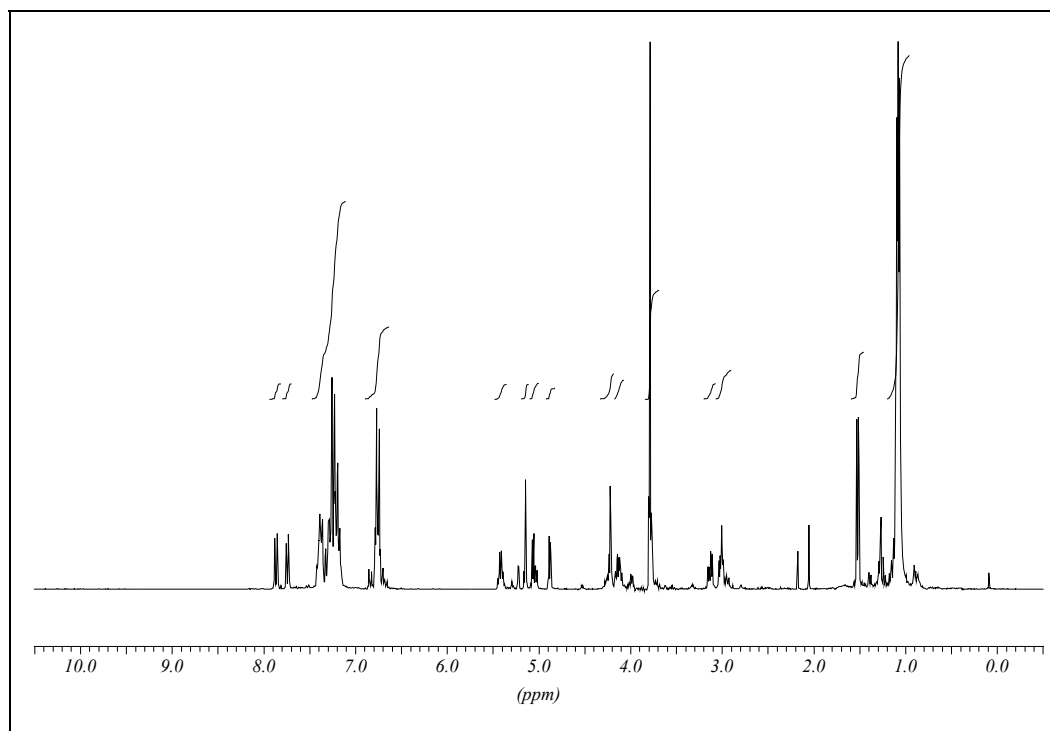


Figure 5.15 $^1\text{H-NMR}$ spectrum of **9b**

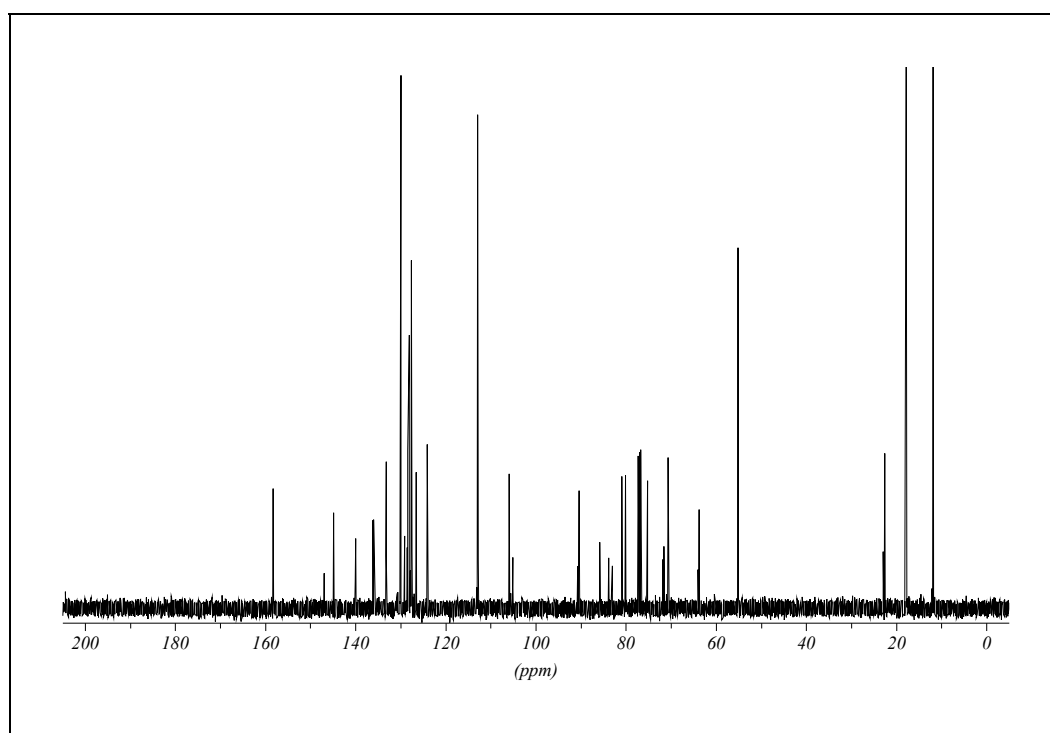
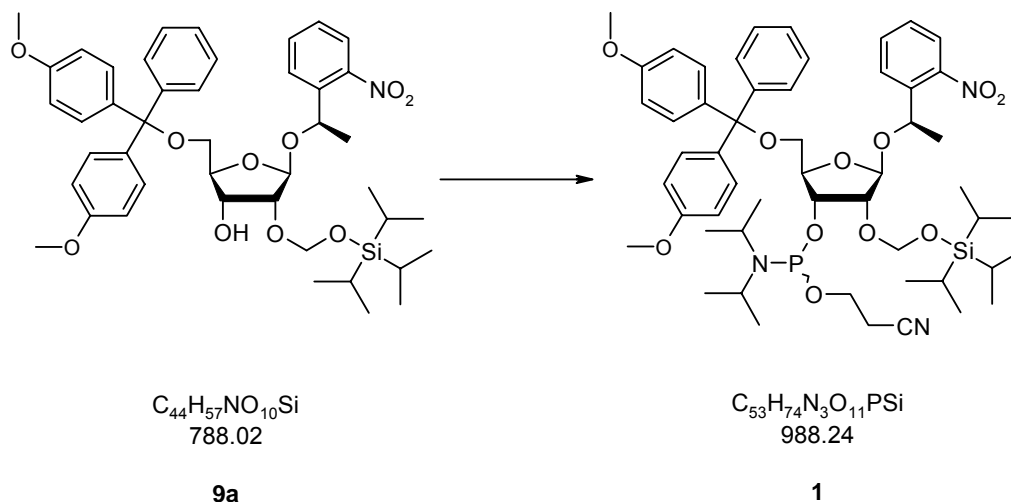


Figure 5.16 $^{13}\text{C-NMR}$ spectrum of **9b**

5.3.10 1'-[(*R*)-1-(2-Nitrophenyl)ethyl]-5'-[(4,4'-dimethoxy)triphenyl]-2'-[[triisopropyl)silyloxy] methyl]-ribofuranose 3'-(2-cyanoethyl diisopropylphosphoramidite) (1**)**



To solution of alcohol **9a** (1.29 g, 1.64 mmol) in THF (32 ml) under argon, iPr_2NEt (813 μ l, 4.8 mmol, 2.9 eq.) and 2-cyanoethyl diisopropylchlorophosphoramidite (532 μ l, 2.4 mmol, 1.45 eq.) are added. The mixture is allowed to stand for 14 hours. The suspension is taken up in ethyl acetate (100 ml) and washed with $NaHCO_3$ (2 x 50 ml). The aqueous layers are then extracted with CH_2Cl_2 (2 x 50 ml). The organic layers are dried (Na_2SO_4) and evaporated under reduced pressure. The residue is chromatographed on silicagel (70 g, eluted with ethyl acetate/hexane 1:4 + 1 % triethylamine) to give diastereomeric **1** (1.41 g, 87 %) as a colorless resin.

TLC (ethyl acetate/hexane 1:3): R_f 0.44

1H -NMR (300 MHz, $CDCl_3$): δ 7.84-7.88 (*m*, 1 H, Ar); 7.74-7.80 (*m*, 1 H, Ar); 7.16-7.40 (*m*, 12 H, Ar); 6.73-6.77 (*m*, 4 H, Ar); 5.41-5.49 (*m*, 1 H, HCM_e); 5.28 (*s*, 1 H, H-C(1')); 5.13 (*d*, $J = 4.8$, 1 H, OCH_2O); 5.02 (*dd*, $J = 11.6, 5.0$, 1 H, OCH_2O); 4.46-4.53, 4.32-4.39 (*2m*, 1 H, H-C(3')); 4.22-4.28 (*m*, 1 H, H-C(2')); 4.10-4.15 (*m*, 1 H, H-C(4')); 3.74-3.90 (*m*, 7 H, $OMe, (Me_2CH)_2N$); 3.45-3.64 (*m*, 3 H, $POCH_2, (Me_2CH)_2N$); 3.27 (*ddd*, $J = 27.6, 6.6, 3.7$, 1 H, H-C(5')); 2.88-2.96 (*m*, 1 H, H-C(5')); 2.62 (*t*, $J = 6.3$, 1 H, CH_2CN); 2.31 (*dt*, $J = 6.3, 2.2$, 1 H, CH_2CN); 1.51 (*d*, $J = 6.6$, 1 H, HCM_e); 0.98-1.17 (*m*, 33 H, $iPr_3Si, (Me_2CH)_2N$).

^{13}C -NMR (75 MHz, $CDCl_3$): δ 158.3 (*s*, Ar); 146.9, 146.8 (*2s*, npe); 144.9, 144.8 (*2s*, Ar); 140.4, 140.3 (*2s*, npe), 136.2, 136.1, 136.0, 135.9 (*4s*, Ar); 133.3, 133.2 (*2d*, npe),

130.1, 130.0 (*2d*, Ar); 128.4, 128.3, 128.2 (*3d*, npe), 127.6, 127.5 (*2d*, Ar); 126.6 (*d*, Ar)124.2, 124.1 (*d*, npe), 117.6, 117.5 (*2s*, CN); 112.9, 112.8 (*2d*, Ar); 105.2, 105.0 (*2d*, C(1')); 89.8 (*t*, OCH₂O); 85.9, 85.7 (*2s*, Ar₃-C-O); 82.0, 81.9, 81.6, 81.5 (*4d*, C(4')); 80.1, 80.0, 79.8, 79.0 (*4d*, C(2')); 72.3, 72.1, 71.9 (*3d*, C(3')); 71.4, 71.3 (*2d*, HCMe); 63.6, 63.1 (*2t*, C(5')); 58.7, 58.5, 58.3, 58.1 (*4t*, OCH₂CH₂CN); 55.2, 55.1 (*2q*, OMe); 43.3, 43.1, 43.0, 42.9 (*4d*, (Me₂CH)₂N); 24.7, 24.6, 24.5, 24.4 (*4q*, (Me₂CH)₂N); 22.8 (*q*, HCMe); 20.3, 20.2, 20.0, 19.9 (*4t*, OCH₂CH₂CN); 17.9, 17.8 (*2q*, (Me₂CH)₃Si); 12.0, 11.9 (*2d*, (Me₂CH)₃Si).

³¹P-NMR (121 MHz, CDCl₃): δ 150.71; 150.65.

LR-ESIMS (M+H⁺) for C₅₃H₇₄N₃O₁₁PSi. Calculated: 989.25. Found: 989.65.

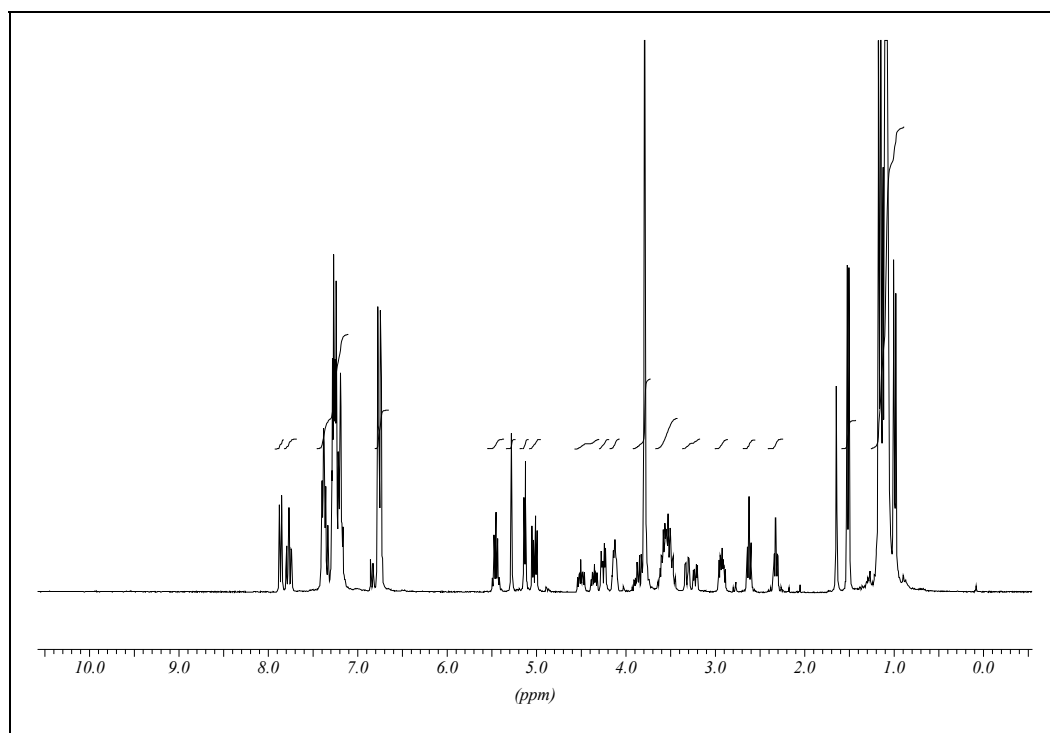


Figure 5.17 ¹H-NMR spectrum of **1**

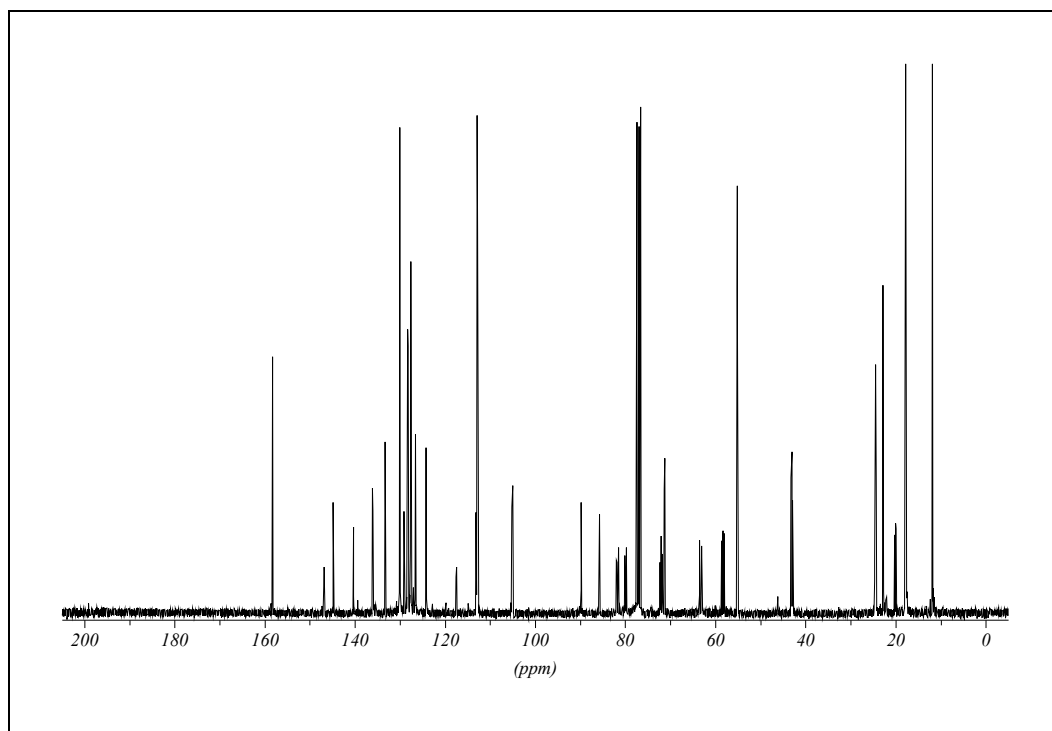


Figure 5.18 ^{13}C -NMR spectrum of **1**

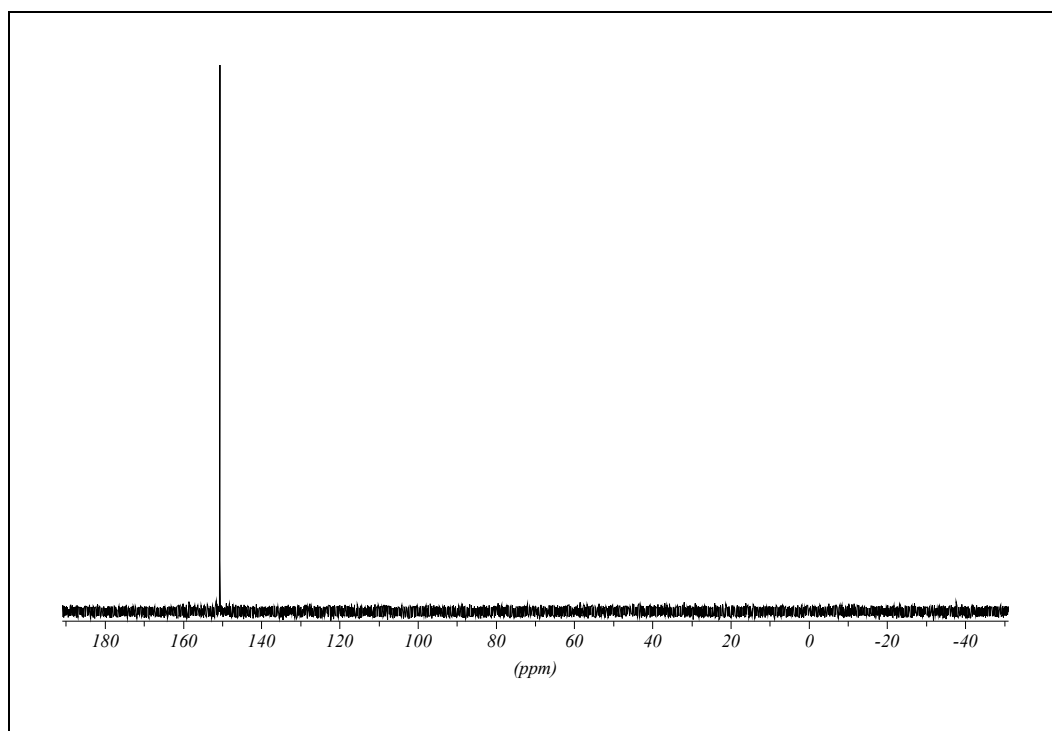
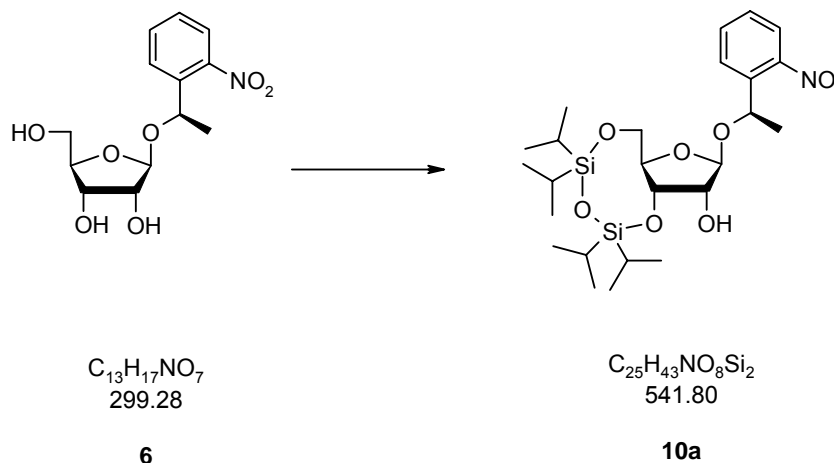


Figure 5.19 ^{31}P -NMR of **1**

5.4 Synthesis of the 2'-O-methylated RNA Abasic Site Precursor

5.4.1 1'-[(*R*)-1-(2-Nitrophenyl)ethyl]-3'-5'-*O*-(1,1,3,3-tetraisopropylidisiloxane-1,3-diyl)-ribofuranose (**10a**)



Triol **6** (1.01 g, 3.4 mmol) is co-evaporated with pyridine (5 ml) and diluted under argon in pyridine (40 ml). 1,3-Dichloro-1,1,3,3-tetraisopropylidisiloxane (1.16 ml, 4.1 mmol, 1.2 eq.) is added and the solution is allowed to stand for 18 hours. The reaction mixture is taken up in ethyl acetate (100 ml), washed with saturated $NaHCO_3$ (2 x 50 ml) and sat. $CuSO_4$ (2 x 50 ml). The aqueous phases are extracted with ethyl acetate (2 x 50 ml) and the organic layers are dried (Na_2SO_4) and evaporated. The residue is chromatographed on silicagel (70 g, eluted with ethyl acetate/hexane 1:9) to give (*R*)-alcohol **10a** (1.51 g, 82 %) as a clear oil that crystallized to give a off-white solid.

TLC (ethyl acetate/hexane 1:9): **10a** R_f 0.22; **10b** R_f 0.15

Spectroscopic data for **10a**:

1H -NMR ($CDCl_3$): δ 7.83-7.86 (*m*, 1 H), 7.66-7.69 (*m*, 1 H), 7.54-7.59 (*m*, 1 H), 7.35-7.40 (*m*, 1 H), 5.25 (*q*, $J = 6.3$, 1 H), 5.07 (*s*, 1 H), 4.36-4.40 (*m*, 1 H), 4.03-4.05 (*m*, 1 H), 3.82-3.88 (*m*, 1 H), 3.61-3.66 (*m*, 1 H), 3.17-3.24 (*m*, 1 H), 2.92 (*s*, 1 H), 1.48 (*d*, $J = 6.3$, 3 H), 0.88-1.04 (*m*, 28 H).

^{13}C -NMR ($CDCl_3$): δ 147.4 (*s*), 139.8 (*s*), 133.0 (*d*), 128.4 (*d*), 127.8 (*d*), 124.0 (*d*), 104.7 (*d*), 82.2 (*d*), 76.1 (*d*), 75.0 (*d*), 70.3 (*d*), 65.4 (*t*), 22.4 (*q*), 17.44 (*q*), 17.43 (*q*),

17.3 (*q*), 17.25 (*q*), 17.18 (*q*), 17.00 (*q*), 16.95 (*q*), 16.92 (*q*), 13.21 (*d*), 13.11 (*d*), 12.58 (*d*).

HR-ESIMS ($M+H^+$) for $C_{25}H_{43}NO_8Si_2$. Calculated: 542.2605. Found: 542.2610.

Starting the synthesis from the diastereomeric mixture of diol **6**, the two diastereomers of **10** are separable by column chromatography.

Spectroscopic data for **10b**:

1H -NMR ($CDCl_3$): δ 7.87-7.90 (*m*, 1 H), 7.58-7.68 (*m*, 2 H), 7.37-7.43 (*m*, 1 H), 5.32 (*q*, $J = 6.3$, 1 H), 4.56-4.62 (*m*, 2 H), 3.95-4.10 (*m*, 3 H), 3.78-3.84 (*m*, 1 H), 2.92 (*s*, 1 H), 1.48 (*d*, $J = 6.3$, 3 H), 0.97-1.12 (*m*, 28 H).

^{13}C -NMR ($CDCl_3$): δ 148.5 (*s*), 138.8 (*s*), 133.6 (*d*), 128.2 (*d*), 128.0 (*d*), 124.4 (*d*), 103.7 (*d*), 82.7 (*d*), 75.8 (*d*), 74.7 (*d*), 69.1 (*d*), 66.0 (*t*), 23.9 (*q*), 17.50 (*q*), 17.45 (*q*), 17.44 (*q*), 17.35 (*q*), 17.17 (*q*), 16.98 (*q*), 16.91 (*q*), 13.30 (*d*), 13.28 (*d*), 12.90 (*d*), 12.53 (*d*).

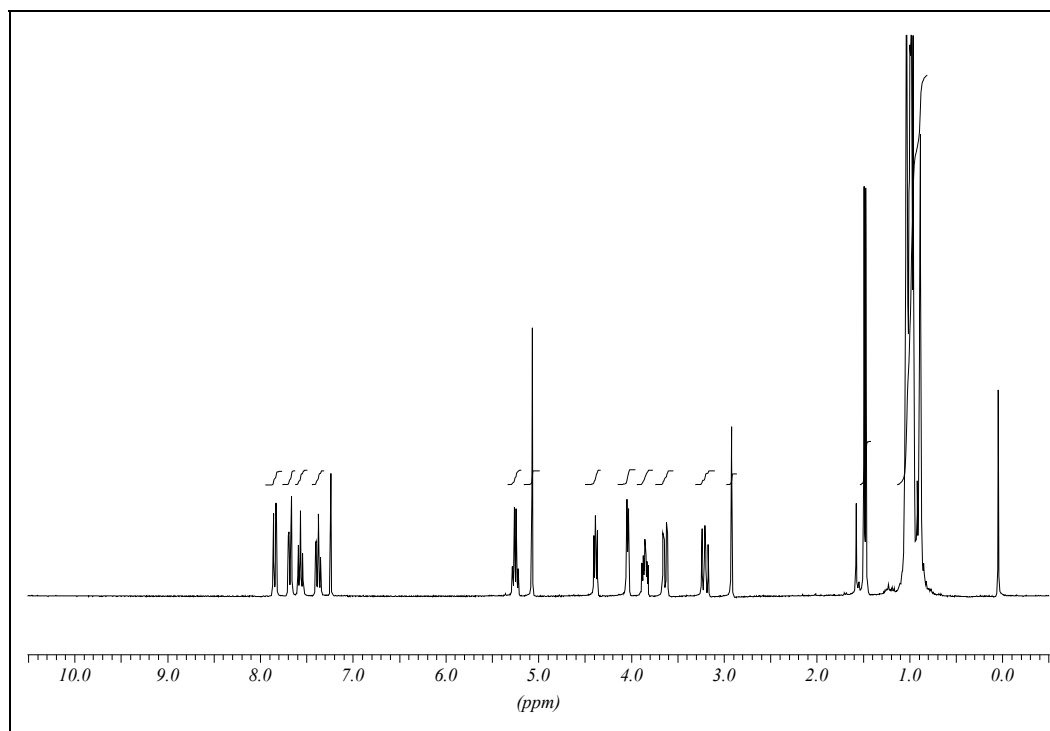


Figure 5.20 $^1\text{H-NMR}$ spectrum of **10a**

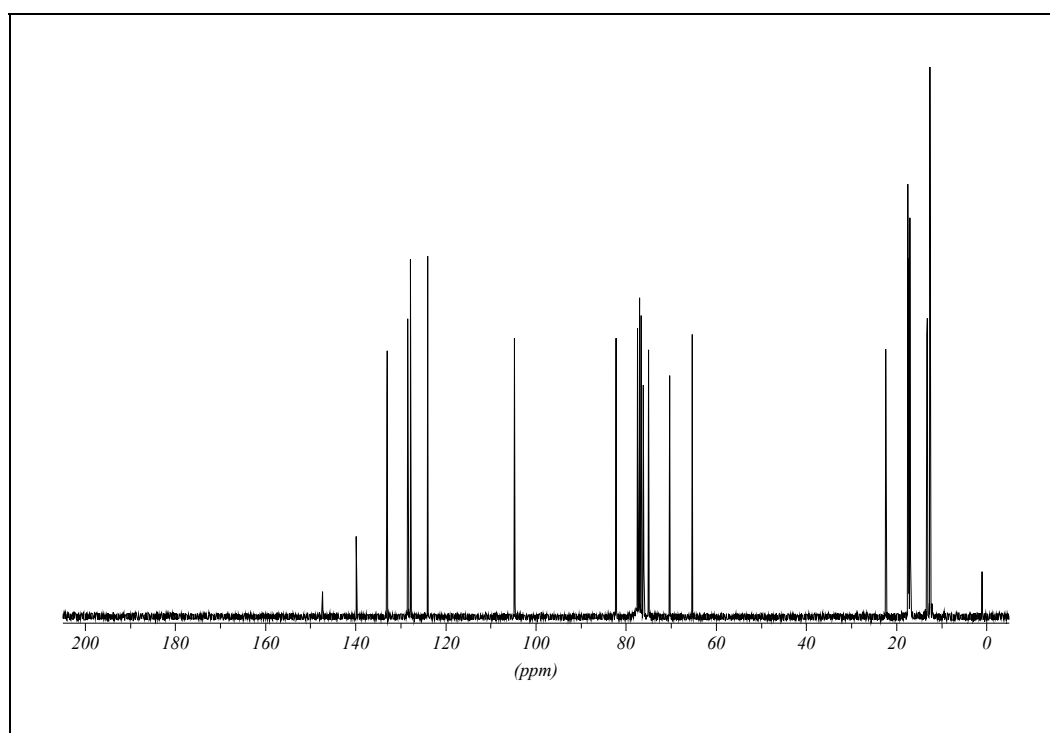


Figure 5.21 $^{13}\text{C-NMR}$ spectrum of **10a**

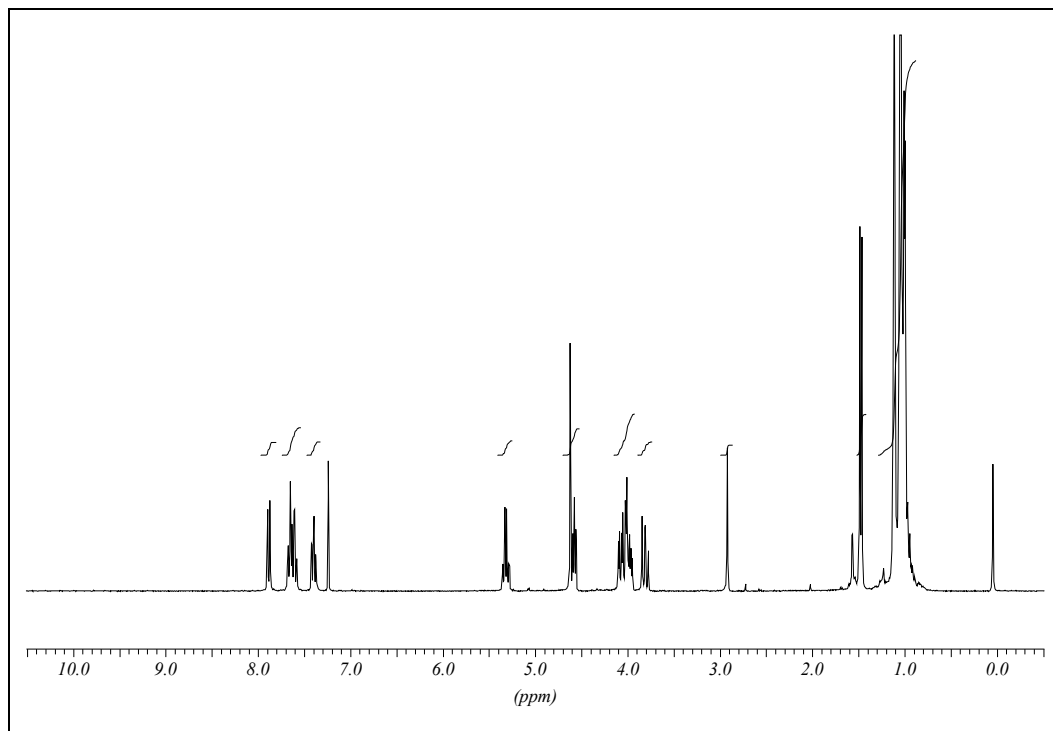


Figure 5.22 $^1\text{H-NMR}$ spectrum of **10b**

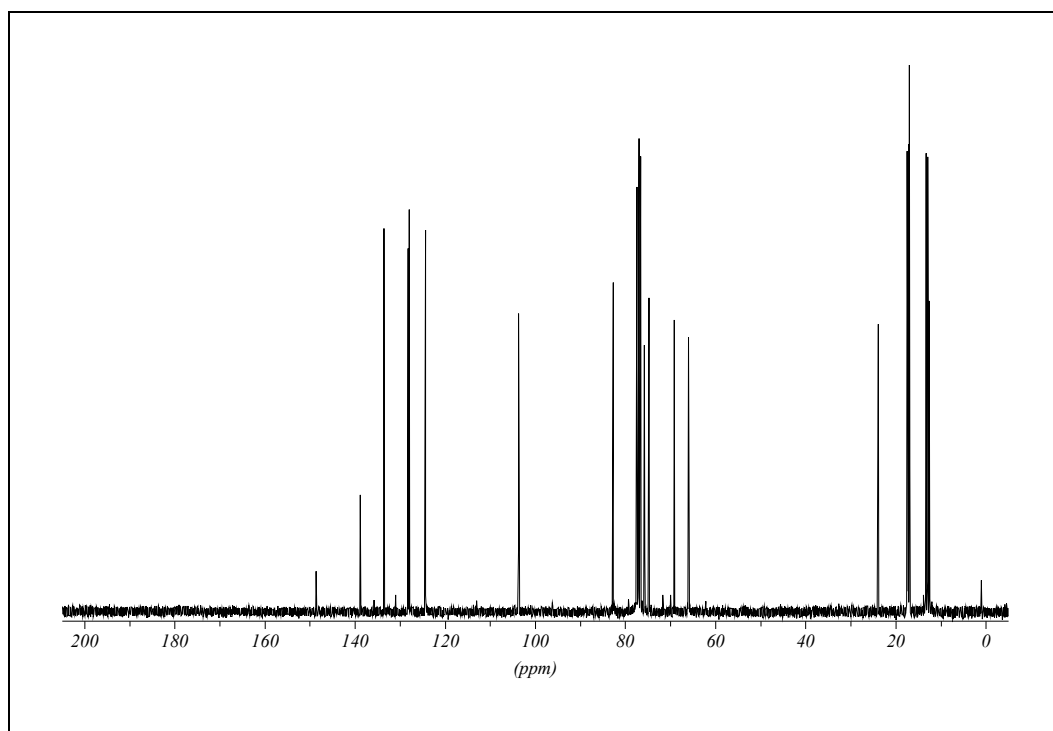
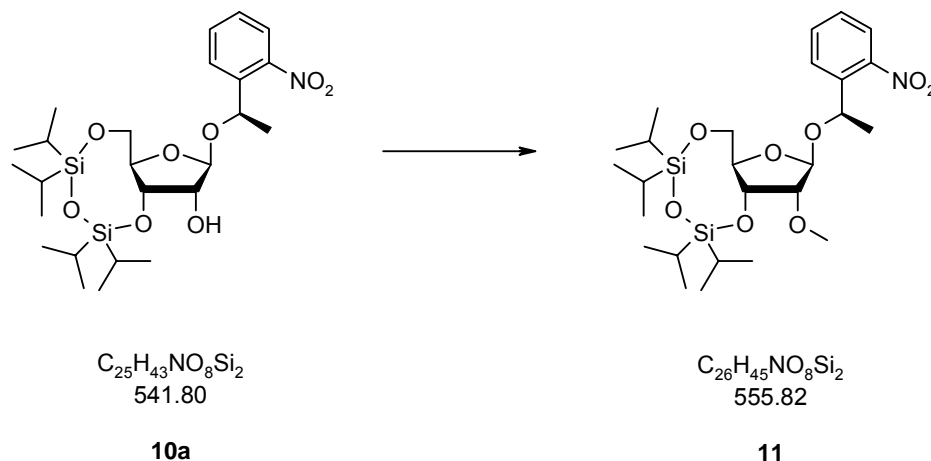


Figure 5.23 $^{13}\text{C-NMR}$ spectrum of **10b**

5.4.2 1'-[(R)-1-(2-Nitrophenyl)ethyl]-2'-O-methyl-3'-5'-O-(1,1,3,3-tetraisopropylidisiloxane-1,3-diyl)-ribofuranose (11)

Alcohol **10a** (1.0 g, 1.85 mmol) and silver(I)oxide (3.43 g, 14.7 mmol, 8 eq.) in methyl iodide (20 ml) are refluxed for 72 h. The suspension is diluted in ethyl acetate and filtered over a pad of Celite. After evaporation of the solvents, the oily residue is chromatographed on silicagel (85 g, eluted with ethyl acetate/hexane 1:14) to give **11** (925 mg, 90 %) as a yellow oil.

TLC (ethyl acetate/hexane 1:14): R_f 0.35.

1H -NMR ($CDCl_3$): δ 7.83-7.86 (*m*, 1 H), 7.77-7.74 (*m*, 1 H), 7.52-7.58 (*m*, 1 H), 7.33-7.38 (*m*, 1 H), 5.26 (*q*, $J = 6.3$, 1 H), 4.95 (*s*, 1 H), 4.40-4.44 (*m*, 1 H), 3.83-3.89 (*m*, 1 H), 3.63-3.71 (*m*, 2 H), 3.55 (*s*, 3 H), 3.39-3.45 (*m*, 1 H), 1.47 (*d*, $J = 6.3$, 1 H), 0.87-1.09 (*m*, 28 H).

^{13}C -NMR ($CDCl_3$): δ 147.4 (*s*), 139.9 (*s*), 132.9 (*d*), 128.8 (*d*), 127.7 (*d*), 123.9 (*d*), 103.7 (*d*), 84.8 (*d*), 80.8 (*d*), 73.9 (*d*), 70.8 (*d*), 63.4 (*t*), 59.4 (*q*), 22.7 (*q*), 17.41 (*q*), 17.39 (*q*), 17.33 (*q*), 17.29 (*q*), 17.24 (*q*), 17.01 (*q*), 16.98 (*q*), 13.37 (*d*), 13.08 (*d*), 12.77 (*d*), 12.52 (*d*).

HR-ESIMS ($M+Na^+$) for $C_{26}H_{45}NO_8Si_2$. Calculated: 578.2581. Found: 578.2598.

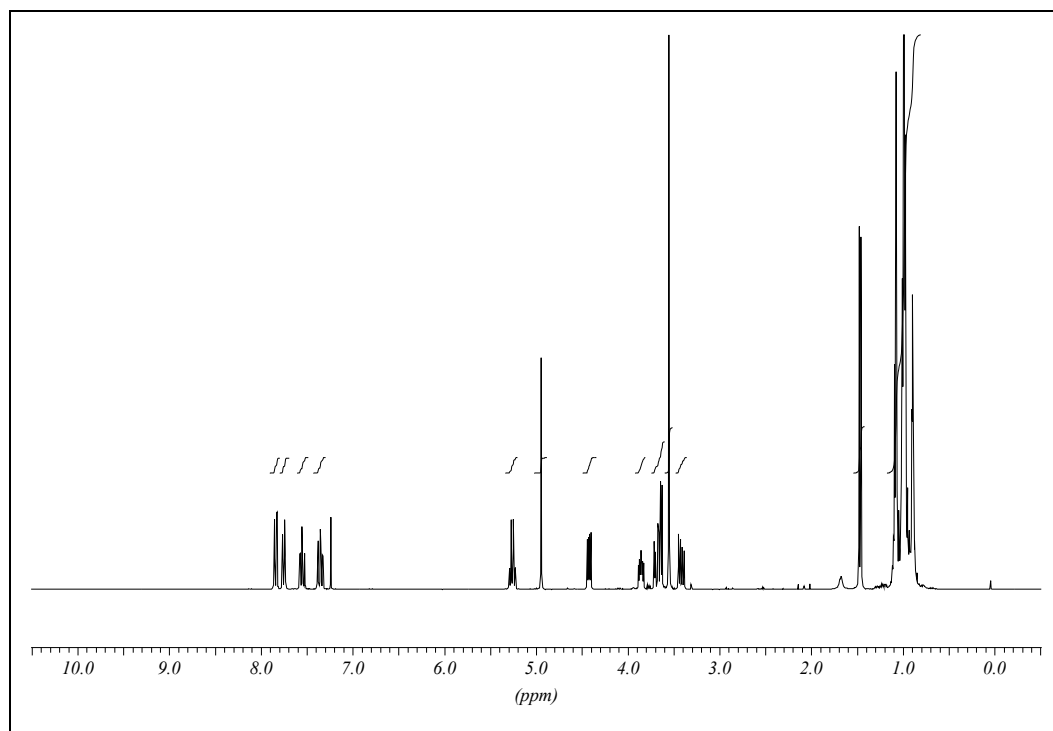
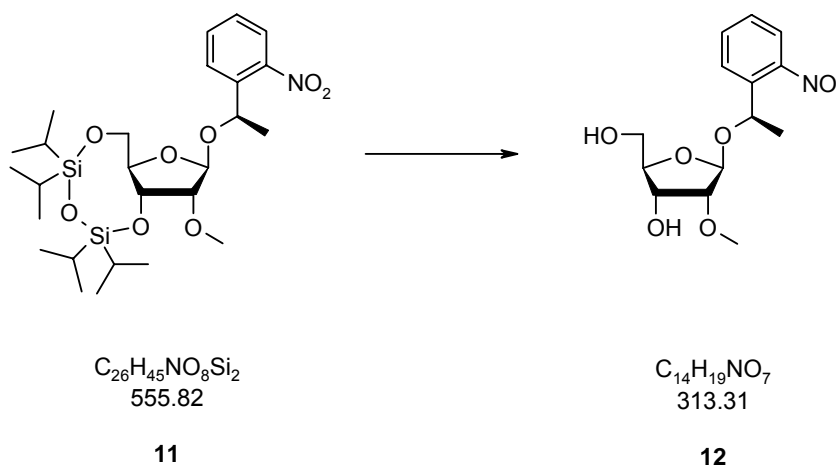


Figure 5.24 $^1\text{H-NMR}$ spectrum of **11**

5.4.3 1'-[(R)-1-(2-Nitrophenyl)ethyl]-2'-O-methyl-ribofuranose (12)

Compound **11** (900 mg, 1.6 mmol) is dissolved in THF (30 ml). After addition of acetic acid (146 μ l, 2.6 mmol, 1.6 eq.) and tetrabutylammonium fluoride (1.54 g, 4.9 mmol, 3 eq.) the solution is stirred for 30 minutes at room temperature. The reaction mixture is then evaporated and chromatographed twice on silicagel (2 x 80 g, eluted with ethyl acetate) to give **12** (432 mg, 85 %) as a colorless solid.

TLC (ethyl acetate): R_f 0.46

1H -NMR ($CDCl_3$): δ 7.83-7.86 (*m*, 1 H), 7.58-7.71 (*m*, 2 H), 7.37-7.43 (*m*, 1 H), 5.30 (*q*, $J = 6.3$, 1 H), 5.11 (*s*, 1 H), 4.11-4.17 (*m*, 1 H), 3.80-3.85 (*m*, 1 H), 3.68 (*d*, 1 H), 3.49-3.55 (*m*, 4 H), 3.22-3.32 (*m*, 1 H), 2.57 (*d*, $J = 8.5$, 1 H), 1.67-1.71 (*m*, 1 H), 1.53 (*d*, $J = 6.3$, 3 H).

^{13}C -NMR ($CDCl_3$): δ 147.6 (*s*), 139.3 (*s*), 133.3 (*d*), 128.2 (*d*), 128.1 (*d*), 124.1 (*d*), 103.7 (*d*), 84.8 (*d*), 84.5 (*d*), 71.3 (*d*), 70.4 (*d*), 62.7 (*t*), 58.4 (*q*), 22.7 (*q*).

HR-ESIMS ($M+Na^+$) for $C_{14}H_{19}NO_7$. Calculated: 336.1059. Found: 336.1043.

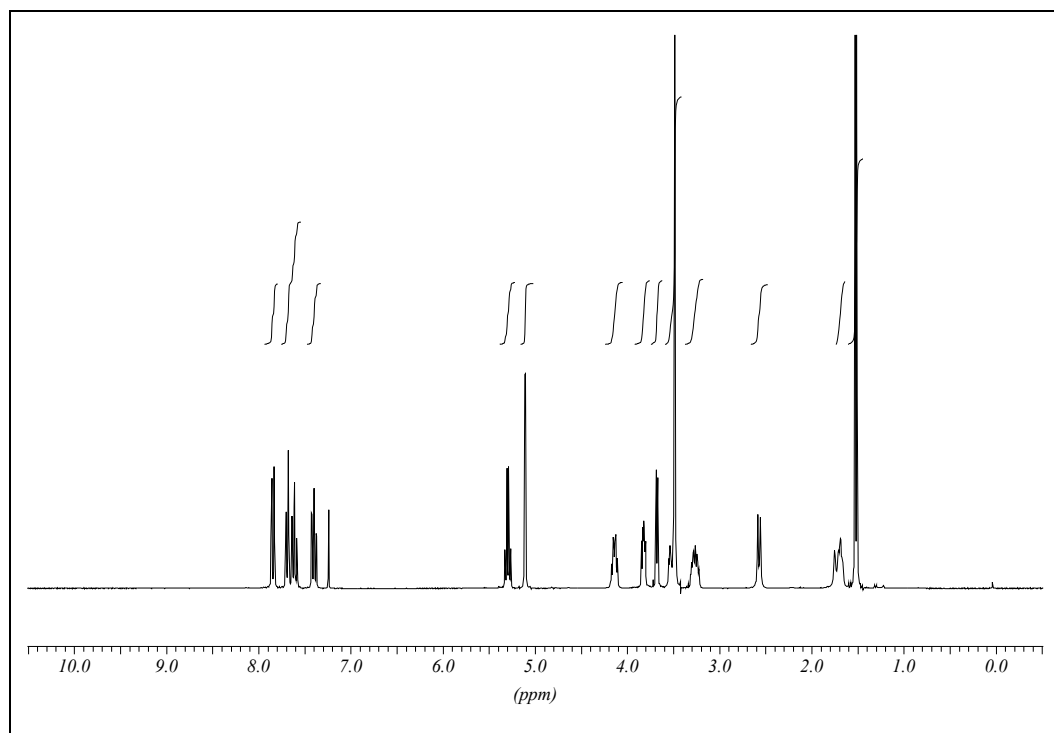
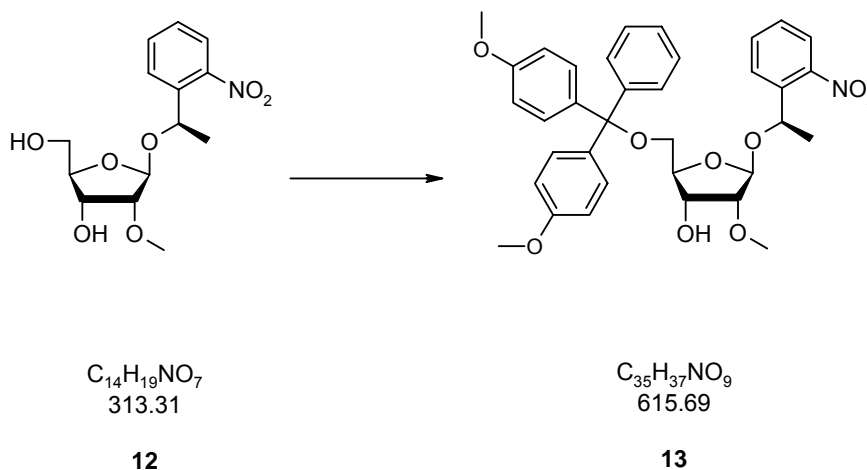


Figure 5.25 $^1\text{H-NMR}$ spectrum of **12**

5.4.4 1'-[(R)-1-(2-Nitrophenyl)ethyl]-5'-[(4,4'-dimethoxy)triphenyl]-2'-O-methyl-ribofuranose (13)

Diol **12** (390 mg, 1.2 mmol) is co-evaporated with pyridine (2 x 2 ml) and diluted under argon in pyridine (7 ml). 4,4'-Dimethoxytriphenylmethyl chloride (508 mg, 1.5 mmol, 1.2 eq.) is added in four equal portions every 15 min. After 90 min. the solution is taken up in ethyl acetate (25 ml) and washed with saturated $NaHCO_3$ (3 x 15 ml). The aqueous phases are extracted with ethyl acetate (2 x 15 ml) and the organic layers are dried (Na_2SO_4) and evaporated. The residue is chromatographed on silicagel (50 g, eluted with ethyl acetate/hexane 1:2 + 1 % triethylamine) to give **13** (716 mg, 94 %) as a yellow foam.

TLC (ethyl acetate/hexane 1:2): R_f 0.25

1H -NMR ($CDCl_3$): δ 7.84-7.87 (*m*, 1 H), 7.69-7.72 (*m*, 1 H), 7.16-7.40 (*m*, 11 H), 5.39 (*q*, $J = 6.3$, 1 H), 5.15 (*s*, 1 H), 4.20-4.25 (*m*, 1 H), 3.91-3.96 (*m*, 1 H), 3.77-3.79 (*m*, 7 H), 3.53 (*m*, 3 H), 3.06-3.11 (*m*, 1 H), 2.96-3.00 (*m*, 1 H), 2.50 (*d*, $J = 7.2$, 1 H), 1.53 (*d*, $J = 6.3$, 3 H)

^{13}C -NMR ($CDCl_3$): δ 158.4 (*s*), 147.1 (*s*), 144.8 (*s*), 139.9 (*s*), 136.0 (*s*), 135.9 (*s*), 133.2 (*d*), 130.0 (*d*), 128.5 (*d*), 128.2 (*d*), 127.7 (*d*), 126.6 (*d*), 124.0 (*d*), 113.0 (*d*), 103.7 (*d*), 86.0 (*s*), 84.5 (*d*), 83.2 (*d*), 71.6 (*d*), 71.4 (*d*), 64.0 (*t*), 58.4 (*q*), 55.2 (*q*), 22.9 (*q*)

HR-ESIMS ($M+Na^+$) for $C_{35}H_{37}NO_9$. Calculated: 638.2366. Found: 638.2371.

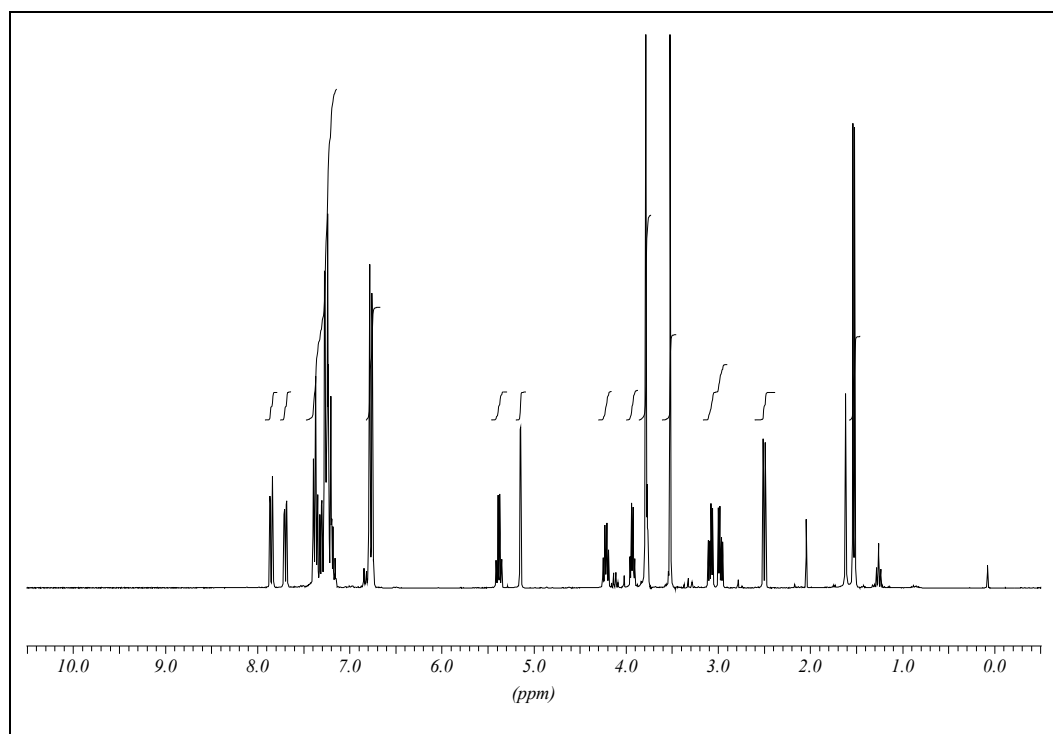
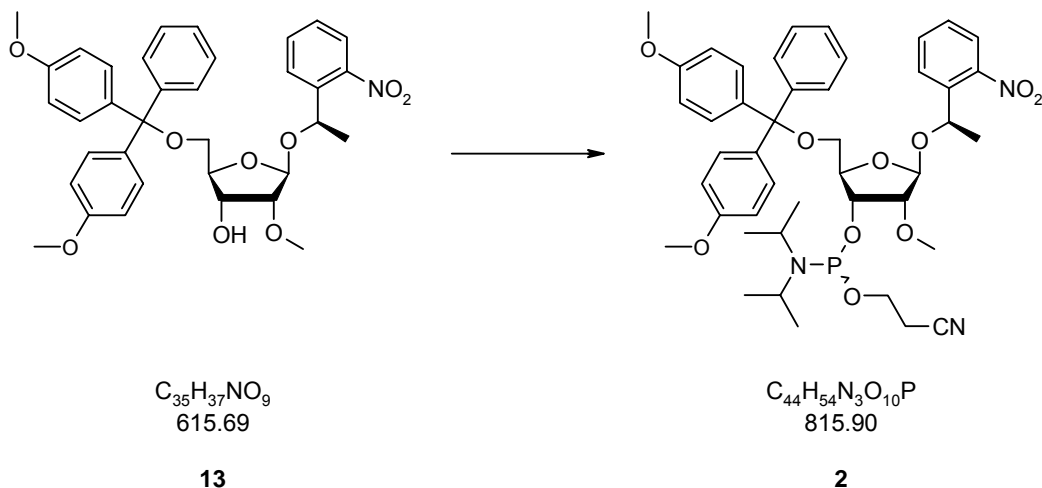


Figure 5.26 1H -NMR spectrum of **13**

5.4.5 1'-[(R)-1-(2-Nitrophenyl)ethyl]-5'-[(4,4'-dimethoxy)triphenyl]-2'-O-methyl-ribofuranose-3'-cyanoethylphosphoramidite (**2**)



Alcohol **13** (500 mg, 0.81 mmol) is dissolved in THF (16 ml) under argon. iPr_2NEt (403 μ l, 2.39 mmol, 2.9 eq.) and 2-cyanoethyl diisopropylchlorophosphoramidite (263 μ l, 1.45 eq.) are added. The solution is allowed to stand for 4 hours at room temperature. Afterwards the solution is taken up in ethyl acetate (50 ml) and washed with saturated $NaHCO_3$ (2 x 25 ml). The aqueous phases are extracted with CH_2Cl_2 (2 x 25 ml) and the organic layers are dried (Na_2SO_4) and evaporated. The residue is chromatographed on silicagel (20 g, eluted with ethyl acetate/hexane 1:2 + 1 % triethylamine) to give **2** (516 mg, 78 %) as a colorless resin.

TLC (ethyl acetate/hexane 1:2): R_f 0.36

1H -NMR ($CDCl_3$): δ 7.76-7.79 (*m*, 1 H), 7.65-7.71 (*m*, 1 H), 7.08-7.33 (*m*, 11 H), 6.67-6.70 (*m*, 4 H), 5.31-5.39 (*m*, 1 H), 5.07-5.08 (*m*, 1 H), 4.33-4.40, 4.19-4.26 (2 *m*, 1 H), 3.98-4.06 (*m*, 1 H), 3.67-3.82 (*m*, 8 H), 3.40-3.57 (*m*, 6 H), 3.09-3.21 (*m*, 1 H), 2.82-2.87 (*m*, 1 H), 2.53-2.58 (*m*, 1 H), 2.25-2.30 (*m*, 1 H), 1.46-1.48 (*m*, 3 H), 1.05-1.11 (*m*, 12 H), 0.91-0.93 (*m*, 2 H)

^{13}C -NMR ($CDCl_3$): δ 158.3 (*s*), 147.2 (*s*), 147.1 (*s*), 144.81 (*s*), 144.78 (*s*), 140.0 (*s*), 136.0 (*s*), 135.98 (*s*), 135.94 (*s*), 133.3 (*d*), 133.2 (*d*), 130.15 (*d*), 130.13 (*d*), 130.09 (*d*), 130.06 (*d*), 129.1 (*d*), 128.51 (*d*), 128.49 (*d*), 128.32 (*d*), 128.23 (*d*), 127.8 (*d*), 127.7 (*d*), 127.61 (*d*), 126.63 (*d*), 124.09 (*d*), 124.05 (*d*), 117.7 (*s*), 117.5 (*s*), 113.1 (*d*), 112.93

(*d*), 112.92 (*d*), 112.90 (*d*), 104.5 (*d*), 103.8 (*d*), 85.99 (*s*), 85.85 (*s*), 84.32 (*d*), 84.29 (*d*), 83.89 (*d*), 83.80 (*d*), 82.40 (*d*), 82.35 (*d*), 81.89 (*d*), 81.85 (*d*), 72.2 (*d*), 72.1 (*d*), 71.98 (*d*), 71.88 (*d*), 71.5 (*d*), 71.4 (*d*), 63.5 (*t*), 63.2 (*t*), 58.8 (*t*), 58.6 (*t*), 58.49 (*t*), 58.47 (*t*), 58.36 (*t*), 58.16 (*t*), 58.15 (*q*), 58.13 (*q*), 55.18 (*q*), 55.16 (*q*), 43.3 (*d*), 43.2 (*d*), 43.1 (*d*), 42.98 (*d*), 24.6 (*t*), 24.54 (*q*), 24.50 (*q*), 24.46 (*q*), 22.98 (*q*), 22.93 (*q*), 20.27 (*t*), 20.21 (*t*), 20.1 (*t*), 20.0 (*t*)

^{31}P -NMR (CDCl_3): δ 150.14, 149.85.

LR-ESIMS ($\text{M}+\text{Na}^+$) for $\text{C}_{44}\text{H}_{54}\text{N}_3\text{O}_{10}\text{P}$. Calculated: 838.88. Found: 838.36.

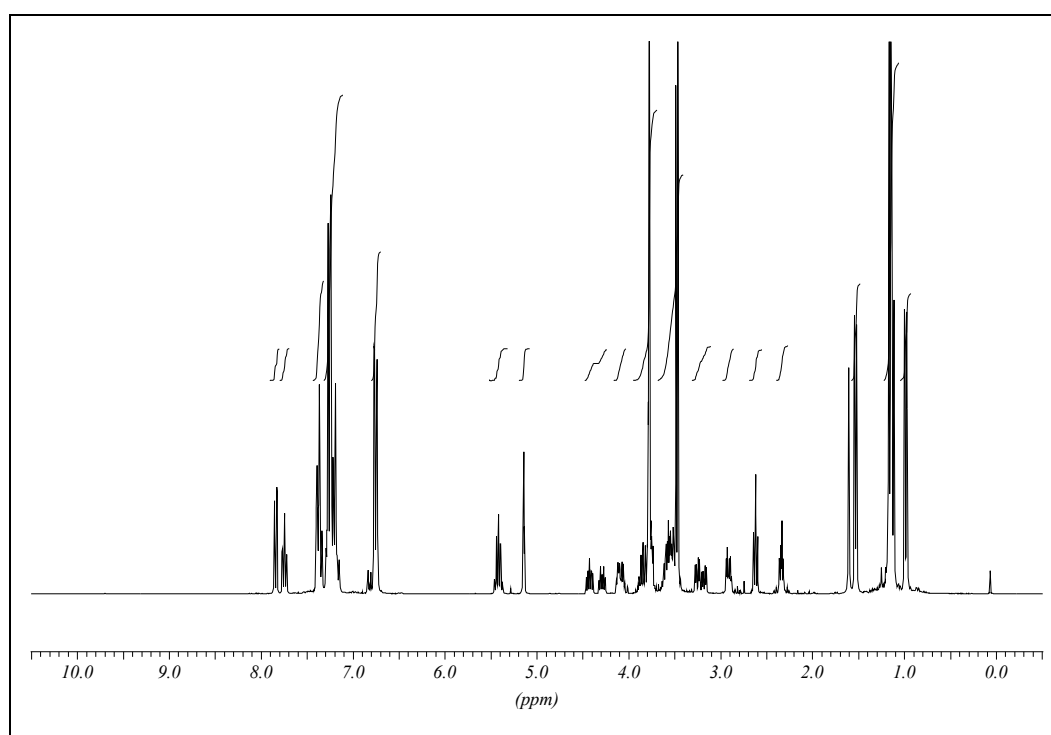


Figure 5.27 ^1H -NMR spectrum of **2**

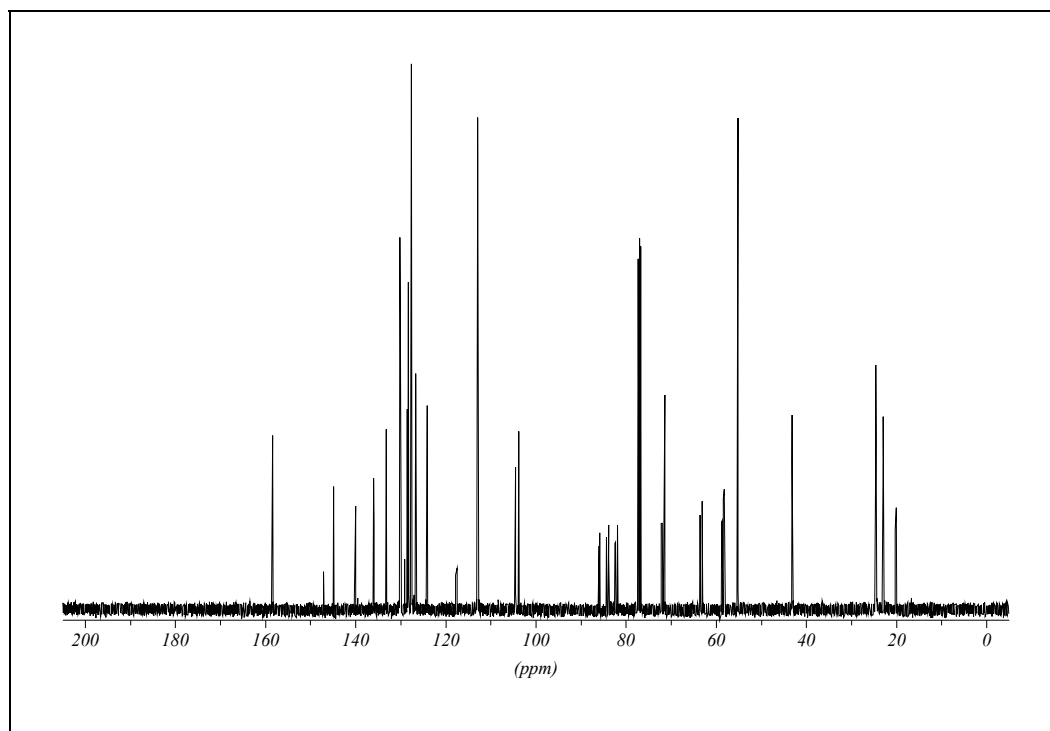


Figure 5.28 ^{13}C -NMR spectrum of **2**

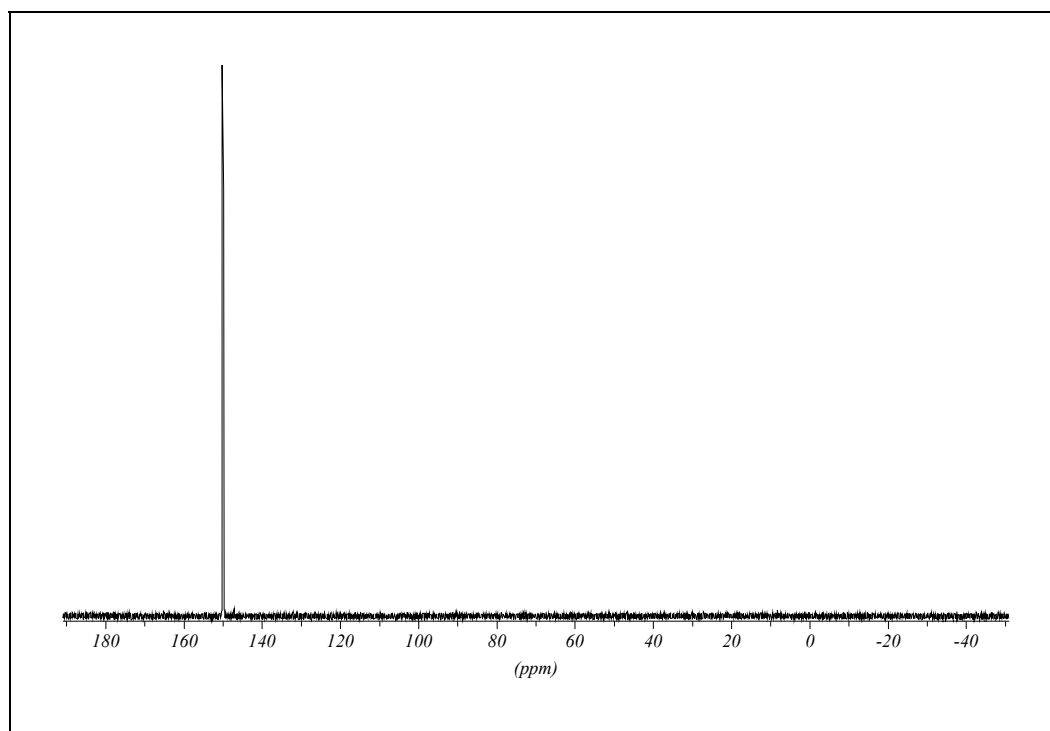
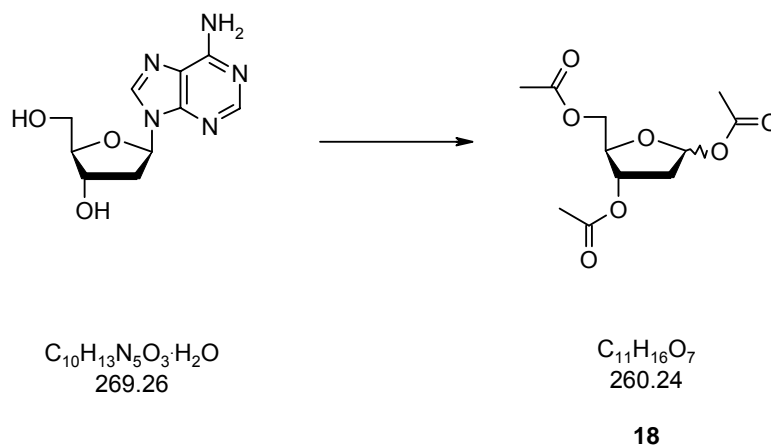


Figure 5.29 ^{31}P -NMR spectrum of **2**

5.5 Synthesis of the DNA Abasic Site Precursor

5.5.1 1', 3', 5'-Tri-*O*-acetyl-2'-deoxy-D-ribofuranose (**16**)



2-Deoxyadenosine monohydrate (3 g, 11.1 mmol) is suspended under argon in pyridine (6.4 ml). The solution is then cooled to 0 °C and acetic anhydride (6.3 ml, 66.6 mmol, 6 eq.) is added dropwise. The suspension clears up after 20 min. The reaction mixture is then stirred for 20 h at room temperature. After evaporation of the solvent under reduced pressure, the colorless syrup is diluted in hot ethanol-toluene (3 x 5 ml, 5:1) and evaporated again. The crude syrup is then diluted in glacial acetic acid (6.7 ml) and acetic anhydride (1.7 ml) and the solution is heated at 105 °C for four hours. After 20 min. colorless crystals begin to form. The reaction mixture is cooled with ice and the colorless crystals are removed by filtration. The filter cake is washed with chloroform (10 ml) and the solvent from the filtrates is removed under reduced pressure. Chloroform (40 ml) is added to the residue and it is washed with cold H₂SO₄ (3 M, 20 ml), water (20 ml), NaHCO₃ (20 ml) and with water (20 ml) again. The organic layer is dried (Na₂SO₄), filtrated and evaporated under reduced pressure. The residue is chromatographed on silicagel (200 g, eluted with ethyl acetate/hexane 1:2) to give **16** (2.18 g, 75 %) as a colorless oil.

TLC (ethyl acetate/hexane 1:2): *R_f* 0.28

¹H-NMR (300 MHz, CDCl₃): δ 6.33-6.38 (*m*, 1 H, H-C(1')); 5.20-5.25, 5.08-5.12 (*2m*, 1 H, H-C(3')); 4.37-4.41, 4.23-4.30, 4.10-4.17 (*3m*, 3 H, H₂-C(5'), H-C(4')); 2.42-2.51 (*m*, 1 H, H-C(2')); 2.25-2.33, 2.03-2.17 (*2m*, 10 H, H-C(2'), 3 OAc).

^{13}C -NMR (75 MHz, CDCl_3): δ 170.71, 170.56, 170.52, 170.48, 170.22, 169.94 (6s, Ac); 98.28, 98.09 (2d, C(1')); 83.14, 82.67 (2d, C(3')); 73.91, 73.71 (2d, C(4')); 64.15, 63.66 (2t, C(5')); 38.29, 38.16 (2t, C(2')); 21.24, 21.21, 20.95, 20.87, 20.79, 20.76 (6q, Ac).

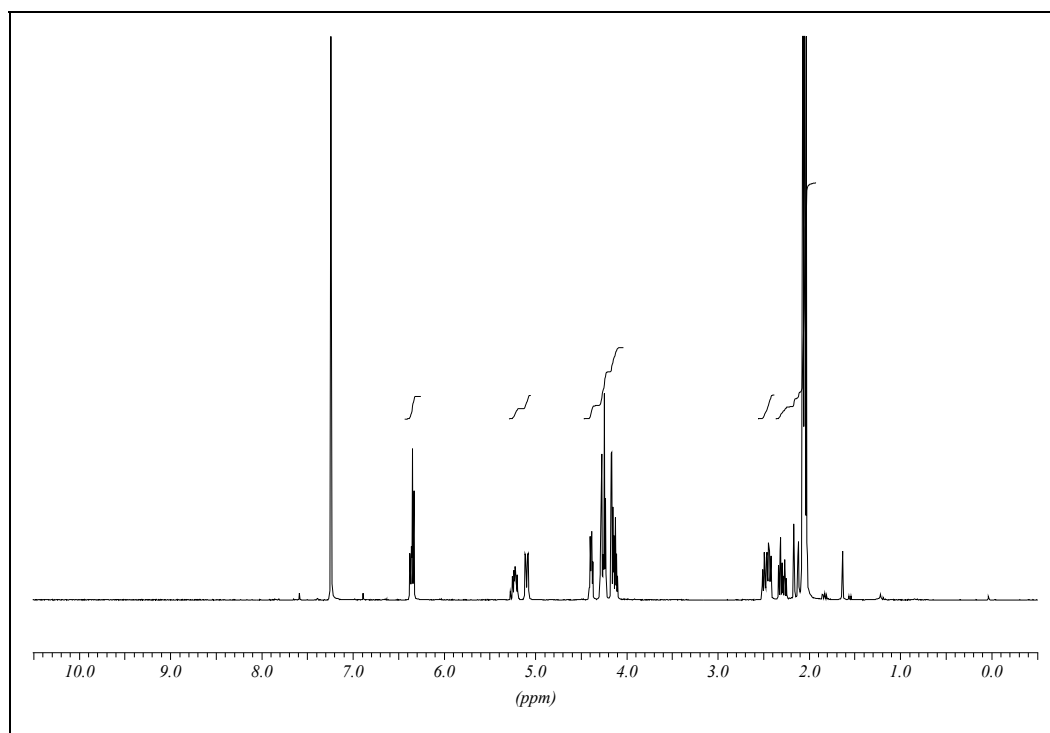
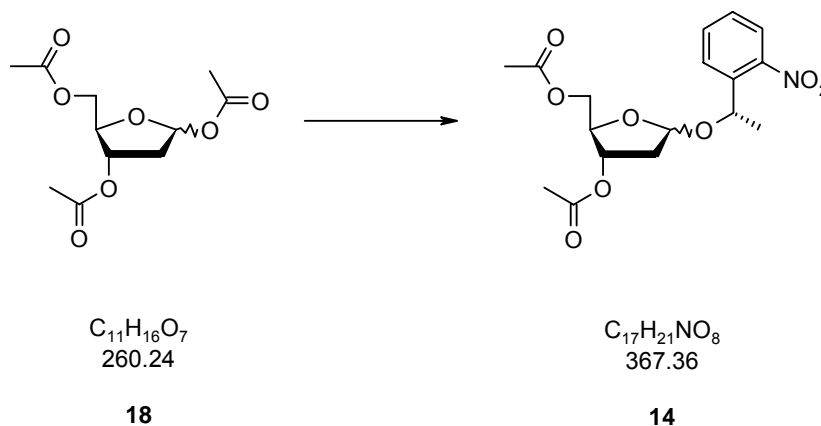


Figure 5.30 ^1H -NMR spectrum of **18**

5.5.2 1'-[1(*S*)-(2-Nitrophenyl)-ethyl]-3', 5'-di-*O*-acetyl-2'-deoxy-ribofuranose (14)



1',3',5'-Tri-*O*-acetyl-2'-deoxy-D-ribofuranose **18** (760 mg, 2.92 mmol) and (*S*)-1-(2-nitrophenyl)ethanol **4b** (585 mg, 3.5 mmol, 1.2 eq.) are diluted under argon in acetonitrile (15 ml). The solution is then cooled to -20 °C and trimethylsilyl-trifluoromethanesulfonate (105 μ l, 0.58 mmol, 0.2 eq.) is added dropwise. The reaction mixture is stirred for 1 h at -20 °C and allowed to warm up to room temperature. The mixture is then taken up in ethyl acetate (50 ml) and washed with saturated NaHCO₃ (3 x 25 ml), dried (Na₂SO₄) and the organic layer is concentrated under reduced pressure. The residue is chromatographed on silicagel (110 g, eluted with ethyl acetate/hexane 1:2) to give anomeric **14** (957 mg, 84 %) as a yellow oil.

TLC (ethyl acetate/hexane 1:2): R_f 0.32, 0.27

¹H-NMR (CDCl₃): δ 7.80-7.92 (*m*, 2 H), 7.55-7.65 (*m*, 1 H), 7.32-7.43 (*m*, 1 H), 5.19-5.39 (*m*, 2 H), 4.93-5.00 (*m*, 1 H), 4.13-4.32, 3.90-4.04, 3.63-3.67 (3*m*, 3 H), 2.27-2.42 (*m*, 1 H), 1.98-2.12 (*m*, 7 H), 1.48-1.52 (*m*, 3 H).

¹³C-NMR (CDCl₃): δ 170.80 (*s*), 170.52 (*s*), 141.26 (*s*), 138.96 (*s*), 133.38 (*d*), 133.87 (*d*), 128.31 (*d*), 128.15 (*d*), 127.93 (*d*), 127.54 (*d*), 124.26 (*d*), 124.11 (*d*), 103.65 (*d*), 102.36 (*d*), 81.72 (*d*), 81.7 (*d*), 74.99 (*d*), 74.32 (*d*), 71.23 (*d*), 70.07 (*d*), 64.83 (*t*), 63.68 (*t*), 39.09 (*t*), 38.94 (*t*), 23.72 (*q*), 23.17 (*q*), 21.02 (*q*), 20.94 (*q*), 20.86 (*q*), 20.72 (*q*).

HR-ESIMS (M+Na⁺) for C₁₇H₂₁NO₈. Calculated: 390.1164. Found: 390.1172.

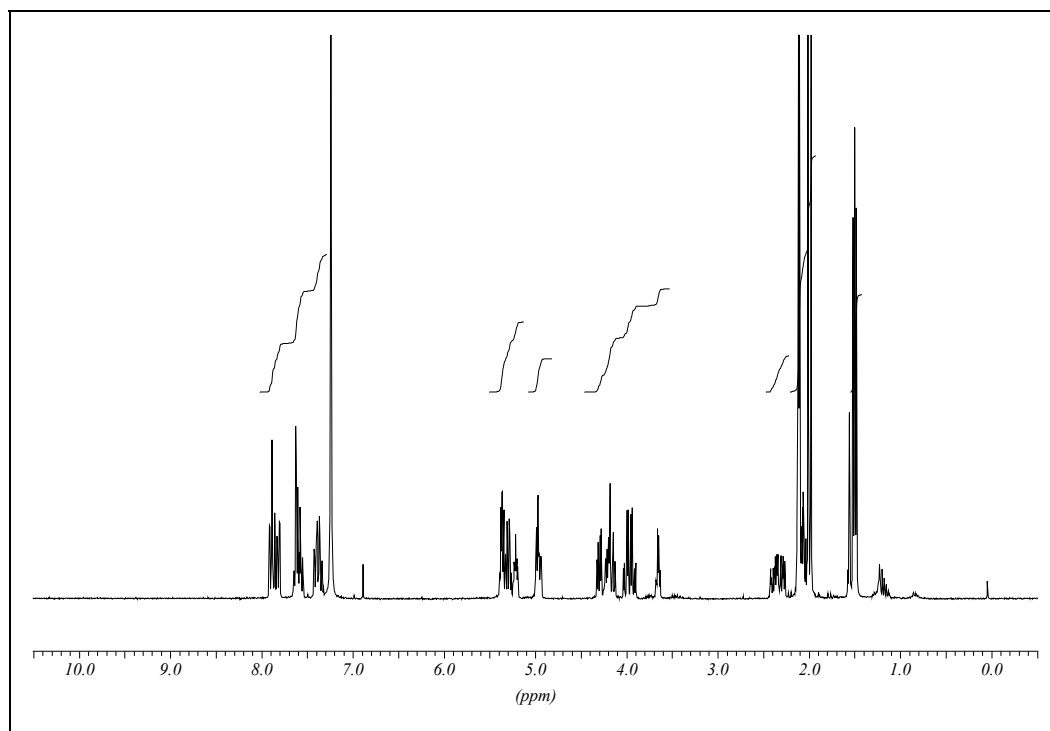
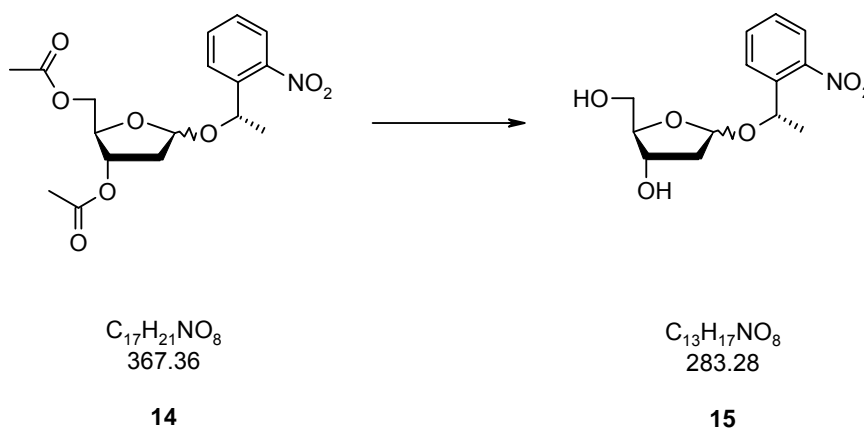


Figure 5.31 $^1\text{H-NMR}$ spectrum of **14**

5.5.3 1'-[1(S)-(2-Nitrophenyl)-ethyl]-2'-deoxy-ribofuranose (**15**)



1'-[1(*S*)-(2-Nitrophenyl)-ethyl]-3',5'-di-*O*-acetyl-2'-deoxy-D-ribofuranose **14** (800 mg, 2.06 mmol) is diluted under argon in methanol (8 ml). Na_2CO_3 (218 mg, 2.06 mmol, 1 eq.) is then added in one portion and the resulting suspension is stirred for 20 hours at room temperature. The reaction mixture is taken up in ethyl acetate (50 ml) and washed with saturated $NaHCO_3$ (3 x 25 ml), dried (Na_2SO_4) and the organic layer is concentrated under reduced pressure. The residue is chromatographed on silicagel (40 g, eluted with ethyl acetate) to give anomeric **15** (534 mg, 91 %) as a yellow oil.

TLC (ethyl acetate): R_f 0.34

1H -NMR ($CDCl_3$): δ 7.84-7.90 (*m*, 1 H), 7.59-7.72 (*m*, 2 H), 7.35-7.43 (*m*, 1 H), 5.27-5.42, 4.97-5.00 (2*m*, 2 H), 4.51-4.56, 4.06-4.11 (2*m*, 1 H), 3.99-4.03, 3.65-3.78, 3.56-3.59, 3.38-3.50 (4*m*, 3 H), 2.53-2.71 (*m*, 1 H), 1.76-2.31 (*m*, 3 H), 1.51-1.54 (*m*, 3 H).

^{13}C -NMR ($CDCl_3$): δ 140.15 (*s*), 138.78 (*s*), 133.51 (*d*), 133.26 (*d*), 128.29 (*d*), 127.98 (*d*), 124.34 (*d*), 124.04 (*d*), 103.97 (*d*), 102.49 (*d*), 87.54 (*d*), 87.09 (*d*), 72.73 (*d*), 72.27 (*d*), 70.93 (*d*), 70.47 (*d*), 63.57 (*t*), 62.75 (*t*), 42.44 (*t*), 41.98 (*t*), 23.86 (*q*), 22.57 (*q*).

HR-ESIMS ($M+Na^+$) for $C_{13}H_{17}NO_6$. Calculated: 306.0953. Found: 306.0962.

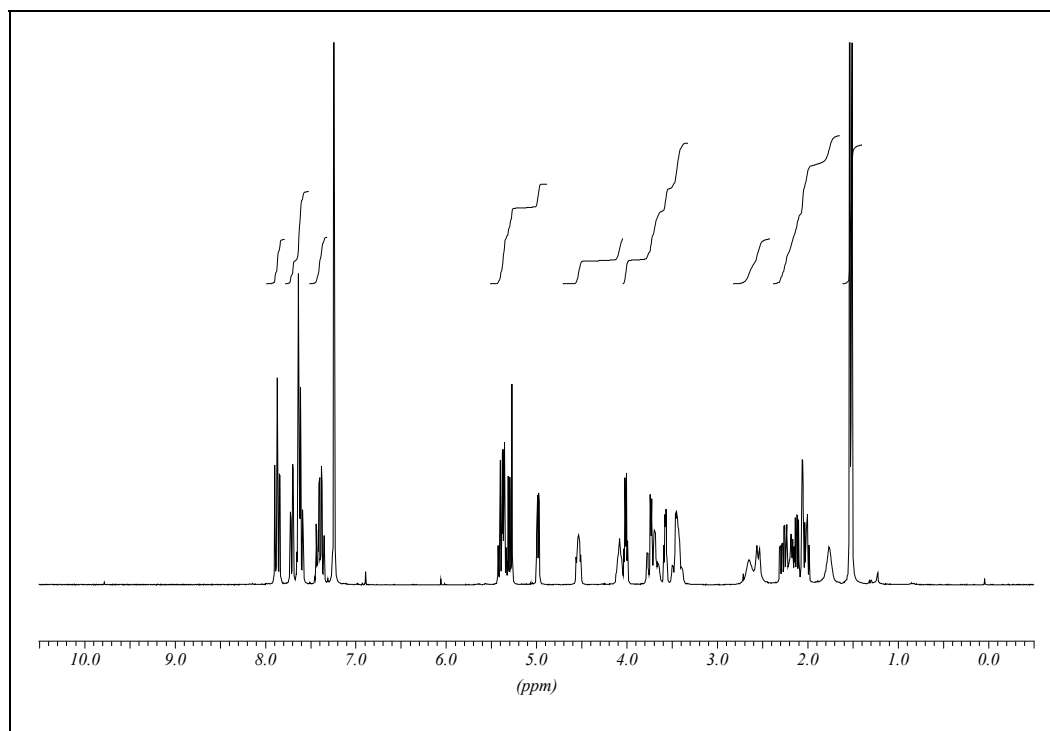
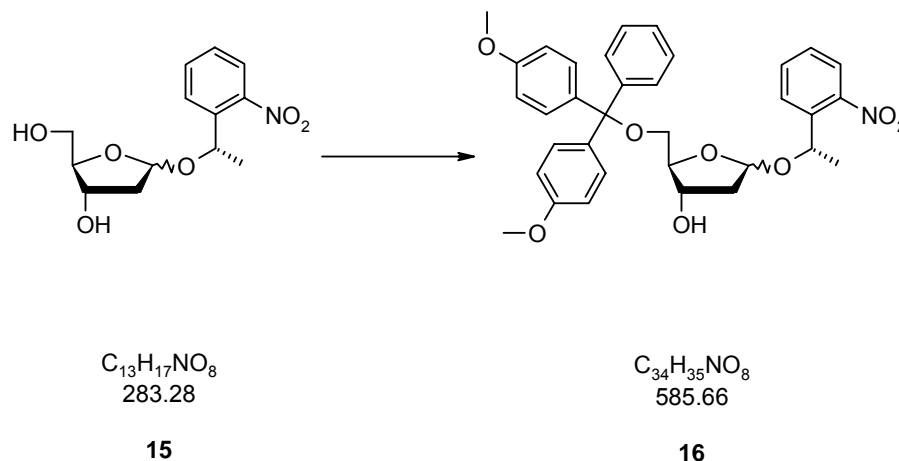


Figure 5.32 $^1\text{H-NMR}$ spectrum of **15**

5.5.4 1'-[1(S)-(2-Nitrophenyl)-ethyl]-5'-[(4,4'-dimethoxy)triphenyl]-2'-deoxy-ribofuranose (**16**)



1'-[1(S)-(2-Nitrophenyl)-ethyl]-2'-deoxy-D-ribofuranose **15** (400 mg, 1.41 mmol) is diluted under argon in pyridine (4 ml). 4,4'-Dimethoxytriphenylmethyl chloride (575 mg, 1.69 mmol, 1.2 eq.) is then added in four equal portions every 15 min. After 90 min. the solution is taken up in ethyl acetate (50 ml) and washed with saturated $NaHCO_3$ (2 x 25 ml). The water layer is extracted with ethyl acetate (2 x 25 ml), the organic layers are dried (Na_2SO_4) and filtered over a pad of charcoal and Celite. The solvent is evaporated after filtration under reduced pressure. The residue is chromatographed on silicagel (90 g, eluted with ethyl acetate/hexane 1:2 + 1 % triethylamine) to give anomeric **16** (723 mg, 74 %) as a pale yellow foam.

TLC (ethyl acetate/hexane 1:1): R_f 0.52, 0.38

1H -NMR ($CDCl_3$): δ 7.87-7.91 (*m*, 1 H), 7.74-7.77, 7.57-7.66 (2*m*, 2 H), 7.48-7.51 (*m*, 1 H), 7.19-7.42 (*m*, 9 H), 6.79-6.88 (*m*, 4 H), 5.43, 4.89 (*d* $J = 4.4$, *dd* $J = 5.5, 1.8$, 1 H), 5.29-5.40 (*m*, 1 H), 4.44-4.52, 4.09-4.16 (2*m*, 1 H), 3.95-4.01, 3.75-3.80 (2*m*, 7 H), 3.32-3.37, 3.16-3.21, 2.92-3.01 (3*m*, 2 H), 2.59, 2.10 (2*d*, $J = 9.9$, *s*, 1 H), 2.18-2.30, 1.88-2.01 (2*m*, 2 H), 1.56, 1.33 (2*d*, $J = 6.6$, 3 H).

^{13}C -NMR ($CDCl_3$): δ 158.49 (*s*), 158.40 (*s*), 147.52 (*s*), 148.39 (*s*), 144.84 (*s*), 144.72 (*s*), 140.49 (*s*), 139.37 (*s*), 136.01 (*s*), 135.99 (*s*), 135.90 (*s*), 135.81 (*s*), 133.49 (*d*), 133.33 (*d*), 133.26 (*d*), 130.04 (*d*), 130.01 (*d*), 129.96 (*d*), 129.91 (*d*), 128.29 (*d*), 128.11 (*d*), 128.04 (*d*), 127.98 (*d*), 127.93 (*d*), 127.87 (*d*), 127.85 (*d*), 127.81 (*d*), 127.75 (*d*),

127.73 (*d*), 127.67 (*d*), 127.05 (*d*), 126.80 (*d*), 126.71 (*d*), 124.34 (*d*), 124.22 (*d*), 124.09 (*d*), 113.14 (*d*), 113.04 (*d*), 103.86 (*d*), 101.55 (*d*), 86.38 (*d*), 84.73 (*d*), 86.18 (*s*), 85.96 (*s*), 73.48 (*d*), 73.32 (*d*), 70.79 (*d*), 69.46 (*d*), 65.15 (*t*), 63.82 (*t*), 55.20 (*q*), 55.17 (*q*), 41.42 (*t*), 41.08 (*t*), 23.82 (*q*), 22.71 (*q*).

HR-ESIMS ($M+Na^+$) for $C_{34}H_{35}NO_8$. Calculated: 608.2260. Found: 608.2249.

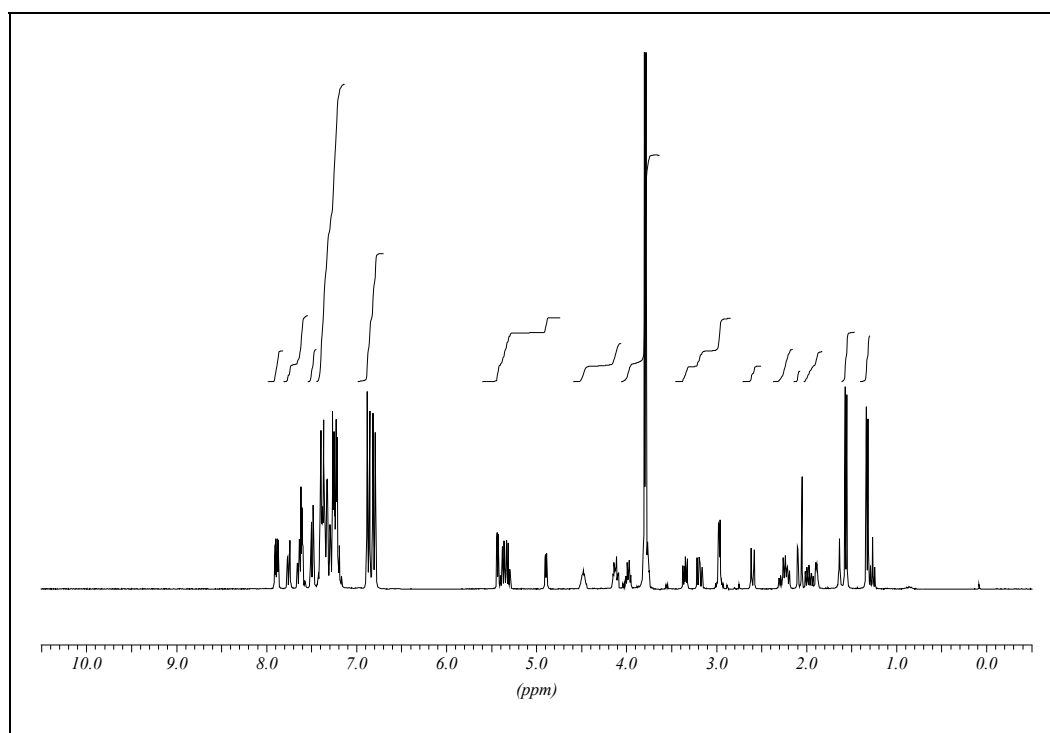
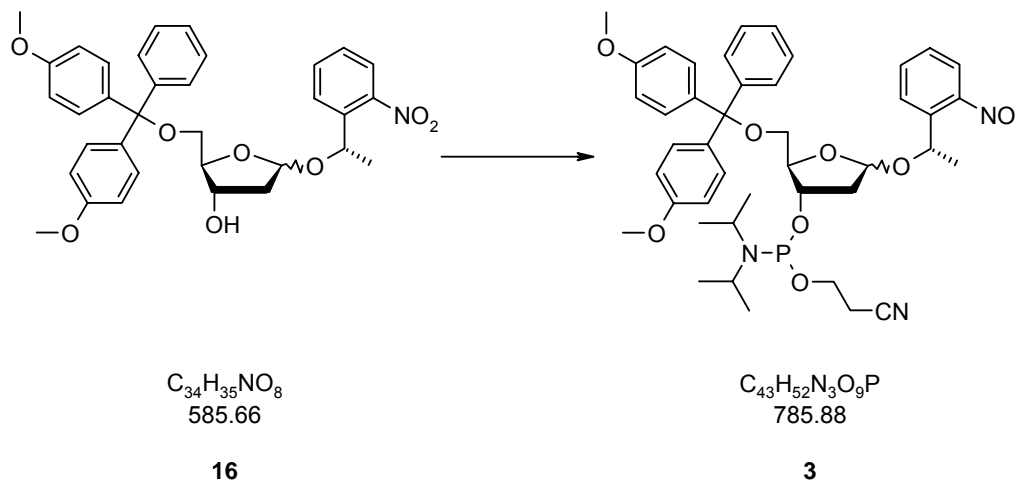


Figure 5.33 1H -NMR spectrum of **16**

5.5.5 1'-[1(S)-(2-Nitrophenyl)-ethyl]-5'-[(4,4'-dimethoxy)triphenyl]-2'-deoxy-ribofuranose-3'-(2-cyanoethyl diisopropylphosphoramidite) (**3**)



To a solution of alcohol **16** (200 mg, 0.34 mmol) in THF (5 ml) under argon, iPr_2NEt (170 μ l, 0.99 mmol, 2.9 eq.) and 2-cyanoethyl diisopropylchlorophosphoramidite (110 μ l, mmol, 1.45 eq.) are added under argon. The mixture is allowed to stand for 1 hour. The suspension is then taken up in ethyl acetate (30 ml) and washed with saturated $NaHCO_3$ (2 x 15 ml). The aqueous layers are then extracted with CH_2Cl_2 (2 x 15 ml). The organic layers are dried (Na_2SO_4) and evaporated under reduced pressure. The residue is chromatographed on silicagel (50 g, eluted with ethyl acetate/hexane 1:2 + 1 % triethylamine) to give anomeric **3** (206 mg, 77 %) as a colorless foam.

TLC (ethyl acetate/hexane 1:2): R_f 0.50, 0.44, 0.36

1H -NMR ($CDCl_3$): δ 7.79-7.90, 7.49-7.56 (2m, 3 H), 7.41-7.45 (m, 1 H), 7.08-7.33 (m, 9 H), 6.67-6.79 (m, 4 H), 5.22-5.36, 4.85 (m, dd, $J = 5.3, 2.1, 2$ H), 4.39-4.54, 4.07-4.24 (2m, 1 H), 4.03-4.06, 3.63-3.74 (2m, 8 H), 3.35-3.61 (m, 3 H), 3.15-3.24, 3.05-3.12 (2m, 1 H), 2.89-2.95, 2.73-2.78 (2m, 1 H), 2.46-2.55 (m, 1 H), 1.91-2.34 (m, 3 H), 1.42-1.45, 1.24-1.28 (2m, 3 H), 0.88-0.96, 1.02-1.10 (m, 12 H).

^{13}C -NMR ($CDCl_3$): δ 158.40 (s), 158.38 (s), 158.33 (s), 158.31 (s), 148.53 (s), 148.49 (s), 146.86 (s), 146.81 (s), 144.95 (s), 144.92 (s), 144.81 (s), 142.01 (s), 141.86 (s), 139.62 (s), 139.53 (s), 136.16 (s), 136.08 (s), 135.99 (s), 135.89 (s), 135.86 (s), 133.42 (d), 133.33 (d), 133.04 (d), 133.01 (d), 130.17 (d), 130.12 (d), 130.07 (d), 130.02 (d), 129.99 (d), 129.97 (d), 128.78 (d), 128.29 (d), 128.23 (d), 128.15 (d), 128.10 (d), 127.99

(*d*), 127.94 (*d*), 127.75 (*d*), 127.66 (*d*), 127.30 (*d*), 127.28 (*d*), 126.71 (*d*), 126.65 (*d*), 126.61 (*d*), 124.26 (*d*), 123.96 (*d*), 123.94 (*d*), 117.66 (*s*), 117.53 (*s*), 117.50 (*s*), 113.04 (*d*), 112.93 (*d*), 104.35 (*d*), 104.34 (*d*), 101.86 (*d*), 101.80 (*d*), 85.93 (*s*), 85.91 (*s*), 85.73 (*s*), 85.71 (*s*), 84.73 (*d*), 84.67 (*d*), 84.58 (*d*), 84.49 (*d*), 83.81 (*d*), 83.72 (*d*), 83.66 (*d*), 74.24 (*d*), 74.05 (*d*), 74.01 (*d*), 73.95 (*d*), 73.80 (*d*), 73.72 (*d*), 73.61 (*d*), 73.36 (*d*), 71.83 (*d*), 71.79 (*d*), 69.72 (*d*), 69.68 (*d*), 64.73 (*t*), 64.46 (*t*), 63.66 (*t*), 63.36 (*t*), 58.48 (*t*), 58.37 (*t*), 58.24 (*t*), 58.20 (*t*), 58.17 (*t*), 58.13 (*t*), 57.96 (*t*), 57.91 (*t*), 55.20 (*q*), 55.18 (*q*), 55.16 (*q*), 43.28 (*d*), 43.19 (*d*), 43.17 (*d*), 43.15 (*d*), 43.11 (*d*), 43.03 (*d*), 43.01 (*d*), 42.98 (*d*), 41.09 (*t*), 41.05 (*t*), 40.87 (*t*), 40.81 (*t*), 40.77 (*t*), 40.72 (*t*), 40.51 (*t*), 40.46 (*t*), 24.63 (*q*), 24.60 (*q*), 24.56 (*q*), 24.54 (*q*), 24.50 (*q*), 24.47 (*q*), 24.37 (*q*), 24.36 (*q*), 23.91 (*q*), 23.87 (*q*), 23.68 (*q*), 20.35 (*t*), 20.31 (*t*), 20.26 (*t*), 20.21 (*t*), 20.14 (*t*), 20.11 (*t*), 20.05 (*t*), 20.02 (*t*).

^{31}P -NMR (CDCl_3): δ 149.13, 148.75, 148.53, 148.27.

HR-ESIMS ($\text{M}+\text{H}^+$) for $\text{C}_{43}\text{H}_{52}\text{N}_3\text{O}_9\text{P}$. Calculated: 786.3519. Found: 786.3538.

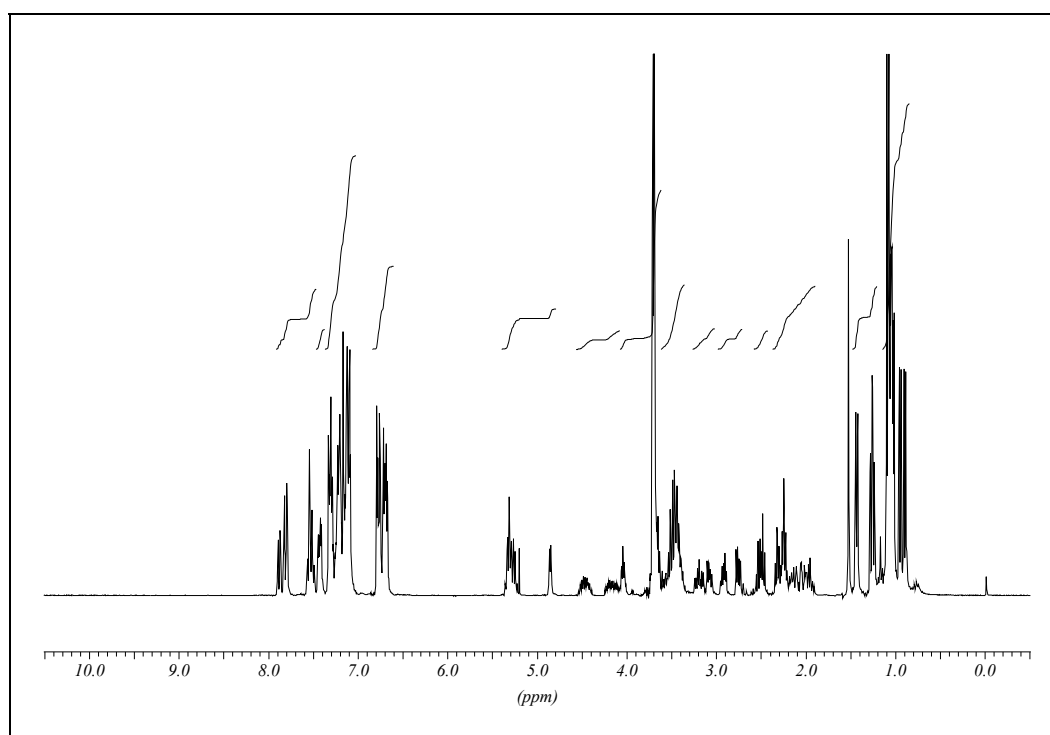


Figure 5.34 ^1H -NMR spectrum of **3**

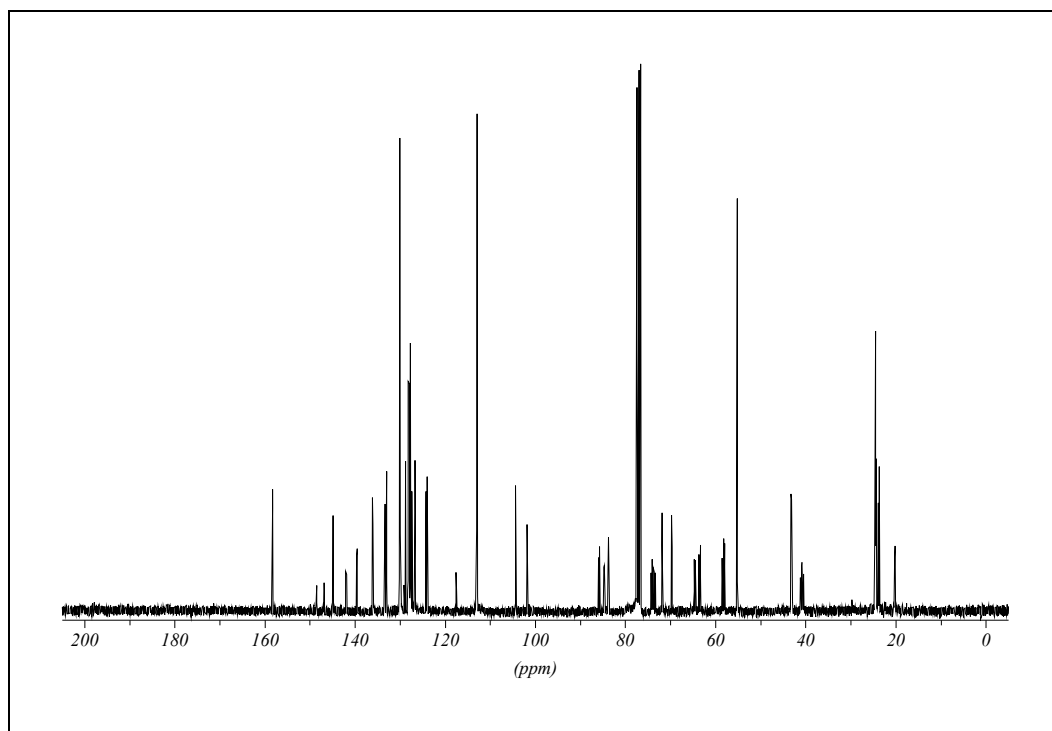


Figure 5.35 ^{13}C -NMR spectrum of **3**

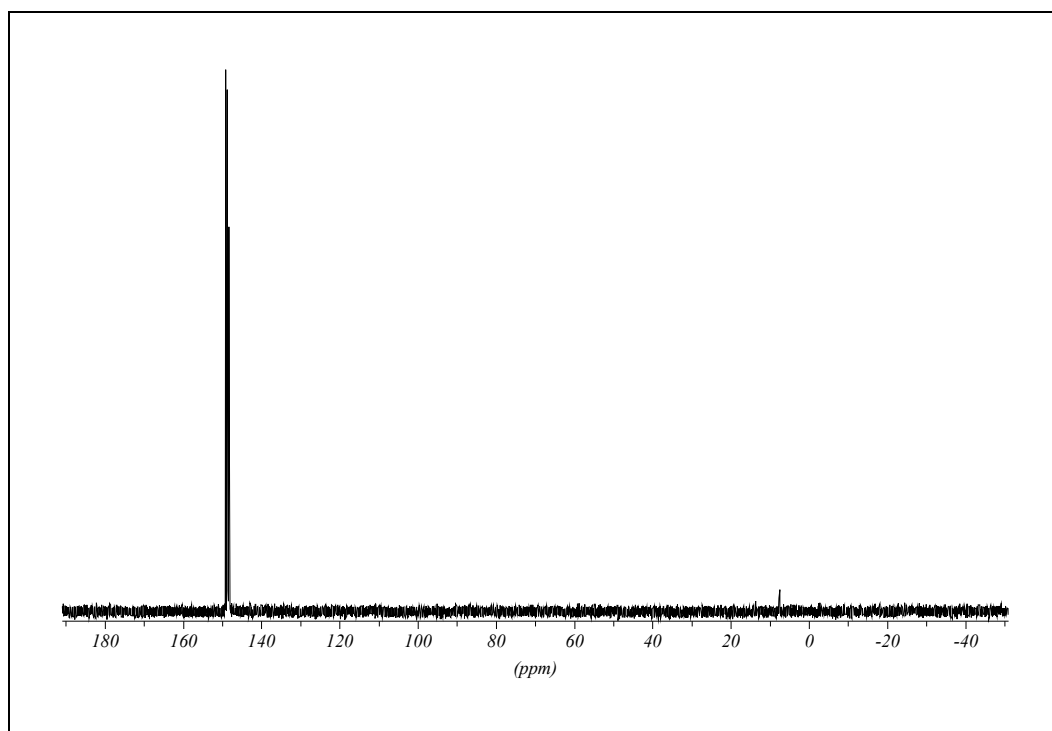


Figure 5.36 ^{31}P -NMR spectrum of **3**

5.6 Synthesis and Purification of Oligonucleotides

5.6.1 Ribonuclease-free laboratory environment

Gloves washed with ethanol are worn at all times when working with RNA or touching laboratory equipment used with RNA. To prevent RNase contamination in solutions, Milli-Q-water were treated with 0.1 % diethyl pyrocarbonate (DEPC, *Fluka*) shaken thoroughly and incubated for one hour at room temperature before autoclaving.^[206,207] Tris buffers were prepared with DEPC-treated, autoclaved water and were then reautoclaved.^[206] All used glass bottles (plastic tops excluded), eppendorf tubes and pipette tips were autoclaved at 150 °C/10 bar/20 min. Screw-top eppendorf tubes and Falcon[®] tubes (*Becton-Dickinson*) were purchased sterilized. Other plasticware was rinsed first with 0.1 M NaOH/1 mM EDTA and then with DEPC-treated water.^[208] Electrophoresis and electroelution tanks were cleaned and dried with ethanol. Then they were filled with 3 % H₂O₂, incubated for 10 minutes and rinsed with DEPC-treated water.

DEPC reacts with histidyl residues in proteins to yield an *N*-carbethoxyhistidyl derivative.^[209,210] DEPC destroys enzymatic activity by modifying -NH₂, -SH and -OH groups in RNases and other proteins.

5.6.2 Synthesis of oligonucleotides

All oligonucleotides were prepared by automated oligonucleotide synthesis with an Expedite 8900 nucleic-acid synthesis system (*PerSeptive Biosystems Inc., Framingham MA*) by using the cyanoethyl-phosphoramidite approach. For RNA synthesis, 2'-*O*-TBDMS protected PAC-phosphoramidites (*Glen Research Corp., Sterling VA*) and polystyrene solid supports (*Amersham Biotech*) were used. For DNA synthesis benzoyl (dA, dC) and isobutyryl (dG) protected phosphoramidites and controlled pore-glass solid supports (*Glen Research*) were used. The synthesis was performed by using the same standard coupling protocol for DNA and RNA with 5-(ethylthio)-1*H*-tetrazole (*Aldrich*) as activator and a coupling time of 90 seconds for DNA and 6 minutes for RNA. The modified phosphoramidites were allowed to couple for 6 min and 12 min for DNA and RNA, respectively.

[206] Blumberg, D. D., *Methods Enzymol.* **1987**, 152, 20-24.

[207] Mabic, S., Kano, I., in *The R&D Notebook No. RD008*, Millipore Corporation, Bedford, USA, **2002**.

[208] in *RNA Analysis Notebook*, Part# BR120 ed., Promega Corporation, Madison, USA, **2003**.

[209] Miles, E. W., *Methods Enzymol.* **1977**, 47, 431-442.

[210] Melchior, W. B., Jr., Fahrney, D., *Biochemistry* **1970**, 9, 251-258.

5.6.2.1 Solutions for oligonucleotides synthesis

Deblocking:	3 ml dichloroacetic acid, 97 ml dichloroethane
Activator 0.25 M:	1 g 5-(ethylthio)-1H-tetrazole, 31 ml acetonitrile, molsieves
Capping A:	6.15 g DMAP, 100 ml acetonitrile
Capping B:	25 ml acetonitrile, 10 ml Ac ₂ O, 15 ml syn.collidine, molsieves
Oxidizing:	104 ml acetonitrile, 412 mg I ₂ , 9.6 ml syn-collidine, 48 ml H ₂ O

5.6.2.2 Oligonucleotide synthesis protocol

The following protocol was used for the synthesis of all sequences. The different coupling times were achieved by changing the appropriate time intervals.

```

/* ----- */
/*      Function             Mode   Amount  Time(sec)      Description      */
/*      /Arg1 /Arg2                                     */
/* ----- */
$Deblocking
144 /*Index Fract. Coll.  */ NA       1       0 "Event out ON"
0 /*Default                */ WAIT      0     1.5 "Wait"
141 /*Trityl Mon. On/Off  */ NA       1       1 "START data collection"
16 /*Dblk                  */ PULSE    10      0 "Dblk to column"
16 /*Dblk                  */ PULSE    50     49 "Deblock"
38 /*Diverted Wash A     */ PULSE    60      0 "Flush system with Wash A"
141 /*Trityl Mon. On/Off  */ NA       0       1 "STOP data collection"
38 /*Diverted Wash A     */ PULSE    60      0 "Flush system with Wash A"
144 /*Index Fract. Coll.  */ NA       2       0 "Event out OFF"
$Coupling
1 /*Wash                   */ PULSE    5       0 "Flush system with Wash"
2 /*Act                    */ PULSE    5       0 "Flush system with Act"
23 /*6 + Act              */ PULSE    5       0 "Monomer + Act to column"
23 /*6 + Act              */ PULSE    2     30 "Couple monomer"
2 /*Act                    */ PULSE    3    120 "Couple monomer"
1 /*Wash                   */ PULSE    7    210 "Couple monomer"
1 /*Wash                   */ PULSE    8       0 "Flush system with Wash"
$Capping
12 /*Wash A                */ PULSE   20       0 "Flush system with Wash A"
13 /*Caps                  */ PULSE    8       0 "Caps to column"
12 /*Wash A                */ PULSE    6     15 "Cap"
12 /*Wash A                */ PULSE   25       0 "Flush system with Wash A"
$Oxidizing
15 /*Ox                    */ PULSE   15       0 "Ox to column"
12 /*Wash A                */ PULSE   25       0 "Flush system with Wash A"
$Capping
13 /*Caps                  */ PULSE    7       0 "Caps to column"
12 /*Wash A                */ PULSE   40       0 "End of cycle wash"

```

Figure 5.37 Synthesis protocol from the Expedite machine. Time settings in red were changed to achieve different coupling times: 1.5 minutes (16 + 24 + 56 sec), 6 minutes (30 + 120 + 210 sec) and 12 min (60 + 240 + 420 sec)

5.6.3 Deprotection of oligonucleotides^[211]

5.6.3.1 Deprotection of DNA sequences

The synthesis column was opened and the dry solid support was poured into a screw-top eppendorf tube. 1 ml of concentrated ammonia (25%) was added and the vessel was sealed and allowed to stand for 30 minutes at room temperature. The tubes were then shaken overnight at 55 °C. After centrifugation, the supernatant was removed with a

[211] Schulhof, J. C., Molko, D., Teoule, R., *Nucleic Acids Res.* **1987**, *15*, 397-416.

syringe and filtered through a teflon filter (0.45 μm). The support was rinsed twice with 1 ml water. The combined solutions are evaporated to dryness. Heptamers were purified by RP-HPLC whereas primer sequences were purified by gel electrophoreses.

5.6.3.2 Deprotection of RNA sequences

The synthesis column was opened and the dry solid support was poured into a screw-top eppendorf tube. 1 ml of ethanolic ammonium hydroxide (EtOH/NH₄OH 1:3) was added and the vessel was sealed and allowed to stand for 30 minutes at room temperature. Ethanol prevents the hydrolysis of the silyl groups.^[212-214] The tubes were then shaken overnight at 55 °C. From then on sterile conditions applied for RNA sequences. After centrifugation, the supernatant was removed with a syringe and filtered through a teflon filter (0.45 μm). The support was rinsed twice with 1 ml of an EtOH/H₂O/CH₃CN 3:1:1 mixture (recommended when using polystyrene support).^[215] The combined solutions were evaporated to dryness. Heptamers were purified by RP-HPLC before removal of the silyl groups. RNA template sequences were directly silyl deprotected before gel electrophoresis.

Silyl deprotection was achieved by treatment with Bu₄NF (1 M in THF) for at least 6 h at room temperature. For RNA sequences, 0.5 ml of a TBAF solution (*Fluka*, 1 M in THF) was added to the residue.^[160,215,216] The eppendorf tube was shaken at room temperature. Again the samples were evaporated using a *Savant Speed-Vac SC 110* to give an oily residue. The residue was taken up in water was desalted by using Sep-Pak[®] C₁₈ columns (*Waters Corp., Milford MA*) before re-purification by RP-HPLC.

5.6.4 Purification of oligonucleotides by RP-HPLC

The DNA and RNA heptamers were purified by using RP-HPLC on an ÄKTA 900 HPLC system (*Amersham Pharmacia Biotech*). UV absorptions were detected at 280, 260 and 215 nm. A SOURCE[™] 15RPC ST 4.6/100 (polystyrene/divinyl benzene, 15 μm , 100/4.6 mm) column (*Amersham Biosciences, Uppsala, Sweden*) was used with a gradient of solvent A (0.1 M Et₃NOAc in H₂O) and solvent B (0.1 M Et₃NOAc, CH₃CN/H₂O (4:1)).

Purified oligonucleotides were dissolved in DEPC-treated water and the concentration was determined by using a NanoDrop[®] ND-100 UV/Vis spectrophotometer (*NanoDrop Technologies, Wilmington DE*).

[212] Wu, T., Ogilvie, K. K., Pon, R. T., *Ibid.* **1989**, *17*, 3501-3517.

[213] Wu, T., Ogilvie, K. K., *J. Org. Chem.* **1990**, *55*, 4717-4724.

[214] Scaringe, S. A., Francklyn, C., Usman, N., *Nucleic Acids Res.* **1990**, *18*, 5433-5441.

[215] in *Technical Bulletin RNA Deprotection*, Glen Research, Sterling, USA, **1999**.

[216] in *Technical Bulletin TOM*, Glen Research, Sterling, USA, **1999**.

[160] Weiss, P. A., *Glen Research Report* **1998**, *11*, 2-4.

5.6.5 Desalting the oligonucleotides

TEAA buffer (1 M): Acetic acid (28.6 ml) is dissolved in water. Triethylamine (69.7 ml) is added slowly. The volume is filled up to 500 ml and the buffer is adjusted to pH 7. The buffer was stored at 4 °C.

The oligonucleotides were desalted using Sep-Pak[®] C₁₈ columns (*Waters*). The longer end of the column was attached to a 10 ml syringe without plunger. The column was first washed with 5 ml acetonitrile and then conditioned with 10 ml 100 mM TEAA buffer. The oligonucleotide was loaded as a 300 mM TEAA solution (up to ~4 ml overall) on the column. After washing with 5 ml (10 ml for shorter sequences) 100 mM TEAA and 10 ml (5 ml) water the oligonucleotide is eluted with 3-4 ml water/acetonitrile 1:1. Sequences were evaporated to dryness.

5.6.6 Purification of oligonucleotides by gel electrophoreses^[217-219]

TBE 10X buffer: (Tris[hydroxymethyl]amino)methane (108.0 g, TRIZMA[®]-base, *Sigma*) and boric acid (55 g, *Fluka*) were diluted in DEPC-treated water. After addition of EDTA (40 ml, 0.5 M solution, pH 8, *Fluka* or 9.3 g Na₂EDTA · 2 H₂O alternatively) the volume was filled up to 1000 ml, reautoclaved and stored at 4 °C. The concentration of the TBE 1X buffer was 89 mM tris-borate and 2 mM EDTA, the pH ~ 8.3.

Glass plates were treated prior to experiments with Sigmacote[®] (*Sigma*) to ensure good gel release properties. The 10 % APS solution was prepared anew weekly.

5.6.6.1 Preparative gel electrophoreses

For a gel (385 mm x 310 mm x 2 mm) the following procedure applied.

Urea (150 g, *Sigma*) was dissolved at ~50 °C in acrylamide-*N,N'*-methylene-bisacrylamide solution (150 ml, 19:1, 40 % (w/v), *Serva*) and TBE 10X (30 ml) was added. To the filtered solution ammonium peroxydisulfate (1.94 ml, 10 % in water, APS, *Fluka*) was added under stirring and polymerisation was then initiated by the addition of *N,N,N',N'*-tetramethylethylenediamine (120 µl, TEMED, *Fluka*). After polymerisation the wells were immediately washed with TBE 1X and the gel was run for 5 min. at 60 W before loading. The desalted samples were dissolved in urea (7 M in water), heated to 80°C for 5 min. and aliquots of 100 µl thereof were placed in the wells. The gel was run overnight at 20 W. The apparatus was then dismantled and after removing the upper glass plate the gel was covered with Saran Wrap[®] Plastic Film. The second glass plate was removed and the gel on the film was put on a fluorescent TLC plate (*Macherey-Nagel*). Under UV-light (254 nm) the desired bands were then cut out with a scalpel and electroeluted.

[217] Maniatis, T., Efstratiadis, A., *Methods Enzymol.* **1980**, 65, 299-305.

[218] Sambrook, J., Fritsch, E. F., Maniatis, T., *Molecular Cloning: A Laboratory Manual, Vol. 1-3*, 2nd ed., Cold Spring Harbor Laboratory Press, **1989**.

[219] Ogden, R. C., Adams, D. A., *Methods Enzymol.* **1987**, 152, 61-87.

5.6.6.2 Analytical gel electrophoreses

For a gel (385 mm x 310 mm x 0.35 mm) the following procedure applied.

Urea (45 g) was dissolved at ~50 °C in acrylamide-*N,N'*-methylenebisacrylamide solution (45 ml) and TBE 10X (9 ml) was added. To the filtered solution, APS (600 µl) was added under stirring. The bottom of the two glass plates was sealed using a syringe filled with the described solution (2 ml) and TEMED (5 µl) for fast polymerisation. The mixture was immediately put between the plates at the bottom side to seal. To the rest of the solution TEMED (28 µl) was added and allowed to slowly polymerize. The gel was preheated at 60-80 W for up to 30 min. and then treated the same way as above and run at 40 W for 3-6 hours.

The gels were run in a *Gibco-BRL Model S2 Sequencing Gel Electrophoresis Apparatus* from *Life Technologies Inc.* with a Power Pac 3000 Power Supply from Bio-Rad Laboratories.

5.6.6.3 Electroelution^[220]

The collected slices from the preparative gels were electroeluted with an *Elutrap*[®] *Electroelution System* apparatus (*Schleicher & Schuell*) according to the manufacturer's protocol.^[221] The oligomers were eluted in TBE 1X buffer at 100 V (10 W) for two hours. After elution the polarity was reversed for 20 sec at 200 V to remove any material attached to the final BT1 membrane.

5.6.6.4 Autoradiography

The analytical gels were transferred to a filter paper (3MM Chr, *Whatman*) and covered with *Saran Wrap*[®] Plastic Film. The gel was then dried using a gel dryer apparatus (*Labcono*) for one hour at 70 °C under vacuum. The dried and gel was then exposed to the blanked phosphor screen (30 min of light) and stored overnight at room temperature. The phosphor screen was then analyzed using a *Storm 820 PhosphorImager* and *ImageQuant*[™] *Image Analysis Software* from *Amersham Biosciences*. A resolution of 200 µ (50 dots/cm) was sufficient for all applications except enzyme kinetics where a resolution of 50 µ (200 dots/cm) was used.

Alternatively the gel was transferred to the filter paper and directly exposed to the screen without drying. In this case the phosphor screen was placed in the fridge overnight to prevent diffusion.

[220] Smith, H. O., *Methods Enzymol.* **1980**, 65, 371-380.

[221] in *Protocols & References*, Schleicher & Schuell GmbH, Dassel, Germany, **2004**.

5.7 Kinetic Studies

5.7.1 Kinetic studies of abasic site deprotection

Purified 1-NPE protected oligonucleotides were diluted with water to a concentration of $1 \text{ OD}_{260}\text{ml}^{-1}$. From this solution 0.4 ml aliquots were placed in a 1 ml quartz cuvette and exposed for different time intervals to UV light (150 W immersion lamp, TQ 150 UV-RS-2, *Heraeus*). The cuvette was therefore placed in a distance of 1 cm from the cooling vessel of the lamp. The samples were immediately analyzed by RP-HPLC using a Brownlee Aquapore RP-300 (C8, 7 μm , 250/4.6 mm) column (*PerkinElmer*). The integrals of the occurring peaks detected at 280 nm were computed directly by the UNICORN v3.00 software and were for each spectrum set to 100%. The areas of the deprotected oligonucleotides were plotted and fitted with a first order exponential decay (*OriginPro 7.5, OriginLab Corporation, Northhampton, MA*). Furthermore the curves were linearized to prove the first-order character of the reactions. From the equation of the fit the half-life times were calculated.

Table 5.1 *RP-HPLC retention times of oligonucleotides used for the deprotection study*

Sequence	Gradient	Retention time
d(AGGY _p TTC)	0-50 % B in 30 min	14.7 min
d(AGGYTTC)	0-50 % B in 30 min	11.3 min
r(AGGX _p UUC)	0-50 % B in 30 min	14.5 min
r(AGGXUUC)	0-50 % B in 30 min	10.8 min

5.7.2 Strand cleavage in the presence of hydroxide at pH 13

Oligonucleotides were diluted to a concentration of $1 \text{ OD}_{260}\text{ml}^{-1}$. Thereof aliquots of 0.3 ml (for cyclophosphate formation kinetics of r(aggX_puuC) and for the strand cleavage kinetics of a true abasic site of r(aggXuuC)) or 0.4 ml (for the DNA abasic site kinetics of d(AGGY_pTTC) and for the β -elimination kinetics of r(aggx_puuC)) were measured, depending on the amount of material available. The aliquots were deprotected by using a slide projector for 6 minutes (for oligoribonucleotides) or the UV lamp (for oligodeoxynucleotides) mentioned above.

For deprotection with the slide projector, the aliquots were placed in 1.5 ml eppendorf tubes and placed horizontally in front of the slide projector (distance lamp to sample: ~ 20 cm). The glass objective is removed; the lens system remained in place.

The samples were then adjusted to pH 13 by addition of 0.9 M NaOH (50 μl for 0.4 ml samples or 37.5 μl for 0.3 ml samples, respectively) to a final concentration of 0.1 M NaOH. The aliquots were then shaken at 37 $^{\circ}\text{C}$ (± 0.5 $^{\circ}\text{C}$) for different time intervals. The samples were quenched with a stoichiometric amount of 1 M HCl and the reaction

mixtures were immediately analyzed by RP-HPLC using a SOURCE 15RPC ST 4.6/100 column (*Amersham Biosciences*).

5.7.3 Strand cleavage in the presence of aniline at pH 4.6

Deprotected oligonucleotides were diluted to a final conc. of $1 \text{ OD}_{260}\text{ml}^{-1}$ in 0.5 M aniline-HCl, pH 4.6 (0.4 ml). The aliquots are incubated at 37 °C for different time intervals. To quench the reactions, aniline was removed by quick DEAE-HPLC (Nucleogen[®] 60-7 125/4 mm column, *Macherey-Nagel*) with the following gradient: 100 % solvent A (0.25 mM Na_2HPO_4 + 0.25 mM NaH_2PO_4 in 20 % acetonitrile) for 10 min, 100 % solvent B (A + 1 M NaCl) for 5 min. The oligonucleotides eluted with solvent B are collected and carefully (low temperature) concentrated to a volume of ~0.4 ml and further analyzed by RP-HPLC as described above.

5.7.4 Evaluation of the kinetic parameters

The calculated substrate integrals are fitted with first order exponential fits using *OriginPro 7.5*. In some of the performed experiments the calculated curve does not intersect the y-axis at $y = 1$. This is because the reactions had already started. To be able to calculate the appropriate half-life times of the described reactions the equations of the resulting curves are corrected in a way to cut the y-axis at $y = 1$. This is just a translation of the curve along the x-axis and therefore does not change the character of the curve. To calculate the velocity constant k $-\ln[S]/[S_0]$ is plotted against the time. The linear fits were calculated with *OriginPro 7.5*. Although the linear fits do not always intersect at the origin the curves were left unchanged since the velocity constant is the slope.

Table 5.2 shows all data from the exponential and linear fits and the calculated half-life times and velocity constants.

Reaction	Exponential fit	Corrected exponential fit	$T_{1/2}$	Linear fit ($-\ln [S]/[S_0]$)	k
RNA deprotection	$y = 0.92 \cdot e^{\frac{-x}{18.75}} - 0.029$ $R^2 > 0.991$	$y = 0.92 \cdot e^{\frac{-x+2.099}{18.75}} - 0.029$	12.5 sec	$y = 0.05677 \cdot x + 0.11388$ $R^2 > 0.987$	$5.68 \cdot 10^{-2} \text{ s}^{-1}$
	DNA deprotection	$y = 0.99 \cdot e^{\frac{-x}{4.82}} + 0.01$ $R^2 > 0.999$	3.4 sec	$y = 0.2105 \cdot x - 0.02367$ $R^2 > 0.999$	$2.11 \cdot 10^{-1} \text{ s}^{-1}$
$\beta_2\delta$ -elimination of abasic RNA	$y = 0.92 \cdot e^{\frac{-x}{12.53}} + 0.08$ $R^2 > 0.998$	-	9 h 54 min	$y = 0.0705 \cdot x + 0.00118$ $R^2 > 0.999$	$1.96 \cdot 10^{-5} \text{ s}^{-1}$
	cyclophosphate formation	$y = 1.02 \cdot e^{\frac{-x}{5.96}} - 0.03$ $R^2 > 0.996$	-	3 h 41 min	$y = 0.21422 \cdot x - 0.12708$ $R^2 > 0.994$
cleavage of a natural RNA abasic site	$y = 0.84 \cdot e^{\frac{-x}{1.67}} - 0.001$ $R^2 > 0.997$	$y = 0.84 \cdot e^{\frac{-x+0.293}{1.67}} - 0.001$	69 min	$y = 0.62115 \cdot x + 0.153$ $R^2 > 0.999$	$1.73 \cdot 10^{-4} \text{ s}^{-1}$
	$\beta_2\delta$ -elimination of abasic DNA	$y = 0.84 \cdot e^{\frac{-x}{6.29}} - 0.02$ $R^2 > 0.997$	$y = 0.84 \cdot e^{\frac{-x+1.109}{6.29}} - 0.02$	4.1 min	$y = 0.18147 \cdot x + 0.13901$ $R^2 > 0.996$
cleavage of a natural RNA abasic site (aniline)	$y = 0.72 \cdot e^{\frac{-x}{21.51}} - 0.04$ $R^2 > 0.997$	$y = 0.72 \cdot e^{\frac{-x+7.91}{21.51}} - 0.04$	14 min	$y = 0.05134 \cdot x + 0.38154$ $R^2 > 0.997$	$8.56 \cdot 10^{-4} \text{ s}^{-1}$
	cleavage of a natural DNA abasic site (aniline)	$y = 0.86 \cdot e^{\frac{-x}{1.26}} + 0.005$ $R^2 > 0.995$	$y = 0.86 \cdot e^{\frac{-x+0.184}{1.26}} + 0.005$	53 sec	$y = 0.77741 \cdot x + 0.10664$ $R^2 > 0.996$

5.8 Enzyme Assays

This sample protocol describes the assays done for all three reverse transcriptases. Here a number of 30 samples with the following final concentrations were prepared:

- template (RNA):	100 nM
- primer (DNA):	50 nM
- each dNTP used:	20 μ M

The DNA/RNA oligonucleotides were stored as 5/10 μ M solutions in water at -20 °C.

5.8.1 Labeling of the primer

T4 PNK 10X Buffer (Fermentas): 500 mM Tris-HCl, pH 7.6, 100 mM MgCl₂, 50 mM DTT, 1 mM spermidine, 1 mM EDTA

30 pmol of DNA primer were phosphorylated at the 5'-OH using 10 units of T4 Polynucleotide Kinase (PNK, *Fermentas*) and [γ -³²P]ATP (*Hartmann Analytic*) as follows:

RNase-free H ₂ O	5 μ l
T4 PNK 10X Buffer	2 μ l
Primer solution (5 μ M)	6 μ l
[γ - ³² P]ATP (3000 Ci/mmol, 10 mCi/ml)	6 μ l
T4 Polynucleotide Kinase (10 u/ μ l)	1 μ l
Total volume	20 μ l

The solution was incubated at 37 °C for 30 minutes. The PNK was then inactivated by heating the sample up to 90 °C for 2 minutes.

5.8.2 Preparation of the reaction mix

Reaction 5X Buffer for HIV and AMV Reverse Transcriptases: 250 mM Tris (pH 8.3), 250 mM NaCl, 40 mM MgCl₂, 5 mM DTT.

Reaction 5X Buffer for M-MLV RT (H-): 250 mM Tris-HCl (pH 8.3), 375 mM KCl, 15 mM MgCl₂, 50 mM DTT.

With two different templates, the natural and the modified RNA, two different reaction mixes had to be prepared

The reaction mix containing 60 pmol of template RNA and 30 pmol of primer DNA was prepared as follows:

	modified	natural	total
Labeled primer			20 μ l
RNase-free H ₂ O			118 μ l
Reaction 5X Buffer			36 μ l
	139.2 μ l	34.8 μ l	174 μ l
Template (10 μ M)	4.8 μ l	1.2 μ l	<u>6 μl</u>
Total volume	144 μ l	36 μ l	180 μ l

The mixture was heated for 5 minutes at 60 °C and then allowed to cool to room temperature. Assays containing a modified RNA template were deprotected for 2 minutes using UV light or the slide projector for 6 minutes.

5.8.3 Enzyme reaction

Per sample following solution was prepared using dNTPs (*Roche Diagnostics*):

Reaction mix	6 μ l
dNTP (100 μ M)	2 μ l
Enzyme	<u>2 μl</u>
Total reaction volume	10 μ l

The reactions took place at 37 °C for 1 hour for all enzymes. After addition of 50 μ l of loading dye, the mixture was heated to 90 °C for 5 minutes. 5 μ l per reaction were analyzed by gel electrophoresis.

5.8.4 Enzyme storage buffers

Enzymes are diluted in their storage buffers.

AMV RT storing 1X buffer: 200 mM K₃PO₄, pH 7.2, 2 mM DTT, 50 % glycerol

K ₃ PO ₄ · H ₂ O	460.6 mg
DTT (1 M)	20 μ l
Glycerol	5 ml
RNase-free H ₂ O	<u>5 ml</u>
	10 ml

rHIV RT storing 1X buffer: 10 mM K₃PO₄, pH 7.4, 1 mM DTT, 20 % glycerol

K ₃ PO ₄ · H ₂ O	23.0 mg
DTT (1 M)	10 µl
Glycerol	2 ml
RNase-free H ₂ O	8 ml
	<hr/>
	10 ml

pH is adjusted with aqueous H₃PO₄ to 7.2 or 7.4 respectively.

5.8.5 Kinetic assays

For the kinetic assay the samples were prepared as described above. A standing start primer-template system was used. All reactions were carried out at 37 °C with a reaction time of 2 minutes. The final substrate concentrations used were 1000, 800, 500, 300, 200, 100, 80, 50, 40, 30, 20, 10 µM. Enzyme concentrations found to work best in time course experiments were: 0.5 u (dATP vs. AS), 1.0 u (dGTP), 1.5 u (dTTP and dCTP). After addition of 50 µl of loading dye, the mixture was heated to 90 °C for 2 minutes. 2 µl per reaction were analyzed by analytical gel electrophoresis. After exposure of the gels the screen was measured at a resolution of 50 micron (200 dots/cm). The spots were quantified with *ImageQuant 5.2* from *Molecular Dynamics*. The starting material was represented with one ellipse that was the same size for all evaluated lanes of a gel. The elongation products were represented with ellipses of a second size. If an elongation product was no more visible at lower dNTP concentration the ellipse was taken into computation nonetheless. Between the starting material and the elongated products the background was measured with an ellipse of the size for elongated products. The percentage of the total elongation was calculated and converted to a concentration. The concentrations were then plotted and fitted with a Michaelis-Menten equation in *KaleidaGraph 4.0* from *Synergy Software*.

6 References

- [1] Macgregor, R. B., Poon, G. M. K., *Comput. Biol. Chem.* **2003**, 27, 461-467.
- [2] Klug, A., *J. Mol. Biol.* **2003**, 335, 3-26.
- [3] Dahm, R., *Dev. Biol.* **2005**, 278, 274-288.
- [4] Miescher, F., *Hoppe-Seyler's Med. Chem. Unters.* **1871**, 4, 441-460.
- [5] Levene, P. A., Jacobs, W. A., *Ber.* **1909**, 42, 2102-2106.
- [6] Levene, P. A., Jacobs, W. A., *Ber.* **1909**, 42, 3247-3251.
- [7] Levene, P. A., Mikeska, L. A., Mori, T., *J. Biol. Chem.* **1930**, 85, 785-787.
- [8] Beadle, G. W., Tatum, E. L., *Proc. Natl. Acad. Sci. U. S. A.* **1941**, 27, 499-506.
- [9] Avery, O. T., MacLeod, C. M., McCarty, M., *J. Exp. Med.* **1944**, 79, 137-158.
- [10] Chargaff, E., *Fed. Proc.* **1951**, 10, 654-659.
- [11] Watson, J. D., Crick, F. H., *Nature* **1953**, 171, 737-738.
- [12] Wilkins, M. H. F., Stokes, A. R., Wilson, H. R., *Nature* **1953**, 171, 738-740.
- [13] Franklin, S. E., Gosling, R. G., *Nature* **1953**, 171, 740-741.
- [14] Watson, J. D., Crick, F. H. C., *Nature* **1953**, 171, 737-738.
- [15] Rich, A., Davies, D. R., *J. Am. Chem. Soc.* **1956**, 78, 3548-3549.
- [16] Puglisi, J. D., Chen, L., Blanchard, S., Frankel, A. D., *Science* **1995**, 270, 1200-1203.
- [17] Battiste, J. L., Mao, H., Rao, N. S., Tan, R., Muhandiram, D. R., Kay, L. E., Frankel, A. D., Williamson, J. R., *Science* **1996**, 273, 1547-1551.
- [18] Correll, C. C., Freeborn, B., Moore, P. B., Steitz, T. A., *Cell* **1997**, 91, 705-712.
- [19] Arnott, S., Hukins, D. W., Dover, S. D., *Biochem. Biophys. Res. Commun.* **1972**, 48, 1392-1399.
- [20] Saenger, W., *Principles of Nucleic Acid Structure*, Springer-Verlag, New York, **1984**.
- [21] Hall, K., Cruz, P., Tinoco, I., Jr., Jovin, T. M., Van de Sande, J. H., *Nature* **1984**, 311, 584-586.
- [22] Adamiak, R. W., Galat, A., Skalski, B., *Biochim. Biophys. Acta* **1985**, 825, 345-352.
- [23] Popena, M., Milecki, J., Adamiak, R. W., *Nucleic Acids Res.* **2004**, 32, 4044-4054.
- [24] Pohl, F. M., Jovin, T. M., *J. Mol. Biol.* **1972**, 67, 375-396.
- [25] Knippers, R., *Molekulare Genetik*, 7th ed., Georg Thieme Verlag, Stuttgart, **1997**.
- [26] <http://newark.rutgers.edu/~babis/research/cell.jpg>.
- [27] http://www.mun.ca/biology/scarr/4241F2_ribosome.jpg.

- [28] Blackburn, G. M., Gait, M. J., *Nucleic Acids in Chemistry and Biology*, 2nd ed., Oxford University Press Inc., New York, **1996**.
- [29] Limbach, P. A., Crain, P. F., McCloskey, J. A., *Nucleic Acids Res.* **1994**, *22*, 2183-2196.
- [30] Rozenski, J., Crain, P. F., McCloskey, J. A., *Nucleic Acids Res.* **1999**, *27*, 196-197.
- [31] Mattick, J. S., Makunin, I. V., *Hum. Mol. Genet.* **2005**, *14*, R121-R132.
- [32] Plath, K., Mlynarczyk-Evans, S., Nusinow, D. A., Panning, B., *Annu. Rev. Genet.* **2002**, *36*, 233-278.
- [33] Valadkhan, S., *Curr. Opin. Chem. Biol.* **2005**, *9*, 603-608.
- [34] Bachellerie Jean, P., Cavaille, J., Huttenhofer, A., *Biochimie* **2002**, *84*, 775-790.
- [35] Elbashir, S. M., Lendeckel, W., Tuschl, T., *Genes Dev.* **2001**, *15*, 188-200.
- [36] Ambros, V., Bartel, B., Bartel, D. P., Burge, C. B., Carrington, J. C., Chen, X., Dreyfuss, G., Eddy, S. R., Griffiths-Jones, S., Marshall, M., Matzke, M., Ruvkun, G., Tuschl, T., *RNA* **2003**, *9*, 277-279.
- [37] Kruger, K., Grabowski, P. J., Zaug, A. J., Sands, J., Gottschling, D. E., Cech, T. R., *Cell* **1982**, *31*, 147-157.
- [38] Carola, C., Eckstein, F., *Curr. Opin. Chem. Biol.* **1999**, *3*, 274-283.
- [39] Byer, C. O., Shainberg, L. W., Galliano, G., Shriver, S. P., Shriver, P., *Dimensions In Human Sexuality*, 5 ed., The McGraw-Hill Companies, **1999**.
- [40] Lindahl, T., Nyberg, B., *Biochemistry* **1972**, *11*, 3610-3618.
- [41] Lindahl, T., Andersson, A., *Biochemistry* **1972**, *11*, 3618-3623.
- [42] Manoharan, M., Ransom, S. C., Mazumder, A., Gerlt, J. A., Wilde, J. A., Withka, J. A., Bolton, P. H., *J. Am. Chem. Soc.* **1988**, *110*, 1620-1622.
- [43] Wilde, J. A., Bolton, P. H., Mazumder, A., Manoharan, M., Gerlt, J. A., *J. Am. Chem. Soc.* **1989**, *111*, 1894-1896.
- [44] Kochetkov, N. K., Budovskii, E. I., in *Organic Chemistry of Nucleic Acids* (Eds.: N. K. Kochetkov, E. I. Budovskii), Plenum, New York, **1972**, pp. 425-448.
- [45] Zielonacka-Lis, E., *Nucleosides Nucleotides* **1989**, *8*, 383-405.
- [46] Venner, H., *H.-S. Z. Physiol. Chem.* **1964**, *339*, 14-27.
- [47] Zoltewicz, J. A., Clark, D. F., Sharpless, T. W., Grahe, G., *J. Am. Chem. Soc.* **1970**, *92*, 1741-1750.
- [48] Shapiro, R., Danzig, M., *Biochemistry* **1972**, *11*, 23-29.
- [49] Brown, D. M., Fasman, G. D., Magrath, D. I., Todd, A. R., *J. Chem. Soc., Chem. Commun.* **1954**, 46-52, 1448-1455.
- [50] Wempen, I., Doerr, I. L., Kaplan, L., Fox, J. J., *J. Am. Chem. Soc.* **1960**, *82*, 1624-1629.
- [51] Lhomme, J., Constant, J.-F., Demeunynck, M., *Biopolymers* **2000**, *52*, 65-83.
- [52] Vasseur, J. J., Rayner, B., Imbach, J. L., *Biochem. Biophys. Res. Commun.* **1986**, *134*, 1204-1208.

- [53] Bertrand, J. R., Vasseur, J. J., Rayner, B., Imbach, J. L., Paoletti, J., Paoletti, C., Malvy, C., *Nucleic Acids Res.* **1989**, *17*, 10307-10319.
- [54] Bailly, V., Verly, W. G., *Biochem. J.* **1987**, *242*, 565-572.
- [55] Stuart, G. R., Chambers, R. W., *Nucleic Acids Res.* **1987**, *15*, 7451-7462.
- [56] Kumar, N. V., Varshney, U., *Nucleic Acids Res.* **1994**, *22*, 3737-3741.
- [57] Groebke, K., Leumann, C., *Helv. Chim. Acta* **1990**, *73*, 608-617.
- [58] Peoc'h, D., Meyer, A., Imbach, J. L., Rayner, B., *Tetrahedron Lett.* **1991**, *32*, 207-210.
- [59] Iocono, J. A., Gildea, B., McLaughlin, L. W., *Tetrahedron Lett.* **1990**, *31*, 175-178.
- [60] Laayoun, A., Decout, J.-L., Defrancq, E., Lhomme, J., *Tetrahedron Lett.* **1994**, *35*, 4991-4994.
- [61] Shishkina, I. G., Johnson, F., *Chem. Res. Toxicol.* **2000**, *13*, 907-912.
- [62] in *Technical Bulletin Abasic Site*, Glen Research, Sterling, USA, **2001**.
- [63] Kojima, N., Sugino, M., Mikami, A., Ohtsuka, E., Komatsu, Y., *Org. Lett.* **2005**, *7*, 709-712.
- [64] Coleman, R. S., Pires, R. M., *Nucleosides Nucleotides* **1999**, *18*, 2141-2146.
- [65] Millican, T. A., Mock, G. A., Chauncey, M. A., Patel, T. P., Eaton, M. A. W., Gunning, J., Cutbush, S. D., Neidle, S., Mann, J., *Nucleic Acids Res.* **1984**, *12*, 7435-7453.
- [66] Pochet, S., Huynh-Dinh, T., Neumann, J. M., Tran-Dinh, S., Taboury, J. A., Taillandier, E., Igolen, J., *Tetrahedron Lett.* **1985**, *26*, 2085-2088.
- [67] Raap, J., Dreef, C. E., Van der Marel, G. A., Van Boom, J. H., Hilbers, C. W., *J. Biomol. Struct. Dyn.* **1987**, *5*, 219-247.
- [68] Kotera, M., Bourdat, A.-G., Defrancq, E., Lhomme, J., *J. Am. Chem. Soc.* **1998**, *120*, 11810-11811.
- [69] Povirk, L. F., Houlgrave, C. W., Han, Y. H., *J. Biol. Chem.* **1988**, *263*, 19263-19266.
- [70] Faure, V., Constant, J.-F., Dumy, P., Sapparbaev, M., *Nucleic Acids Res.* **2004**, *32*, 2937-2946.
- [71] Povirk, L. F., Goldberg, I. H., *Proc. Natl. Acad. Sci. U. S. A.* **1985**, *82*, 3182-3186.
- [72] Wang, Y., Sheppard, T. L., Tornaletti, S., Maeda, L. S., Hanawalt, P. C., *Chem. Res. Toxicol.* **2006**, *19*, 234-241.
- [73] Meijler, M. M., Zelenko, O., Sigman, D. S., *J. Am. Chem. Soc.* **1997**, *119*, 1135-1136.
- [74] Berthet, N., Roupioz, Y., Constant, J.-F., Kotera, M., Lhomme, J., *Nucleic Acids Res.* **2001**, *29*, 2725-2732.
- [75] Kroeger, K. M., Jiang, Y. L., Kow, Y. W., Goodman, M. F., Greenberg, M. M., *Biochemistry* **2004**, *43*, 6723-6733.
- [76] Thomas, M., Castaing, B., Fourrey, J.-L., Zelwer, C., *Nucleosides Nucleotides* **1999**, *18*, 239-243.

- [77] Takeshita, M., Chang, C. N., Johnson, F., Will, S., Grollman, A. P., *J. Biol. Chem.* **1987**, *262*, 10171-10179.
- [78] Kim, J., Weledji, Y. N., Greenberg, M. M., *J. Org. Chem.* **2004**, *69*, 6100-6104.
- [79] Chen, J., Stubbe, J., *Biochemistry* **2004**, *43*, 5278-5286.
- [80] Mosimann, M., Kuepfer, P. A., Leumann, C. J., *Org. Lett.* **2005**, *7*, 5211-5214.
- [81] Bailly, V., Verly, W. G., *Biochem. J.* **1988**, *253*, 553-559.
- [82] Bailly, V., Derydt, M., Verly, W. G., *Biochem. J.* **1989**, *261*, 707-713.
- [83] Vodicka, P., Hemminki, K., *Chem.-Biol. Interact.* **1988**, *68*, 153-164.
- [84] Suzuki, T., Ohsumi, S., Makino, K., *Nucleic Acids Res.* **1994**, *22*, 4997-5003.
- [85] Livingston, D. C., *Biochim. Biophys. Acta* **1964**, *87*, 538-540.
- [86] McHugh, P. J., Knowland, J., *Nucleic Acids Res.* **1995**, *23*, 1664-1670.
- [87] Male, R., Fosse, V. M., Kleppe, K., *Nucleic Acids Res.* **1982**, *10*, 6305-6318.
- [88] Georgakilas Alexandros, G., Bennett Paula, V., Sutherland Betsy, M., *Nucleic Acids Res.* **2002**, *30*, 2800-2808.
- [89] Vasseur, J. J., Rayner, B., Imbach, J. L., Verma, S., McCloskey, J. A., Lee, M., Chang, D. K., Lown, J. W., *J. Org. Chem.* **1987**, *52*, 4994-4998.
- [90] Behmoaras, T., Toulme, J. J., Helene, C., *Nature* **1981**, *292*, 858-859.
- [91] Pierre, J., Laval, J., *J. Biol. Chem.* **1981**, *256*, 10217-10220.
- [92] Fkyerat, A., Demeunynck, M., Constant, J. F., Michon, P., Lhomme, J., *J. Am. Chem. Soc.* **1993**, *115*, 9952-9959.
- [93] Belmont, P., Boudali, A., Constant, J.-F., Demeunynck, M., Fkyerat, A., Michon, P., Serratrice, G., Lhomme, J., *New J. Chem.* **1997**, *21*, 47-54.
- [94] Alarcon, K., Demeunynck, M., Lhomme, J., Carrez, D., Croisy, A., *Bioorg. Med. Chem. Lett.* **2001**, *11*, 1855-1858.
- [95] Nakamura, J., Swenberg, J. A., *Cancer Res.* **1999**, *59*, 2522-2526.
- [96] Atamna, H., Cheung, I., Ames, B. N., *Proc. Natl. Acad. Sci. U. S. A.* **2000**, *97*, 686-691.
- [97] Boturyn, D., Constant, J.-F., Defrancq, E., Lhomme, J., Barbin, A., Wild, C. P., *Chem. Res. Toxicol.* **1999**, *12*, 476-482.
- [98] Loeb, L. A., Preston, B. D., *Annu. Rev. Genet.* **1986**, *20*, 201-230.
- [99] Pages, V., Fuchs, R. P. P., *Oncogene* **2002**, *21*, 8957-8966.
- [100] Sagher, D., Strauss, B., *Biochemistry* **1983**, *22*, 4518-4526.
- [101] Randall, S. K., Eritja, R., Kaplan, B. E., Petruska, J., Goodman, M. F., *J. Biol. Chem.* **1987**, *262*, 6864-6870.
- [102] Strauss, B. S., *BioEssays* **1991**, *13*, 79-84.
- [103] Cai, H., Bloom, L. B., Eritja, R., Goodman, M. F., *J. Biol. Chem.* **1993**, *268*, 23567-23572.
- [104] Cancio, R., Spadari, S., Maga, G., *Biochem. J.* **2004**, *383*, 475-482.
- [105] Shibutani, S., Takeshita, M., Grollman, A. P., *J. Biol. Chem.* **1997**, *272*, 13916-13922.

- [106] Dianov, G. L., Sleeth, K. M., Dianova, I. I., Allinson, S. L., *Mutat. Res.* **2003**, *531*, 157-163.
- [107] Friedberg Errol, C., *Nature* **2003**, *421*, 436-440.
- [108] Fleck, O., Nielsen, O., *J. Cell Sci.* **2004**, *117*, 515-517.
- [109] Schaerer, O. D., *Angew. Chem., Int. Ed. Engl.* **2003**, *42*, 2946-2974.
- [110] Hoeijmakers, J. H., *Nature* **2001**, *411*, 366-374.
- [111] Cappelli, E., Hazra, T., Hill, J. W., Slupphaug, G., Bogliolo, M., Frosina, G., *Carcinogenesis* **2001**, *22*, 387-393.
- [112] Peattie, D. A., *Proc. Natl. Acad. Sci. U. S. A.* **1979**, *76*, 1760-1764.
- [113] Waldmann, R., Gross, H. J., Krupp, G., *Nucleic Acids Res.* **1987**, *15*, 7209.
- [114] Thiebe, R., Zachau, H. G., *Eur. J. Biochem.* **1968**, *5*, 546-555.
- [115] Wintermeyer, W., Zachau, H. G., *FEBS Lett.* **1970**, *11*, 160-164.
- [116] Wintermeyer, W., Zachau, H. G., *FEBS Lett.* **1975**, *58*, 306-309.
- [117] Nishikawa, K., Adams, B. L., Hecht, S. M., *J. Am. Chem. Soc.* **1982**, *104*, 326-328.
- [118] Trzuppek, J. D., Sheppard, T. L., *Org. Lett.* **2005**, *7*, 1493-1496.
- [119] Stirpe, F., *Toxicon* **2004**, *44*, 371-383.
- [120] Stirpe, F., Battelli, M. G., *Cell. Mol. Life Sci.* **2006**, *63*, 1850-1866.
- [121] Peumans, W. J., Hao, Q., Van Damme, E. J. M., *FASEB J.* **2001**, *15*, 1493-1506.
- [122] Olsnes, S., *Toxicon* **2004**, *44*, 361-370.
- [123] Schramm, V. L., *Curr. Opin. Chem. Biol.* **1997**, *1*, 323-331.
- [124] Endo, Y., Mitsui, K., Motizuki, M., Tsurugi, K., *J. Biol. Chem.* **1987**, *262*, 5908-5912.
- [125] Endo, Y., Gluck, A., Wool, I. G., *J. Mol. Biol.* **1991**, *221*, 193-207.
- [126] Stirpe, F., Bailey, S., Miller, S. P., Bodley, J. W., *Nucleic Acids Res.* **1988**, *16*, 1349-1357.
- [127] Barbieri, L., Ferreras, J. M., Barraco, A., Ricci, P., Stirpe, F., *Biochem. J.* **1992**, *286*, 1-4.
- [128] Correll, C. C., Munishkin, A., Chan, Y.-L., Ren, Z., Wool, I. G., Steitz, T. A., *Proc. Natl. Acad. Sci. U. S. A.* **1998**, *95*, 13436-13441.
- [129] Beigelman, L., Karpeisky, A., Usman, N., *Bioorg. Med. Chem. Lett.* **1994**, *4*, 1715-1720.
- [130] *Glen Report* **2003**, *16*.
- [131] Ogasawara, T., Sawasaki, T., Morishita, R., Ozawa, A., Madin, K., Endo, Y., *EMBO J.* **1999**, *18*, 6522-6531.
- [132] Sawasaki, T., Morishita, R., Ozawa, A., Ogasawara, T., Madin, K., Endo, Y., *Nucleic Acids Symp. Ser.* **1999**, *42*, 257-258.
- [133] Ozawa, A., Sawasaki, T., Takai, K., Uchiumi, T., Hori, H., Endo, Y., *FEBS Lett.* **2003**, *555*, 455-458.
- [134] Yoon, J.-H., Lee, C.-S., O'Connor, T. R., Yasui, A., Pfeifer, G. P., *J. Mol. Biol.* **2000**, *299*, 681-693.

- [135] Ravanat, J.-L., Douki, T., Cadet, J., *J. Photochem. Photobiol., B* **2001**, *63*, 88-102.
- [136] Sinha, R. P., Hader, D.-P., *Photochem. Photobiol. Sci.* **2002**, *1*, 225-236.
- [137] Liu, F.-T., Yang, N. C., *Biochemistry* **1978**, *17*, 4865-4876.
- [138] Vink, A. A., Roza, L., *J. Photochem. Photobiol., B* **2001**, *65*, 101-104.
- [139] Durbeej, B., Eriksson, L. A., *J. Photochem. Photobiol., A* **2002**, *152*, 95-101.
- [140] Koning, T. M. G., Van Soest, J. J. G., Kaptein, R., *Eur. J. Biochem.* **1991**, *195*, 29-40.
- [141] Gibbs, P. E. M., Lawrence, C. W., *Nucleic Acids Res.* **1993**, *21*, 4059-4065.
- [142] Taylor, J.-S., *Mutat. Res.* **2002**, *510*, 55-70.
- [143] Glickman, B. W., Schaaper, R. M., Haseltine, W. A., Dunn, R. L., Brash, D. E., *Proc. Natl. Acad. Sci. U. S. A.* **1986**, *83*, 6945-6949.
- [144] Kundu, L. M., Linne, U., Marahiel, M., Carell, T., *Chem. Eur. J.* **2004**, *10*, 5697-5705.
- [145] Aas, P. A., Otterlei, M., Falnes, P. O., Vagbo, C. B., Skorpen, F., Akbari, M., Sundheim, O., Bjoras, M., Slupphaug, G., Seeberg, E., Krokan, H. E., *Nature* **2003**, *421*, 859-863.
- [146] Bellacosa, A., Moss, E. G., *Curr. Biol.* **2003**, *13*, R482-R484.
- [147] Bregeon, D., Sarasin, A., *Mutat. Res.* **2005**, *577*, 293-302.
- [148] Bochet, C. G., *J. Chem. Soc., Perkin Trans. 1* **2002**, 125-142.
- [149] Ohtsuka, E., Tanaka, S., Ikehara, M., *Nucleic Acids Res.* **1974**, *1*, 1351-1357.
- [150] Bartholomew, D. G., Broom, A. D., *J. Chem. Soc., Chem. Commun.* **1975**, 38.
- [151] Hayes, J. A., Brunden, M. J., Gilham, P. T., Gough, G. R., *Tetrahedron Lett.* **1985**, *26*, 2407-2410.
- [152] Walker, J. W., Reid, G. P., McCray, J. A., Trentham, D. R., *J. Am. Chem. Soc.* **1988**, *110*, 7170-7177.
- [153] Chaulk, S. G., MacMillan, A. M., *Nucleic Acids Res.* **1998**, *26*, 3173-3178.
- [154] Schwartz, M. E., Breaker, R. R., Asteriadis, G. T., deBear, J. S., Gough, G. R., *Bioorg. Med. Chem. Lett.* **1992**, *2*, 1019-1024.
- [155] Walker, J. W., McCray, J. A., Hess, G. P., *Biochemistry* **1986**, *25*, 1799-1805.
- [156] Corrie, J. E. T., Reid, G. P., Trentham, D. R., Hursthouse, M. B., Mazid, M. A., *J. Chem. Soc., Perkin Trans. 1* **1992**, 1015-1019.
- [157] Gerlach, H., Kappes, D., Boeckman, R. K., Jr., Maw, G. N., *Org. Synth.* **1993**, *71*, 48-55.
- [158] Vorbrueggen, H., Krolkiewicz, K., Bennua, B., *Chem. Ber.* **1981**, *114*, 1234-1255.
- [159] Vorbrueggen, H., Hoefle, G., *Chem. Ber.* **1981**, *114*, 1256-1268.
- [160] Weiss, P. A., *Glen Research Report* **1998**, *11*, 2-4.
- [161] Benneche, T., Gundersen, L. L., Undheim, K., *Acta Chem. Scand.* **1988**, *B42*, 384-389.
- [162] Benneche, T., Strande, P., Undheim, K., *Synthesis* **1983**, 762-763.

- [163] Pitsch, S., Weiss, P. A., Jenny, L., Stutz, A., Wu, X., *Helv. Chim. Acta* **2001**, *84*, 3773-3795.
- [164] Markiewicz, W. T., *J. Chem. Res., Synop.* **1979**, 24-25.
- [165] Zhang, N., Chen, H.-M., Koch, V., Schmitz, H., Liao, C.-L., Bretner, M., Bhadti, V. S., Fattom, A. I., Naso, R. B., Hosmane, R. S., Borowski, P., *J. Med. Chem.* **2003**, *46*, 4149-4164.
- [166] Robins, M. J., Robins, R. K., *J. Am. Chem. Soc.* **1965**, *87*, 4934-4940.
- [167] Beaucage, S. L., *Methods Mol. Biol.* **1993**, *20*, 33-61.
- [168] Mueller, S., Wolf, J., Ivanov, S. A., *Curr. Org. Synth.* **2004**, *1*, 293-307.
- [169] Blanc, A., Bochet, C. G., *J. Am. Chem. Soc.* **2004**, *126*, 7174-7175.
- [170] Il'ichev, Y. V., Schwoerer, M. A., Wirz, J., *J. Am. Chem. Soc.* **2004**, *126*, 4581-4595.
- [171] Gaplovsky, M., Il'ichev, Y. V., Kamdzhilov, Y., Kombarova, S. V., Mac, M., Schwoerer, M. A., Wirz, J., *Photochem. Photobiol. Sci.* **2005**, *4*, 33-42.
- [172] Pitsch, S., *Helv. Chim. Acta* **1997**, *80*, 2286-2314.
- [173] Anslyn, E., Breslow, R., *J. Am. Chem. Soc.* **1989**, *111*, 4473-4482.
- [174] Breslow, R., *Acc. Chem. Res.* **1991**, *24*, 317-324.
- [175] Breslow, R., *Proc. Natl. Acad. Sci. U. S. A.* **1993**, *90*, 1208-1211.
- [176] Hilal, S. H., Karickhoff, S. W., Carreira, L. A., *Quant. Struct.-Act. Relat.* **1995**, *14*, 348-355.
- [177] Stahlberg, A., Kubista, M., Pfaffl, M., *Clin. Chem.* **2004**, *50*, 1678-1680.
- [178] Zuker, M., *Nucleic Acids Res.* **2003**, *31*, 3406-3415.
- [179] Castro, H. C., Loureiro, N. I. V., Pujol-Luz, M., Souza, A. M. T., Albuquerque, M. G., Santos, D. O., Cabral, L. M., Frugulhetti, I. C., Rodrigues, C. R., *Curr. Med. Chem.* **2006**, *13*, 313-324.
- [180] Yu, H., Goodman, M. F., *J. Biol. Chem.* **1992**, *267*, 10888-10896.
- [181] Kati, W. M., Johnson, K. A., Jerva, L. F., Anderson, K. S., *J. Biol. Chem.* **1992**, *267*, 25988-25997.
- [182] Bebenek, K., Abbotts, J., Wilson, S. H., Kunkel, T. A., *J. Biol. Chem.* **1993**, *268*, 10324-10334.
- [183] Huang, H., Chopra, R., Verdine, G. L., Harrison, S. C., *Science* **1998**, *282*, 1669-1675.
- [184] Roberts, J. D., Preston, B. D., Johnston, L. A., Soni, A., Loeb, L. A., Kunkel, T. A., *Mol. Cell. Biol.* **1989**, *9*, 469-476.
- [185] Roth, M. J., Tanese, N., Goff, S. P., *J. Biol. Chem.* **1985**, *260*, 9326-9335.
- [186] Das, D., Georgiadis, M. M., *Structure (Cambridge, MA, U. S.)* **2004**, *12*, 819-829.
- [187] DeStefano, J. J., Mallaber, L. M., Fay, P. J., Bambara, R. A., *Nucleic Acids Res.* **1994**, *22*, 3793-3800.
- [188] DeStefano, J. J., Buiser, R. G., Mallaber, L. M., Myers, T. W., Bambara, R. A., Fay, P. J., *J. Biol. Chem.* **1991**, *266*, 7423-7431.
- [189] Dudding, L. R., Nkabinde, N. C., Mizrahi, V., *Biochemistry* **1991**, *30*, 10498-10506.

- [190] Fuentes, G. M., Fay, P. J., Bambara, R. A., *Nucleic Acids Res.* **1996**, *24*, 1719-1726.
- [191] Goodman, M. F., Cai, H., Bloom, L. B., Eritja, R., in *Ann. N. Y. Acad. Sci.*, Vol. 726, **1994**, pp. 132-143.
- [192] Withka, J. M., Wilde, J. A., Bolton, P. H., Mazumder, A., Gerlt, J. A., *Biochemistry* **1991**, *30*, 9931-9940.
- [193] Goljer, I., Withka, J. M., Kao, J. Y., Bolton, P. H., *Biochemistry* **1992**, *31*, 11614-11619.
- [194] Fouilloux, L., Berthet, N., Coulombeau, C., Coulombeau, C., Dheu-Andries, M. L., Garcia, J., Lhomme, J., Vattton, P., *J. Mol. Struct. (Theochem)* **1995**, *330*, 417-422.
- [195] Coppel, Y., Berthet, N., Coulombeau, C., Coulombeau, C., Garcia, J., Lhomme, J., *Biochemistry* **1997**, *36*, 4817-4830.
- [196] Wang, K. Y., Parker, S. A., Goljer, I., Bolton, P. H., *Biochemistry* **1997**, *36*, 11629-11639.
- [197] Gelfand, C. A., Plum, G. E., Grollman, A. P., Johnson, F., Breslauer, K. J., *Biochemistry* **1998**, *37*, 7321-7327.
- [198] Barsky, D., Foloppe, N., Ahmadi, S., Wilson, D. M., III, MacKerell, A. D., Jr., *Nucleic Acids Res.* **2000**, *28*, 2613-2626.
- [199] Sagi, J., Guliaev, A. B., Singer, B., *Biochemistry* **2001**, *40*, 3859-3868.
- [200] Moore, M. J., Sharp, P. A., *Science* **1992**, *256*, 992-997.
- [201] Spirin, A. S., Baranov, V. I., Ryabova, L. A., Ovodov, S. Y., Alakhov, Y. B., *Science* **1988**, *242*, 1162-1164.
- [202] Nakano, H., Yamane, T., *Biotechnol. Adv.* **1998**, *16*, 367-384.
- [203] Shimizu, Y., Inoue, A., Tomari, Y., Suzuki, T., Yokogawa, T., Nishikawa, K., Ueda, T., *Nat. Biotechnol.* **2001**, *19*, 751-755.
- [204] Katzen, F., Chang, G., Kudlicki, W., *Trends Biotechnol.* **2005**, *23*, 150-156.
- [205] Gottlieb, H. E., Kotlyar, V., Nudelman, A., *J. Org. Chem.* **1997**, *62*, 7512-7515.
- [206] Blumberg, D. D., *Methods Enzymol.* **1987**, *152*, 20-24.
- [207] Mabic, S., Kano, I., in *The R&D Notebook No. RD008*, Millipore Corporation, Bedford, USA, **2002**.
- [208] in *RNA Analysis Notebook*, Part# BR120 ed., Promega Corporation, Madison, USA, **2003**.
- [209] Miles, E. W., *Methods Enzymol.* **1977**, *47*, 431-442.
- [210] Melchior, W. B., Jr., Fahrney, D., *Biochemistry* **1970**, *9*, 251-258.
- [211] Schulhof, J. C., Molko, D., Teoule, R., *Nucleic Acids Res.* **1987**, *15*, 397-416.
- [212] Wu, T., Ogilvie, K. K., Pon, R. T., *Nucleic Acids Res.* **1989**, *17*, 3501-3517.
- [213] Wu, T., Ogilvie, K. K., *J. Org. Chem.* **1990**, *55*, 4717-4724.
- [214] Scaringe, S. A., Francklyn, C., Usman, N., *Nucleic Acids Res.* **1990**, *18*, 5433-5441.
- [215] in *Technical Bulletin RNA Deprotection*, Glen Research, Sterling, USA, **1999**.
- [216] in *Technical Bulletin TOM*, Glen Research, Sterling, USA, **1999**.

-
- [217] Maniatis, T., Efstratiadis, A., *Methods Enzymol.* **1980**, *65*, 299-305.
- [218] Sambrook, J., Fritsch, E. F., Maniatis, T., *Molecular Cloning: A Laboratory Manual, Vol. 1-3*, 2nd ed., Cold Spring Harbor Laboratory Press, **1989**.
- [219] Ogden, R. C., Adams, D. A., *Methods Enzymol.* **1987**, *152*, 61-87.
- [220] Smith, H. O., *Methods Enzymol.* **1980**, *65*, 371-380.
- [221] in *Protocols & References*, Schleicher & Schuell GmbH, Dassel, Germany, **2004**.

Appendix

The following articles were published during this work:

- Küpfer P. A., Leumann C. J., “RNA abasic sites: Preparation and trans-lesion synthesis by HIV-1 reverse transcriptase”, *ChemBioChem* **2005**, *6*, 1970-1973.
- Mosimann M., Küpfer P. A., Leumann C. J., “Synthesis and Incorporation into DNA of a Chemically Stable, Functional Abasic Site Analogue”, *Org. Lett.* **2005**, *7*, 5211-5214.
- Küpfer P. A. Leumann C. J., “The Chemical Stability of Abasic RNA Compared to Abasic DNA”, *Nucleic Acids Res.* **2007**, *35*, 58-68.

RNA Abasic Sites: Preparation and Trans-Lesion Synthesis by HIV-1 Reverse Transcriptase


Pascal A. Küpfer and Christian J. Leumann^{*[a]}

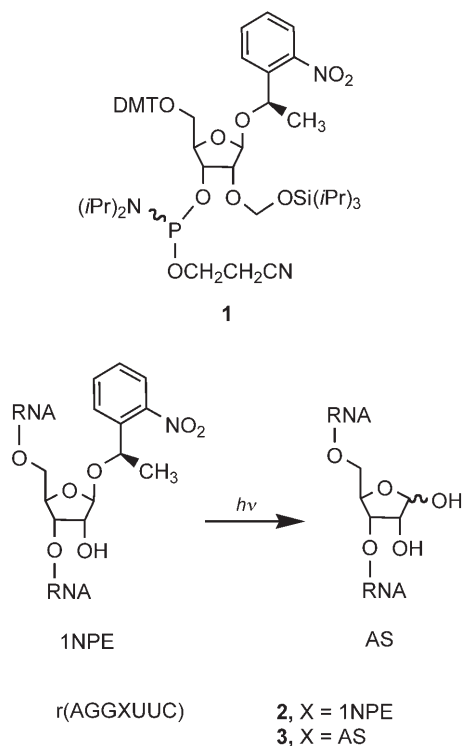
Abasic sites are well-known DNA lesions that occur spontaneously under acidic or oxidative stress, or as intermediates after enzymatic excision of damaged bases.^[1] Due to the missing genetic information such sites are highly mutagenic. Therefore, nature has developed a ubiquitous cellular DNA-repair machinery for genome housekeeping.^[2] However, cellular RNA lesions are less well known, and, with the exception of a few cases, their biological impact is unclear. For example, RNA abasic sites can occur as a result of the action of RNA *N*-ribohydrolases and can severely affect the vitality of a cell. A famous example of the occurrence of RNA abasic sites is when the peptide toxin, ricin, depurinates a specific adenosine residue on 28S rRNA, which is one of the RNA chains of eukaryotic ribosomes. This leads to poor binding of elongation factors and thus the abortion of protein synthesis. A single molecule of ricin is sufficient to kill a whole cell.^[3] Besides this, there is evidence for a new class of RNA-specific lyases in wheat germ that act on rRNA apurinic sites,^[4] and, very recently, a repair mechanism for alkylated RNA was found.^[5] However, data on the intrinsic chemical mechanism and kinetics of the decay of abasic RNA in comparison to abasic DNA are virtually nonexistent.^[6] This prompted us to study the chemistry and chemical biology of RNA abasic sites in vitro in more detail. Here we report preliminary results on the synthesis and translesion-polymerase activity of HIV-1 reverse transcriptase on a RNA template–DNA primer system with an abasic site in the template.

Our synthesis started with the RNA abasic site building block **1** (Scheme 1), the synthesis of which will be described in detail elsewhere. A very similar approach to obtaining abasic RNA was published independently recently;^[7] however, only the synthesis but no further biological data was described. Building block **1** contains the photocleavable *R*-1-(2-nitrophenyl)ethyl (1NPE) group at the anomeric center. This group was recently used in oligoribonucleotide synthesis as a 2'-*O* protecting group and has proven superior to the *O*-nitrobenzyl group during photolysis.^[8] 2'-*O*-[(Triisopropylsilyl)oxy]methyl (TOM) was chosen as a 2'-*O* protecting group.^[9]

To test the performance of this amidite building block in synthesis, we first prepared the RNA 7-mer **2**, which contains

[a] *Dipl.-Chem. P. A. Küpfer, Prof. C. J. Leumann
Department of Chemistry & Biochemistry, University of Bern
Freiestrasse 3, 3012 Bern (Switzerland)
Fax: (+41) 31-631-3422
E-mail: leumann@ioc.unibe.ch*

 Supporting information for this article is available on the WWW under <http://www.chembiochem.org> or from the author: ESI⁻ mass spectra of oligonucleotides **2** and **3**.



Scheme 1. Chemical structures of the RNA abasic site (AS), its building block (1), and the protected intermediate, 1NPE.

this unit in the center of the sequence. RNA synthesis was performed on a commercial DNA synthesizer by using standard protocols. 2'-O-*t*-Butyldimethylsilyloxy (TBDMS) phosphoramidites were used as regular RNA building blocks. The coupling time was set to 12 min for unit 1, and 5-(ethylthio)-1*H*-tetrazole was used as activator. According to the standard trityl assay, all steps in the synthesis proceeded with coupling yields of > 98%. Detachment from solid support was followed by base and phosphate deprotection with concentrated NH₃/EtOH (4:1) at 55 °C for 16 h. Subsequently, the silyl groups were removed with 1 M tetrabutylammonium fluoride (TBAF) in tetrahydrofuran (THF). RP-HPLC purification afforded the abasic RNA 7-mer precursor 2, the mass of which was confirmed by ESI-MS (see Supporting Information).

We then determined the kinetics of cleavage of the photolabile 1NPE group. An aqueous solution of 2 was irradiated with a UV lamp (see Experimental Section), and the amount of 1NPE cleavage as a function of time was quantified by HPLC (Figure 1). The half-life for 1NPE photolysis was determined to be 13 s. Deprotection was virtually quantitative after 1 min, as can be seen from the HPLC traces and as was found by ESI-MS data (> 99.8%). Interestingly, besides the molecular mass at m/z 2085.9, the MS of the deprotected abasic RNA 3 showed an additional peak with a mass difference of $\Delta m/z = +18$. This indicates that the aldehyde function at the abasic site might exist to a non-negligible extent in its hydrated form in solution. A thorough analysis of the chemical stability and kinetics of decay of abasic RNA in comparison to DNA is currently underway and will be published in due course.

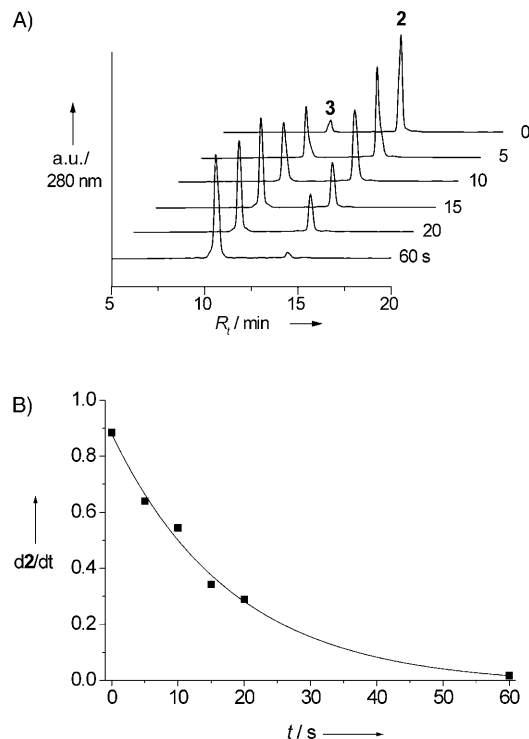


Figure 1. Time course of the photolytic-cleavage reaction of oligomer 2. A) HPLC traces (280 nm) after UV irradiation for the indicated time. B) Normalized fraction of residual starting material 2 fitted with a first order exponential decay.

RNA can also act as genetic material as, for example, is the case for retroviruses. In order to determine the potential mutagenicity of an RNA abasic site we studied its effect on reverse transcriptase. This enzyme is responsible for reverse transcription of a retroviral RNA single strand into a DNA single strand. Subsequent hydrolysis of the RNA in the hybrid duplex and synthesis of the complementary DNA strand result in a DNA duplex that contains the original RNA information. We chose HIV-1 reverse transcriptase as a model enzyme due to its well-characterized structural and biophysical properties.^[10] We synthesized a 31-mer RNA template–DNA primer system that contained the abasic-RNA site adjacent to the 3'-end of the DNA primer (Figure 2). In order to follow translesion synthesis, the primer was ³²P labeled at the 5' end by using T4-poly nucleotide kinase. The purified, 1NPE-protected RNA template was annealed to its DNA primer and subjected to UV irradiation for 2 min to reveal the abasic site. The protected 1NPE-containing template–primer duplex was used as a control. Both binary mixtures were then incubated with each of the four dNTPs and enzyme at two different concentrations. The reactions were quenched after 60 min at 37 °C and the products separated by PAGE and visualized on a Phosphorimager (Figure 2).

Inspection of the gel revealed that HIV-1 reverse transcriptase readily bypassed RNA abasic sites at concentrations as low as 0.5 units and yielded full-length products in the presence of all four dNTPs (Figure 2A). Elongation is not as efficient as in the case of an intact template strand (X=U). Experiments with single dNTPs show that dATP is preferentially inserted op-

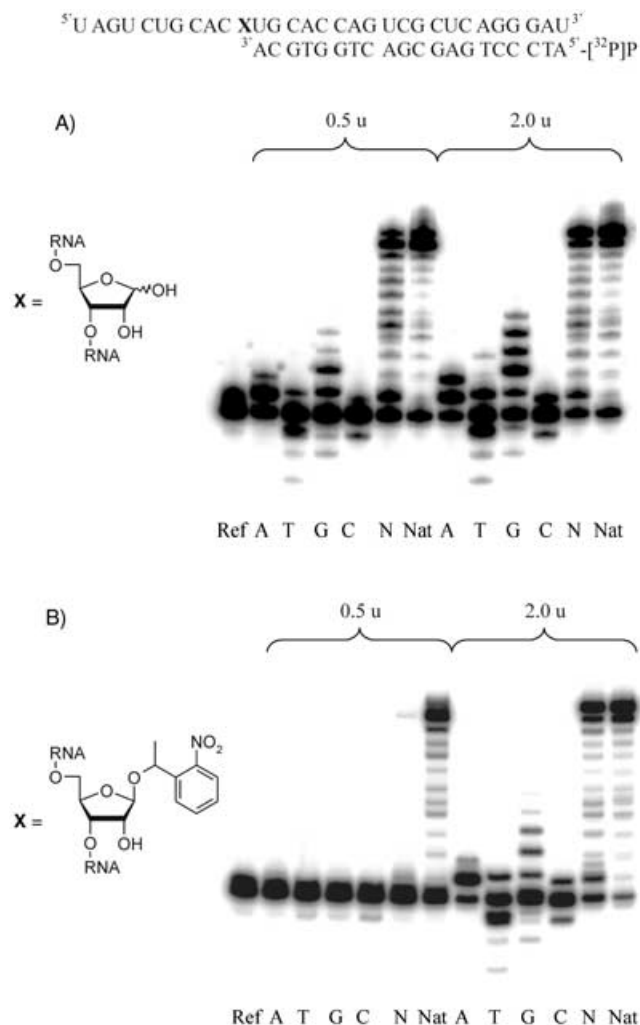


Figure 2. Denaturing PAGE gel (20%) of primer–template elongation products obtained with HIV-1 reverse transcriptase at 37 °C for 60 min. A) Abasic site template; B) 1NPE-protected template; enzyme concentrations 0.5 and 2.0 units. Ref: without enzyme and dNTPs. A, T, G, C: reactions in presence of the corresponding dNTPs; N: reactions in presence of all four dNTPs; Nat: unmodified template (X=U) and all four dNTPs.

posite the abasic lesion. Qualitatively, the dNTPs are incorporated in the order $A > G > T \approx C$. Some exonuclease activity is observed on the primer strand in the case of (slow) pyrimidine-nucleotide incorporation.

We also tested the template strand that contained the protected abasic residue (Figure 2B) for dNTP incorporation by HIV-1 reverse transcriptase. This experiment was performed so as to determine the difference between an abasic site and a noncoding, non-hydrogen bonding, stereochemically demanding base replacement. In contrast to the situation at the abasic site, essentially no dNTP incorporation was observed at low enzyme concentration. Incorporation and full-length extension were observed only at fourfold higher enzyme concentration. Again, dA was preferentially introduced opposite the bulky 1NPE group, while the other three dNTPs were incorporated at substantially slower rates.

We also checked for the RNase H activity of HIV-1 reverse transcriptase. For this, the abasic (X=AS) and unmodified (X=

U) template strands were ^{32}P 5'-end labeled and the primer was not labeled (Figure 3).

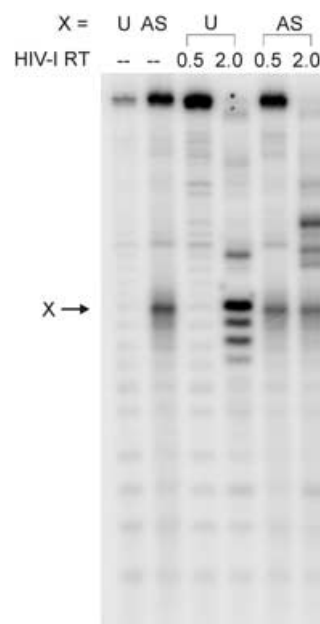


Figure 3. RNase H activity of HIV-1 reverse transcriptase on primer–template complexes that either contained the unmodified template (X=U) or the RNA abasic site (X=AS). Experimental conditions were the same as those used for primer-elongation experiments. HIV-1 reverse transcriptase (RT) concentrations are indicated.

Control experiments performed in the absence of HIV-1 reverse transcriptase (Figure 3, left 2 lanes) show that the RNA template is partially cleaved at the abasic site, presumably by β -elimination at the 3' terminus of the RNA. We assume, however, that most of this cleavage occurs under denaturation conditions (5 min, 90 °C) prior to application to the gel and not during incubation. We note that partial cleavage is not expected to interfere with primer extension as the RNA template is used in excess. At low enzyme concentration essentially no RNase H activity is observed. Increasing the enzyme concentration to 2 units results in complete disappearance of the full-length RNA template. Interestingly, there are differences in the RNA degradation pattern as a function of the presence or absence of the RNA abasic site. In the unmodified RNA template, cleavage occurs predominantly at the junction between the double-helical part and the RNA single strand. However, in the abasic template, cleavage is effected predominantly in the double helical primer–template region. This differential cleavage pattern is in accord with the enzyme predominantly cleaving in the unextended primer part due to slow elongation in the latter case.

We draw the following conclusions from these preliminary results: phosphoramidite **1** is a useful building block for the synthesis of abasic RNA. It is readily incorporated by conventional RNA solid-phase synthesis, and the 1NPE group is almost quantitatively cleaved after 1 min of irradiation with a UV immersion lamp. Furthermore, an RNA abasic site is readily by-

passed by HIV-1 reverse transcriptase. As in the case of DNA templates,^[11] a deoxyadenosine residue is preferentially introduced opposite the abasic site; this demonstrates that the "A rule"^[12] is also valid when the template is an abasic RNA strand. In addition, RNase H activity is not inhibited by the presence of an abasic site. Work towards a comprehensive kinetic characterization of reverse transcriptase action on abasic RNA templates is currently underway.

The study of the biological role of abasic RNA has so far been hampered by the lack of a reliable method for its synthesis. With this technique at hand it might now become possible to incorporate such lesions into larger, biologically relevant RNA molecules by, for example, splint ligation methods.^[13] The study of such constructs will be of interest, for instance, in the context of RNA viral evolution, rRNA function, mRNA translation, and of a possible existence of an RNA repair mechanism.

Experimental Section

Synthesis, deprotection, and purification of oligonucleotides: All oligonucleotides were prepared by automated oligonucleotide synthesis with an Expedite 8900 nucleic-acid synthesis system (PerSeptive Biosystems, Inc., Framingham, MA) by using the cyanoethylphosphoramidite approach. For RNA synthesis 2'-O-TBDMS protected PAC-phosphoramidites (GlenResearch) and polystyrene solid supports (Amersham Biotech) were used. For DNA synthesis benzoyl (dA, dC) and isobutyryl (dG) protected phosphoramidites and controlled pore-glass solid supports (GlenResearch) were used. The synthesis was performed by using the same standard coupling protocol for DNA and RNA with 5-(ethylthio)-1H-tetrazole (Aldrich) as activator and a coupling time of 90 s for DNA and 6 min for RNA. The modified phosphoramidite was allowed to couple for 12 min. Solid supports were treated with EtOH/NH₄OH (1:4) at 55 °C, overnight. RNA sequences were further deprotected by treatment with Bu₄NF (1 M in THF) for 6 h at RT. Oligonucleotides were desalted by using Sep-Pak[®] C₁₈ columns (Waters, Milford, MA) before application to HPLC.

The DNA primer for the primer-template extension reactions and the RNA heptamer were purified by using RP-HPLC on an ÄKTA 900 HPLC system (Amersham Pharmacia Biotech). A Brownlee Aquapore RP-300 (C₈, 7 µm, 250/4.6 mm) column (PerkinElmer) was used with a gradient of solvent A (0.1 M Et₃NOAc in H₂O, pH 7.0) and solvent B (0.1 M Et₃NOAc, CH₃CN/H₂O (4:1)). The 31-mer RNA templates were purified on a 20% preparative denaturing (7 M urea) polyacrylamide gel. The oligoribonucleotides were then electroeluted with an Elutrap[®] electroelution system (Schleicher & Schuell) according to the manufacturer's protocol and desalted by using Sep-Pak[®] C₁₈ columns. Purified oligonucleotides were dissolved in DEPC-treated water and the concentration was determined by using a NanoDrop[®] ND-100 UV/Vis spectrophotometer (NanoDrop Technologies, Inc., Wilmington, DE).

Kinetics of 1NPE deprotection: 1NPE-protected oligonucleotides were deprotected at RT by using a UV immersion lamp TQ 150 (UV-RS-2, Heraeus). Aliquots (0.4 mL) of a 1 OD₂₆₀ mL⁻¹ solution of 1NPE-protected RNA heptamer **2** were exposed to UV light for different time intervals in a quartz cuvette and immediately analyzed by RP-HPLC. The ratio of **2:3** was determined by peak integration. From the first order rate law for disappearance of **2** we calculated a deprotection extent of > 99.99% after irradiation for 2 min. Inte-

gration of ESI-MS peaks at the *m/z* of **2** and **3** confirmed this result and showed a deprotection extent of > 99% after 2 min.

HIV-1 reverse transcriptase assays: HIV-1 reverse transcriptase (Worthington Biochemical Corporation, Lakewood, NJ) was diluted in storage buffer (10 mM K₃PO₄, pH 7.4, 1 mM DTT, 20% glycerol). For the primer-extension experiments the DNA primer (30 pmol) was labeled by using T4-polynucleotide kinase (10 units, Fermentas) and [γ -³²P]ATP (Hartmann Analytik GmbH, Braunschweig, Germany) in T4 buffer (50 mM Tris-HCl pH 7.6, 10 mM MgCl₂, 5 mM DTT, 0.1 mM spermidine, 0.1 mM EDTA) for 30 min at 37 °C. T4-Polynucleotide kinase was then inactivated by heating to 90 °C for 2 min. For the RNase H assay the RNA templates (X=U or 1NPE) were 5'-end labeled as described above and used together with unlabeled DNA primer. The 1NPE-protected RNA template and DNA primer were annealed in a molar ratio of 2:1 in HIV-1 reverse transcriptase buffer. For the assays with abasic RNA this mixture was irradiated with a UV lamp for 2 min as described before. Final reaction mixtures contained RNA template (100 nM), DNA primer (50 nM), and dNTP (20 µM) in buffer (50 mM Tris pH 8.3, 50 mM NaCl, 8 mM MgCl₂, 1 mM DTT). After addition of the enzyme the mixtures were incubated for 60 min at 37 °C. The reactions were then quenched with loading buffer (98% formamide, 0.1% xylene cyanol (FF), 0.1% bromophenol blue), heated to 90 °C for 5 min and applied to a denaturing PAGE gel (20%). Radioactivity was detected and quantified on a Storm 820 Phosphorimager with ImageQuant software (Amersham Biosciences).

Acknowledgements

The authors wish to thank Dr. Caroline Crey-Desbiolles for valuable experimental advice on the primer-template elongation experiments. Financial support from the Swiss National Science Foundation (grant No.: 200020-107692) is gratefully acknowledged.

Keywords: abasic sites • bioorganic chemistry • nucleic acids • RNA damage • RNA

- [1] J. Lhomme, J. F. Constant, M. Demeunynck, *Biopolymers* **1999**, *52*, 65–83.
- [2] O. D. Schärer, *Angew. Chem.* **2003**, *115*, 3052–3082; *Angew. Chem. Int. Ed.* **2003**, *42*, 2946–2974.
- [3] V. L. Schramm, *Curr. Opin. Chem. Biol.* **1997**, *1*, 323–331.
- [4] T. Ogasawara, T. Sawasaki, R. Morishita, A. Ozawa, K. Madin, Y. Endo, *EMBO J.* **1999**, *18*, 6522–6531.
- [5] P. A. Aas, M. Otterlei, P. O. Falnes, C. B. Vagbo, F. Skorpen, M. Akbari, O. Sundheim, M. Bjoras, G. Slupphaug, E. Seeberg, H. E. Krokan, *Nature* **2003**, *421*, 859–863.
- [6] Y. Nishikawa, B. L. Adams, S. M. Hecht, *J. Am. Chem. Soc.* **1982**, *104*, 326–328.
- [7] J. D. Trzuppek, T. L. Sheppard, *Org. Lett.* **2005**, *7*, 1493–1496.
- [8] S. Pitsch, P. A. Weiss, X. Wu, D. Ackermann, T. Honegger, *Helv. Chim. Acta* **1999**, *82*, 1753–1761.
- [9] S. Pitsch, P. A. Weiss, L. Jenny, A. Stutz, X. Wu, *Helv. Chim. Acta* **2001**, *84*, 3773–3795.
- [10] L. Menendez-Arias, *Prog. Nucleic Acid Res. Mol. Biol.* **2002**, *71*, 91–147.
- [11] H. Cai, L. B. Bloom, R. Eritja, M. F. Goodman, *J. Biol. Chem.* **1993**, *268*, 23567–23572.
- [12] B. S. Strauss, *Bioessays* **1991**, *13*, 79–84.
- [13] M. J. Moore, P. A. Sharp, *Science* **1992**, *256*, 992–997.

Received: May 17, 2005

Synthesis and Incorporation into DNA of a Chemically Stable, Functional Abasic Site Analogue

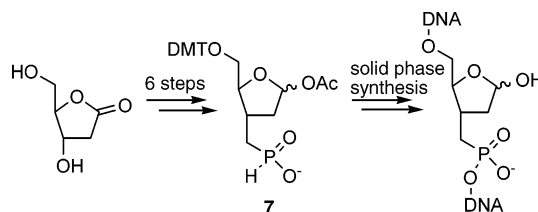
Markus Mosimann, Pascal A. K pfer, and Christian J. Leumann*

Department of Chemistry & Biochemistry, University of Bern, Freiestrasse 3,
CH-3012 Bern, Switzerland

leumann@ioc.unibe.ch

Received August 24, 2005

ABSTRACT



The abasic site building block 7 for DNA synthesis, containing a methylenephosphonic acid group at C3', was prepared in six steps and was incorporated into DNA via a combination of H-phosphonate and phosphoramidite chemistry. Corresponding oligodeoxynucleotides were shown to be chemically stable under basic conditions and fully functional at the respective hemiacetal center.

Abasic sites are DNA lesions that either occur spontaneously by hydrolysis of purine bases or enzymatically as intermediates in the base excision pathway of the DNA repair machinery.¹ Due to the missing coding information, such sites are highly mutagenic and are thus a threat to the integrity of the genome. Chemically, abasic sites contain a hemiacetal function at the anomeric center and are thus intrinsically unstable leading to DNA strand scission at the 3'- and 5'-site of the abasic unit via β - and δ -elimination (Figure 1).

Due to the low chemical stability, most of the investigations on the biological, biophysical, and structural impact of abasic sites in the past have been performed on analogues in which the hemiacetal function was reduced to a cyclic ether (THF analogue) or to open-chain analogues (propanediol analogues). Both of these variants are not optimal as the chemical characteristics of the hemiacetal function that crucially determine its reactivity and that may also influence its structural and biophysical properties is lost.

A conceptually simple way to preserve the hemiacetal function and to maintain chemical stability of the DNA

backbone exists in the conversion of the 3'-oxygen of an abasic site into a methylene unit, resulting in a phosphonate

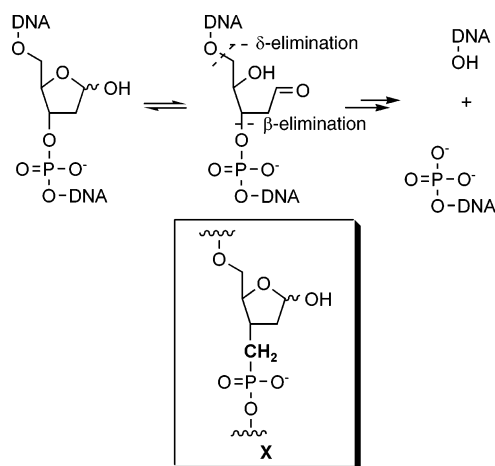


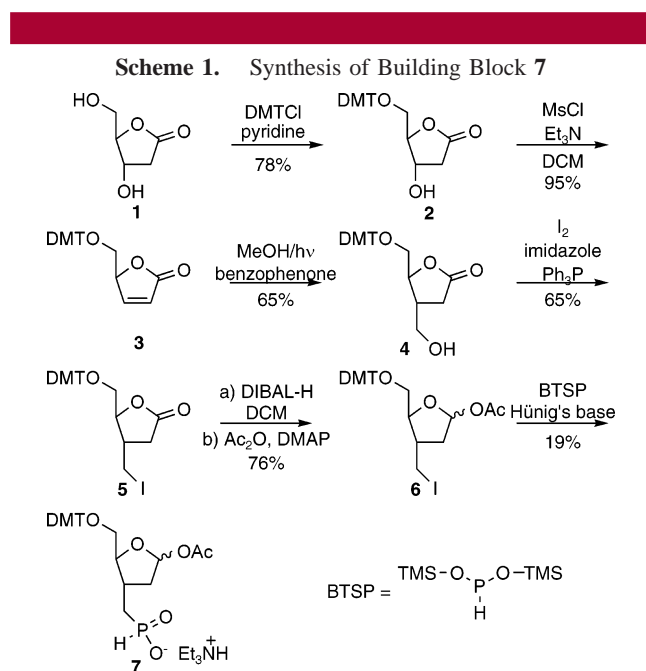
Figure 1. β , δ -Elimination pathways leading to DNA strand cleavage at abasic sites, as well as the chemical structure of the 3'-methylene analogue X.

(1) (a) Lhomme, J.; Constant, J. F.; Demeunynck, M. *Biopolymers* **1999**, 52, 65. (b) Sch rer, O. D. *Angew. Chem., Int. Ed.* **2003**, 42, 2946.

function that is isostructural and isoelectrostatic to a natural backbone phosphodiester function. This modification is expected to block the β -elimination reaction at abasic sites, thus inhibiting strand scission.

3'-Deoxy-3'-hydroxymethylene nucleosides and corresponding phosphonates were synthesized before. Their syntheses typically started from the natural nucleosides using different C-1 synthons.² DNA oligonucleotides containing phosphonate backbone linkages were also prepared before in the context of antisense research, and it was shown that they slightly enhance duplex stability,³ indicating that the mutation of a 3'-oxygen into a methylene group does not interfere with double helix formation.

Here, we report on the successful synthesis of oligodeoxynucleotides containing the 3'-methylene abasic site analogue **X** (Figure 1) and the characterization of its functional properties and its chemical stability.



We planned to use the H-phosphinate **7** (Scheme 1) as a building block for **X**, reasoning that it could be directly used in the automated synthesis of oligodeoxynucleotides and that it would be compatible with standard phosphoramidite chemistry. For the elaboration of the C–C bond between the methylene unit and the deoxyribose ring we intended to utilize the photoinduced radical conjugate addition of methanol, previously developed by Mann.⁴ As a protecting group for the anomeric center we chose an acetyl group which would liberate the hemiacetal function concomitantly

(2) (a) Sanghvi, Y. S.; Bharadwaj, R.; Debart, F.; De Mesmaeker, A. *Synthesis* **1994**, 1163. (b) Collingwood, S. P.; Douglas, M. E.; Natt, F.; Pieleś, U. *Phosphorus, Sulfur Silicon Relat. Elem.* **1999**, 144–146, 645.

(3) An, H.; Wang, T.; Dan Cook, P. *Tetrahedron Lett.* **2000**, 41, 7813. (d) Winqvist, A.; Strömberg, R. *Eur. J. Org. Chem.* **2001**, 4305.

(4) (a) Mann, J.; Weymouth-Wilson, A. *Synlett* **1992**, 67. (b) Gould, J. H. M.; Mann, J. *Nucleosides, Nucleotides* **1997**, 16, 193.

during deprotection and detachment from the solid support of the oligonucleotide. The synthesis of building block **7** is outlined in Scheme 1.

While the synthesis up to iodide **6** proceeded smoothly and in good yields, the following Arbusov reaction proved to be difficult. Reaction of **6** with in situ prepared bis-trimethylsilylphosphonite (BTSP) led to only ca. 20% of the desired building block **7** after aqueous workup, even after considerable efforts of optimization. A major side reaction observed was the (known) reduction by BTSP to the corresponding 3'-methyl derivative.⁵ Changing the leaving group to a tosylate inhibited the reduction pathway but surprisingly did not improve the yield. Attempts to use the more active triflate leaving group failed due to the instability of the corresponding compound. To test whether a TMS-based Lewis acid originating from the TMS phosphinate intermediate of **7** was responsible for the low yield, we also subjected lactone **5** to BTSP treatment. But again the corresponding Arbusov product could only be isolated in ca. 25% yield, indicating that Lewis acid-catalyzed elimination of the anomeric acetate group is not a significant side reaction responsible for the low yields of **7**. Despite the difficulties in the last synthetic step, **7** could be produced in sufficient quantities for the following synthetic and biophysical studies.

In a series of model experiments using 3'-*O*-TBDMS-protected thymidine and **7** we first tested a variety of carbodiimide-, uronium-, and phosphonium-based coupling reagents and were surprised to find that, contrary to the reported high coupling efficiencies in the ribo series, building block **7** reacted not at all under standard coupling conditions (30 min, rt, 20-fold molar excess). It thus seems that a missing electronegative substituent at the remote 2'-position decelerates the condensation reaction for a yet unknown reason. A way out was finally found by adding a nucleophilic catalyst to the coupling mixture as was recently reported for the synthesis of boranophosphates.⁶ We found that the combination of BOP-Cl and 3-nitro-1,2,4-triazole was perfectly suited for coupling the H-phosphinate intermediate (Figure 2), leading to complete conversion within 30 min. The related NEP-Cl was under these conditions less active and needed 24 h for complete conversion.

Having optimized the coupling conditions in solution, we next approached the solid-phase oligonucleotide synthesis. Within the amidite protocol, a separate coupling and oxidation step for **7** had to be accommodated. Coupling was effected with BOP-Cl and 3-nitro-1,2,4-triazole as activator while oxidation was performed using iodine (200 mM) under basic (1 M NEt₃) conditions for 5 min.⁷ The detailed protocol is described in the Supporting Information. With this protocol, we prepared the two oligonucleotides **8** and **9** (Table 1). Coupling efficiencies for the incorporation of **7** as determined from the trityl assay were typically >95%. Oligonucleotides were detached from solid support and deprotected under standard conditions (NH₃ concd, 55 °C,

(5) Winqvist, A.; Strömberg, R. *Eur. J. Org. Chem.* **2002**, 1509.

(6) Shimizu, M.; Wada, T.; Oka, N.; Saigo, K. *J. Org. Chem.* **2004**, 69, 5261.

(7) Winqvist, A.; Strömberg, R. *Eur. J. Org. Chem.* **2002**, 3140.

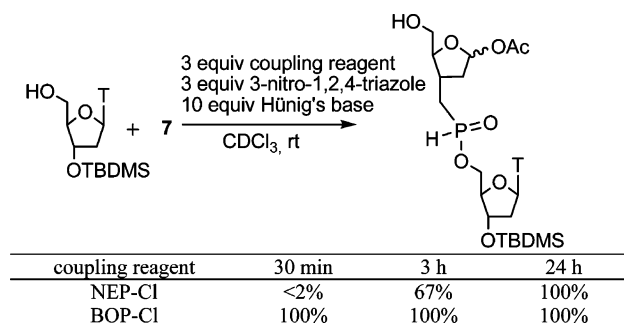


Figure 2. Coupling yields for H-phosphinate **7** as judged from integration of ^{31}P NMR peaks after the indicated reaction time. NEP-Cl = 2-chloro-5,5'-dimethyl-1,3,2-dioxaphosphorinane-2-oxide; BOP-Cl = bis(2-oxo-3-oxazolidinyl)phosphinic chloride.

16 h) and purified by standard RP-HPLC. Isolated yields after purification were in the range of 20–30%, and ESI-mass spectrometric analysis confirmed the expected masses (Table 1). From these results we conclude that the condensation chemistry for the introduction of **7** is orthogonal to the phosphoramidite chemistry of oligonucleotide synthesis despite the fact that there is no protecting group on the newly formed phosphonate function.

For comparison, we also prepared oligonucleotides **10** and **11** having a natural protected or unprotected abasic site **Y** from a phosphoramidite building block containing a photocleavable *S*-1-(2-nitrophenyl)ethyl (1NPE) group at the anomeric center.

The next task was to prove the presence of the hemiacetal function in oligonucleotides. For this we recorded a ^1H NMR spectrum of **8**, of which the aromatic and anomeric proton section is depicted in Figure 3.

Table 1. Sequence and Analytical Data of Oligonucleotides Containing the Abasic Site Analogue **X** or the Natural Abasic Site **Y**

sequence	ESI ⁻ -MS calcd	ESI ⁻ -MS found	yield ^a	
			OD ²⁶⁰	%
8 d(TTTXTTT)	1957.3	1956.7	17.3	27.0
9 d(GTACXATCG)	2603.7	2602.9	23.9	23.1
10 d(GTACY ^p ATCG)	2754.9	2754.1	27.8	26.8
11 d(GTACYATCG)				

^a All oligonucleotides were synthesized on a 1.3 μmol scale. Yields are calculated after RP-HPLC purification.

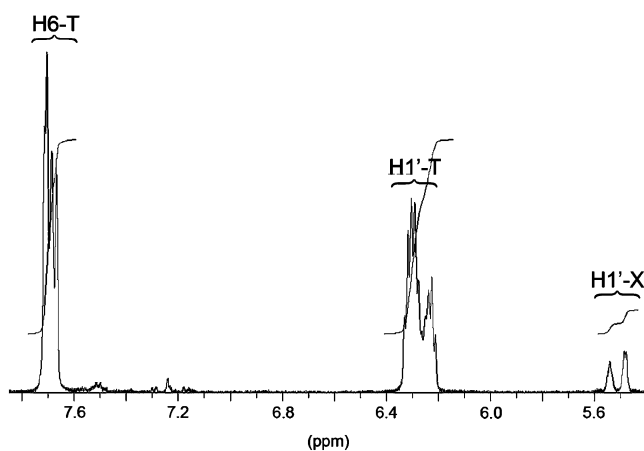


Figure 3. Section of the ^1H NMR spectrum of **8** (D_2O , ≈ 0.65 mM, 500 MHz).

Besides the typical resonances of the aromatic H6 and the anomeric H1' of the thymidine residues there appear two signals at around 5.5 ppm that can be assigned to the H1' of the two anomeric forms of the corresponding abasic unit **X**. No signal at around 10 ppm could be detected ruling out a significant contribution of the aldehyde form to the equilibrium mixture.

To prove the functionality of the abasic site, we incubated oligonucleotide **8** with varying amounts of dansylhydrazine (DNSH), a reagent typically used for labeling aldehydes and ketones,⁸ and analyzed the progress of hydrazone formation by polyacrylamide gel electrophoresis (PAGE). As can be seen from Figure 4, a new (fluorescent) band with lower

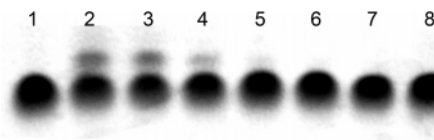


Figure 4. UV shadow of a denaturing 20% PAGE of mixtures of **8** with varying amounts of dansylhydrazine (DNSH). Each lane contains 0.4 OD²⁶⁰ (13.2 μg , 6.75 nmol) of **8**. Lane 1: control without DNSH. Lanes 2–8: 10, 5, 2, 1, 0.5, 0.25, 0.1 equiv of DNSH.

mobility than the parent oligonucleotide **8** occurred at high DNSH excess in a concentration dependent manner. This band is ascribed to the hydrazone of oligonucleotide **8** and fully proves the functionality of the abasic site analogue **X**.

Last but not least, we determined the base stability of the abasic site analogue **X**. For this oligonucleotide **9** and for comparison also **10** and **11**, containing a protected and unprotected natural abasic site were radiolabeled at their 5'-end with T4 polynucleotide kinase and $[\gamma\text{-}^{32}\text{P}]\text{ATP}$. Oligo-

(8) Yan, B.; Li, W. *J. Org. Chem.* **1997**, *62*, 9354.

nucleotides were then incubated in 0.2 M NaOH at 65 °C for 30 min and the reaction products analyzed by PAGE.

As can be seen from Figure 5, no degradation of

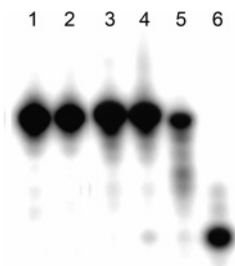


Figure 5. Denaturing 20% PAGE of radiolabeled **9** and control oligonucleotides **10** and **11**. Lanes 1, 3, and 5: oligonucleotides **9**, **10**, and **11**, without base treatment. Lane 2, 4, and 6: oligonucleotides **9**, **10**, and **11** after treatment with 0.2 M NaOH at 65 °C for 30 min.

oligonucleotide **9**, containing the abasic site analogue **X**, was observed under these conditions, while oligonucleotide **11**, having a natural abasic site, underwent complete β - and δ -elimination leading to a shorter labeled fragment with higher mobility. This experiment clearly demonstrates the stability of **X** toward basic conditions.

In conclusion, we have shown that phosphinate **7** is a useful building block for the abasic site analogue **X**. The underlying coupling and oxidation chemistry was found to be orthogonal to the phosphoramidite chemistry despite the missing protecting group at the phosphonate function. Further

improvement in the synthesis of **7** has to be achieved in future work in order to make the use of this building block more practical.

We also showed that **X**-containing oligonucleotides can be deprotected via standard methods and that **X** occurs in aqueous solution as expected predominantly in the two hemiacetal forms. A hydrazine dye labeling test and NaOH treatment clearly demonstrated the functionality and the base stability of oligonucleotides containing **X**. Thus, this phosphonate unit constitutes the first chemically stable and functional abasic site analogue.

Potential applications of this unit can be envisaged in experiments directed to determine the effect of the hemiacetal function on duplex structure and stability as well as on DNA polymerase dependent template primer extension reactions. Furthermore, this unit could be of interest in the context of reactivity based screening or inhibition of enzymes involved in the DNA base excision repair pathway.

Acknowledgment. This work was supported by the Swiss National Science Foundation (Grant No. 200020-107692) and by the University of Bern.

Supporting Information Available: Procedures and analytical data for the synthesis of compounds **2–7** as well as oligonucleotides **8** and **9**. Detailed procedures for the experiments summarized in Figures 4 and 5 as well as ^1H and ^{13}C NMR spectra for compounds **2–7**. This material is available free of charge via the Internet at <http://pubs.acs.org>.

OL052045G

The chemical stability of abasic RNA compared to abasic DNA

Pascal A. Küpfer and Christian J. Leumann*

Department of Chemistry and Biochemistry, University of Bern, Freiestrasse 3, CH-3012 Bern, Switzerland

Received September 11, 2006; Revised and Accepted October 20, 2006

ABSTRACT

We describe the synthesis of an abasic RNA phosphoramidite carrying a photocleavable 1-(2-nitrophenyl)ethyl (NPE) group at the anomeric center and a triisopropylsilyloxymethyl (TOM) group as 2'-O-protecting group together with the analogous DNA and the 2'-OMe RNA abasic building blocks. These units were incorporated into RNA-, 2'-OMe-RNA- and DNA for the purpose of studying their chemical stabilities towards backbone cleavage in a comparative way. Stability measurements were performed under basic conditions (0.1 M NaOH) and in the presence of aniline (pH 4.6) at 37°C. The kinetics and mechanisms of strand cleavage were followed by High pressure liquid chromatography and ESI-MS. Under basic conditions, strand cleavage at abasic RNA sites can occur via β,δ -elimination and 2',3'-cyclophosphate formation. We found that β,δ -elimination was 154-fold slower compared to the same mechanism in abasic DNA. Overall strand cleavage of abasic RNA (including cyclophosphate formation) was still 16.8 times slower compared to abasic DNA. In the presence of aniline at pH 4.6, where only β,δ -elimination contributes to strand cleavage, a 15-fold reduced cleavage rate at the RNA abasic site was observed. Thus abasic RNA is significantly more stable than abasic DNA. The higher stability of abasic RNA is discussed in the context of its potential biological role.

INTRODUCTION

Abasic sites are well known DNA lesions that occur spontaneously via depurination at a frequency of $\sim 10\,000$ per genome per day in mammalian cells (1). Acidic or alkylating conditions as well as oxidative stress greatly enhance this number. Abasic DNA is unstable and undergoes strand cleavage 3' to the abasic site with an average lifetime of 8 days at 37°C, pH 7.4 and physiological ionic strength (2). Due to the degradation of the genetic material and to missing coding

information such sites are highly mutagenic and a major threat to living cells (3,4). Living organisms have therefore evolved a highly efficient and complex DNA repair machinery that maintains genome integrity (5). One component of this machinery is the base excision repair pathway in which abasic sites are produced as intermediates by DNA glycosylases and cleaved either by AP-endonucleases or by AP-lyases. It is only recently that cellular repair processes were also found in RNA. For example, the human oxidative demethylase hABH3 that reverse alkylation of bases in DNA were found to repair also RNA (6). When expressed in *Escherichia coli* they were found to reactivate methylated RNA bacteriophage MS2 *in vivo*. This illustrates the biological relevance of such a repair activity and points towards RNA repair being a potentially important defense mechanism in living cells.

Spontaneous or induced abasic lesions are *a priori* not restricted to DNA but can also occur in RNA. Given the fact that not only short lived mRNA but long-lived tRNAs and ribosomal RNAs are present at all times in a cell in much higher concentrations than DNA, and given also the fact that RNA viruses as well as retroviruses store their genetic information in form of RNA, it is not excluded that abasic RNA plays a significant biological role. Literature about the chemistry and chemical biology of RNA abasic sites is, however, scarce and their biological impact is largely unexplored with a few exceptions. For example, RNA abasic sites are known to be the result of the action of RNA N-ribohydrolases (7). A famous example is the peptide toxin ricin which depurinates a specific adenosine residue on 28S rRNA, one of the RNA chains of eukaryotic ribosomes. This leads to poor binding of elongation factors and knockout of protein synthesis. A single molecule of ricin suffices to kill a whole cell. Besides this there is evidence for a class of RNA specific lyases that act on rRNA abasic sites, leading to complete inactivation of ribosomes (8,9).

Data on the mechanism and kinetics of strand scission of abasic RNA in comparison to abasic DNA is virtually inexistent. *In vitro* generation and cleavage of abasic RNA has been of some interest in the context of RNA sequencing via base alkylation and depurination followed by strand scission induced by aniline under neutral to slightly acidic conditions. It is believed that under these conditions only β -elimination of the phosphate unit on the 3'-side occurs,

*To whom correspondence should be addressed. Tel: +41 31 631 4355; Fax: +41 31 631 3422; Email: leumann@ioc.unibe.ch

leaving behind a 5'-oligonucleotide with a pendent 4,5-dihydroxy-2-oxovaleraldehyde moiety. In another example similar chemistry was used to excise one specific abasic nucleotide out of yeast tRNA^{Phe}. Here the intrinsic lability of the glycosidic bond of wybutosine was used to selectively produce one abasic site, followed by treatment with 2-aminopyridine to effect β,δ -elimination, leaving behind 3' and 5'-phosphorylated ends that were religated in three consecutive enzymatic steps (10).

Given the lack of knowledge on the chemistry and chemical biology of RNA abasic sites we set out to investigate this in more detail. More precisely we synthesized an abasic RNA precursor phosphoramidite that carries a photocleavable protecting group at the anomeric center (11). This unit can be introduced into oligoribonucleotides via automated RNA synthesis and the abasic site can be revealed after detachment from solid support and high pressure liquid chromatography (HPLC) purification by photolysis. In preliminary work we reported on the *trans*-lesion synthesis of HIV-1 reverse transcriptase on a RNA-template/DNA-primer system with an abasic site in the RNA template, and on the degradation of the damaged template by the RNase H activity of the polymerase in comparison to a non-damaged template (12). We found efficient incorporation of deoxynucleotides opposite the lesion following the 'A-rule', previously described for DNA-templated *trans*-lesion synthesis (13). Here we present now a detailed analysis of the kinetics and mechanisms of strand cleavage of RNA abasic sites at various conditions in comparison to abasic DNA.

MATERIALS AND METHODS

Synthesis, deprotection and purification of oligonucleotides

Full experimental details on the synthesis of the RNA and DNA abasic site phosphoramidites **1–3** (Scheme 1) containing the photocleavable 1-(2-methyl)nitrophenethyl (NPE) group is given in the supplementary data section. All oligonucleotides were prepared by automated oligonucleotide synthesis with an Expedite 8909 nucleic-acid synthesis system (PerSeptive Biosystems Inc., Framingham, MA) by using the cyanoethyl-phosphoramidite approach. RNA synthesis was performed with 2'-*O*-TBDMS protected PAC-phosphoramidites (Glen Research Corp., Sterling, VA) on polystyrene solid supports (Amersham Biotech). 2'-OMe-RNA oligoribonucleotides were prepared with benzoyl (A, C) and dimethylformamidino (G) protected 2'-OMe RNA phosphoramidites (Glen Research Corp., Sterling, VA). All 2'-OMe-RNA sequences were synthesized on normal RNA solid supports thus leading to oligonucleotides with an unmodified 3'-terminus. For DNA synthesis benzoyl (dA, dC) and isobutyryl (dG) protected phosphoramidites and controlled pore-glass solid supports (Glen Research Corp., Sterling, VA) were used. The syntheses were performed using the standard coupling protocols for DNA and RNA synthesis, with 5-(ethylthio)-1*H*-tetrazole (Aldrich) as activator and a coupling time of 90 s for DNA and 6 min for RNA and 2'OMe-RNA building blocks. The modified phosphoramidites **1–3** were allowed to couple for 6 min and 12 min for DNA and RNA, respectively. Solid supports were treated with EtOH/NH₄OH (1:4) at 55°C,

overnight. The DNA and RNA heptamers were purified by using RP-HPLC on an ÄKTA 900 HPLC system (Amersham Pharmacia Biotech). A SOURCE™ 15RPC ST 4.6/100 (polystyrene/divinyl benzene, 15 μ m, 100/4.6 mm) column (Amersham Biosciences, Uppsala, Sweden) was used with a linear gradient of solvent A (0.1 M Et₃NOAc in H₂O) and solvent B [0.1 M Et₃NOAc, CH₃CN/H₂O (4:1)]. RNA sequences were further silyl deprotected by treatment with Bu₄NF (1 M in THF) for 16 h at RT. Deprotected oligoribonucleotides were desalted by using Sep-Pak® C₁₈ columns (Waters Corp., Milford, MA) before purification by RP-HPLC. Purified oligonucleotides were dissolved in DEPC-treated water and the concentrations of these stock solutions (O.D. 260 nm) were determined with a NanoDrop® ND-100 UV/Vis spectrophotometer (NanoDrop Technologies, Wilmington, DE). All abasic oligonucleotides as well as their NPE-protected precursors were analyzed by ESI-MS.

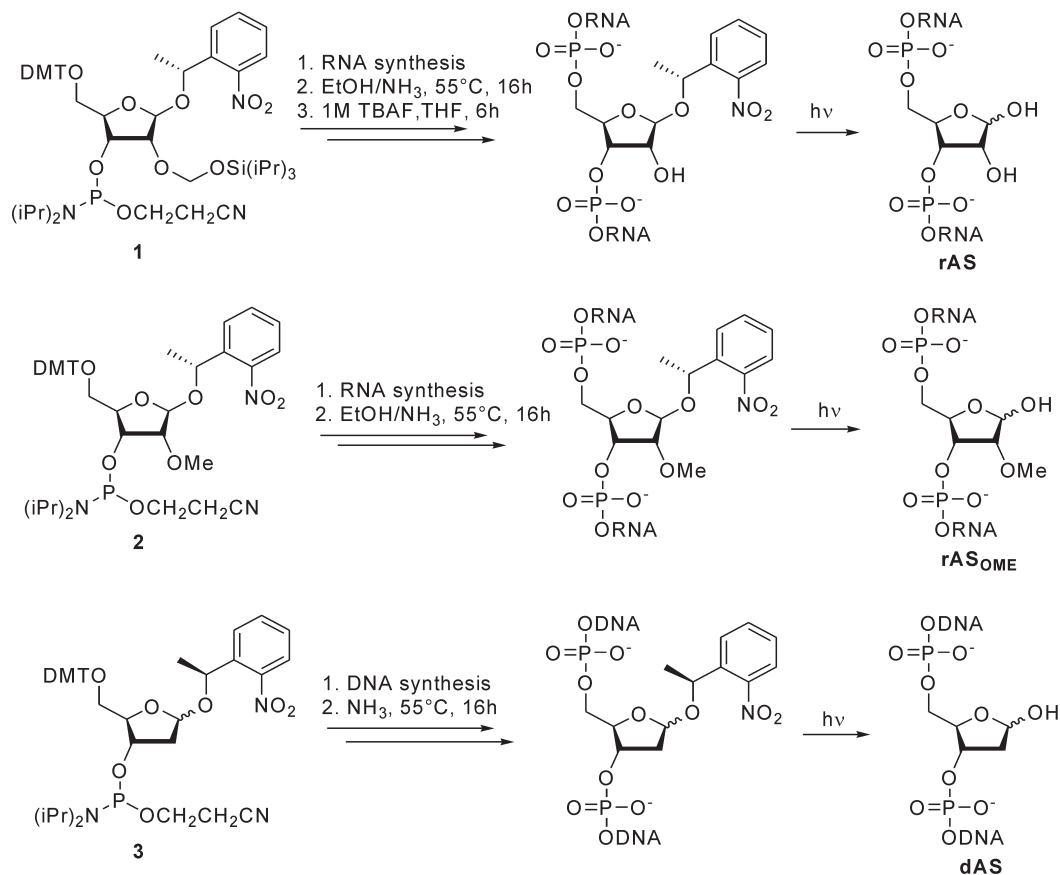
Strand cleavage kinetics

Sample preparation. Aliquots (0.3 or 0.4 ml of a 1 OD₂₆₀ ml⁻¹ solution) of NPE-protected RNA heptamers in H₂O in a quartz cuvette were deprotected at room temperature by using a UV immersion lamp TQ 150 (UV-RS-2, Heraeus) for 2 min. Alternatively, deprotection was achieved using a slide projector with a 250 W tungsten halogen lamp for 6 min. For both methods a conventional glass plate was used as a filter to remove light with wavelengths <300 nm to avoid damage to the oligonucleotides.

Alkaline strand cleavage. Deprotected oligonucleotides were treated with 1 M NaOH to a final concentration of 0.1 M NaOH and incubated at 37°C. Samples were quenched with a stoichiometric amount of 1 M HCl and the reaction mixtures were immediately analyzed by RP-HPLC. The ratio of the remaining abasic heptamer to reaction products was determined by peak integration. The resulting values were fitted with a first order exponential decay using OriginPro 7.5 software (OriginLab Corp., Northampton, MA). Resulting half-life times $T_{1/2}$ were calculated from the fitted curves that were corrected, where necessary, for the observed amount of products already present at $t = 0$. Alternatively, the $\ln([\text{oligo}]/[\text{oligo}]_0)$ was plotted against the time t . In all cases a linear relationship was observed, indicating first order kinetics. The first order rate constants for strand scission k_s (s⁻¹) were obtained from the slopes of the respective linear fits.

Strand cleavage in the presence of aniline at pH 4.6. Deprotected oligonucleotides were diluted to a final concentration of 1 OD₂₆₀ ml⁻¹ in 0.5 M aniline-HCl, pH 4.6 (0.4 ml). The aliquots are incubated at 37°C for different time intervals. To quench the reactions, aniline was removed by quick DEAE HPLC (Nucleogen® 60-7 125/4 mm column, Macherey-Nagel) with the following gradient: 0% solvent A (0.25 mM Na₂HPO₄ + 0.25 mM NaH₂PO₄ in 20% acetonitrile) for 10 min, 100% solvent B (A + 1 M NaCl) for 5 min. The oligonucleotides eluted with solvent B are collected and carefully concentrated (Speedvac) to a volume of ~0.4 ml and further analyzed by RP-HPLC as described above.

Fragment identification. Cleavage products of three independent cleavage reactions each were separated by RP-HPLC as described, pooled, lyophilized and analyzed by ESI mass



oligonucleotide	+NPE ^a		-NPE ^b	
	a		b	
	m/z calc.	m/z found	m/z calc.	m/z found
4 r(AGG-rAS-UUC)	2235.4	2236.4	2086.3	2086.3
5 r(A _{OMe} G _{OMe} G _{OMe} -rAS _{OME} -U _{OMe} U _{OMe} C)	2320.6	2320.1	2171.5	2171.0
6 r(A _{OME} G _{OME} G _{OME} -rAS-U _{OME} U _{OME} C)	2306.6	2306.6	2157.4	2157.5
7 d(AGG-dAS-TTC)	2151.5	2151.9	2002.3	2002.9

a) Oligonucleotides before NPE deprotection, b) Oligonucleotides after NPE deprotection

Scheme 1. Synthesis and sequences of rAS-, rAS_{OME}- and dAS-containing oligonucleotide heptamers.

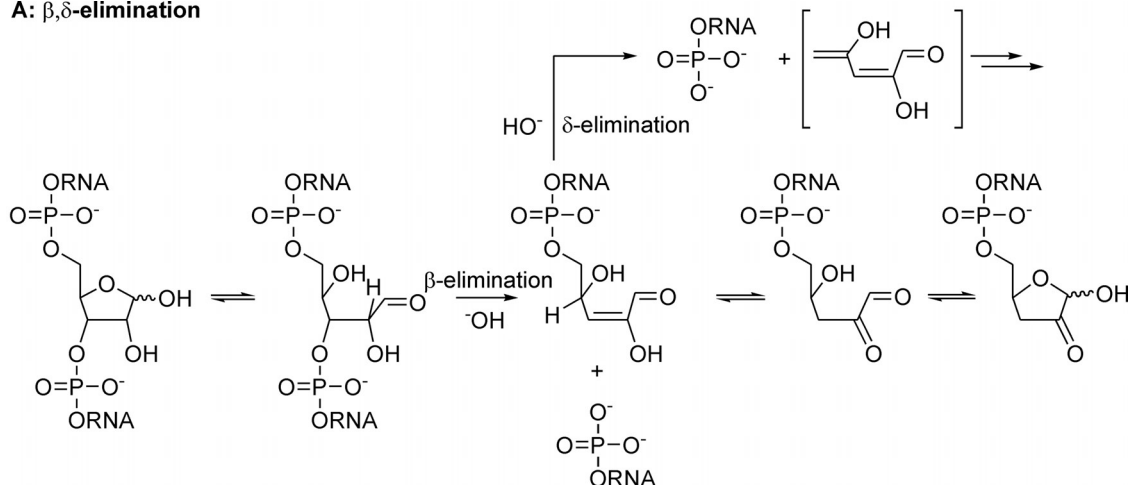
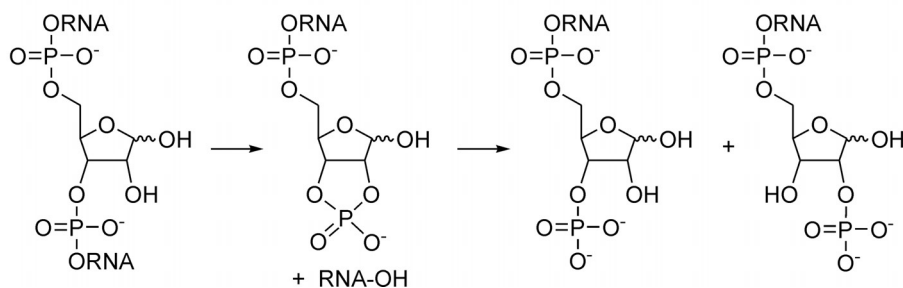
spectrometry. In the case of oligonucleotide **4b** the pooled fragments after aniline removal were desalted over Sep-Pak[®] C₁₈ columns (Waters Corp., Milford, MA) and measured directly by ESI-MS without RP-HPLC separation.

RESULTS

Synthesis of abasic building blocks and oligonucleotides

The synthesis of the RNA and DNA abasic site phosphoramidites **1–3** (Scheme 1) containing the photocleavable 1-(2-nitrophenyl)ethyl (NPE) group, which was used successfully before in oligonucleotide synthesis as protecting group for the 2'-OH function of ribonucleosides (14) or for caging

RNA and DNA bases (15–17), is described in the supplementary data section. Their synthesis is straight forward and resulted in overall yields of 21% for the rAS and 32% for the rAS_{OME} phosphoramidite starting from tetraacetyl ribose, as well as 44% for the dAS building block starting from 1,3,5-tri-*O*-acetyl-2'-deoxy-D-ribose. Both configurations at the chiral center of the NPE protecting group were used for reasons of synthetic economy and in both cases photolytic removal was quantitative (see Supplementary Data). These building blocks were stable for more than 1 year when kept in the dark at -20°C. Direct contact to sunlight was avoided but otherwise no special light protection was used during synthesis or manipulation of these abasic site precursors. The synthesis of oligonucleotides was performed

A: β,δ -elimination**B: cyclophosphate formation**

Scheme 2. (A and B) Mechanisms of strand cleavage of abasic RNA at high pH.

by standard phosphoramidite chemistry (Scheme 1) and resulted in coupling yields for building blocks **1–3** that are in the same range as for natural nucleoside phosphoramidites (>95%). Typically, oligoribonucleotides were HPLC purified before silyl deprotection. We found that this lead to purer oligonucleotide samples after desilylation.

In a first step we determined the deprotection kinetics of the NPE group in the ribonucleotide **4a** at a concentration of $1 \text{ OD}_{260} \text{ ml}^{-1}$ with glass-filtered light from a UV immersion lamp and followed the progress of deprotection by RP-HPLC at different time intervals. The HPLC traces (see Supplementary Data) showed clean conversion to the AS-containing oligonucleotide **4b** following first order kinetics. The half-life time was calculated to be 12.5 s. Traces of **4b** (<5%) resulting from deprotection during manipulations could already be seen at the beginning. An irradiation time of 2 min was found to be sufficient to achieve almost quantitative deprotection. In an alternative setup we used a slide projector with a halogen lamp for irradiation. Due to its lenses, UV light <365 nm was filtered out. Irradiation times of 6–10 min were found sufficient to promote full NPE-cleavage. This latter method is very mild and was generally preferred in further experiments.

We applied the same NPE-deprotection protocols also to the dAS precursor **7a**. Again we found first order kinetics for NPE deprotection to **7b** with a half-life time of 3.4 s. Long time (~15 min) UV irradiation with the UV lamp lead to a side product that was not identified but that was

clearly not the result of strand cleavage. Most likely it is a product resulting from T-T cyclobutane formation. Again irradiation with the slide projector for 5 min effected complete revelation of the abasic site without producing traces of this side product and was therefore considered superior.

Mechanisms of RNA abasic site cleavage

The presence of the 2'-OH group at an RNA- compared to a DNA abasic site substantially influences the mechanism of cleavage at high pH. The structurally and kinetically relevant intermediates for hydroxide induced strand scission are depicted in Scheme 2. As in the case of DNA, β -elimination of the oligonucleotide fragment 3' to the abasic site can occur from the aldehyde form yielding a 5'-phosphorylated 3'-fragment and an enol intermediate which after enol-ketone tautomerization leads to a 4,5-dihydroxy-2-oxovaleraldehyde unit attached to the 5'-fragment of the original RNA (Scheme 2A). Alternatively, the enol form is suited to a further δ -elimination step leading to complete excision of the abasic ribose unit and leaving behind a 3'-phosphorylated 5' end. Besides this an alternative mechanism via cyclophosphate formation (Scheme 2B) does also apply under basic conditions producing a 5'-fragment with an abasic site that is phosphorylated in the 2' or 3' position and a 3'-fragment with a 5'-OH end. Cyclophosphate formation must not only occur in the hemiacetal form but can also happen in the aldehyde form of the abasic site (not shown in Scheme 2B).

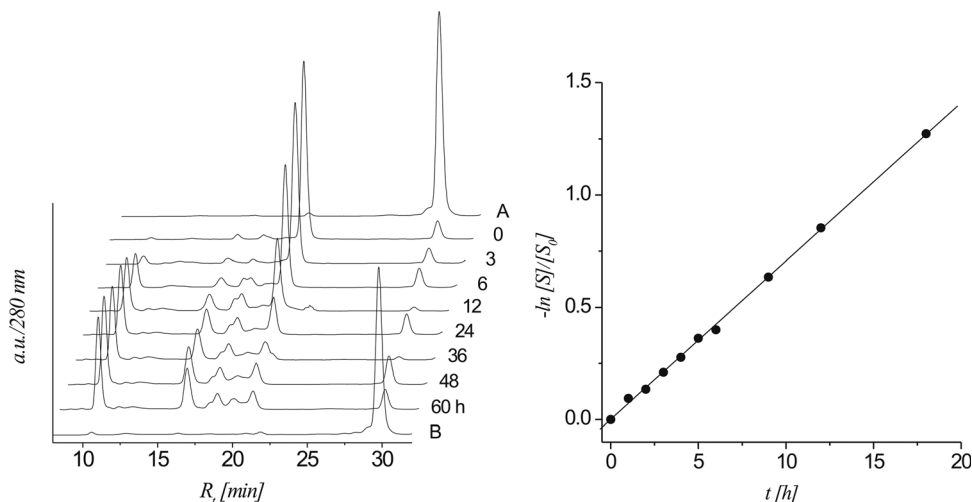


Figure 1. left: HPLC traces (280 nm) of the β -elimination reaction of the 2'-OMe heptamer **5b** at different time intervals; controls: trace A: protected heptamer **5a**; trace B: protected **5a** after treatment with 0.1 M NaOH for 48 h at 37°C; right: linear fit ($R^2 > 0.999$) of $\ln[S]/[S_0]$ versus t calculated from the HPLC traces.

To determine the contribution of each of these mechanisms to overall strand scission we performed separate kinetic analyses with oligonucleotide **5b** and **6a** and compared the results to that of **6b** in which both mechanisms are active simultaneously. In **5b**, the 2'-OH positions are methylated (with the exception of the 3' terminal C) and the abasic site is deprotected, thus excluding cyclophosphate formation, but admitting β -elimination. In **6a** the abasic site is still NPE protected, while the 2'-position of the abasic ribose is free. Here β -elimination is excluded but cyclophosphate formation at the abasic ribose is allowed. Oligonucleotide **7b** served as the DNA abasic site model that was used for comparison. The kinetics of strand scission was followed by reversed phase HPLC after incubating the oligonucleotides (Na^+ form) with 0.1 M NaOH at 37°C. In regular time intervals samples were injected and the relative amount of residual starting material determined by peak integration. The half-life times ($T_{1/2}$) were calculated from a first order exponential fit while the first order rate constants k_s for strand scission were obtained from the slope of a linear plot of $\ln[S]/[S_0]$ versus t where $[S]/[S_0]$ means the relative amount of unreacted abasic oligonucleotide at the time t .

β,δ -elimination at an RNA abasic site

The time course of strand cleavage of oligonucleotide **5b** is depicted in Figure 1. From the HPLC traces it becomes clear that the abasic heptamer **5b** (peak 4) decreases while at the same time three major fragments with lower retention times appear (peaks 1–3). Lane B is a control with protected oligonucleotide **5a** proving that no cleavage occurs if the anomeric center is still protected. The $T_{1/2}$ and k_s for **5b** under these conditions were calculated to be 594 min and $1.96 \times 10^{-5} \text{ s}^{-1}$, respectively. Peaks 1–3 were isolated and analyzed by ESI-MS (Table 1). Peaks 2 and 3 contain the two 5'-RNA-fragments after β -elimination and β,δ -elimination, respectively, while peak 1 corresponds to the phosphorylated 3'-fragment. Thus it is clear that both β - and δ -elimination steps take place, however at much slower rates compared to DNA **7b** (Table 4).

Table 1. Fragment analysis of cleavage of **5b**

peak	R_t [min]	Structure	Formula	m/z calc.	m/z found
1	10.5	r(pU _{OMe} U _{OMe} C)	C ₂₉ H ₄₀ N ₇ O ₂₄ P ₃	963.60	963.64
2	16.1	r(A _{OMe} G _{OMe} G _{OMe} P)	C ₃₃ H ₄₄ N ₁₅ O ₂₁ P ₃	1079.73	1079.26
3	18.2	r(A _{OMe} G _{OMe} G _{OMe} prb) ^a	C ₃₉ H ₅₂ N ₁₅ O ₂₄ P ₃	1207.86	1207.34

^arb = 4,5-dihydroxy-2-methoxy-2-pentenal.

Table 2. Fragment analysis of cleavage of **6a**

Peak	R_t [min]	Structure	Formula	m/z calc.	m/z found
1	11.6	r(U _{OMe} U _{OMe} C)	C ₂₉ H ₃₉ N ₇ O ₂₁ P ₂	883.62	883.20
2	19.5	r(A _{OMe} G _{OMe} G _{OMe} ASp)	C ₃₃ H ₄₄ N ₁₅ O ₂₁ P ₃	1440.98	1440.35
3	20.6	r(A _{OMe} G _{OMe} G _{OMe} ASp)	C ₃₉ H ₅₂ N ₁₅ O ₂₄ P ₃	1440.98	1440.34

Cyclophosphate formation at the RNA abasic site

To study strand scission via cyclophosphate formation independently from β,δ -elimination chemistry, oligonucleotide **6a** was subjected to the same basic conditions and its decay followed again by HPLC (Figure 2).

The HPLC traces show as expected a decrease of peak 4 corresponding to the heptamer **6a** and the appearance of three novel fragments (peaks 1–3) with lower retention times. Trace A shows oligonucleotide **6b** in which the abasic site was deprotected as a control. The absence of this peak in the other traces clearly shows that the 1NPE group is stable under the basic conditions and that no β,δ -elimination can be observed. We calculated again the $T_{1/2}$ for the disappearance of **6a** as described before and found a value of 221 min k_s in this case was found to be $5.95 \times 10^{-5} \text{ s}^{-1}$.

To follow the mechanism of cleavage we isolated the newly arising peaks 1–3 and analyzed the RNA fragments by ESI-MS (Table 2). Peak 1 contains the 3'-RNA fragment with a free 5'-OH group which is in accord with hydrolysis via cyclophosphate formation. Peaks 2 and 3 both contain fragments with the same mass that correspond to the isomeric 5'-fragment in which the terminal phosphate group is located

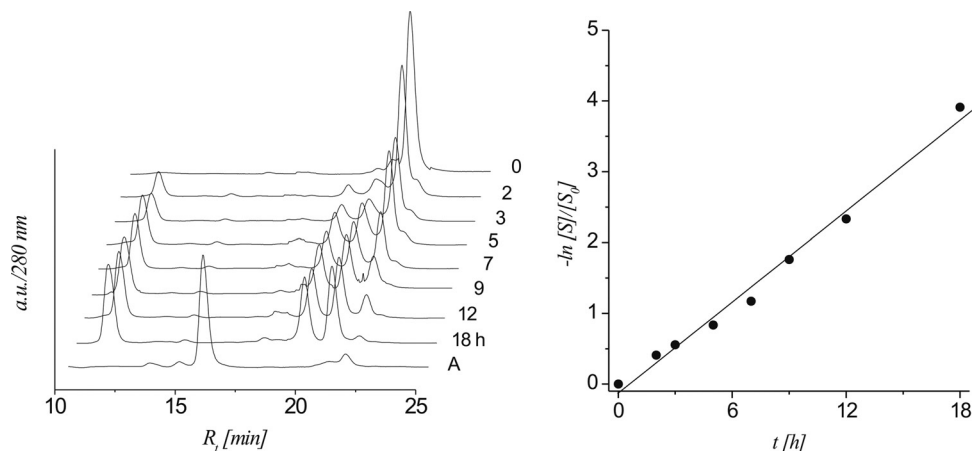


Figure 2. HPLC left: traces of strand cleavage via cyclophosphate formation of **6a** (0.1 M NaOH, 37°C) at different time intervals; controls: trace A: oligomer **6b**; right: linear fit ($R^2 > 0.994$) of $\ln[S]/[S_0]$ versus t calculated from the HPLC traces.

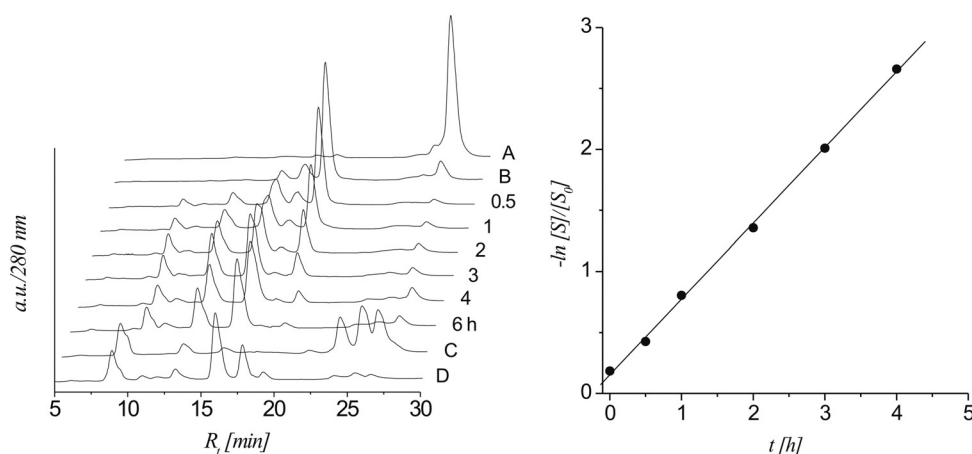


Figure 3. left: HPLC traces of strand cleavage via cyclophosphate formation and β,δ -elimination of **6b** (0.1 M NaOH, 37°C) at different time intervals; controls: trace A: **6a**, trace B: **6b**, trace C: **6a** (0.1 M NaOH, 6.5 h, 37°C), trace D: **6a** (0.1 M NaOH, 6.5 h, 37°C, followed by photolysis); right: linear fit ($R^2 > 0.999$) of $\ln[S]/[S_0]$ versus t calculated from the HPLC traces.

either at O2' or O3'. The corresponding cyclophosphate intermediate could not be isolated in this case.

Combination of β,δ -elimination and cyclophosphate formation in strand cleavage at the RNA abasic site

Since the two strand cleavage mechanisms studied separately so far act in concert in abasic RNA, it was necessary to study the effect of their combination on strand cleavage efficiency. For this purpose oligonucleotide **6b** was subjected to 0.1 M NaOH and strand cleavage analyzed as described before (Figure 3).

Oligonucleotide **6b** disappears under standard basic conditions with a $T_{1/2}$ of 69 min and a k_s of $1.73 \times 10^{-4} \text{ s}^{-1}$ as can be seen from the fit. This is considerably faster compared to **6a** and **6b** and is due to the overlay of the two mechanisms for strand scission (Table 4). A calculated $T_{1/2}$ for **6b** from those of **5b** and **6a** resulted in a value of 165 min. The difference between calculated and measured value is in reasonable agreement and validates the 2'-OME modification as a model for studying the β -elimination mechanism.

The overlay of the two modes for strand cleavage gives rise to an increased number of fragments. Fractions of the newly arising three main peaks (peaks 1–3) in the HPLC were again isolated and subjected to fragment analysis (Table 3). To have a first indication whether cyclophosphate formation would be dominant, protected heptamer **6a** was also submitted to basic conditions (0.1 M NaOH at 37°C, 6.5 h, trace C) and deprotected afterwards (trace D). Fraction 1 contained the 5'-phosphorylated 3'-fragment of **6b** arising from β,δ -elimination while fraction 2 contained the corresponding non-phosphorylated fragment which is expected from strand scission via cyclophosphate formation. The MS spectrum of fraction 3 revealed four major signals from four different fragments which could be identified as the 3'-phosphorylated 5'-fragment of **6b** together with that with the pending 4,5-dihydroxy-2-oxo-pentanal residue, arising from β,δ - and β -elimination, respectively. A second set of signals could be attributed to the same RNA fragment with the abasic ribose unit in its cyclophosphate and its hydrolyzed phosphate form. These products clearly arise from the hydrolytic strand scission pathway. Thus, fragment analysis clearly proves that both strand scission mechanisms are simultaneously active

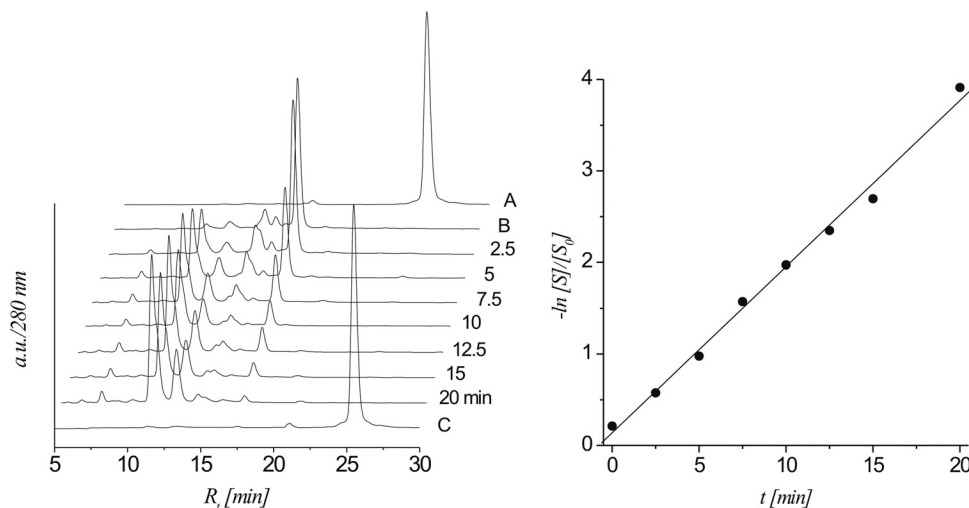


Figure 4. left: HPLC traces of strand cleavage via β,δ -elimination of **7b** (0.1 M NaOH, 37°C) at different time intervals; controls: trace A: **7a**; trace B: **7b**; trace C: **7a** after treatment with 0.1 M NaOH, 37°C for 20 min; right: linear fit ($R^2 > 0.996$) of $\ln[S]/[S_0]$ versus t calculated from the HPLC traces.

Table 3. Fragment analysis of strand scission of **6b**

Nr	R_t (min)	Fragment ^a	Formula	m/z calc.	m/z found
1	10.3	r(pU _{OMe} U _{OMe} C)	C ₂₉ H ₄₀ N ₇ O ₂₄ P ₃	963.60	963.26
2	13.6	r(U _{OMe} U _{OMe} C)	C ₂₉ H ₃₉ N ₇ O ₂₁ P ₂	883.62	883.22
3	16.2	r(A _{OMe} G _{OMe} G _{OMe} P)	C ₃₃ H ₄₄ N ₁₅ O ₂₁ P ₃	1079.73	1079.34
		r(A _{OMe} G _{OMe} G _{OMe} -rb)	C ₃₈ H ₅₂ N ₁₅ O ₂₅ P ₃	1211.85	1211.51
		r(A _{OMe} G _{OMe} G _{OMe} AScp)	C ₃₈ H ₅₁ N ₁₅ O ₂₇ P ₄	1273.81	1273.36
		r(A _{OMe} G _{OMe} G _{OMe} ASp)	C ₃₈ H ₅₃ N ₁₅ O ₂₈ P ₄	1291.83	1291.34

^arb = 4,5-dihydroxy-2-oxo-pentanal, cp = 2',3'-cyclophosphate, AS = abasic residue.

and contribute to the observed faster overall rate of strand cleavage as compared to **5b** and **6a**.

β,δ -elimination at a DNA abasic site

To compare the relative stability of the RNA abasic site with its DNA analogue, the abasic DNA heptamer **7b** was prepared and subjected to basic degradation under the same conditions (0.1 M NaOH, 37°C). The mechanism and kinetics of decay were measured as described before (Figure 4).

Oligodeoxynucleotide **7b** rapidly degrades into at least one intermediate and two stable products with a $T_{1/2}$ of only 4.1 min and a k_s of $3.02 \times 10^{-3} \text{ s}^{-1}$. HPLC analysis indicated the d(pTTC) fragment ($m/z = 915.15$) to be the faster eluting and d(AGGp) ($m/z = 989.38$) to be the slower eluting fragment, both being the expected products of β,δ -elimination. We assume that the transiently formed intermediate corresponds to the 5'-DNA fragment after β -elimination with the pending 4,5-dihydroxypent-2-enal unit but we did not investigate this in further detail.

For an overview of abasic site decay under alkaline conditions, all measured first order rate constants and the corresponding half-life times were summarized in Table 4, together with k_{rel} , indicating relative differences in the rates of abasic site cleavage. It becomes immediately evident that β,δ -elimination at a DNA abasic site is 154-fold faster than at an RNA abasic site. This highlights the strong influence

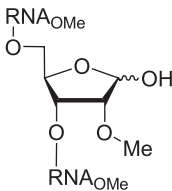
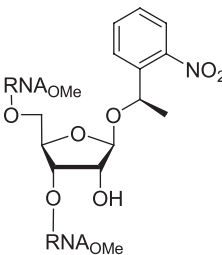
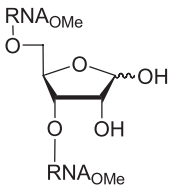
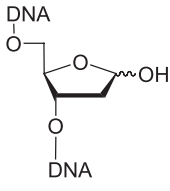
of the 2'-OH group on this mechanism for strand scission. Interestingly, strand cleavage via cyclophosphate formation is 3-fold faster compared to strand cleavage via β,δ -elimination in RNA. In the case of an unperturbed abasic site, where both mechanisms can contribute to strand cleavage, the RNA abasic site shows ~ 16 -fold enhanced stability compared to a DNA abasic site.

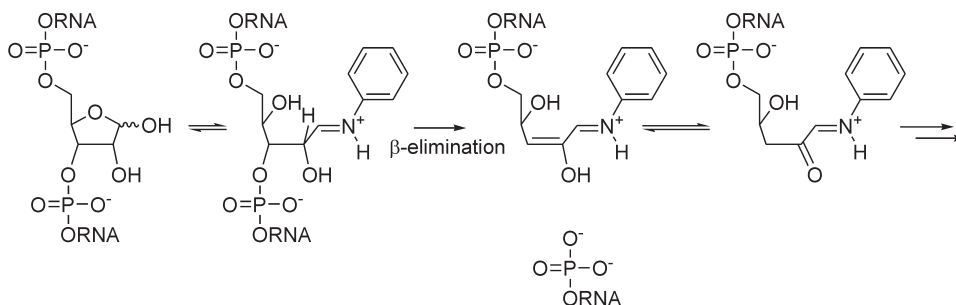
Aniline mediated strand cleavage at pH 4.6

It is long known that strand cleavage of abasic DNA at physiological ionic strength and neutral to slightly acidic pH is greatly enhanced in the presence of amines (2). It was therefore of interest to investigate strand cleavage of abasic RNA in the presence of an amine and compare it to DNA. We have chosen aniline as a model amine because abasic RNA cleavage by this amine at pH 4.6 was used in the past for sequencing and site specific modification of RNA (10,18). A potentially simplified mechanism for the aniline mediated abasic RNA decay is given in Scheme 3.

It is beyond doubt that strand cleavage is initiated by immonium ion formation which renders the 2'-H base-labile and the 3'-phosphate unit prone to β -elimination. The intermediate enol strongly prefers the keto tautomeric form which renders δ -elimination that could in principle be initiated via vinylogous deprotonation of 4'-H slow. Given the fact that strand cleavage occurs in a slightly acidic medium, concomitant cyclophosphate formation, as observed under under alkaline conditions, is no longer obscuring β -elimination and for this reason the following experiments were performed with the 2'-unmodified abasic RNA oligonucleotide **4b**. Again, abasic DNA **7b** was used for comparison. The extent of cleavage was followed also in this case by HPLC (Figures 5 and 6). $T_{1/2}$ and the apparent first order rate constant for strand scission k_s were determined as described before. We found a $T_{1/2}$ of 14 min and a k_s of $8.56 \times 10^{-4} \text{ s}^{-1}$ for the abasic RNA **4b**. The control experiments at neutral pH (Figure 5, trace B and C) clearly show that strand cleavage is much slower in the absence of aniline and essentially does not progress significantly over the time

Table 4. Summary of the $T_{1/2}$ and k_s and k_{rel} data measured for alkaline induced strand scission of the abasic RNA and DNA heptamers

	Oligonucleotide			
Abasic site				
	5b	6a	6b	7
Mechanism of strand scission	β,δ -elimination	cyclophosphate formation	β,δ -elimination + cyclophosphate formation	β,δ -elimination
$T_{1/2}$ (min)	594	221	69	4.1
k_s (s^{-1})	1.96×10^{-5}	5.95×10^{-5}	1.73×10^{-4}	3.02×10^{-3}
k_{rel}	1	3	9	154

**Scheme 3.** Structurally and kinetically relevant intermediates in the aniline mediated strand scission at RNA abasic sites at slightly acidic pH.

course of the experiment. The same analysis in the case of the DNA abasic oligomer **7b** resulted in a $T_{1/2}$ of 53 s and a k_s of $1.29 \times 10^{-2} s^{-1}$. Also, here strand cleavage in the absence of aniline was negligible over the time course of the experiment (Figure 6, trace B and C).

Fragment analysis in the case of aniline induced strand cleavage by ESI-MS proved more difficult than in the case of base induced cleavage for a yet unknown reason. We were unable to obtain masses for cleavage products in all isolated fractions. Those that could be identified for **4b** and **7b** were listed in Table 5. In both cases, the trimers 3' to the abasic sites, as expected from β -elimination, were identified. Interestingly, in the case of the deoxyoligonucleotide **7b**, the 5'-fragment containing the abasic residue bound to aniline as well as the aniline adduct of the intact abasic heptamer could be identified. This is a direct proof of the intermediacy of imines or hemiaminals in the cleavage mechanism.

From these experiments, it becomes clear that amines greatly accelerate strand cleavage near neutral pH also in abasic RNA. But again, abasic DNA is cleaved 15-fold faster. If one compares the k_s values of cleavage via β -elimination in the presence of aniline with those obtained for alkaline cleavage it becomes clear that a DNA abasic site is only cleaved 4-fold faster while a RNA abasic site decays 42-fold faster. Thus the 2'-OH group seems to

increase the β -elimination chemistry next to the immonium group.

DISCUSSION

We describe here the first direct comparison of the chemical stability of an RNA versus a DNA abasic site under basic conditions and under slightly acidic conditions in the presence of an amine. While under basic conditions no other mechanism than β -elimination is operative in DNA, the situation is more complex in the case of RNA, where cyclophosphate formation is acting in concert with β -elimination. In order to analyze the contribution of each mechanism to strand scission separately we used a 2'-OMe abasic site analogue, incapable of cyclophosphate formation, and a 1'-protected abasic RNA analogue incapable of β -elimination as well as a true abasic site within a 2'-OMe-oligoribonucleotide.

An initial concern was whether the 2'-OMe-RNA abasic site analogue would be an adequate model reflecting correctly the β -elimination properties of a true RNA abasic site. This was a *priori* not clear as e.g. reversible, competitive deprotonation at 2'-OH or the shift of the keto function from C1' to C2' via a C1'-C2' dienolate could interfere with β -elimination kinetics (Figure 7).

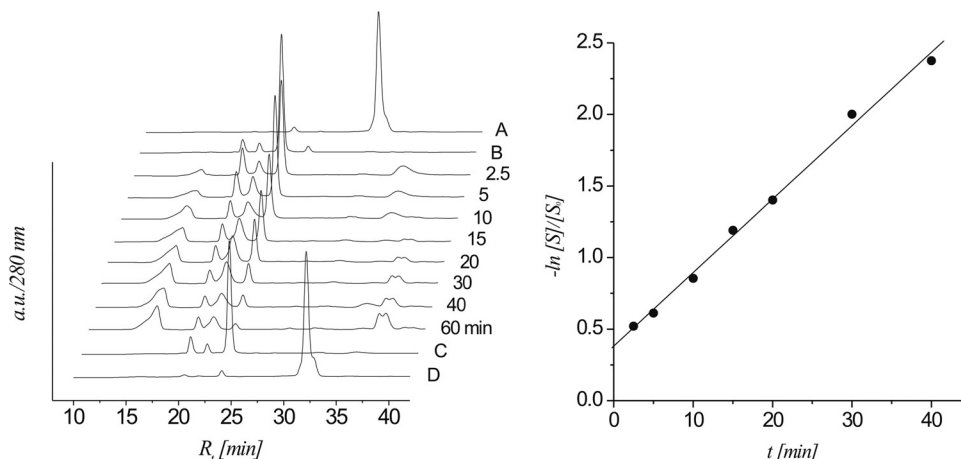


Figure 5. left: HPLC traces of aniline-induced strand cleavage reaction of **4b** at the given time intervals; controls: trace A: protected heptamer **4a**; trace B: deprotected heptamer **4b**; trace C: **4b** after 60 min in 0.3 M TEAA buffer, pH 7.0 at 37°C in the absence of aniline; trace D: protected heptamer **4a** after treatment with aniline for 60 min; right: linear fit ($R^2 > 0.997$) of the $\ln[S]/[S_0]$ versus t for **4b**.

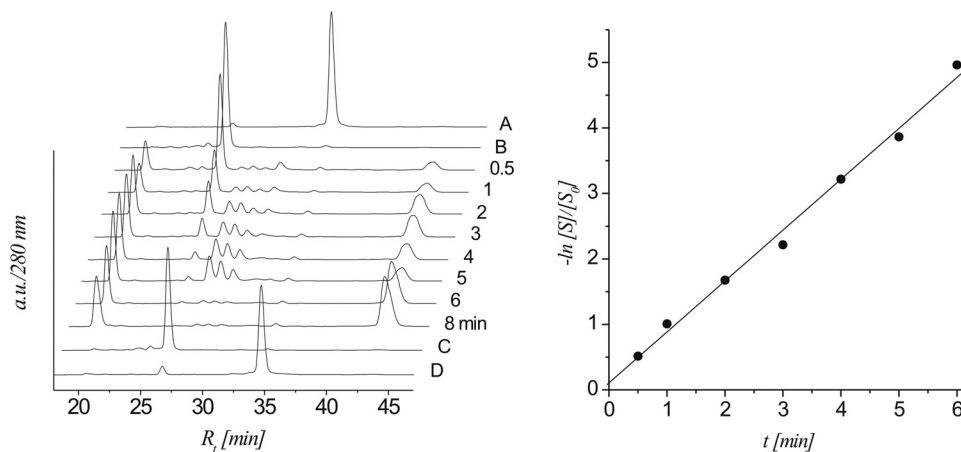


Figure 6. left: HPLC traces of aniline-induced strand cleavage reaction of **7b** at the given time intervals; controls: trace A: protected heptamer **7a**; trace B: deprotected heptamer **7b**; trace C: deprotected heptamer **7b** after 10 min in 0.3 M TEAA buffer, pH 7.0 at 37°C in the absence of aniline; trace D: protected heptamer **7a** after treatment with aniline for 10 min; right: linear fit ($R^2 > 0.996$) of the $\ln[S]/[S_0]$ versus t for **7b**.

Table 5. Identified fragments of aniline induced cleavage at pH 4.6 of oligonucleotides **4b** and **7b**

oligonucleotide	R_t (min)	Identified fragments ^a	Formula	m/z calc.	m/z found
7b	16.5	r(UUC)	$C_{27}H_{35}N_7O_{21}P_2$	855.6	855.1
	20.3	r(pUUC)	$C_{27}H_{36}N_7O_{24}P_3$	953.5	935.1
4b	20.5	d(pTTC)	$C_{29}H_{40}N_7O_{21}P_3$	915.6	915.2
	20.5	d(TTC)	$C_{29}H_{39}N_7O_{18}P_2$	835.6	835.2
	28.3–30.3	d(AGG)-AS-NHC ₆ H ₅	$C_{41}H_{48}N_{16}O_{19}P_3$	1161.9	1162.3
		d(AGG-AS-NHC ₆ H ₅ -TTC)	$C_{70}H_{88}N_{23}O_{40}P_6$	2077.4	2077.4

^aAS-NHC₆H₅ = imine or hemiaminal between the abasic site and aniline.

We compared therefore $T_{1/2}$ of **6b** with that calculated from the sum of the measured exponential decays of **6a** and **5b**. We found a theoretical $T_{1/2}$ of 165 min which is 2.5-fold longer than that measured for **6b**. From this we conclude that O2'-methylation slightly but not significantly retards β -elimination in abasic RNA which validates the O2'-methylated ribose unit as abasic site model. At the same

time this comparison also validates the NPE protected abasic RNA unit with a free 2'-OH group to be a valid model. In a true RNA abasic site not only the hemiacetal form but also the open chain, aldehyde form can undergo strand cleavage via the cyclophosphate pathway. The above described comparison underlines that if this is the case there is either no significant difference in the velocity of cyclophosphate

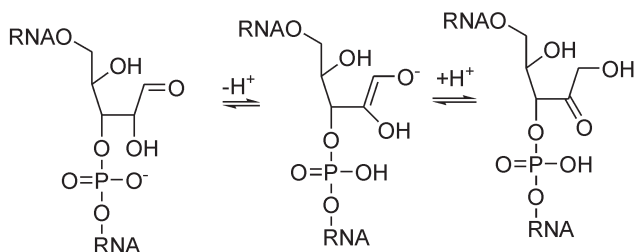


Figure 7. 1',2'-shift of keto function via a dienolate intermediate.

formation between the open chain and the furanose form, or the open chain form is kinetically not relevant. By comparing the relative rate of strand cleavage we noted that cleavage via cyclophosphate formation is ca 3-fold faster than cleavage by β -elimination. Extrapolated to longer RNA as, e.g. viral RNA this means that under basic conditions strand scission via cyclophosphate formation is clearly the dominant mechanism of decay even in the presence of an abasic site.

From the mechanistic point of view by far the most challenging fact is the roughly 150-fold higher stability of an RNA abasic site towards β -elimination compared to DNA under alkaline conditions. Several factors could be responsible for this. A thermodynamic argument would invoke differences in the pK_a of the $\text{C}2'$ -H as a function of the presence or absence of an OH function. We calculated the $\text{C}2'$ -H acidity of a DNA and RNA abasic site model using the SPARC calculator (19) and found only minor differences in pK_a (Figure 8A). According to theory, the $\text{C}2'$ -H of the RNA abasic site is slightly less acidic compared to DNA but the ΔpK_a of only 0.34 can not explain the differences in reactivity. Also retardation of β -elimination via competitive, reversible deprotonation of the 2'-OH group can be excluded as the reason due to the fact that the corresponding 2'-OMe derivative shows slightly slower strand scission kinetics as compared to the non-methylated abasic residue. Also to be excluded are statistical effects resulting from 2 scissile $\text{C}2'$ -H bonds in DNA compared to only one in RNA, as this certainly does not explain a more than 150-fold rate difference.

The origin of the stability differences could in principle arise from differential stereoelectronic effects in a concerted *trans*- β -elimination mechanism (Figure 8B). The conformer for which less reactivity of RNA over DNA can be expected is that with the anti-arrangement of the $\text{C}2'$ - $\text{C}3'$ -bond (Figure 8B, right). Although steric arguments favor this conformation, stereoelectronic effects disfavor this arrangement in the case of RNA due to the anti-alignment of the $\text{C}2'$ -O- and the $\text{C}3'$ -O-bond, violating the gauche effect. Thus, there is no strong stereoelectronic argument in support of the higher reactivity of a DNA over RNA abasic site.

If one assumes that β -elimination follows a polar, non-concerted pathway, another hypothesis opens up. Under the basic conditions applied it seems likely that $\text{C}2'$ -H dissociation is fast and reversible and therefore dissociation of the $\text{C}3'$ - $\text{O}3'$ bond is rate determining. An important role has then to be attributed to the $\text{C}2'$ - $\text{O}2'$ σ -bond in RNA which renders dissociation of the $\text{C}3'$ - $\text{O}3'$ bond more difficult compared to the $\text{C}2'$ -H bond in DNA due to less hyperconjugative stabilization of the transition state upon progressing

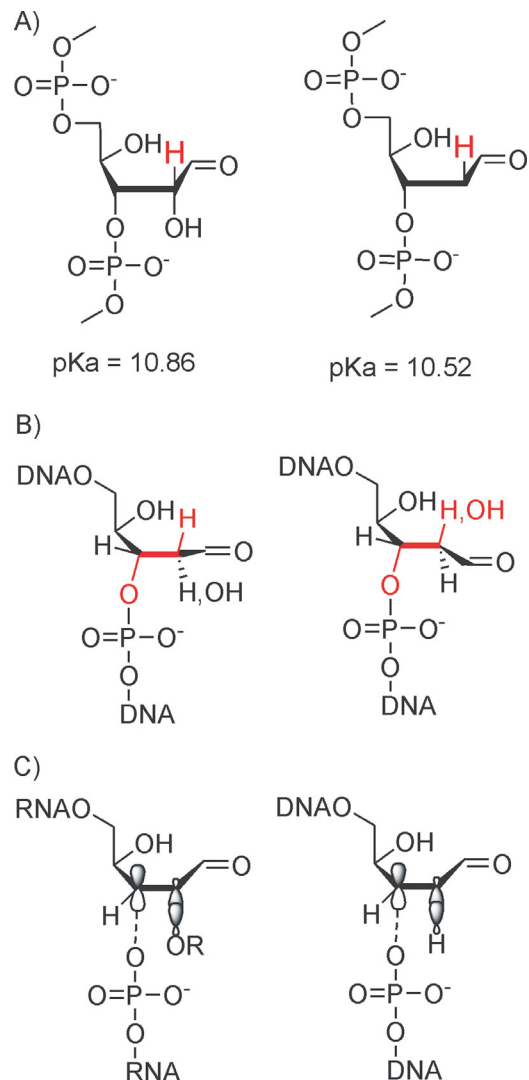


Figure 8. (A) $\text{C}2'$ -H acidities of an RNA and a DNA abasic site in the aldehyde form; (B) syn and anti conformers at the $\text{C}2'$ - $\text{C}3'$ -bond and implications on the concerted *trans*- β -elimination process for RNA and DNA; (C) Model of differential hyperconjugative assistance of $\text{C}3'$ - $\text{O}3'$ bond dissociation by a $\text{C}2'$ -H or $\text{C}2'$ -OH σ -bond in a DNA and RNA abasic site.

$\text{C}3'$ - $\text{O}3'$ bond dissociation (Figure 8C). We currently favor this hypothesis as it is in agreement with our experimental observations.

In the Schiff-base induced β -elimination at pH 4.6, the relative rates of cleavage between an RNA and a DNA abasic site are less different. Under these conditions, abasic RNA is still 15-fold more stable compared to abasic DNA. It may well be that under these conditions the deprotonation of the $2'\text{C}-\text{H}$ becomes kinetically more dominant compared to the $\text{C}3'-\text{O}3'$ bond dissociation in the overall β -elimination mechanism due to the increased difference of the pH of the medium compared to the pK_a of the $\text{C}2'$ -H. Thus the differences in kinetics between RNA and DNA decay are expected to correlate with the differences of the pK_a of the respective $\text{C}2'$ -H which is at least qualitatively the case. As a bottom line it appears that also under these more biorelevant conditions there is an advantage in stability of abasic RNA over abasic DNA.

The relative stability of abasic RNA may have interesting biological consequences for long lived RNAs. It is known that spontaneous generation of abasic RNA is slower compared to DNA (20), but once such lesions are formed, their potential biological effect is expected to be higher due to their relative longevity. Ribosome inactivating proteins (RIPs) are long known, but only recently it was found that class-I RIPs such as the pokeweed antiviral protein can not only depurinate the sarcin/ricin loop of the large rRNA but also specific adenine and guanine residues throughout the sequence of capped mRNAs (21) or other viral RNAs (22). This means that there exist not only spontaneous but also enzymatic pathways for abasic mRNA generation. It will therefore be of interest to study the effect of abasic RNA sites on the translation process in more detail.

Another open question associated with RNA abasic sites in long-lived RNA is whether they have any impact on the evolution of viral RNA. In preliminary experiments we studied the *trans*-lesion synthesis of an abasic RNA template/DNA-primer system by HIV-1 reverse transcriptase and found efficient insertion of purine bases opposite the lesion (12). Thus it is not excluded that abasic RNA also contributes to mutations in viral or retroviral RNA during replication or reversed transcription, in addition to the error rate of RNA dependent RNA polymerases (23) or reversed transcriptases (24).

Finally it will be of interest to find out whether there exists a primitive cellular repair system for abasic RNA. There is a growing list of genes involved in RNA damage control (25,26), and it is assumed that many of them are not yet discovered. There is also evidence that defects in the RNome stability might play a role in cancer formation. The study of mRNA biogenesis over the last years lead to the insight that there exists an elaborate RNA quality control mechanism involving, e.g. proteins that select aberrantly spliced mRNAs and mRNAs with premature termination codons (26). mRNAs are the working copies of the genomic information and a cell should therefore have a great investment in maintaining the integrity of its RNA. So, why should there not be a specific mechanism for dealing with abasic RNA? It could be as simple as just a mechanism for inactivating and metabolizing abasic RNA.

SUPPLEMENTARY DATA

Supplementary Data are available at *NAR* Online.

ACKNOWLEDGEMENTS

Financial support from the Swiss National Science Foundation (grant No. 200020-107692) is gratefully acknowledged. Funding to pay the Open Access publication charges for this article was provided by Swiss National Science Foundation.

Conflict of interest statement. None declared.

REFERENCES

- Lindahl, T. and Nyberg, B. (1972) Rate of depurination of native deoxyribonucleic acid. *Biochemistry*, **11**, 3610–3618.

- Lindahl, T. and Andersson, A. (1972) Rate of chain breakage at apurinic sites in double-stranded deoxyribonucleic acid. *Biochemistry*, **11**, 3618–3623.
- Loeb, L.A. and Preston, B.D. (1986) Mutagenesis by apurinic/aprimidinic sites. *Ann. Rev. Genet.*, **20**, 201–230.
- Lhomme, J., Constant, J.F. and Demeunynck, M. (1999) Abasic DNA structure, reactivity and recognition. *Biopolymers*, **52**, 65–83.
- Scharer, O.D. (2003) Chemistry and biology of DNA repair. *Angew. Chem. Int. Ed. Engl.*, **42**, 2946–2974.
- Aas, P.A., Otterlei, M., Falnes, P.O., Vagbo, C.B., Skorpen, F., Akbari, M., Sundheim, O., Bjoras, M., Slupphaug, G., Seeberg, E. *et al.* (2003) Human and bacterial oxidative demethylases repair alkylation damage in both RNA and DNA. *Nature*, **421**, 859–863.
- Schramm, V.L. (1997) Enzymatic N-riboside scission in RNA and RNA precursors. *Curr. Opin. Chem. Biol.*, **1**, 323–331.
- Ogasawara, T., Sawasaki, T., Morishita, R., Ozawa, A., Madin, K. and Endo, Y. (1999) A new class of enzyme acting on damaged ribosomes: ribosomal RNA apurinic site specific lyase found in wheat germ. *EMBO J.*, **18**, 6522–6531.
- Ozawa, A., Sawasaki, T., Takai, K., Uchiumi, T., Hori, H. and Endo, Y. (2003) RALyase; a terminator of elongation function of depurinated ribosomes. *FEBS Lett.*, **555**, 455–458.
- Nishikawa, Y., Adams, B.L. and Hecht, S.M. (1982) Chemical excision of apurinic acids from rna. a structurally modified yeast tRNA^{Phe}. *J. Am. Chem. Soc.*, **104**, 326–328.
- Trzupek, J.D. and Sheppard, T.L. (2005) Photochemical generation of ribose abasic sites in RNA oligonucleotides. *Org. Lett.*, **7**, 1493–1496.
- Kuepfer, P.A. and Leumann, C.J. (2005) RNA abasic sites: preparation and *trans*-lesion synthesis by HIV-1 reverse transcriptase. *Chem. Bio. Chem.*, **6**, 1970–1973.
- Strauss, B.S. (1991) The ‘A rule’ of mutagen specificity: a consequence of DNA polymerase bypass of non-instructional lesions? *Bioessays*, **13**, 79–84.
- Pitsch, S., Weiss, P.A., Wu, X., Ackermann, D. and Honegger, T. (1999) Fast and reliable automated synthesis of RNA and partially 2'-O protected precursors ('caged RNA') based on two novel orthogonal 2'-O protecting groups. *Helv. Chim. Acta*, **82**, 1753–1761.
- Wenter, P., Furtig, B., Hainard, A., Schwalbe, H. and Pitsch, S. (2005) Kinetics of photoinduced RNA refolding by real-time NMR spectroscopy. *Angew. Chem. Int. Ed. Engl.*, **44**, 2600–2603.
- Wenter, P., Furtig, B., Hainard, A., Schwalbe, H. and Pitsch, S. (2006) A caged uridine for the selective preparation of an RNA fold and determination of its refolding kinetics by real-time NMR. *ChemBiochem*, **7**, 417–420.
- Heckel, A. and Mayer, G. (2005) Light regulation of aptamer activity: an anti-thrombin aptamer with caged thymidine nucleobases. *J. Am. Chem. Soc.*, **127**, 822–823.
- Rajbhandary, U.L. (1980) Recent developments in methods for RNA sequencing using *in vitro* 32P-labeling. *Fed. Proc.*, **39**, 2815–2821.
- Hillal, S.H., Karickhoff, S.W. and Carreira, L.A. (1995) A rigorous test for SPARC's chemical reactivity models: estimation of more than 4300 ionization pK(a)s. *Quant. Struct. -Act. Relat.*, **14**, 348–355.
- Kochetkov, N.K. and Budovskii, E.I. (1972) Hydrolysis of N-glycosidic bonds in nucleosides, nucleotides and their derivatives. In Kochetkov, N.K. and Budovskii, E.I. (eds), *Organic Chemistry of Nucleic Acids*. Plenum, New York, pp. 425–448.
- Hudak, K.A., Bauman, J.D. and Tumer, N.E. (2002) Pokeweed antiviral protein binds to the cap structure of eukaryotic mRNA and depurinates the mRNA downstream of the cap. *RNA*, **8**, 1148–1159.
- Parikh, B.A. and Tumer, N.E. (2004) Antiviral activity of ribosome inactivating proteins in medicine. *Mini. Rev. Med. Chem.*, **4**, 523–543.
- Castro, C., Arnold, J.J. and Cameron, C.E. (2005) Incorporation fidelity of the viral RNA-dependent RNA polymerase: a kinetic, thermodynamic and structural perspective. *Virus Res.*, **107**, 141–149.
- Menendez-Arias, L. (2002) Molecular basis of fidelity of DNA synthesis and nucleotide specificity of retroviral reverse transcriptases. *Prog. Nucleic Acid Res. Mol. Biol.*, **71**, 91–147.
- Bregeon, D. and Sarasin, A. (2005) Hypothetical role of RNA damage avoidance in preventing human disease. *Mutat. Res.*, **577**, 293–302.
- Bellacosa, A. and Moss, E.G. (2003) RNA repair: damage control. *Curr. Biol.*, **13**, R482–R484.

Curriculum Vitae

- 1975 Born on the 26th of June in Interlaken
- 1982-1986 Primary school in Interlaken
- 1986-1991 Secondary school in Interlaken
- 1991-1996 High school in Interlaken
- 1996-2002 Undergraduate studies in Chemistry at the University of Bern
Diploma work with PD Dr. Jürg Hunziker at the Department of
Chemistry and Biochemistry, University of Bern
- 2002 Diploma in Chemistry: 17th of January
- 2002-2006 PhD thesis with Prof. Dr. Christian J. Leumann at the Department
of Chemistry und Biochemistry, University of Bern